EFFECT OF OFF-ROAD SURFACE ROUGHNESS ON TYRE PERFORMANCE

by

FUMIHARU EIYO

A thesis submitted to the Faculty of Graduate Studies and Research in partial fulfillment of the requirements for the degree of Doctor of Philosophy

Department of Civil Engineering and Applied Mechanics

McGill University

Montreal, Quebec, Canada

May 1989

EFFECT OF OFF-ROAD SURFACE ROUGHNESS ON TYRE PERFORMANCE

by

Fumiharu Eiyo

ABSTRACT

In this thesis, the effect of geometrical roughness of a non-deformable road surface on the mobility performance of a pneumatic tyre is investigated. A system function which represents the theoretical relationship between the drawbar-pull and the random traction surface geometry is developed in the frequency domain, associated with the energy conservation law.

Prior to the analysis, measurement of road profile is achieved using an ultrasonic distance detector, and characterization of the stochastic road profile is evaluated by a power spectral density function. Further to this, the resulting drawbar-pull and tractive efficiency for a given slip rate, applied torque, tyre characteristics (as a function of inflation pressure) and vehicle moving velocity are evaluated through the above-mentioned system function.

The enveloping function, describing the modification effect of the original road profile by a flexible tyre, is also experimentally investigated. Systematic laboratory

tests are carried out by using four pseudo-random rough traction surfaces, for comparison and verification of the theoretical predictions.

Through combined theoretical and experimental investigations, the following conclusions are obtained:

(1) As the traveling speed increases, tractive efficiency is gradually decreased.

(2) Higher slip rates give less tractive efficiency, however, an optimum slip rate between 2% and 10% provides the highest efficiency.

(3) Tractive efficiency increases hyperbolically with an increase in the inflation pressure of the tyre.

(4) A substantial decrease in tractive efficiency is obtained when the condition of the road surface becomes sufficiently rough that the road would be classified as "poor" or rougher under the ISO recommendations, at a speed of 5 m/s (18 km/h).

EFFETS DES SURFACES RUGUEUSES HORS ROUTE SUR LA PERFORMANCE DES PNEUS

RÉSUMÉ

Les effets de rugosite geometrique d'une surface routiere non-déformable sur la performance d'un pneu sont etudies dans cette thèse. Un systeme fonctionnel qui represente les relations théoriques entre le couple moteur et la traction aléatoire de la surface geometrique a ete developpe dans le domaine de la modulation, conformement a la loi de la conservation de l'energie.

Avant l'analyse, un profil de la surface routiere est obtenu à l'aide d'un détecteur de distance à ultra-sons. Le profil «stochastique» routier est caracterise au moyen d'une fonction de densite du pouvoir spectral. De plus, le couple moteur et le coefficient de frottement sont evalues a l'aide du système mentionne ci-haut, en fonction d'un taux de glissement donné, du couple appliqué, des caracteristiques du pneu selon la pression d'air, et de la vitesse du véhicule.

La fonction globale qui décrit les modifications du profil routier original par un pneu flexible est egalement étudiée. Des tests ont ete effectués en laboratoire a l'aide de quatre surfaces tractives rugueuses dites «pseudo-aléatoires», afin de comparer et de verifier les predictions theoriques.

A partir des resultats des études theoriques et experimentales combines, les conclusions suivantes ont été degagees :

1) l'efficacite tractive décroît proportionnellement à l'augmentation de la vitesse du vehicule;
2) un plus haut taux de glissement entraîne une reduction de l'efficacité tractive, l'efficacité optimale correspondant à un taux de glissement se situant entre 2 et 10 %;
3) l'efficacite tractive croît hyperboliquement en fonction de l'augmentation de la pression de l'air dans le pneu;
4) l'efficacite tractive diminue considérablement lorsque l'etat de la surface routière se dégrade et que la chaussee correspond au mieux à la catégorie «mediocre» de la classification ISO, pour une vitesse de 5 m/s (18 km/hr).

ACKNOWLEDGMENTS

The author wishes to express his sincere appreciation and gratitude to:

-Professor R. N. Yong, William Scott Professor of Civil Engineering and Applied Mechanics, and Director of the Geotechnical Research Center at McGill University, for his invaluable guidance and continued encouragement throughout this study;

-Professor M. Kitano, Professor of Mechanical Engineering of National Defense Academy, Japan, for his incessant guidance and encouragement;

-Japan Self Defense Force, for their support and continuous encouragement during my study leave;

-Dr. P. Boonsinsuk, for his helpful advice and discussions;

-Dr. D. Xu, for his encouragement, and invaluable suggestions and helpful discussions;

-Mr. F. Caporuscio, for his technical assistance;

-Special appreciation is extended to my family, especially my mother and my wife for their encouragement and understanding. My wife, Hiroko, who was of great assistance in typing the manuscript.

TABLE OF CONTENTS

LIST OF FIGURES

LIST OF TABLES

NOTATION

d	half of contact length
r_o	original tyre radius
r_r	rolling tyre radius
D	deflection of tyre
N	normal load to tyre axle
P_i	tyre inflation pressure
k_T	tyre stiffness
c_T	tyre damping
k'	distributed tyre stiffness
c'	distributed tyre damping
q	contact length coefficient
h	amplitude of sinusoidal road surface
V	horizontal translational velocity
Vv	vertical velocity
DBP	drawbar-pull
T	input torque
s_i	slip rate
MR	motion resistance
RR	rolling resistance
$S_{(f)}, S_{(\Omega)}$	one-sided power spectral density
Go	roughness constant
n	slope constant
y_1	amplitude of original road profile
y_2	amplitude of filtered road profile

y_3	vertical response of tyre axle
$H_{E(f)}$	enveloping function
$H_{sy(f)}$	system function
E_{in}	input energy
E_{out}	output energy
E_s	slip (interfacial) energy
E_T	tyre deformation energy
$E[\ ]$	expected value
σ	standard deviation
ϵ	linearization equivalence parameter
ζ	damping ratio
ξ	energy recovery factor
ω_T	angular velocity of tyre
ω , f	excitation frequency (rad,Hz)
Ω	spatial frequency (c/m)
η	tractive efficiency
η_n	nominal tractive efficiency

ABBREVIATION

ASAE	American Society of Agricultural Engineers
ASME	American Society of Mechanical Engineers
ASTM	American Society for Testing and Materials
ISTVS	International Society for Terrain-Vehicle System
NASA	National Aeronautic and Space Administration
SAE	Society of Automotive Engineers
VSD	Vehicle System Dynamics

CHAPTER 1

INTRODUCTION

1.1 General

In this study, the tractive performance of a pneumatic tyre will be theoretically and experimentally investigated in relation to the ground surface characteristics (rough and non-deformable), together with the effect of inflation pressure of tyre, running speed and slip rate at tyre-ground interface.

An off-road vehicle such as a bulldozer, agricultural tractor or heavy duty military truck is normally operated under severe terrain and/or operational conditions. In other words, off-road i.e. an unpaved outdoor snowy, muddy or rough field, supplies poor operational conditions for the vehicles as compared with a properly paved road. The most significant differences between on-road and off-road characteristics are the deformability of the road and the conditions of terrain (road) cover. As for the deformability, which is related to the strength of the soil, many studies have been given in the consideration of flotation and traction (Schuring,1966; Bekker,1969; Yong and Fattah,1976; Gee-Clough,1980 and others). If the terrain material can provide the necessary flotation and traction to maintain a vehicle in constant travel and produce the required pull force, terrain cover characteristics can constitute another factor which could restrict vehicle travel speed or even cause total vehicle immobilization. Terrain cover factors can be identified as: i) ground slope, ii) obstacles (mound and ditches), iii) roughness and iv) vegetation (Fig. 1.1.1).

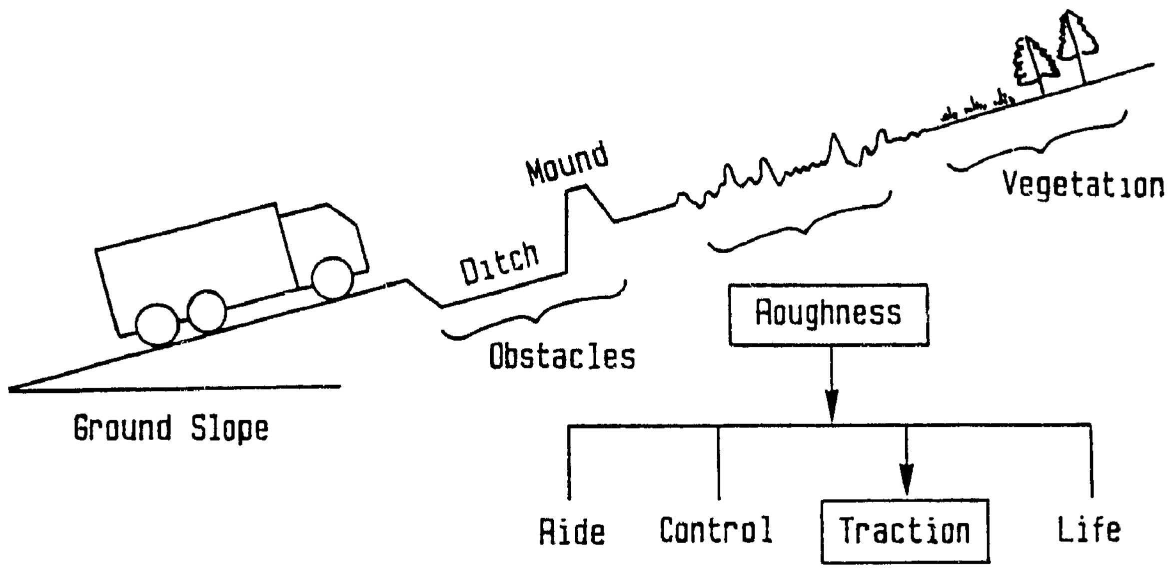

Fig. 1.1.1 Types of terrain cover and major problems due to terrain roughness

i) Ground slope

Ground slope increases vehicle motion resistance due to the gravitational component of the vehicle. The maximum ground slope which a vehicle can climb is an important performance criterion. Overturning phenomenon is also to be considered on a inclined road.

ii) Obstacles

These include surface features such as boulders, stumps, logs, potholes, mounds, ditches etc., which cause impediments to vehicles (immobilization). The main concern to the vehicle traction is the capability to climb over these obstacles.

iii) Roughness

This can be defined as small ground surface irregularities. When a vehicle travels on such a ground surface, resultant vibrations are generated which cause many problems to both the vehicle and the human body.

iv) Vegetation

Vegetation can be regarded in a very broad sense to include the surface vegetation (muskeg, moss etc. or even ground surface contamination by oil or water etc.) and obstacle effect due to tall trees etc..

In this investigation, the terrain surface roughness is considered to be one of the biggest problems faced in off-road vehicle mobility in order to achieve efficient transportation, which means that a vehicle transverses as fast as possible with a minimum energy spent. As for a rough road operation, several important problems arise with the resultant effect of changes in vehicle performance.

The main areas in the problems of off-road vehicle performance on rough road surfaces are ride, controllability, vehicle's life cycle cost (durability) and tractive performance.

(1) Ride comfort

Vehicle speed across rough terrain is usually limited by the ability of the operator to withstand the transmitted accelerations. Therefore, vehicle performance is also affected by ride comfort. Vertical accelerations or displacements of a vehicle/driver were mainly investigated (Kozin et al.,1960, 1966; Matthews,1966; Sireteanu,1984).

(2) Vehicle control (handling)

Off-road vehicles are today operated not only at low speeds but also at high speeds. For example, in a tactical situation (for the military), a high speed generally has to be maintained. Therefore, when a vehicle bounces due to vertical excitation from a rough ground surface, and as vehicle speed or terrain roughness increases, the running gear no longer contacts the ground all the time. The more the running gear loses contact with the terrain surface, the less controllability is evidenced.

(3) Life cycle cost

With the excitation from the ground, a problem of long life, durability and maintainability of vehicles is created. To develop optimum productivity, high payload and high speed are essentially required. However, these two quantities have an inversely proportional relationship based on the life cycle cost. In order to decrease life cycle cost over a certain time period, it is necessary to reduce efficient payload and/or vehicle speed on a rough terrain. In doing so, a penalty for productivity must be paid. Few reports have been published on both controllability and life cycle cost related to the ground surface roughness.

(4) Tractive performance

As expected, the off-road vehicle may jump or bounce on a rough ground. This severely limits the speed of the vehicle because of excessive vibrations leading to total immobilization. The slip rate of the running gear (wheel/track) may be increased as a result of this phenomenon. Furthermore, the energy of vibratory motion is dissipated in vehicles in many ways, which may cause deterioration of tractive performance (normally evaluated by the drawbar-pull) of the vehicle due to an increase in the motion resistance resulting from the off-road surface roughness (Fig. 1.1.2).

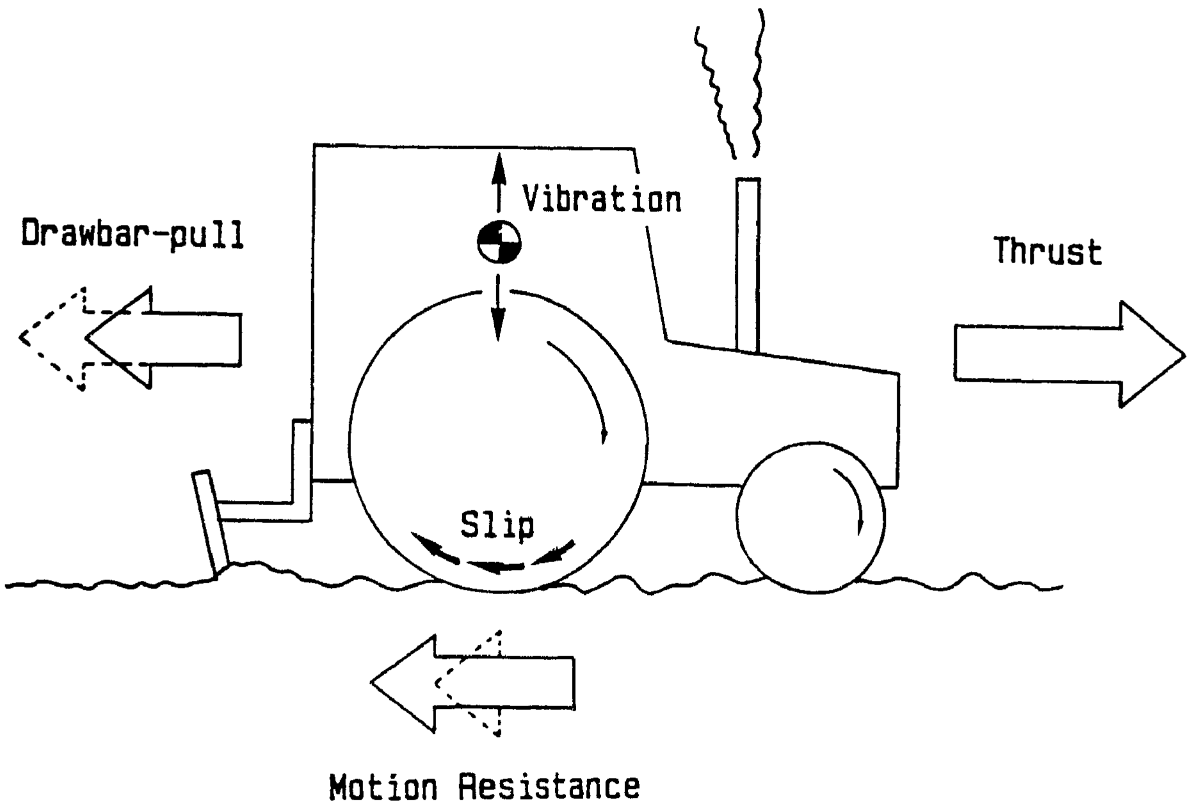

Fig. 1.1.2 Decrease in drawbar-pull due to increased motion resistance in rough road operation

Although all the preceding factors are very important considerations in the improvement of total off-road vehicle performance over rough ground, the effect of road roughness on tractive performance will be investigated in this study since traction is an essential required capability for off-road vehicles.

Compared to the traction studies on a deformable terrain, relatively little work has been done in regard to a rigorous and rational evaluation of tractive performance as conditioned by the roughness characteristics of the riding surface. Nevertheless, terrain roughness is a representative and inherent off-road characteristic which affects the dynamic behaviors of off-road vehicles.

Moreover, in accordance with the development of high speed off-road vehicles such as HIMAG (High Mobility Agility Test Vehicle) and HSTV-L (High Survivability Test Vehicle-Light Weight), the need for investigation of the effect of terrain roughness on tractive performance is urgent since the surface roughness effect will be intensified with an increased vehicle speed.

In addition, on a rough road, more fuel consumption will be expected compared to that on a smooth road due to change in the rolling resistance. In general, a 10% change in the rolling resistance coefficient results in a 2% change in vehicle fuel consumption, as reported by EPA (Environmental Protection Agency) researchers.

There is now evidence that improvement of the tractive performance of the vehicles on a rough terrain is one of the most important problems to be solved at the present time to achieve optimum work, energy economy and safety in operation of off-road vehicles.

1.2 Statement of the Problem

The investigation of tractive performance on a rough road is very complicated due to the random features of the terrain surface profile which cannot be described by a deterministic function. The resulting contact area, slip rate, normal reacting load to tyre or even moving speed vary randomly at every instant of time.

In solving this problem, the role of a pneumatic tyre is studied hereafter because it is considered as the direct contacting device with the ground, i.e. the tyre carries the vehicle load and transfers the forces which drive, brake and guide the vehicle to the supporting ground. It is expected that the performance of the entire wheeled vehicle can be evaluated, once the analyses are available for a representative tyre.

Fig. 1.2.1 shows the fundamental parameters which have to be considered in the analysis of off-road tyre tractive performance. They can be categorized into three factors, namely terrain, operational and tyre factors. In order to predict the tyre-rough terrain interaction, it is necessary to establish a proper analytical model which reflects the physics of interaction between tyre and rough ground, taking into account all of these parameters in the analysis.

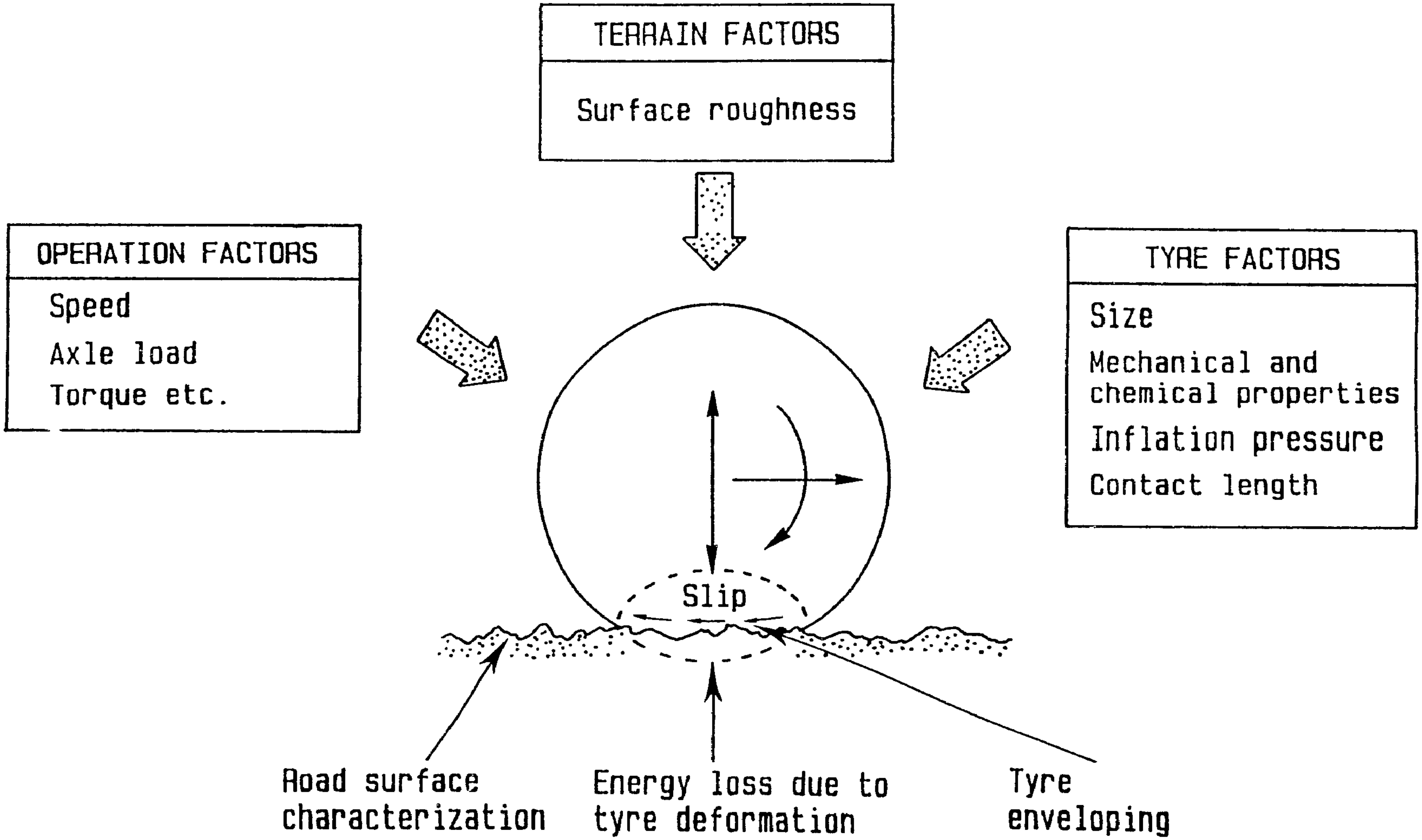

Fig. 1.2.1 Fundamental parameters to be considered in the analysis of tyre tractive performance on a rough road

To predict the tyre traction on a rough road, three complex phases of tyre motions (rotation, vertical and translational motions) simultaneously need to be accounted for. A wheel does not simply rotate, but is driven with a certain slip at the wheel-ground interface. Because of the multi-directional and interdependent dynamic behavior of the tyre-ground interaction system, the analytical procedure adopted in this study is described in terms of scalar quantities, i.e. energies, for the practical evaluation of off-road vehicle performance.

In order to investigate the effect of terrain surface roughness on the tractive performance of tyres, the following problems need to be examined:

(1) Description of terrain surface roughness:
What constitutes surface roughness? How is it to be measured? How do we characterize and quantify terrain roughness so that it can be used in analyses? How do we relate random surface irregularities to tractive force (drawbar-pull)?

(2) Enveloping effect to original ground surface due to flexible tyre:
Fig. 1.2.2 compares the point contact (a) and line contact (b) of the running gear, showing different observation of the terrain profile.

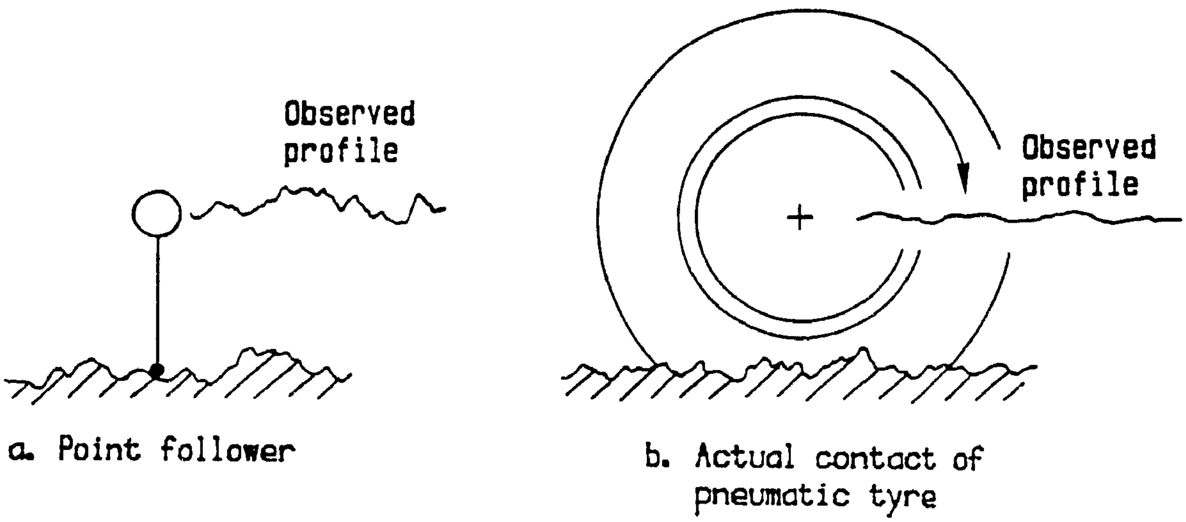

Fig. 1.2.2 Comparison of observed profiles by running gear between point contact and line contact

The profile which a running gear "sees (observes)" is modified depending on the type of contact, and it affects the way of loading to tyre. The trajectoty of the point follower is directly affected by the geometry of the original terrain surface profile. As for the trajectory of the center of a pneumatic tyre, a modified (smoothed) trajectory is expected, since a pneumatic tyre does not replicate exactly the terrain surface profile due to a line (or area) contact with the ground. This is caused by the special characteristics, namely tyre enveloping property on terrain surface geometry. This property has often been neglected in the analysis of ride comfort or tractive performance for simplification of the problem.

However, a modified surface profile has to be considered for the analysis of true reaction loading to a tyre since the loading condition has a significant effect on tyre performance. How do we define this enveloping function in relation to tyre's mechanical properties so that it can be employed in the theoretical analysis of the tractive performance?

(3) Additional energy dissipation by road roughness:

It is presumed that more energy will be spent on a rough ground surface than on a flat and smooth surface. What causes this extra energy dissipation? How can the governing mechanism of energy loss of a rolling tyre be explained, in conjunction with the terrain surface roughness? In other words, what are the principal characteristics of interaction between tyre and rough terrain surface? How do we evaluate the tractive efficiency of a tyre which produces a fluctuating drawbar-pull on a rough terrain? In addition, what is the effect of operational speed, slip rate and inflation pressure on the tractive efficiency?

1.3 Literature Review

Previous experience shows that rolling resistance (or motion resistance), which influences the traction of a vehicle, increases as road roughness increases. Systematic investigation of rolling resistance on rough roads began in the late 1970's with a view to reducing rolling resistance on rough roads (including paved highways).

(1) In the 1950's and 60's, a number of field running tests were performed to relate the skid number to highway/runway grooving and textures. Sugg (1969) stated that rolling resistance (RR) was increased with a low inflated tyre and rougher pavement. However, these experiments were too empirical to predict the effect of the road roughness, and the roughness of the road surface was not characterized in a rational way, but rather by means of harshness.

    DeRaad (1977) conducted indoor and outdoor tests using a dynamometer and a fifth wheel, respectively. He also investigated the effect of the micro-roughness of the paved road on RR. An increase in RR was observed with increasing texture of road.

(2) Wong created a pilot study in order to investigate the excitation effect on friction between a sand and shear plate (1970), and between a sand and rubber plate (1972). He found that there was a significant effect of excitation on the friction. Larger

excitation force and lower shear rate produces less shear force, i.e. traction. However, the effect of excitation frequency was not clearly observed in his experiments within the range of 5-30 Hz, which was presumed as a typical excitation range for off-road vehicle performance.

Cap and Wambold (1984) experimentally investigated the effect of excitation amplitude and frequency with regard to a coefficient of friction. A rolling tyre was shaken with a changing frequency range between 1 and 12 Hz on a concrete surface. A major loss in traction at higher amplitude or higher frequencies was observed, while Wong did not recognize the effect of excitation frequency. As much as 30% of the automobile's traction is lost at 11 Hz.

Orlandi and Matassa (1986, 1987) also performed a laboratory test whose experimental device is shown in Chapter 7. The excitation was applied to a rolling tyre on a sand with various moisture contents and on a rigid surface (Plexiglas). It was also ascertained that the rolling resistance (traction) was drastically changed by the excitation frequency and moisture content, especially at the natural frequency. The traction in the presence of vibrations was always reduced compared to that in the absence of vibrations. Unfortunately, the mechanism of the reduction of RR was not clearly given in these experimental studies.

(3) Dzielski and Hedrick (1984) calculated a train resistance. The resistance force at wheel-rail interface was assumed to be expressed in the form of a quadratic polynomial equation as a function of traveling speed.

(4) In order to theoretically study the effect of rough road surface on vehicle tractive performance, several analytical models were developed. Captain et al.(1979) compared four analytical tyre models for negotiating a rough road. The point contact model, rigid tread band tyre model, fixed foot print tyre model and adaptive foot print tyre model (see Fig.3.1.3) were introduced. Based on these models, horizontal and vertical tyre forces were computed in the time domain, and their usefulness was compared. It was suggested that the vehicle simulations using the simplest point contact model could be improved very conveniently by replacing the terrain profile input by an appropriate filtered profile. Although a nonlinear analysis can be available for the time domain analysis, a tedious computation process is required.

Korst and Funfsinn (1977) and Velinsky and White (1980) calculated the RR by using the deterministic functioned road surface (step, step-wave, up-down ramp and sine wave). At the same time, a coastdown experiment on a highway was performed and their results were compared with the predicted results. They stated that the RR increased up to 20% as compared to an ideal smooth road. The aerodynamic drag coefficient was also found to increase during operation on rough roads.

The nature and magnitude of the component of propulsive force associated with the energy loss of a one-degree-of-freedom vibrating system (simplified vehicle) was estimated by Karnopp (1978). In a certain speed range, the force was found to vary dramatically with speed for several types of periodic road way profiles (sinusoidal, triangular and modified triangular wave). Significant work was accomplished by Segel and Lu (1982) and Lu (1985), who investigated the average RR on rough roads through the transfer function between the road roughness and the tyre-suspension system. RR was obtained by the energy expenditure due to visco-elastic characteristics in the tyre and suspension. At the same time, the effect of vehicle speed on RR was investigated.

From previous studies performed, an increase in RR, together with the effect of excitation amplitude, frequency and traveling speed were demonstrated when road roughness was encountered in vehicle mobility. It was found that terrain roughness significantly affects the tractive performance of vehicles.

However, while these studies can provide certain information about the effect of road roughness, some of them have been achieved in an irrational way using a simplified experimental device which does not properly represent an actual rolling tyre, or deterministic/ periodical simplified road profiles which generally do not exist in real road or field conditions. Even if the random terrain profiles were considered, the description of roughness was briefly attempted by their height Root-Mean-Square values. They have also investigated the change in RR only in relation to road surface roughness. The effect of the tyre's inflation pressure was ignored in spite of its key role on vehicle traction. Although RR is an important part of the investigation of tractive performance of vehicle running gear, future research should now be towards the predictive and analytical investigation of vehicle traction, which is the most inherent and direct performance parameter of an off-road vehicle, in conjunction with a randomly profiled non-deformable rough terrain. It has not yet been achieved due to the aforementioned complex traction mechanism.

1.4 Objective

In view of the previous discussion of tyre-rough terrain interaction and related problems, requirements for a successful predictive/analytical procedure call for the following:

(1) Development of a rational, simple predictive scheme which considers the effects of tyre characteristics on tyre-rough, non-deformable terrain mobility performance.

(2) Development of an appropriate measuring device or technique which can be easily operated to provide information on the following:

  a. road surface profile

  b. tyre enveloping property

  c. tyre tractive parameters e.g. drawbar-pull, torque and angular velocity etc.

(3) Establishment of a system function which describes tyre-rough, non-deformable terrain interaction and portrays the relationships between off-road surface irregularities and tractive efficiency in terms of drawbar-pull with various tyre parameters.

1.5 Study Protocol

Fig. 1.5 briefly illustrates the general research program for this study. The following approaches are considered:

Theoretical Considerations

(1) Characterization and Evaluation of terrain surface roughness so that the random shaped terrain profile can be used in the theoretical analysis.

(2) Definition of the tyre enveloping function that smoothes the original terrain surface profile.

(3) Establishment of an analytical relationship between tractive force and ground surface rou ness, which can also predict the effect of slip, inflation pressure and speed, associated with the energy conservation law.

Experimental Considerations

(1) Design of simple equipment for measurement of surface roughness, and establishment of a measurement method.

(2) Measurement of the filtered profile of the terrain surface and establishment of the mathematical form of the enveloping function.

(3) Performance of running tests on various random rough surfaces in the laboratory with different tyre inflation pressures and slip rates to investigate the synthetic effect on tractive efficiency.

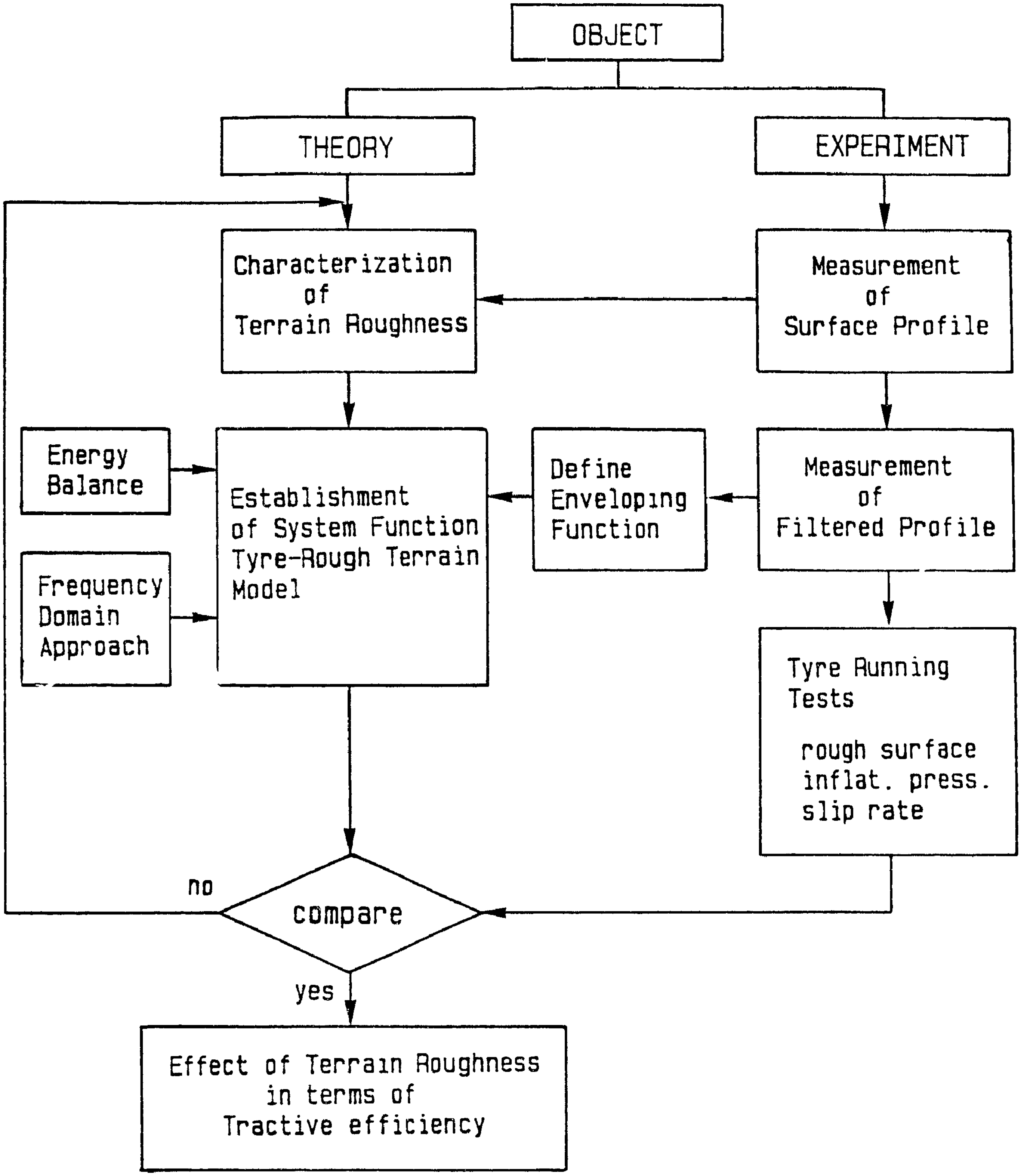

Fig. 1.5 Research program

1.6 Organization of the Thesis

The presentation of this study is arranged in eight chapters (Fig. 1.6) and seven appendices. The seven chapters, excluding Chapter 1, are classified into three major parts, each of which can be described briefly as follows:

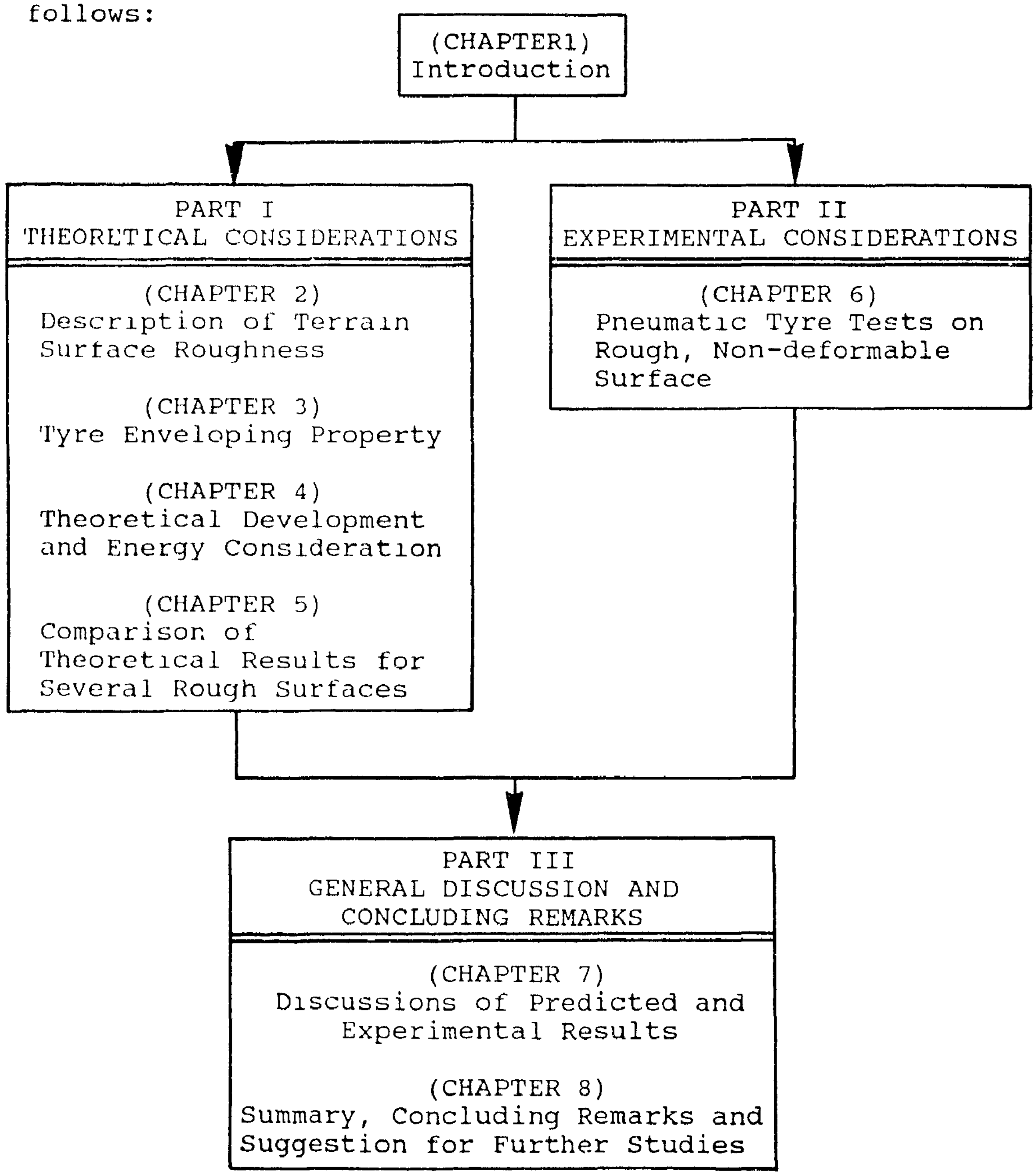

Fig. 1.6 Organization of the main body of the thesis

CHAPTER 1 --- states the nature of problem and the necessity of an analytical model in place of the existing approaches for evaluating the performance of off-road vehicles equipped with pneumatic tyres

PART I THEORETICAL CONSIDERATIONS

(Background considerations)

CHAPTER 2 --- describes the characterization and evaluation of terrain surface roughness together with the roughness classification by ISO recommendation

CHAPTER 3 --- introduces representative tyre enveloping functions

(Present work)

CHAPTER 4 --- describes the predictive procedure, the idealization of the tyre-rough terrain system and the application of the frequency domain approach to obtain the system function representing the relationship between the drawbar-pull and the terrain surface geometry

CHAPTER 5 --- compares the simulated results with flat and smooth surface, sinusoidal surface and randomly rough surfaces as a function of slip

PART II EXPERIMENTAL CONSIDERATIONS

CHAPTER 6 --- presents the experimental results including the measurement techniques engaged

PART III GENERAL DISCUSSION AND CONCLUDING REMARKS

CHAPTER 7 --- compares and discusses the predictive and experimental results

CHAPTER 8 --- presents the summary and conclusion, and recommends certain problems which are worth investigating for further study

APPENDICES

APPENDIX A --- shows the derivation and discrete form of PSD function for the numerical process of measured data

APPENDIX B --- reviews and discusses the previous workers' results on the road surface measurement

APPENDIX C --- shows several nonlinear characteristics of flexible tyre in terms of excitation frequency, amplitude, traveling speed and load dependency regarding to the stiffness and damping of tyre

APPENDIX D --- explains the mechanism of energy dissipation of flexible tyre moving on a rigid rough terrain

APPENDIX E --- explains the human tolerance criteria to the vibration (ISO 2631 and Absorbed Power criteria) for future study of the tractive efficiency in connection with ride comfort

APPENDIX F --- presents the test results in tabular forms for further reference

APPENDIX G --- presents the computer programs transferring the analogue signal to digital computer, calculating PSD functions with those digitized data and computing the nominal tractive efficiency

PART I THEORETICAL CONSIDERATIONS

In Part I, the following four components are presented.

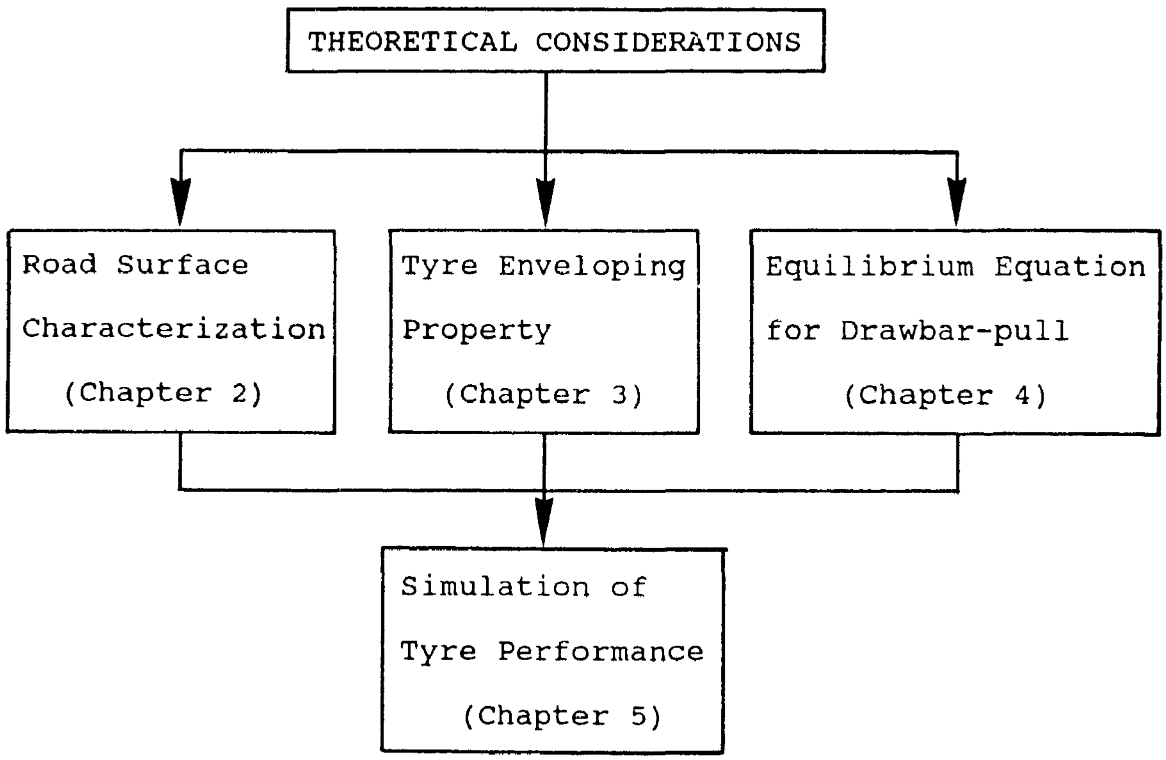

CHAPTER 2

DESCRIPTION OF TERRAIN SURFACE ROUGHNESS

2.1 Introduction

Fig. 2.1 shows that a vehicle driver recognizes terrain surface roughness as a synthesized result of vehicle speed, vehicle dimensions, their mechanical properties, terrain surface geometry, surface and/or soil deformability and finally, human sensitivity. In other words, the degree of terrain surface roughness which is expected to affect the vehicle's performance is determined by these complex factors. As an example, the roughness of the terrain surface works as a severe disturbance for a short wheelbased vehicle with stiff shock absorbers under high speed operations, even if there are very small irregularities on its road surface. On the other hand, the vehicle would not feel an excitation from the ground if the terrain is extremely soft, as on a muddy or snowy road. It is, therefore, required to consider all of these factors in full for the pure description of "wide-sensed" terrain roughness.

It is not necessary, however, to quantify all of these effects for the description of the terrain surface roughness. To simplify the analysis, consideration should be given to the surface roughness effect in terms of a non-deformable surface. This, in effect, reduces the complex problem to the set of issues which pertain to surface geometry, while the randomness of the surface geometry is held. With an assumption that the terrain is non-deformable, the most influential parameter for off-road vehicle dynamics on a rough terrain can be considered to be the terrain surface geometry. Although factors other than surface geometry indicate the response of the vehicle-terrain system to disturbance from the ground, the surface geometry only needs to be used for a universal description of terrain roughness.

In this study, "terrain (off-road) surface roughness" is restricted to a "narrow-sensed" model which can be described in terms of surface geometry only. It is defined as the deviation of a surface from a true planar surface with characteristic dimensions that affect vehicle dynamics, ride quality, dynamic load and drainage. The interesting range of road wavelength to the off-road vehicle mobility falls between 0.1m and 10 m approximately, since an off-road vehicle "sees" these wavelengths most often (Ohmiya, 1986).

Based on this definition, the characterization of terrain surface roughness should be clearly outlined in order to prescribe the exciting (loading) input function to the system. An evaluation of roughness must also be performed based on the regulated classification method, so that ground roughness can be properly characterized.

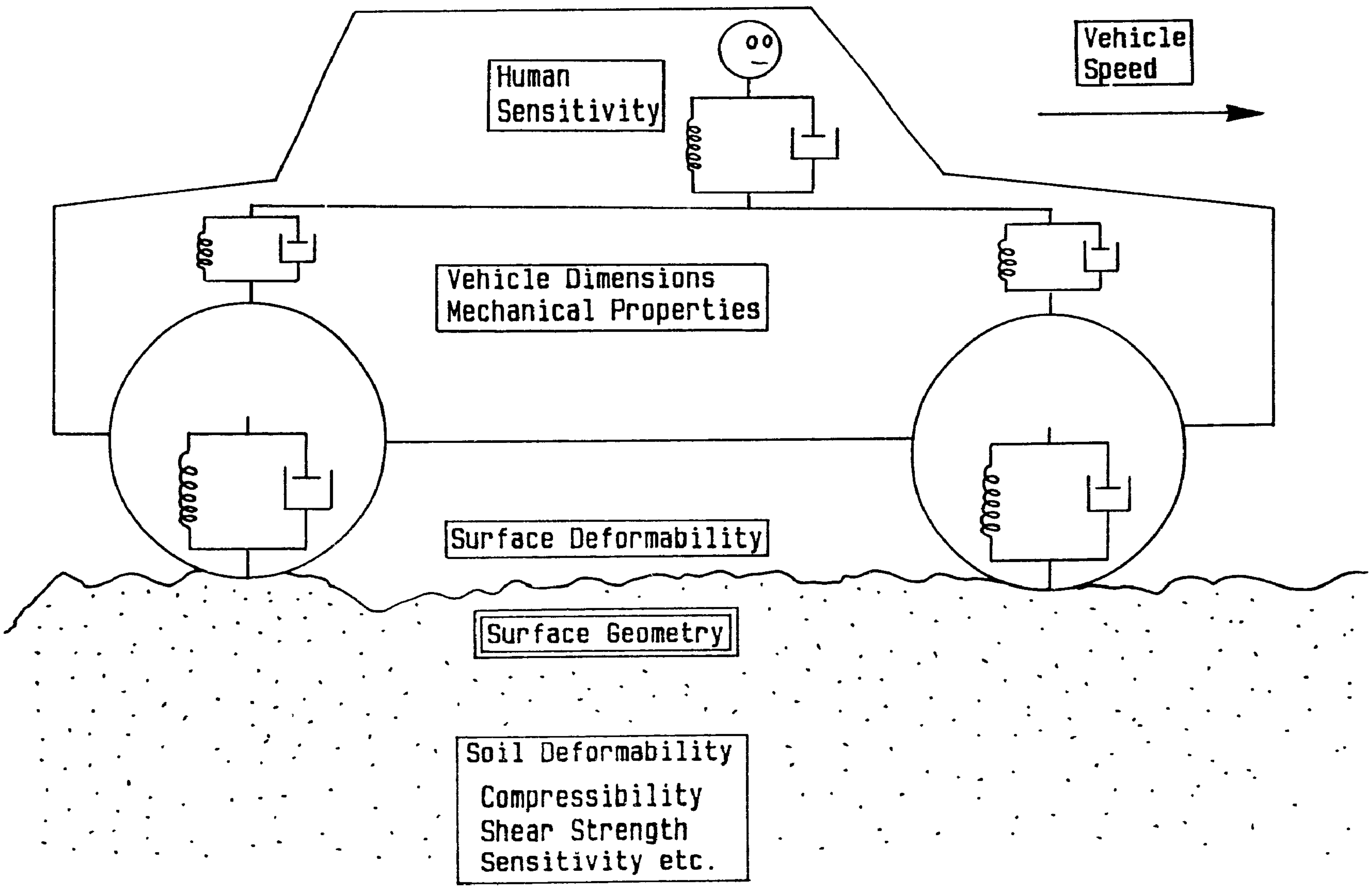

Fig. 2.1 Factors related to off-road surface roughness

2.2 Characterization of Surface Roughness

It can be said that the largest difference in effect between a smooth road surface and a rough, non-deformable road surface is the method in which reaction loading is applied to a rotating tyre. Fig. 2.2.1 schematically illustrates constant loading of a tyre moving on a flat and smooth terrain surface, in contrast to the dynamic loading resulting from vertical movement of the tyre on a rough terrain. The time-varying wheel load resulting from wheel travel over the arbitrary irregularities of rough terrain surface affects tyre slip, tyre deformation and finally tractive performance.

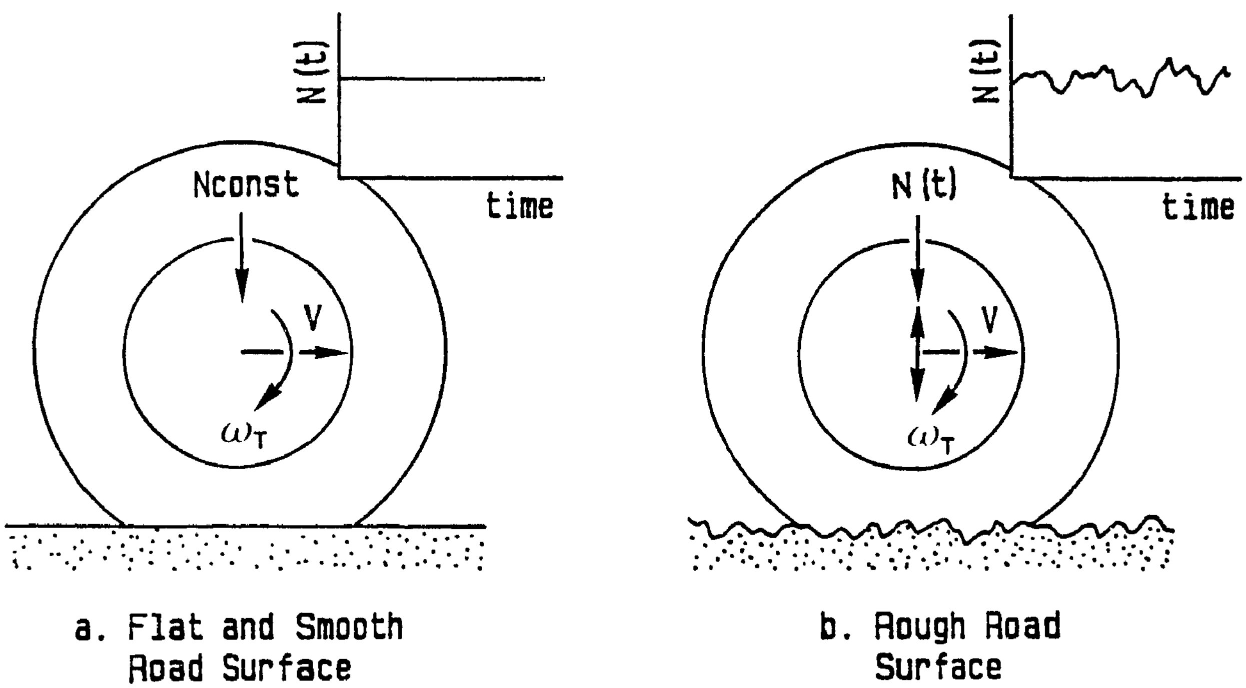

Fig. 2.2.1 Comparison of reaction loading to tyre

Accordingly, surface characterization is of prime interest to vehicle and tyre designers, since the terrain surface profile is the critical function in defining the loading function for a tyre traveling on a rough terrain. It is noted that the enveloping function should be considered together with the terrain surface characterization in order to prescribe the practical reaction loading to a tyre (Fig. 2.2.2).

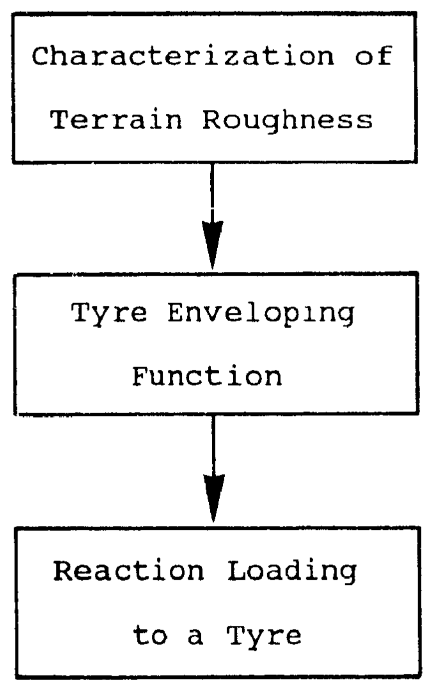

Fig. 2.2.2 Procedure to define reaction load from terrain surface roughness

In the early studies of vehicle performance on a rough road, simple functions such as sine waves, step functions or triangular waves were generally applied as disturbances from the ground. While these inputs provide a basic idea for comparative evaluation of designs, it is recognized that the terrain (road) surface is usually not represented by these simplified functions, and therefore the deterministic irregular shapes cannot serve as a valid basis for studying the actual behavior of the vehicle. In this study, a real road surface, taken as a random exciting function, is used as an input to a tyre-terrain system. A special mathematical expression of random surface profile is developed to characterize terrain roughness, and is used to generate the analyses for determination of terrain roughness effect on mobility efficiency.

Since the main factors in a loading function are its frequency and amplitude, the geometrical characteristics of a non-deformable terrain surface need to be described by these two quantities. The excitation frequencies are directly related to vehicle translational speed and the wavelengths contained in various waveforms of the rough surface profile. This highlights the problem in the expression of roughness i.e. randomness of surface profile.

It is noted that the main characteristic of a random function is uncertainty. That is, there is no way to predict an exact value at a future time. The function must be described in terms of probability statements and statistical averages, rather than by explicit equations. Four main types of statistical functions can be used to describe the basic properties of random data: (1) Root-Mean-Square values, (2) probability density functions, (3) autocorrelation functions and (4) power spectral density functions.

(1) The Root-Mean-Square (RMS) value

This value furnishes a rudimentary description of the intensity of the data. If the mean value is zero, the RMS value represents a dispersion of data. As one of the description of road surface roughness, RMS vertical acceleration (RMSVA) has been used by Hudson et al. (1985). It is obtained by calculating the second derivative with respect to time for the height of an object in contact with a profile moving at a constant horizontal speed. A large value, in general, means a poor condition of the road surface. The approach is attractive for its simplicity, in that a road has a unique roughness value, but it does not recognize that the roughness effects on vehicle mobility are dependent on the speed, nor does it include any frequency information which is required for vibration analysis.

(2) The probability density function

This function furnishes information concerning the properties of the data in the amplitude domain. Therefore, it is possible to determine the output values in that domain with their probability. However, knowledge of the n-th order joint probability is required for the determination of the statistical properties of a stochastic process, which is a difficult procedure. Furthermore, the probability density function may not be suitable for dynamic analysis because of the difficulty of expressing values in the time domain.

The above statistical functions are useful as indices so that one can simply define the terrain surface roughness. However, once again, it is necessary to include information of not only the degree of roughness, but also dynamic properties, such as energy distribution, mean value and/or frequency components in that signal. If one can find a suitable way to satisfy the above requirements, the amplitude data of the surface profile can be used as inputs for dynamic theoretical studies. There are two other statistical functions which may satisfy the requirements:

(3) Autocorrelation function

The autocorrelation function, $R(\tau)$, for a stationary record is a measure of time-related properties in the data, which are separated by fixed time delays, τ. An estimation may be made by delaying the record relative to itself by some fixed time delay, then multiplying the original record with the delayed record, and averaging the resulting product values over the available record length or over some desired portion of this record length (Fig. 2.2.3). The procedure is repeated for all time delays of interest.

$$R_{(\tau)} = \lim_{T \to \infty} \frac{1}{T} \int_{-\frac{T}{2}}^{\frac{T}{2}} y(t) \cdot y(t+\tau) \quad dt \qquad (2.1)$$

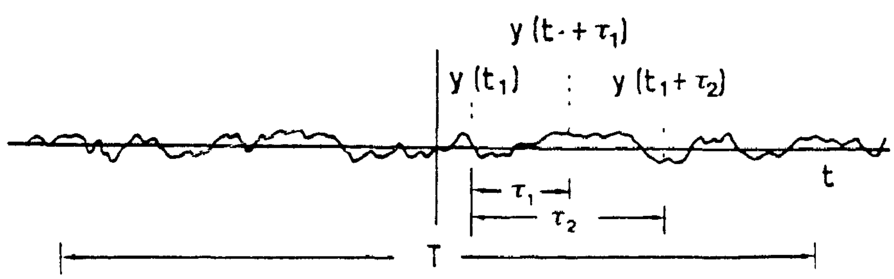

Fig. 2.2.3 Estimation of autocorrelation function

(4) Power spectral density function

The power spectral density (PSD) function for a stationary record represents the rate of change of mean values with frequency. It is estimated by computing the mean square value in a narrow frequency band at various center frequencies, and then dividing by the frequency band. The total area under the PSD curve over all frequencies will be the total mean square value of the record. The partial area under the PSD curve from frequency f_1 to f_2 represents the mean energy value of the record associated with that frequency range.

The autocorrelation function and the PSD function are Fourier transforms of each other (Wiener-Khinchine relation), and therefore furnish similar information in the time domain and frequency domain, respectively. Most importantly, the PSD function may satisfy the requirements for off-road vehicle studies since both amplitudes and frequencies, which are essential factors for vehicle vibration dynamics, are described in terms of energy density. Furthermore, the use of the following simple relationship between inputs and their responses using their PSDs is the most advantageous for this complex problem. The result can be also expressed by RMS values.

$$\boxed{\begin{array}{c}\text{PSD}\\ \text{of}\\ \text{response}\end{array}} = \boxed{\left|\begin{array}{c}\text{Transfer function}\\ \text{of}\\ \text{system}\end{array}\right|^{2}} \times \boxed{\begin{array}{c}\text{PSD}\\ \text{of}\\ \text{input}\end{array}}$$

Fig. 2.2.4 Relationship between input and output of a linear system with PSD

Thus it may be suitable to express the off-road surface profile (representation of surface roughness) by a spectral description such as the PSD function. The PSD function will contribute to a response analysis which will describe, with adequate precision, the motion of the system expressed in terms of displacement, acceleration or stress. This function has been used previously for vehicle mobility analysis by many authors (Matthews,1966; Laib,1975; Sireteanu,1984; Lu,1985).

Since the terrain surface roughness under consideration is a spatial disturbance, rather than a disturbance in time, it is desirable to define the PSD in terms of the spatial frequency, Ω, in cycles per meter, rather than in terms of the conventional time frequency, f, in cycles per second (Walls et al.,1954; Crolla,1981). Spatial frequency is another description of frequency in the space domain. Then off-road surface roughness can be expressed in a concrete manner, disregarding the effect of various operating speeds of the vehicle. In terms of this spatial frequency argument, the PSD of the off-road surface profile is defined in the following manner (Wendenborn, 1966; Bekker,1960):

$$S_{(\Omega)} = \lim_{X \to \infty} \frac{2}{X} \left| \int_0^X y(x) e^{-i2\pi\Omega x} \quad dx \right|^2 \tag{2.2}$$

where $S_{(\Omega)}$: one-sided PSD of the road surface profile (m^3/c)

Ω : spatial frequency (c/m)

X : length of course (m)

x : horizontal distance over surface (m)

$y_{(x)}$: surface height profile from a reference plane (m)

In Appendix A, detailed derivations and discrete forms of PSD are given. This estimated PSD allows a reasonably accurate measurement of the frequency content of a particular surface, and thus is useful for surface roughness classification. Whilst the spatial frequency, Ω, is to be used as a disturbance frequency for a rough road profile, it can be converted to a conventional time-dependent exciting frequency, f, for a given velocity, V, by the following relationship. That is,

$$f = V\Omega \tag{2.3}$$

Therefore each PSD of the ground surface profile can be represented by a respective curve for a given velocity.

$$S_{(f)} = \frac{1}{V} S_{(\Omega)} \tag{2.4}$$

Accordingly, the expression of terrain surface roughness in terms of PSD having the above-mentioned features is acceptable and effective for the analysis of vehicle traction, if the PSD of an actual rough terrain surface profile can be described by a relatively simple mathematical form.

2.3 Classification and Evaluation of Road Surface Roughness by PSD

Several attempts have been made to classify the roughness of a road surface. In the field of construction, the PSR (Present Serviceability Rating) is often used in the AASHO (American Association of State Highway Officials) road test for this purpose, as well as by RMSVA. The PSR are correlated with various objective measurements of pavement features through a regression equation, so that the objective measurements could be used to estimate the PSR. The numerical range of the PSR, and the corresponding general pavement condition, are shown in Table 2.1.

Table 2.1 PSR for paved road

PSR	0-1	1-2	2-3	3-4	4-5
condition	very poor	poor	fair	good	very good

There is yet another method of classification of roughness. Ground surfaces are classified into the following categories by the dominant wavelengths included in the surface profile. This classification is given in Table 2.2.

Table 2.2 Classification of road roughness by road wavelength (after Pottinger and Yager, 1986)

Type of roughness	Range of wavelength
Road microtexture	wavelength(λ) < about 0.5mm
Road macrotexture	about 0.5mm < λ < 10cm
Terrain roughness	about 10cm < λ < 100m
Topographical undulations	λ > about 50m

Although these indices can provide an evaluation for the purpose of road roughness classification, more useful parameters should be included for the analysis of vehicle dynamics, as was previously mentioned. For example, the classification by wavelength may be an unreliable method since a real road surface possesses an infinite number of wavelengths and amplitudes, and therefore is not recommended for classifying the surface roughness based only on the dominant range of wavelength.

The properties of the surface profile can basically be described only in statistical terms, which are themselves expressed in terms of the PSD when the road surface profile is regarded as a random function. Thus, the PSD produces a roughness measure that can be classified in a direct manner so that not only random surface waves, but also their harmonic content and power level, can be accounted for.

Using the PSD, Wendenborn (1965) suggested dividing terrain surface roughness into two categories, as shown in Fig. 2.3.1.

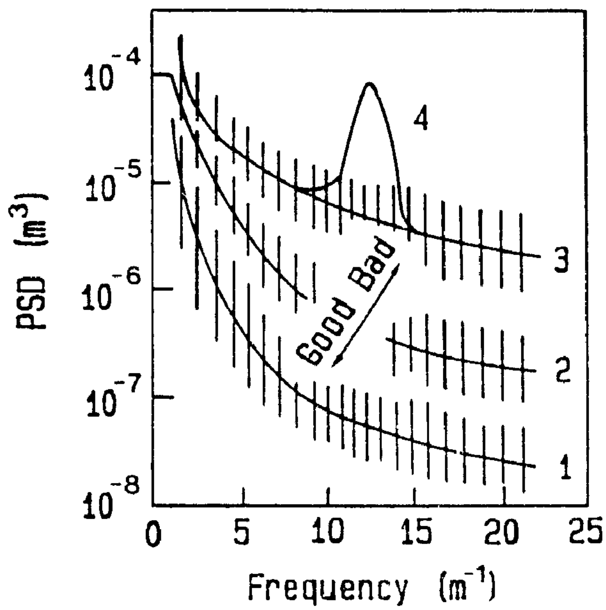

Fig. 2.3.1 Classification of PSD curves for (1) average first class road; (2) average secondary road; (3) average agricultural field; (4) average agricultural field with periodicity (after Wendenborn)

Curve 1 shows the smoothest surface, which represents a paved road. Curve 3 describes the roughest (bad) surface, which is an agricultural field. The borderline between "good" and "bad" is a paved country road (curve 2). Curve 4 shows the periodic component at a wavelength of about 1/12 m. The hatched areas indicate the scatter of PSD of each surface. Though this classification gives a better index representing surface roughness, it is still too coarse for a theoretical analysis. Therefore, a more precise and standardized classification is needed.

The International Organization for Standardization (ISO) has proposed road roughness classification (class A to H) using the PSD values. Fig. 2.3.2 shows the classification by ISO (1982) and corresponding range of PSD values at a particular frequency of $1/2\pi$ c/m. It is indicated that the smoother surface possesses less power over a whole frequency range than the rougher surfaces. In this draft proposal, these amplitude PSD functions of the terrain surfaces can be approximated by means of two straight lines with different slopes, since the PSD curves of many terrain surfaces show concavity. The approximate forms of smoothed PSD (one-sided) are given as follows:

$$S_{(\Omega)} = S_{(\Omega_o)} \left(\frac{\Omega}{\Omega_o}\right)^{-n_1} \quad \text{for } \Omega \leq \Omega_o = \frac{1}{2\pi}\, c/m$$

$$S_{(\Omega)} = S_{(\Omega_o)} \left(\frac{\Omega}{\Omega_o}\right)^{-n_2} \quad \text{for } \Omega > \Omega_o \tag{2.5}$$

where n1 and n2 are 2.0 and 1.5 respectively in the ISO draft. These two values are determined from field measurements. A more simplified mathematical form is suggested as follows (Crolla, 1981):

$$S_{(\Omega)} = G_o \Omega^{-n} \tag{2.6}$$

The advantage of this description is that it presents a very easy simple form. The realization of surface profile by any other method requires much effort, and leads to inaccuracies which cause unavoidable discrepancies in the results due to the approximate method to be applied.

2.4 Summary

In order to characterize the ground surface roughness, description by the PSD is used due to:

(1) simplicity of mathematical form

(2) possession of information on the energy distribution for each included frequency

and

(3) availability of a linear input-output relationship in the frequency domain.

The classification and evaluation of road roughness can be achieved based on the ISO recommendations, using the PSD values at each frequency.

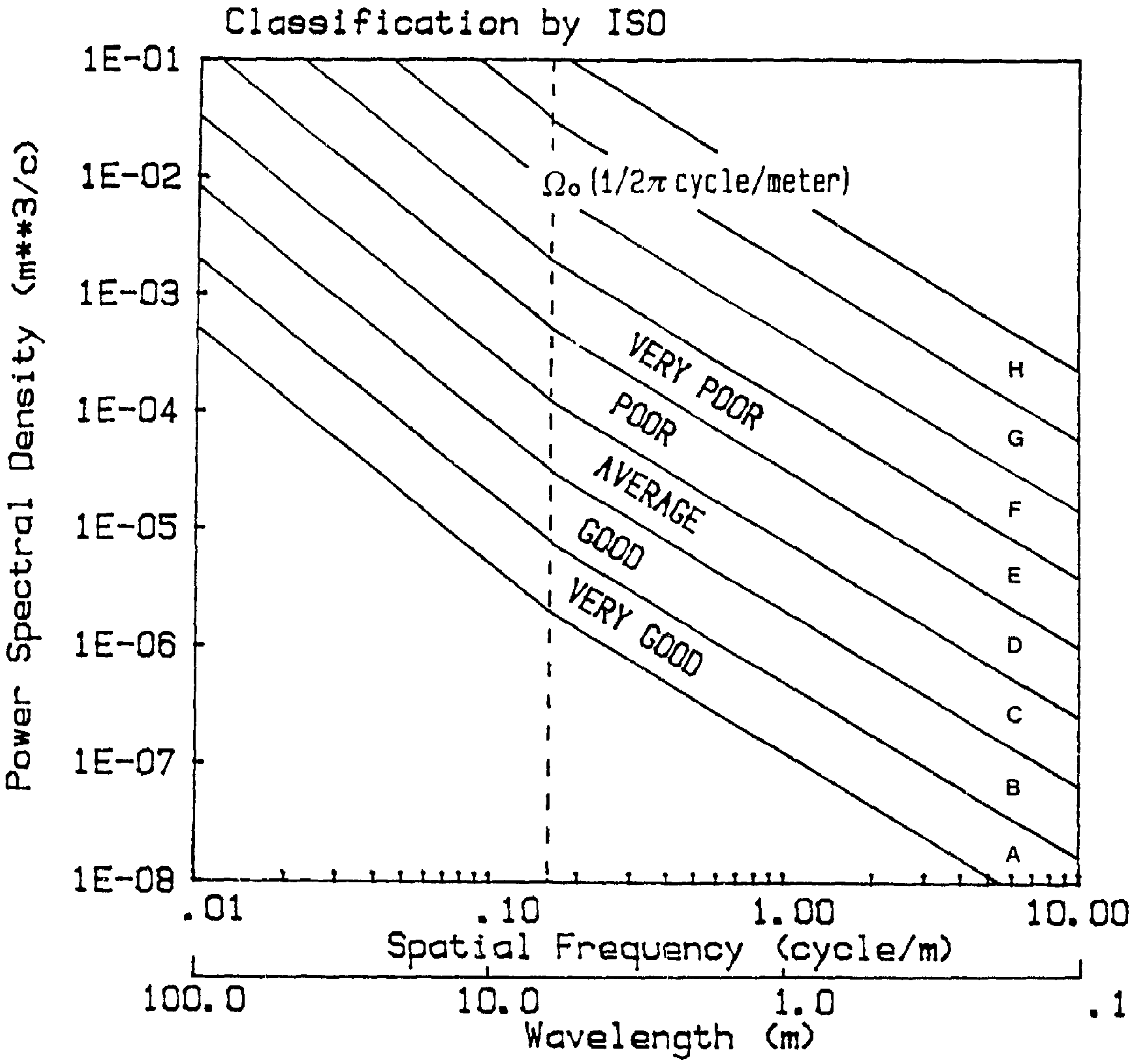

Road Class	Degree of Roughness	S(Ωo) *E-6
	Range	Geometric mean
A (Very Good)	< 8	4
B (Good)	8-32	16
C (Average)	32-128	64
D (Poor)	128-512	256
E (Very Poor)	512-2048	1024
F	2048-8192	4096
G	8192-32768	16384
H	32768 <	

Fig. 2.3.2 Road roughness classification by ISO

CHAPTER 3

TYRE ENVELOPING EFFECT

3.1 Introduction

The PSD of the road surface height profile contributes to a definition of the reaction load of the tyre arising from the rough ground. It was noted that the pneumatic tyre has a special function called the "enveloping effect". Fig. 3.1.1 describes the linear low-pass enveloping effect of a pneumatic tyre moving on a rigid, rough terrain. As previously stated in Chapter 1, the tyre's contacting condition with the ground is not a point contact, but rather a line or area contact (Fig. 1.2.2). The enveloping effect is, thus, characterized as the ability of the tyre to engulf short wavelength irregularities of the road surface. Therefore, the tyre does not replicate the original road surface profile. The tyre moves as if over a "filtered" road profile of the original road profile. This results in a modification of the reaction load to the tyre.

The enveloping function, which defines the relationship between the filtered road profile,y2, and the original road profile,y1, can be basically determined by the ratio of y2 (response) to y1 (input) in the frequency domain. In order to determine a modified reaction load, the enveloping function needs to be derived.

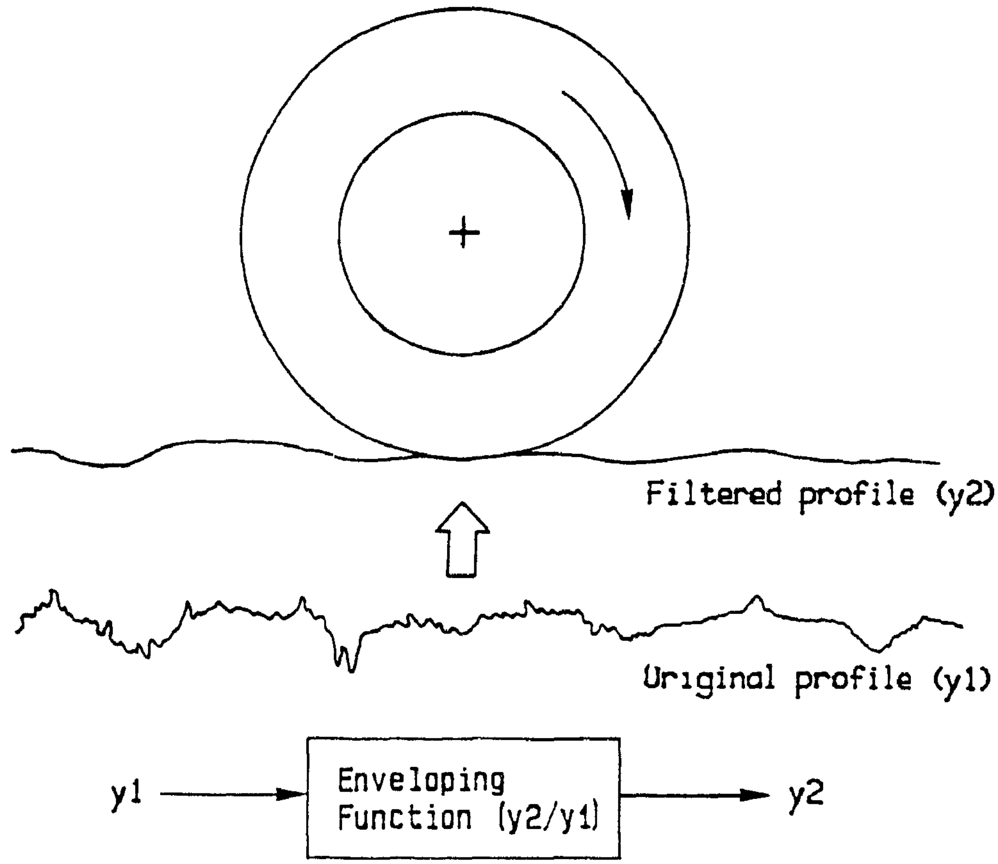

Fig. 3.1.1 Linear low-pass enveloping effect of pneumatic tyre on a rigid rough terrain

Van Deusen (1966) demonstrated very simple models of the tyre enveloping effect for the specific obstacles shown in Fig. 3.1.2. Model (a) is a rigid circular wheel of radius, R, which encounters a bump of height, H. In this representation, the path of the wheel center is an arc of a circle of the same radius, R. The other model (b) is an idealized enveloping wheel where the height of the tyre hub is directly proportional to the percentage of the contact length that has encountered the bump. The exponential function was also introduced as the third model.

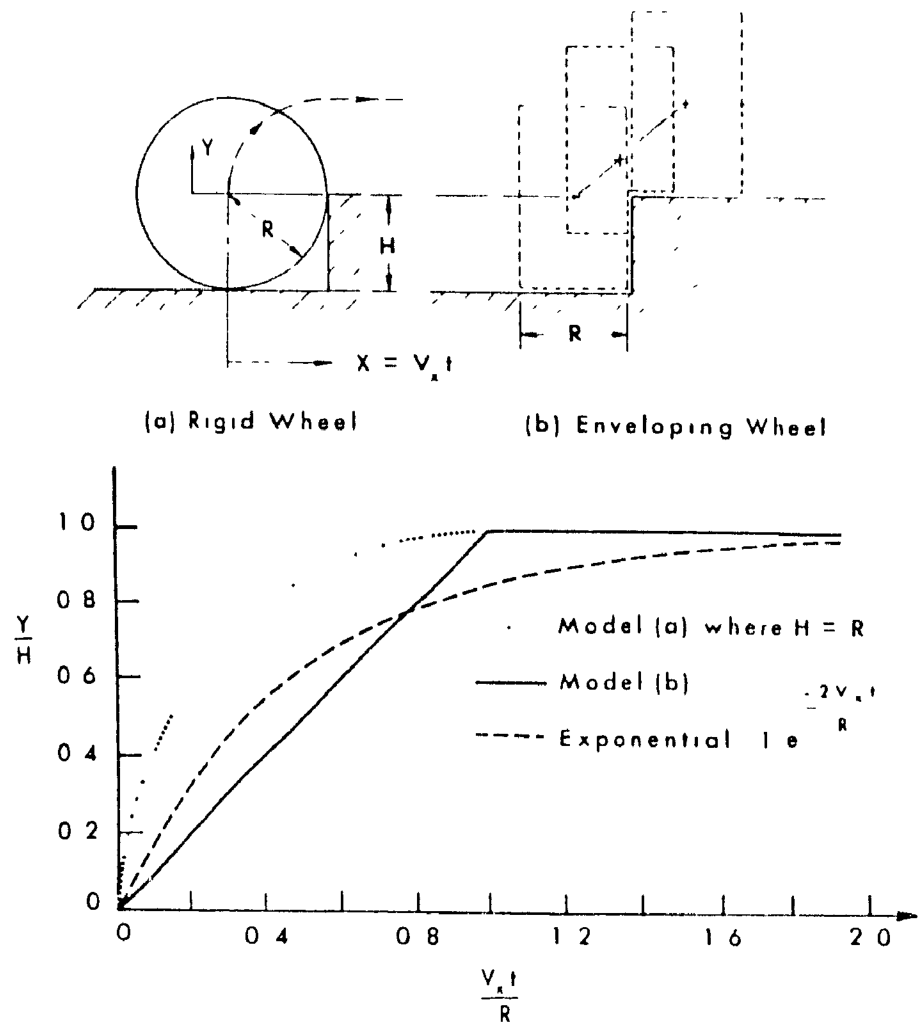

Fig. 3.1.2 Trajectories of tyre center and their enveloping models (after Van Deusen)

Although these models give basic information about the tyre enveloping effect, it is not realistic to apply these to a randomly rough road.

Captain et al. (1979) showed four kinds of representative analytical tyre-rough terrain models, including their enveloping effects (Fig. 3.1.3). The analysis of wheel center motion becomes very complicated

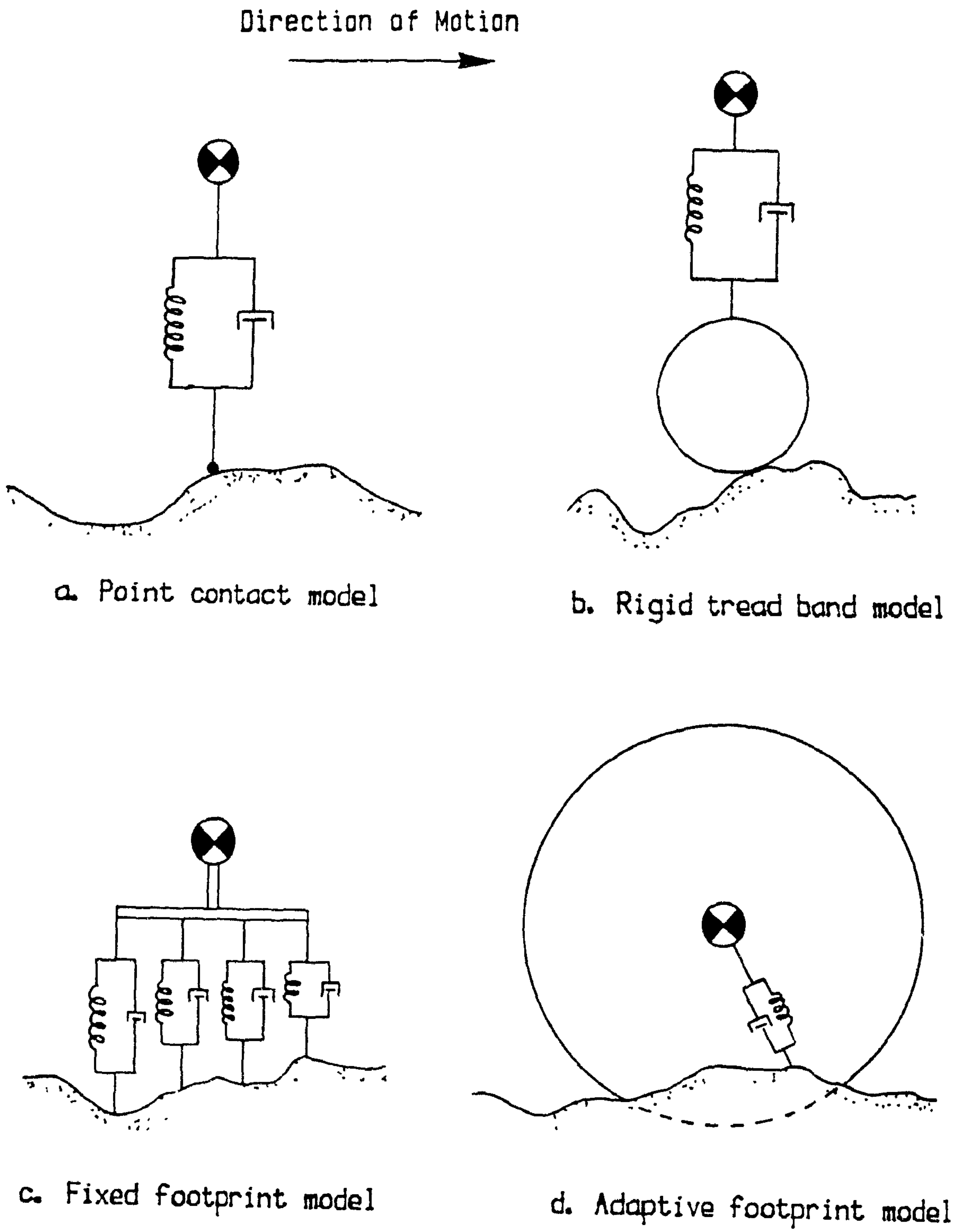

Fig. 3.1.3 Several tyre-terrain models showing enveloping effect (after Captain et al.)

because of the complex contact between the ground and the tyre having distinct properties. In the time domain, a sophisticated calculation procedure is required to estimate the filtered random surface profile and the reaction load.

However, a concise technique to derive the enveloping function can be found by using the frequency domain analysis (Gray and Johnson, 1972). It was suggested that a running tyre on a rough terrain behaves as a low-pass filter which attenuates high spatial frequencies (short road wavelengths). In the frequency domain, the difficulty in modeling the enveloping function could be largely eliminated by considering the low-pass filtering effect, assuming line contact between the tyre and the terrain surface. The enveloping function of a tyre can be derived in terms of a simple attenuating function in this domain. Another advantage of defining the enveloping function in the frequency domain is the possibility of association with the PSD function.

In order to derive a tyre enveloping function, experimental results are required, together with the tyre characteristics. In this chapter, the relationship between the original and filtered surface profile (i.e. enveloping function) is presented, giving the following two basic models.

3.2 Useful Models of Tyre Enveloping Effect

Berés (1986, 1987) introduced several tyre enveloping models as weighting functions. These functions are classified into two types of the enveloping characteristics, depending on the smoothing manner of the terrain profile at tyre-ground interface. They are (1) rectangular type and (2) exponential type (N.B. different from the exponential function stated by Van Deusen) weighting (enveloping) functions as shown in Fig. 3.2. The profiles at the tyre-ground interface are exaggerated in the Figure. The filtering characteristics (functions) are generally expressed as follows:

$h_{E(x)}$ --- weighting function in the road length domain

$H_{E(\Omega)}, H_{E(f)}$ --- frequency response function in the spatial and ordinary frequency domain, respectively

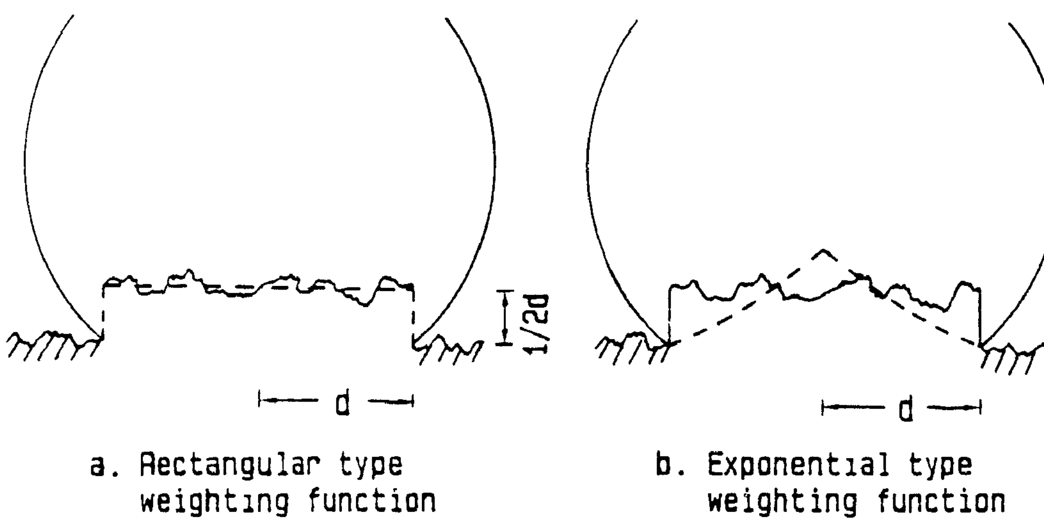

Fig. 3.2 Rectangular type and exponential type weighting (enveloping) functions

(1) Rectangular type weighting function (Fig.3.2a)

This type of function has been used by many authors (Kozin et al., 1966; Segel and Lu, 1982) due to its simplicity and accuracy. It will be assumed that the contact length, 2d, is constant while the running tyre is continuously deformed at the interface between the tyre and the terrain surface due to vibrational motion caused by the terrain surface roughness. The local deformation of the surface asperities is neglected since the ground is rigid.

The various vertical heights of the terrain surface profile at the interface are smoothed by multiplying by this weighting function. In the frequency domain, this is equivalent to stating that each harmonic component included in the signal of the terrain surface profile is attenuated by a certain amount, depending on the tyre flexibility, tyre load and road wavelength.

The rectangular weighting function, $h_{ER(x)}$, is given by the following simple form.

$$h_{ER(x)} = \frac{1}{2d} \qquad \text{for} \quad |x| \leq d$$

$$= 0 \qquad \text{for} \quad |x| > d \tag{3.1}$$

The frequency response function is derived by performing the Fourier transform on the above function.

$$H_{ER(\Omega)} = \frac{\sin 2\pi\Omega d}{2\pi\Omega d}$$

or

$$H_{ER(f)} = \frac{\sin \frac{2\pi f d}{V}}{\frac{2\pi f d}{V}} \qquad (3.2)$$

where x = distance from center of contact line

Ω = spatial frequency (= f/V)

f = temporal time frequency

V = vehicle speed

d = half contact length

(2) Exponential type weighting function (Fig.3.2b)

The theory of this enveloping function is similar to that of the rectangular type function. As shown in Fig. 3.2b, the smoothing of the terrain surface irregularities at the tyre-road interface can be determined by multiplying by the exponential function instead of by the rectangular function. The concept originates from an electrical R-C low-pass filter which decays the outputs at a certain rate by increasing the frequency. The weighting function for the exponential type is expressed as follows:

$$h_{EE(x)} = \pi a e^{-2\pi a|x|} \qquad |x| < \infty \qquad (3.3)$$

where a is the experimental constant. Performing the Fourier transform, the frequency response function is obtained.

$$H_{EE(\Omega)} = \frac{1}{1 + \left(\frac{\Omega}{a}\right)^2}$$

or

$$H_{EE(f)} = \frac{1}{1 + \left(\frac{f}{aV}\right)^2} \tag{3.4}$$

Although other frequency response functions were introduced by Bereś, such as

$$H_{EE1(\Omega)} = \frac{1}{\left[1 + \left(\frac{\Omega}{a}\right)^2\right]^2}$$

$$H_{EE2(\Omega)} = \frac{1}{\left[1 + \left(\frac{\Omega}{a}\right)^2\right]^3}$$

or

$$H_{EE3(\Omega)} = \frac{1}{1 + \left(\frac{\Omega}{a}\right)^4} \tag{3.5}$$

these functions should be determined experimentally by rolling the tyre on the rough terrain surface. However, the general characteristics of these weighting functions are basically similar to each other. The general form of the exponential type weighting function yields

$$H_{EE(\Omega)} = \frac{1}{1 + \left(\frac{\Omega}{a}\right)^b} \tag{3.6}$$

where a and b are the experimental constants.

A comparison between the rectangular enveloping function and the exponential enveloping function will be presented in Chapter 7, using the experimental results.

CHAPTER 4

THEORETICAL INVESTIGATION OF ROUGH NON-DEFORMABLE ROAD SURFACE EFFECT ON TYRE TRACTIVE PERFORMANCE

4.1 Introduction

A schematic diagram of the tyre moving over a rough, non-deformable terrain with an angular velocity, ω_T , is illustrated in Fig. 4.1.1. Three major fields of interest for the theoretical investigation of road roughness effect on tyre tractive performance are shown there. Forces acting on the driven tyre are also shown and they are individually explained as:

Torque

This is produced by the engine to deliver a driving force to the supporting terrain.

Thrust

This is the force developed by a vehicle tractive element (wheel/track) due to applied torque.

Motion Resistance

This can be considered as resistance forces converted from total energy expenditure due to interfacial slip and due to flexing of the running gear (tyre).

Drawbar-pull (DBP)

This represents the ability of the vehicle to pull or push various types of working machinery, including implements of earthmoving agricultural or construction equipment.

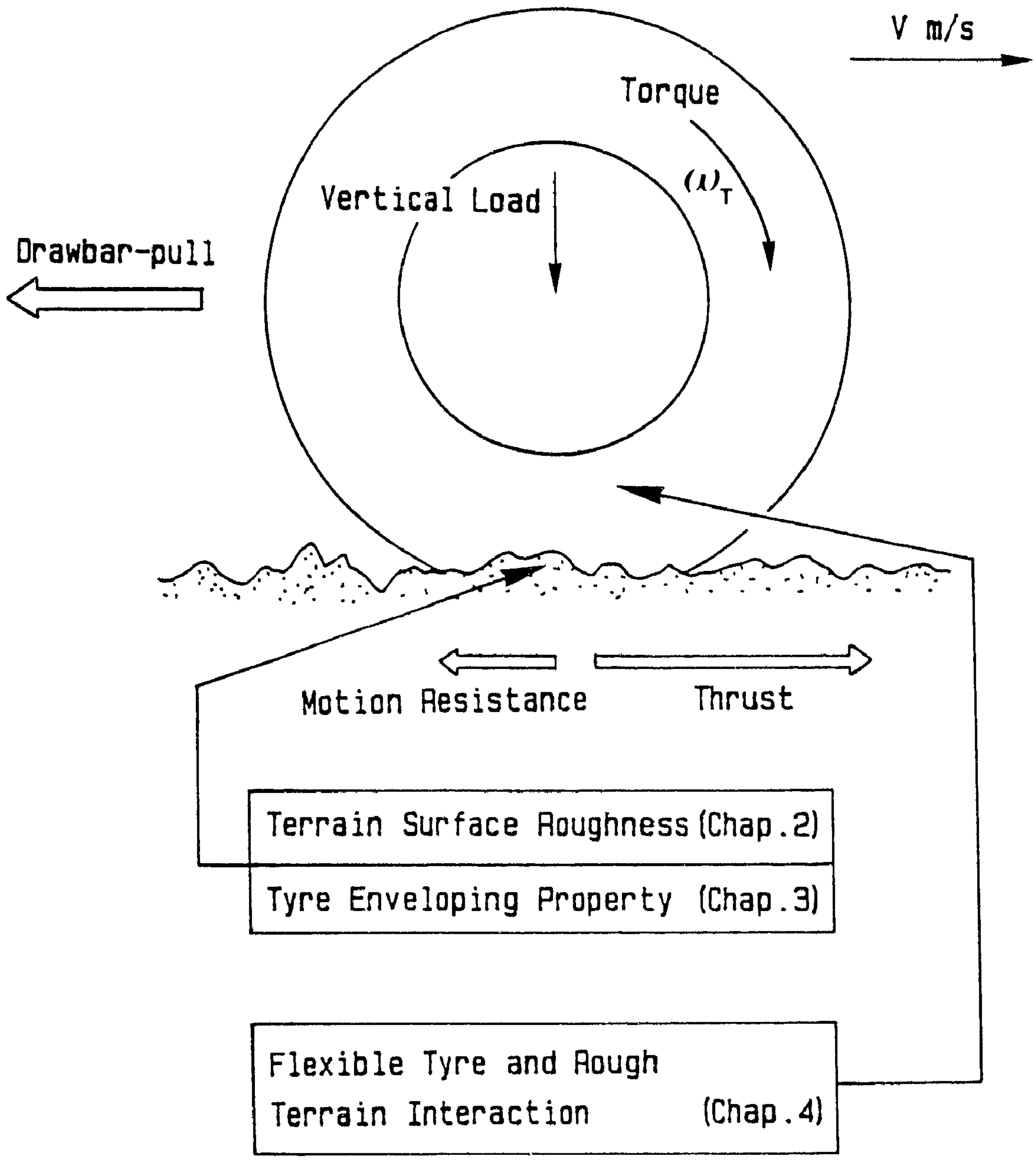

Fig. 4.1.1 Schematic diagram of forces acting on moving tyre over rough terrain and three major problems associated with this operation

The main concern in the theoretical study of the terrain roughness effect on tyre tractive performance is the development of an analytical relationship between the road surface roughness and the DBP produced by the tyre. It is established in a form of system function that defines the resultant DBP from the terrain surface geometry in the frequency domain, in conjunction with the principle of energy conservation.

One of the important factors in the development of a system function is the tyre's mechanical and/or chemical properties which depend on many factors, such as temperature, rotating velocity, loading condition and tyre materials.

The second factor to be considered is the rolling phenomenon of the tyre. The traction is developed by the slip which is originated by the difference in speed between rotation and translation of the tyre. While the mechanism of slip is very sophisticated, as shown in Wolfson (1987), it is important to account for slip in an off-road performance study since a relatively high slip rate is generally engaged in off-road operation.

The third factor is a vibration phenomenon of the tyre. The oscillatory movements of the tractive element are the cause of vibration in tractive force.

Up until now, several investigations of tyre performance on a rough terrain or under the existence of vibration have been attempted. However, there are very few studies which have successfully dealt with these complex factors, together with an analysis of tyre performance because of the difficulties in tyre-rough terrain interaction.

Excitation from a rigid, rough ground is one of the most influential phenomena to be considered for off-road vehicle performance. In developing a theoretical model which can predict and analyze the effect of terrain surface roughness on tyre performance, the effect of base (ground) excitation to the flexible tyre should be the primary focus. Three leading factors, (geometrical characteristics of terrain surface, the mechanical properties of a flexible tyre and operational conditions), control the excitation phenomenon interelatedly. The vibration of a rolling tyre would be expected to cause some change in the tractive performance of the tyre, which is an increase in motion resistance (Fig. 4.1.2). The tractive performance will be offset by an increased motion resistance as a result of extra energy expenditure due to production of heat, noise, slip and vibration etc..

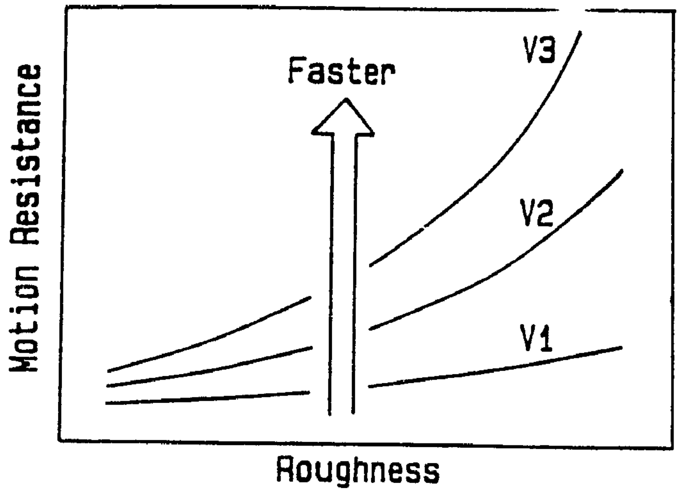

Fig. 4.1.2 Diagram of relationship between motion resistance and road roughness with effect of translational speed (V1<V2<V3)

The objectives of this chapter are:

(1) to develop a theoretical model of a tyre-rough terrain system, including terrain surface characteristics, mechanical properties of the tyre and operational conditions,

(2) to find a predictive/analytical method for the investigation of surface roughness effect on a tyre's tractive performance in the most simple economical and time-saving manner,
and finally,

(3) to establish a system function which can describe the tractive efficiency of a driven tyre with the derived DBP.

The flow chart of the predictive procedure for the determination of DBP on a rigid, rough terrain is shown in Fig. 4.1.3. In Section 4.2, modeling of the tyre-terrain system is discussed. Section 4.3 provides the derivation of time-dependent DBP based on the concept of energy balance. Section 4.4 deals with the development of a system function by using the frequency domain approach. In Section 4.5, a new concept of the tractive efficiency is proposed.

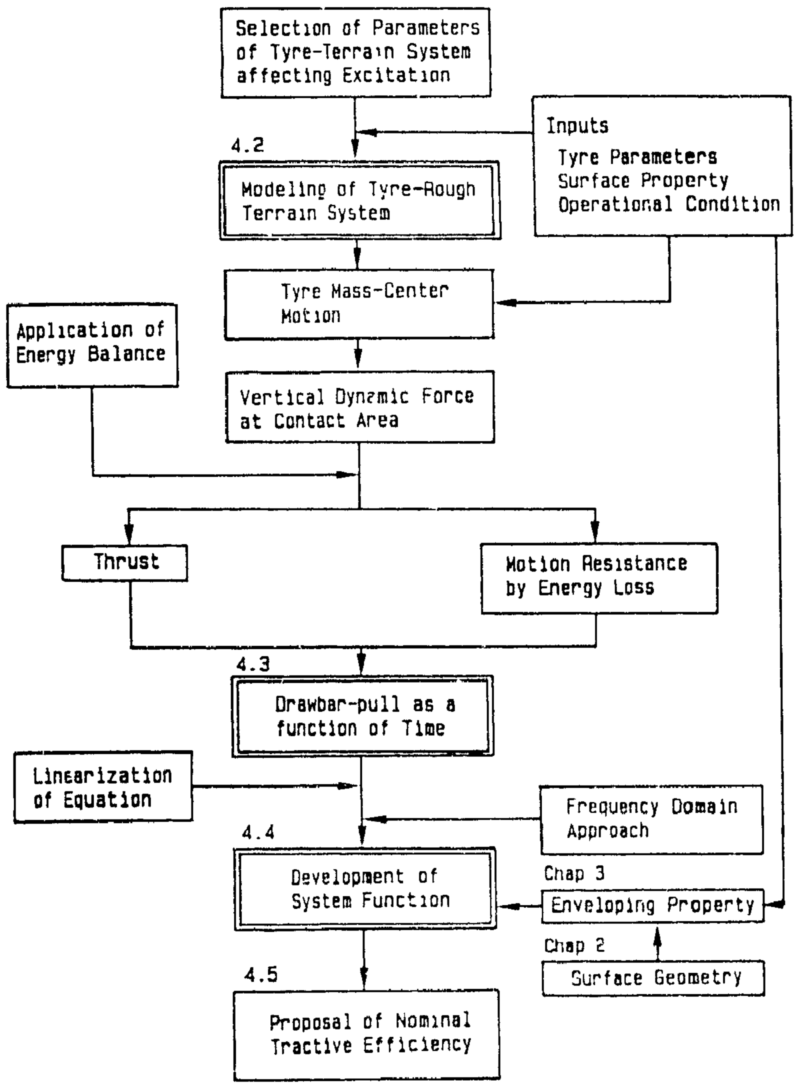

Fig. 4.1.3 Flow chart of predictive/analytical procedure in Chapter4

4.2 Flexible Tyre Model on a Rough Terrain

4.2.1 Parameters affecting the Tyre Performance

Fig. 4.2.1 depicts the parameters concerning tyre, terrain and tyre-terrain interaction individually. The difficulty in this investigation is the treatment of the variability of all the parameters. Tyre deflection is not constant as in the case of flat and smooth surface operation. Torque, slip, inflation pressure and finally the DBP may not be constant, but a function of time, which means a function of surface geometry.

Furthermore, these are related to each other. If one parameter changes, all the others are influenced. Changes in vertical load on the wheels also affect the friction at tyre-ground interface, and changes in friction interfere with the slip rate and translational velocity. If the vehicle velocity is changed, dynamic loading on the wheel is also affected. Therefore, the aspects which cover all these influential parameters for the tractive performance on a rough terrain have not yet been fully understood because of the lack of information concerning the complex mechanisms of the tyre-rough terrain system.

In view of the above, it is clear that a comprehensive traction model including road roughness effect, tyre properties and operational conditions (slip and speed etc.) is needed.

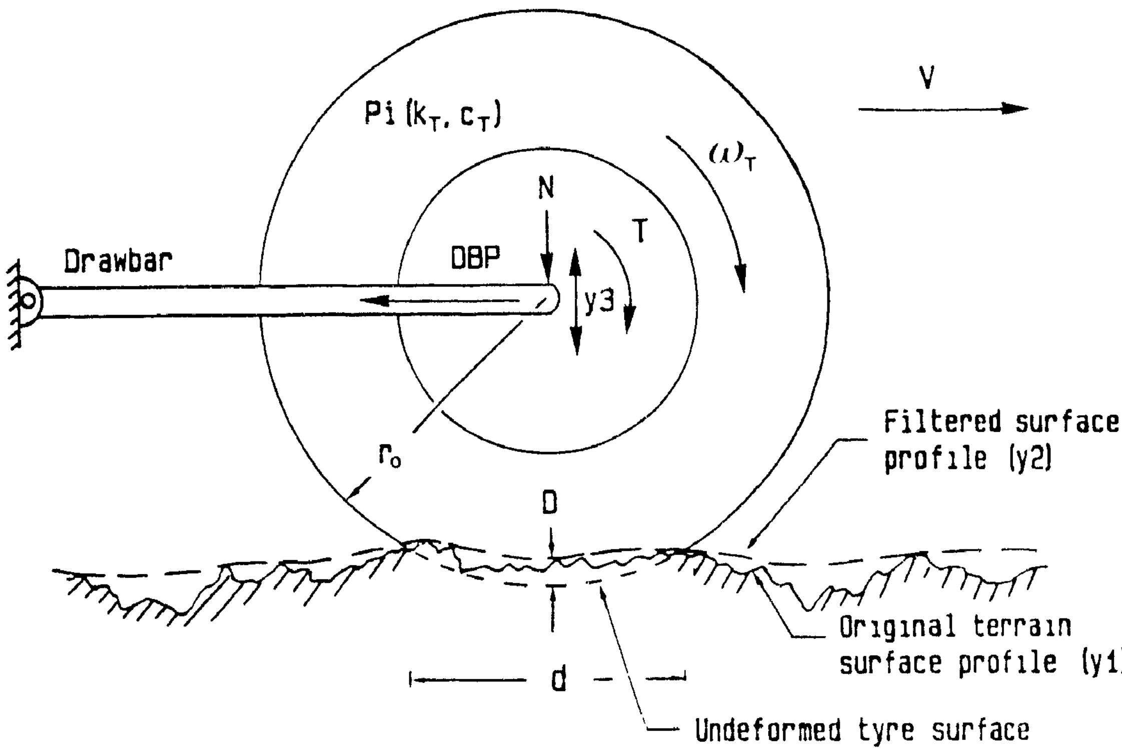

Tyre Parameters		Terrain Parameters	
N	Wheel load	y1	Original terrain surface profile
T	Input torque		
DBP	Drawbar-pull		
V	Translational velocity		
ω_T	Angular velocity	**Tyre-terrain Interactive Parameters**	
r_o	Wheel radius	2d	contact length
P_i	Inflation pressure	D	Tyre deflection
k_T	Stiffness	y2	Filtered surface profile
c_T	Damping	y3	vertical response of tyre

Fig. 4.2.1 Parameters for flexible tyre-rough terrain system

4.2.2 Idealization of Moving Tyre on Rough Terrain and Established Assumptions

Based on the hypothesis that the excitation arising from the rough ground, which is a function of ground surface roughness, tyre properties and translational velocity, is the key concern of the tyre tractive performance study on the rough terrain, the following idealization of the tyre-terrain system is proposed, as illustrated in Fig. 4.2.2. Whilst the ground surface, in fact, has a random profile, the ground which has a flat and smooth surface moves backward at the same speed as the translational speed, V, of the tyre, while oscillating vertically in a random manner. This vertical oscillation characterizes the loading function of the tyre.

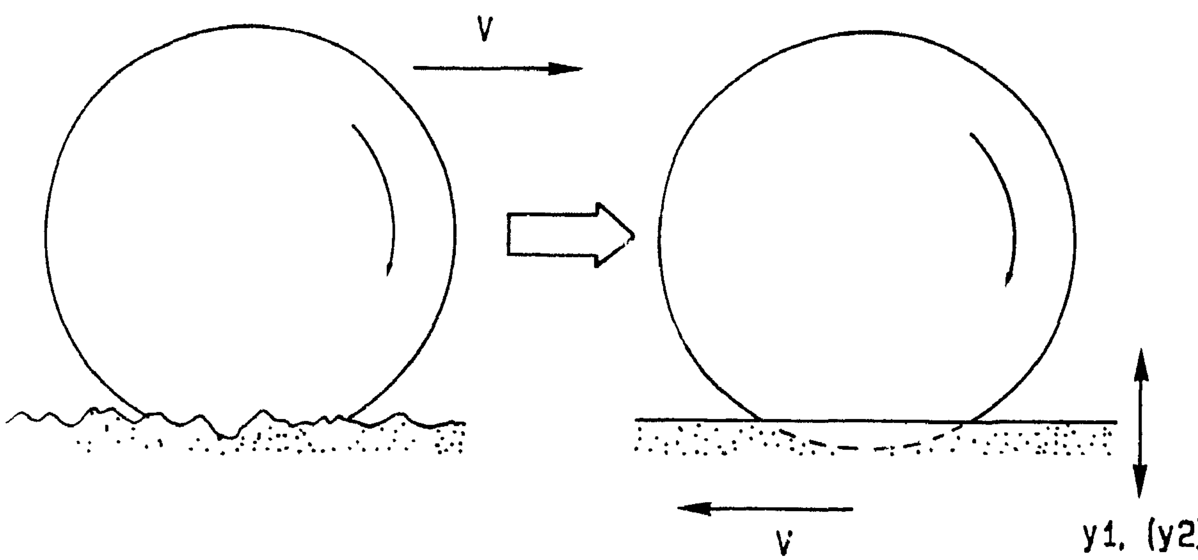

Fig. 4.2.2 Idealization of moving tyre over rough terrain

Accordingly, the following assumptions were established.

Terrain

(1) The random process of terrain surface is weakly stationary (the first and second statistical moments of the process are time-invariant) and ergordic (the first two moments do not differ over the different samples).

(2) Terrain surface is rigid and undeformable, i.e. the coordinates of the profile points do not change as the tyre travels over the ground surface.

Tyre

(1) Translational velocity is relatively low, and not affected by the motion of the tyre but is kept constant. Therefore, the tyre is always in contact with the ground surface.

(2) Wheel surface is buffed (smoothed), i.e. the tyre does not have any tread on its surface.

(3) Moment of inertia about the tyre's lateral axis is neglected since the rotational velocity of an off-road tyre is usually much smaller than that of an on-road tyre.

(4) Inflation pressure during motion is constant and the swelling of the tyre is neglected.

Interface

(1) Shear stress between the tyre and ground surface is generated only at the tyre contact area, and is distributed uniformly.

(2) Frictional characteristics are unique in the contact area.

(3) Contact length is not varied during the dynamic loading, and is determined by the static load of the tyre and the tyre's stiffness.

(4) Horizontal deformation or twisting of rubber tread is neglected.

4.2.3 Flexible Tyre-Rough Terrain System

In order to investigate the effect of ground excitation on tyre tractive performance, an analytical tyre-terrain system is suggested, as shown in Fig. 4.2.3. It consists of uniformly distributed stiffness and damping elements over the foot print length, to represent the inflation pressure and carcass vibrational characteristics. While the rolling radius of the tyre is dependent on its vertical deflection, the foot print length is assumed to be constant, independent of the tyre deflection, during the rough road operation. The finite foot print length provides this model with the ability of enveloping. It will negotiate the small irregularities over the terrain surface. Dynamic reaction load is a function of the filtered profile rather than of the original surface profile because of this property.

Although the tyre is actually driven over a terrain surface and therefore the slip exists at the interface between the tyre and terrain, the distributed elements of the tyre carcass are considered not to be distorted horizontally, but only vertically in the model.

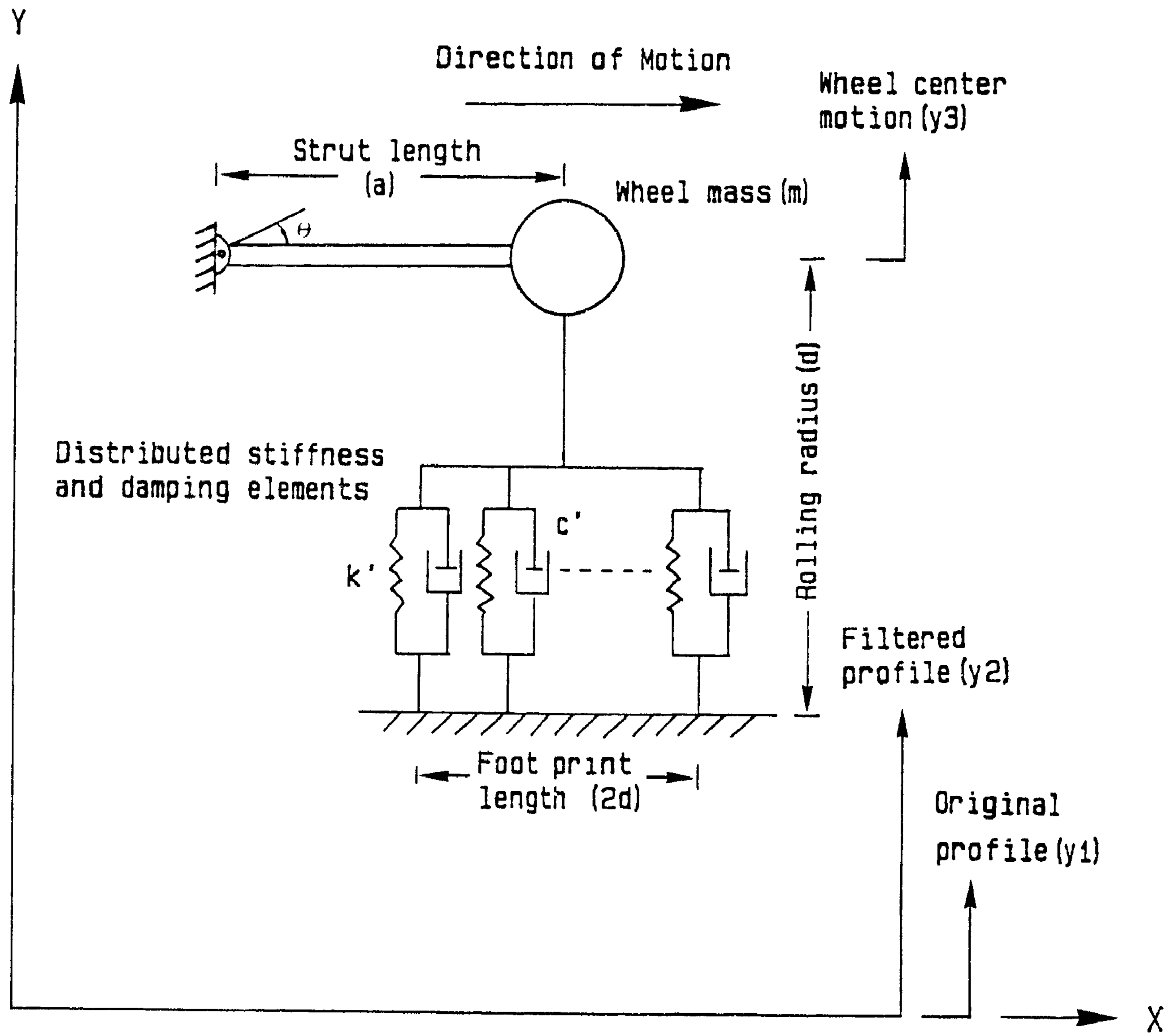

Fig. 4.2.3 Flexible tyre-rough terrain system

4.3 Development of Equilibrium Equation between DBP and Terrain Surface Roughness

4.3.1 Energy Balance of Tyre Moving over Rough Terrain

The principle of energy conservation is one of the basic laws of physics. The input (total) energy must be equal to the sum of output energy and energy loss during the motion of a system. Although several attempts have been made to investigate the DBP based on the force equilibrium, the energy method is preferable in the tyre-rough ground interaction analysis since it has a capability of incorporating all the resultant forces, velocities and displacement of the entire system. As stated earlier, the energy method of analysis may be suitable for application to a problem where a number of parameters are combined in a complex fashion with each other. The energy method considers simultaneously both the force system and the different modes of movement in a tyre-rough ground system, namely the rotational, vertical and translational motions. This method will consequently satisfy the equilibrium requirements both statically and dynamically. It has also been successfully used to evaluate the wheel/track-soil/snow performance, provided the different energy components in that system (Yong et al.,1978; Yong and Muro,1981).

Fig. 4.3.1 shows a schematic representation of the resultant energy components generated by a tractive element (wheel/track) interacting with a terrain surface. Considering the form of evaluation of mobility performance of a tyre-rough terrain system in terms of energy conservation, the governing equation has been written as:

$$E_{in} = E_s + E_T + E_{out} \tag{4.1}$$

where E_{in} = input torque energy which is obtained by subtracting the mechanical energy losses due to gear and bearing friction etc. from net engine power,

E_s = slip (interfacial) energy which is wasted at the interface in forms otner than work done,

E_T = tyre deformation energy which is the amount of energy required to deform the flexible tyre,

E_{out} = output DBP energy which is the remainder for available work from energy accounted for.

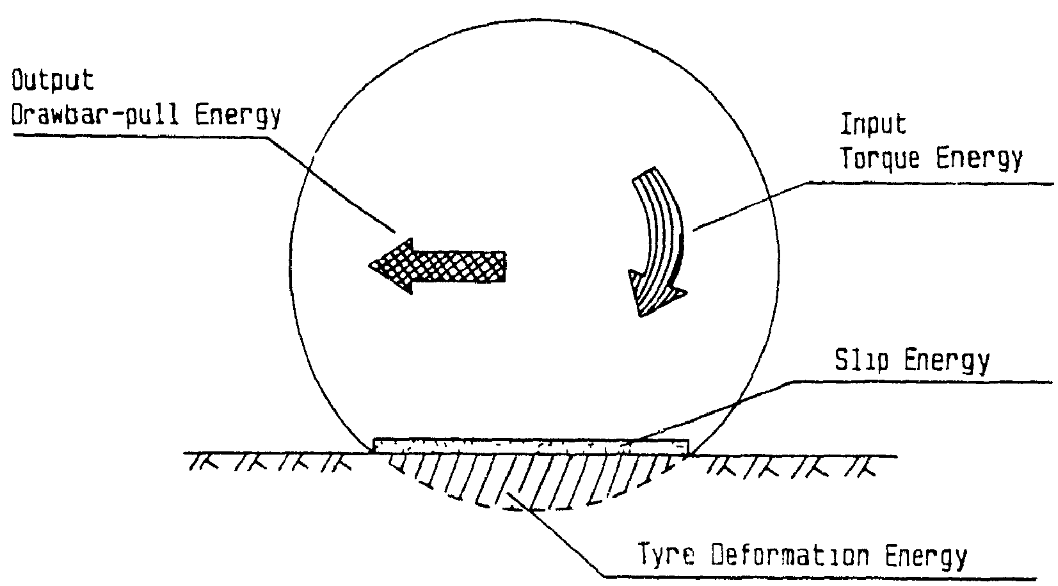

Fig. 4.3.1 Schematic diagram of energy componen.s of rolling wheel on ground

Fig. 4.3.2 schematically shows an increase in the tyre deformation energy due to ground surface roughness, resulting in a decrease of output energy where the same input energy is applied. It is obvious that the energy losses (tyre deformation energy and slip energy) must be reduced if a greater output energy is desired. Therefore, it is necessary to pay proper attention to the design of an optimum running gear system which minimizes these energy losses.

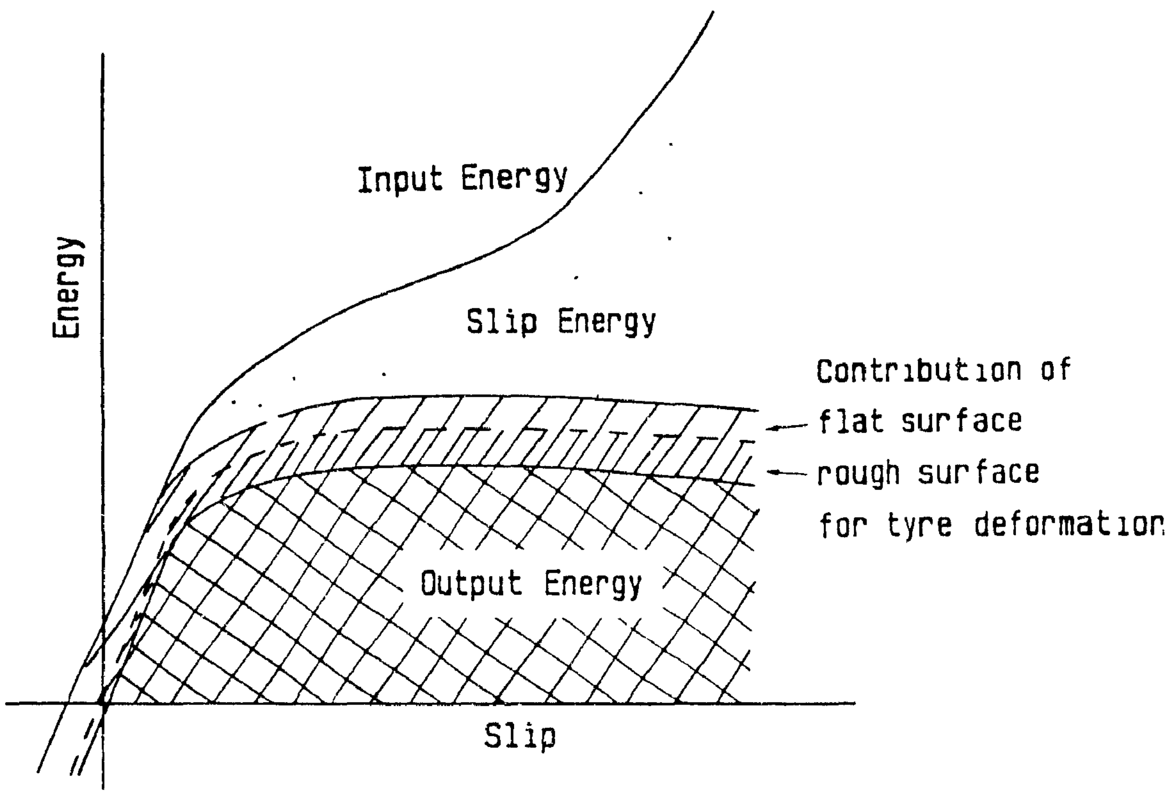

Fig. 4.3.2 Diagram showing effect of terrain surface roughness on tyre deformation energy

In the later analysis, the energy rate (power) will be considered instead of using the energy itself for the benefit of the evaluation of the tyre performance in the same reference frame. Consequently, the performance of a tyre on a rough ground surface can be evaluated in terms of the basic principle of power balance.

$$\dot{E}_{out} = \dot{E}_{in} - (\dot{E}_T + \dot{E}_S)$$

$$\text{output power} = \text{input power} - \text{power loss} \tag{4.2}$$

where (•) indicates a derivative with respect to time.

4.3.2 Derivation of Equation for DBP on a Rough Ground

The prediction of the drawbar-pull (DBP) is an essential part of the requirement for vehicle performance simulation. The DBP is defined as the resultant of the thrust, TH, minus total motion resistance, MR (Bekker, 1960). Thus,

$$DBP = TH - MR \tag{4.3}$$

It is obvious that maximizing the thrust and minimizing the motion resistance will achieve the vehicle's maximum tractive performance. Considering that the thrust is developed by the input power to the wheel and the motion resistance is from the products of the power losses, the useful DBP force would be derived by calculating the thrust and the motion resistance separately, by virtue of a concept of power balance.

(1) Thrust

Thrust can be considered as an input force from the wheel to ground surface. On a rigid, unyielding surface, the input power to apply a wheel torque is directly transmitted to the ground surface to produce the thrust. Taking advantage of the principle that the power induced by the torque transmitted to the tyre must be equal to the power produced by the product of the thrust and constant translational velocity, thrust is given as follows:

$$TH = \frac{T \cdot \omega_T}{V} \tag{4.4}$$

Slip rate is given by

$$s_i = \frac{r_r \omega_T - V}{r_r \omega_T} \tag{4.5}$$

100% slip indicates no-transversal motion while the tyre is rotating. Then,

$$V = r_r \cdot \omega_T (1 - s_i) \tag{4.6}$$

Substituting Eq.(4.6) into Eq.(4.4),

$$TH = \frac{T}{r_r(1 - s_i)} \qquad (s_i \; / \; 1) \tag{4.7}$$

where T = input driving torque

r_r = rolling radius of tyre

ω_T = angular velocity of tyre

s_i = slip rate at tyre-ground interface

(2) Motion resistance

Before considering the motion resistance of a rotating tyre, it may be useful to consider the frictional mechanism of a rubber tyre. Several types of frictional components have been introduced to explain the frictional mechanism between a tyre and a rigid surface. Bowden and Tabor (1954), and Meyer and Kummer (1968) suggested the two major frictional components, which were caused by the adhesion,Fa, (surface friction) and by the deformation,Fd, (internal friction). Therefore, total friction becomes,

$$Ftotal = Fa + Fd \qquad (4.8)$$

Fig. 4.3.3 depicts these two components. Fa is attributed to bonding of exposed surface atoms between sliding members. Fd is a resisting force available when a rubber specimen is rolling on a perfectly lubricated surface with small irregularities. This is due to tyre hysteresis. Any individual rubber surface element goes through a deformation cycle as it passes over an asperity of a terrain surface. A certain energy is dissipated every cycle.

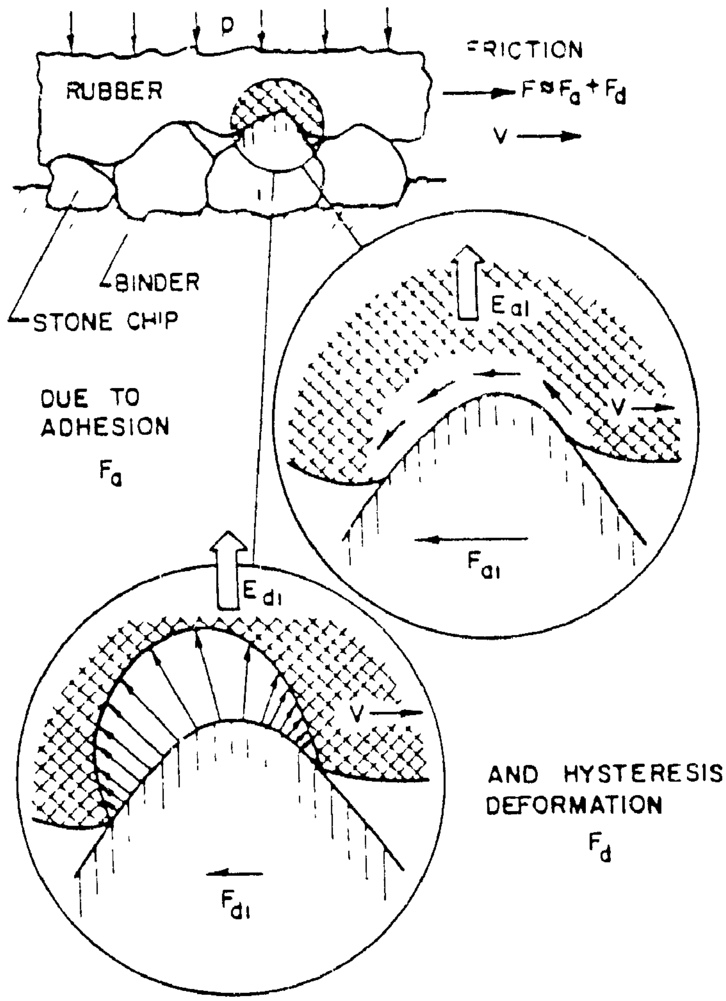

Fig. 4.3.3 Two principal components of pavement friction (after Meyer and Kummer)

Pottinger (1986) added another frictional component to the above-mentioned equation, i.e. wearing (tearing) of rubber tips. Clark (1971) introduced four components to explain frictional mechanism, namely adhesion, deformation, tearing, and viscous components. The viscous frictional component is a resistance created mainly by foreign material (water or surface contamination) entrapped between the tyre and the road surface.

Although many frictional components for a rubber tyre are exhibited here, the most influential ones seem to be the deformation and the adhesion components for the case of the flexible tyre moving on a dry, rigid ground. As shown in Fig. 4.3.4, the rolling flexible tyre undergoes repeated deformation (compression and recovery) during rotation on a rigid, smooth road. In addition, on a rigid rough terrain, another deformation factor, arising from vertical excitation, has to be considered. Furthermore, a driven tyre normally produces a positive slip (sliding) between the rubber surface and the ground surface. When a tyre has a slip, the adhesive bonding between the two surfaces are cut due to the development of excessive shear force, causing an extra energy expenditure. The energies required to deform and slip the tyre do not contribute to increase the DBP, but to increase the motion resistance.

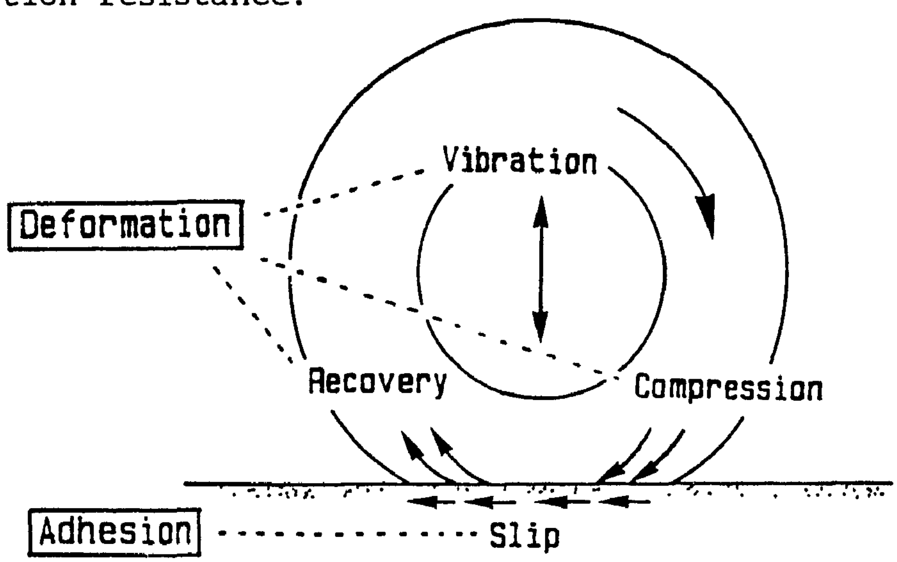

Fig. 4.3.4 Friction components of a driven tyre

Therefore, it is presumed that the two energy expenditure factors which are due to tyre deformation and due to tyre adhesion (slip) must be taken into account for the analysis of motion resistance. Consequently, two types of motion resistance will be considered, i.e. vertical excitation resistant force (MR1) resulting from tyre deformation power loss and the slip resistant force (MR2) produced by the slip power loss.

Vertical Excitation Resistance Force (MR1)

Since this resistance force is a product arising from a hysteresis power loss of tyre damping property, the velocity components of the tyre deformation should be defined in order to derive the damping power loss, which is called the tyre deformation power loss.

Two different kinds of vertical velocities are obtained for a rotating tyre on a rough terrain. One is identified as vertical excitation velocity, $V_{1(t)}$, originating from the rough surface geometry. Euler's theorem (instantaneous axis of rotation) defines another vertical velocity component, $V_{2(t)}$, resulting from the tyre rotation (Fig. 4.3.5).

Euler's Theorem

A motion of a rigid body with both rotation about a fixed point, O, of the body and a translational velocity of V, is equivalent to a rotation about an instantaneous axis of rotation, O', which lies at a vertical distance of r_r (=V/ ω_T) from point O.

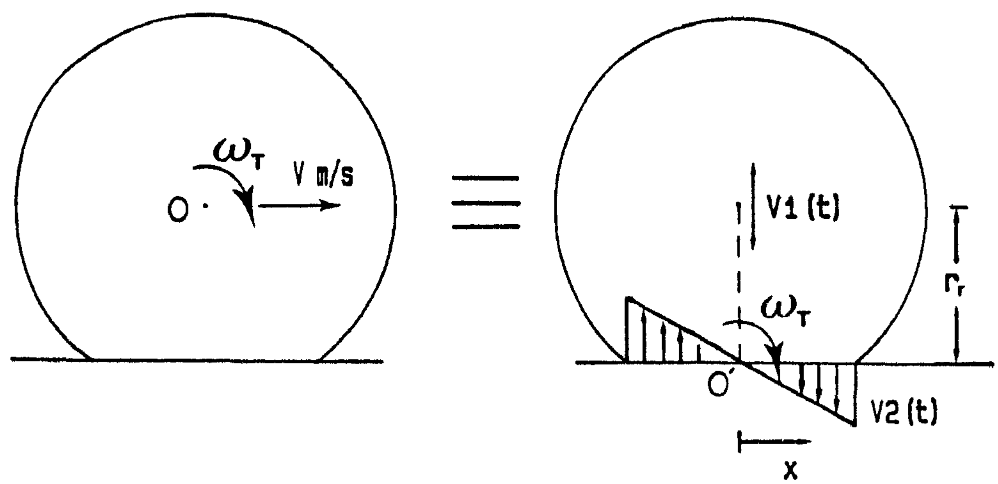

Fig. 4.3.5 Instantaneous axis of rotation (O') and two velocity components

Therefore, the total vertical velocity at each point along the contact portion can be written as:

$$V_V = V_{1(t)} + V_{2(t,x)} \tag{4.9}$$

where

$$V_{1(t)} = \frac{d}{dt}(y3 - y2)$$

$$V_{2(t,x)} = -x \cdot \omega_T$$

where x is a horizontal distance from an instantaneous center of rotation which is a middle point of the contact portion.

When a tyre moves on a completely smooth surface, the velocity, V_1, is equal to zero. Each point along the forward contact portion interacts with the ground surface at a distance-dependent velocity of $-x \cdot \omega_T$. Points along the backward contact portion are being repulsed at a negative velocity (stretching). The dissipation of tyre deformation power by these two velocities is derived in Appendix D.

$$\begin{aligned} \dot{E}_T &= \xi \left(\dot{E}_{V_1} + \dot{E}_{V_2} \right) \\ &= \xi c_T \left\{ V_1^2 + \frac{1}{3} (\omega_T d)^2 \right\} \end{aligned} \qquad \text{(D.1.10)}$$

where $\dot{E}_{V1}$ and $\dot{E}_{V2}$ are power dissipations caused by the velocity V_1 and V_2 respectively. Since the velocity, V_1 is equal to vertical response of the tyre, $\dot{z}$,

$$\dot{E}_T = \xi c_T \left\{ \dot{z}^2 + \frac{1}{3} (\omega_T d)^2 \right\} \qquad \text{(4.10)}$$

where $\dot{z}$ = derivative of relative displacement between the filtered profile and the center of the tyre mass ($=\dot{y}2-\dot{y}3$)

d = half of contact length

c_T = total damping of tyre ($=2dc'$)

ξ = energy recovery factor suggested by Bekker (1983)

$= 1-e^{-AD/H}$

A : constant

D : tyre deflection

H : tyre carcass height

The vertical excitation resistant force could be given by dividing this tyre damping power dissipation by the translational velocity. It is therefore,

$$\mathrm{MR1} = \frac{\dot{E}_T}{V}$$

$$= \frac{\xi c_T}{V}\left\{\dot{z}^2 + \frac{1}{3}(\omega_T d)^2\right\} \tag{4.11}$$

<u>Slip Resistance Force (MR2)</u>

Tyre slip is an inherent phenomenon caused by the difference in relative velocity between the translational velocity and the rotational velocity of the tyre macroscopically. Therefore, a shear force will be developed at the contacting portion between the tyre surface and the ground surface. The shear force is the source of the thrust which permits the tyre to propel forward or backward. Slip is an essential element for tyre traction.

Although the occurrence of slip is necessary for the tractive motion, it is understood that a certain amount of energy is wasted by slip. For example, when a vehicle is stuck on a slippery icy road, all the input energy is dissipated elsewhere without producing any useful output energy (i.e. no actual DBP). A muddy soft terrain could also produce the same situation. In these cases, slip rate is almost 100% since there is little transversal motion. As previously seen in Fig. 4.3.2, a large amount of input energy is wasted at a higher slip because the output energy developed at tyre-ground interface remains the same or is decreased slightly.

For economical mobility purposes, it is desirable that the vehicle is able to move from one point to another with the least amount of input energy. To achieve this, the slip energy loss must be a minimum.

The power loss due to the slip can therefore be converted into another form of the resistance to motion in terms of force units, because it does not contribute to useful work done. The power loss due to the tyre slip is calculated on the basis of the average slip occurring over the tyre-terrain interface. Assuming a uniform distribution of shear forces, the power loss by the slip can be obtained as:

$$\dot{E}_s = T \cdot \omega_T \cdot s_i \tag{4.12}$$

where T = input torque

ω_T = angular velocity of tyre

s_i = slip rate

Thus, the slip resistance force (MR2) is given by

$$\mathrm{MR2} = \frac{\dot{E}_s}{V}$$

$$= \frac{T \cdot \omega_T \cdot s_i}{V} \tag{4.13}$$

(3) Drawbar-pull

As explained by Eq.(4.3), the useful output force can be predicted by taking the difference between the thrust and the motion resistance which are derived from the power balance during motion. Therefore,

$$DBP = TH - (MR1 + MR2)$$

$$= \frac{T}{r_r(1-s_i)} - \left[\frac{\xi c_T}{V}\left\{\dot{z}^2 + \frac{1}{3}(\omega_T d)^2\right\} + \frac{T\omega_T s_i}{V}\right]$$

$$= \frac{T}{r_r} - \frac{\xi c_T}{V}\left\{\dot{z}^2 + \frac{1}{3}(\omega_T d)^2\right\} \tag{4.14}$$

The rolling radius, r_r, is given by a geometrical relationship between the half contact length, d, and the original (undeflected) tyre radius, r_o (Fig. 4.3.6).

$$\frac{1}{r_r} = \frac{1}{\sqrt{r_o^2 - d^2}} \tag{4.15}$$

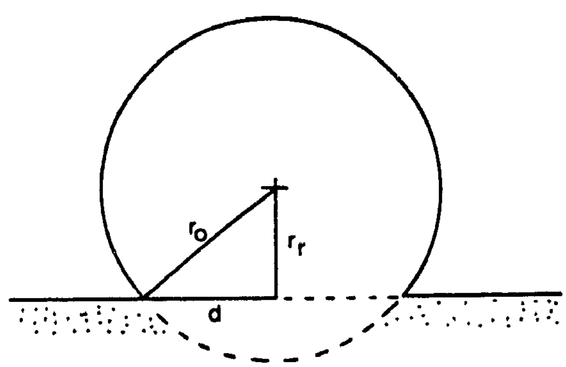

Fig.4.3.6 Geometrical relationship between half contact length, original and rolling radius of tyre

Applying the binomial series expansion to Eq.(4.15) for an approximation,

$$\frac{1}{r_r} = \frac{1}{r_o}\left\{1 + \frac{1}{2}\left(\frac{d}{r_o}\right)^2\right\} \tag{4.16}$$

Substituting Eq.(4.16) into Eq.(4.14),

$$DBP = \frac{T}{r_o}\left\{1 + \frac{1}{2}\left(\frac{d}{r_o}\right)^2\right\} - \frac{\xi c_T}{V}\left\{\dot{z}^2 + \frac{1}{3}(\omega_T d)^2\right\} \tag{4.17}$$

Assuming that the contact length is proportional to the square root of the vertical load from the load-contact area experiments (Fig. 6.3.5), an empirical relationship between the contact length and the vertical load to the tyre axis is given as follows:

$$2\,d = q\,N^{0.5} \tag{4.18}$$

where q = experimental constant named as contact length coefficient (given in Eq.6.3)

N = vertical reaction load $(=c_T\dot{z}+k_T z+mg)$

Substituting Eq.(4.18) into Eq.(4.17), the equation of the DBP on a rigid, rough road can be finally written as:

$$\begin{aligned} DBP &= \frac{T}{r_o}\left\{1 + \frac{1}{8}\left(\frac{q}{r_o}\right)^2 N\right\} - \frac{\xi c_T}{V}\left\{\dot{z}^2 + \frac{1}{12}(q\omega_T)^2 N\right\} \\ &= \frac{T}{r_o} + Jmg - \frac{\xi c_T \dot{z}^2}{V} + J(c_T\dot{z} + k_T z) \end{aligned} \tag{4.19}$$

where

$$J = \left(\frac{T}{8r_o^3} - \frac{\xi\, c_T\, \omega_T^2}{12V}\right) q^2$$

4.4 Derivation of System Function

4.4.1 Frequency Domain Analysis

It has been mentioned several times that the terrain surface profile is a stochastic process. As well, the profile modified by the tyre enveloping effect is also a stochastic process. This profile must be regarded carefully because a pneumatic tyre recognizes the roughness of a filtered profile, rather than that of the original profile. In the analytical prediction of the tyre performance, the time domain analysis can be a powerful and useful concept if the inputs are defined with an adequate mathematical representation. However, it is very difficult to estimate a random stochastic filtered profile signal from a random original surface profile in a deterministic manner without using statistical and probabilistic techniques. Even if it could be done in the time domain, the computation process becomes enormously large due to the tedious convolution integrals.

The requirement is to find a quick, economical prediction method of tyre traction related to the ground surface roughness. Comparing the frequency domain analysis and the time domain analysis, the former is relatively cheap but assumes linearity while the latter is relatively expensive but allows for nonlinearities.

As stated in Chapter 2 and 3, the frequency domain analysis may satisfy the requirements such as accuracy, simplicity and availability of information of dynamic behavior, if the engaged system is linear. The original ground surface profile can be described in terms of the amplitude PSD function. The filtering function due to the tyre enveloping effect is also expressed as a frequency filter. Therefore, the variation of the tractive force of the tyre as output can be estimated by using the following basic, linear input-output relationship:

$$S_{DBP'(f)} = \left| H_{sy(f)} \right|^2 S_{y1(f)} \tag{4.20}$$

where $S_{DBP'(f)}$ = PSD of non-constant component of DBP

$S_{y1(f)}$ = PSD of original surface height profile

$H_{sy(f)}$ = system function of tyre-rough terrain system which relates the terrain surface irregularities to the DBP including tyre enveloping effect

4.4.2 Linearization of Equation

The derived equation for DBP (Eq.4.19) shows a nonlinearity with a vertical response of a tyre axle. An analytical solution of the nonlinear equation is usually quite difficult because the principles of the additive property and homogeneous property cannot be applied to a nonlinear problem.

$f(x_1 + x_2)$	$= f(x_1) + f(x_2)$	additive property
$f(cx)$	$= c\, f(x)$	homogeneous property

Therefore, the solutions of the nonlinear problem are generally obtained by methods specific to the particular problem or by linearization methods. Although several linearization methods have been developed, only two representative methods will be shown here. They are the perturbation method (Crandall, 1963) and the equivalent linearization method (Krylov and Bogoliubov, 1937) which is employed in this study.

(1) Perturbation method

This method can be used when a deviation from linearity is very small. As an example, the motion of a single-degree-of-freedom system is considered. The nonlinear differential equation is given by

$$\ddot{x} + \beta\dot{x} + g_{(x)} = F_{(t)} \qquad (4.4.2.1)$$

The nonlinear restoring force, $g_{(x)}$, is assumed to represent the sum of a linear plus a nonlinear component as follows:

$$g_{(x)} = \omega_o^2 x + \epsilon\, g_{o(x)} \qquad (4.4.2.2)$$

where $\omega_o{}^2$ is a constant and $g_{o(x)}$ is the residual nonlinear function. ϵ is a perturbation parameter and is << 1.

The basic idea behind this method is to assume a response of the system in the form of an expansion of power of ϵ:

$$x_{(t)} = x_{o(t)} + \epsilon x_{1(t)} + \epsilon^2 x_{2(t)} + \cdots \qquad (4.4.2.3)$$

Substituting Eq.(4.4.2.3) in Eq.(4.4.2.1) with $g_{(x)}$ defined by Eq.(4.4.2.2),

$$Dx_o + D\epsilon x_1 + D\epsilon^2 x_2 + \cdots = F_{(t)} - \epsilon g_{o(x_o)} - \epsilon^2 \frac{\partial g_{o(x_o)}}{\partial x_o} x_1 - \cdots \qquad (4.4.2.4)$$

Taylor's series expansion of $g_{o(x)}$ about x_o was used in above calculation. D is a differential operator given by

$$D = \left[\frac{d^2}{dt^2} + \beta \frac{d}{dt} + \omega_o^2 \right]$$

Setting the coefficients of powers of in Eq. (4.4.2.4) to cancel each other,

$$
\left.\begin{aligned}
Dx_o &= F_{(t)} \\
Dx_1 &= -g_{o(x_o)} \\
Dx_2 &= -\frac{\partial g_{o(x_o)}}{\partial x_o} x_1 \\
&\;\;\cdots\cdots
\end{aligned}\right\} \qquad (4.4.2.5)
$$

Thus, Eqs.(4.4.2.5) all involve the same linear operator on the left and the original nonlinearity has been shifted to the sequence of nonlinear operations on the right. Solutions to Eqs.(4.4.2.5) will be given by employing the convolution integrals.

$$
\left.\begin{aligned}
x_o &= \int_{-\infty}^{\infty} h_{(\tau)} F_{(t-\tau)} \; d\tau \\
x_1 &= -\int_{-\infty}^{\infty} h_{(\tau)} g_o[x_{o(t-\tau)}] \; d\tau \\
x_2 &= -\int_{-\infty}^{\infty} h_{(\tau)} \frac{\partial g_o[x_{o(t-\tau)}]}{\partial x_o} x_{1(t-\tau)} \; d\tau \\
&\cdots\cdots
\end{aligned}\right\} \qquad (4.4.2.6)
$$

where $h(\tau)$ is the response function to the unit impulse. When an excitation function, $F_{(t)}$, is a random process, this method can be used to obtain the statistical moment of the nonlinear response. The mean square response is often determined, as follows:

$$
E[x^2] = E[x_o^2] + 2\epsilon E[x_o x_1] + \epsilon^2 \left\{ E[x_1^2] + 2E[x_o x_2] \right\} + \quad \cdots \qquad (4.4.2.7)
$$

In principle, the perturbation method can be used to estimate the response to any order of ϵ. However, results are obtained to the first order of ϵ only, in most cases, because the algebra for higher order estimates becomes very complex. The first two terms on the right hand side of Eq.(4.4.2.7) are given by using auto correlation functions.

$$E[x_o^2] = \int_{-\infty}^{\infty}\int_{-\infty}^{\infty} h_{(\tau_1)}h_{(\tau_2)}E[F_{(t-\tau_1)} \cdot F_{(t-\tau_2)}]\ d\tau_1 d\tau_2$$

$$E[x_o x_1] = -\int_{-\infty}^{\infty}\int_{-\infty}^{\infty} h_{(\tau_1)}h_{(\tau_2)}E\left[F_{(t-\tau_1)}g_{o(x_{o(t-\tau_2)})}\right]\ d\tau_1 d\tau_2$$

(4.4.2.8)

(2) Equivalent linearization method

This is a conversion method where the solution of a system expressed by nonlinear differential equations is approximated by the solution of the equivalent system transformed by linear equations. The main concept in this method is to minimize the difference between the original nonlinear equations and the proposed linear equations, and then to find the equivalence parameters for linear equations.

A linear equation for the nonlinear equation is assumed as follows:

$$\mathrm{DBP}_{\mathrm{linear}} = \epsilon_1 + \epsilon_2 \dot{z} + \epsilon_3 z \qquad (4.21)$$

where ϵ_i (i=1,2,3) are the equivalence parameters. Taking the difference between Eqs.(4.19) and (4.21),

$$M = \mathrm{DBP} - \mathrm{DBP}_{\mathrm{linear}}$$

$$= \frac{T}{r_o} + Jmg - \frac{\xi c_T \dot{z}^2}{V} + J(c_T \dot{z} + k_T z)$$

$$- (\epsilon_1 + \epsilon_2 \dot{z} + \epsilon_3 z) \tag{4.22}$$

where the function,M, is a stationary random process because of the stationarity of process,z(t). If the parameters ϵ_i are chosen so as to minimize M, $\mathrm{DBP}_{\mathrm{linear}}$ can be regarded as to be approximately equal to DBP. A natural optimization for the linearization is to choose ϵ_i so that $E[M^2]$ is minimized. This requires that

$$\left.\begin{aligned} \frac{\partial E[M^2]}{\partial \epsilon_1} &= 0 \\ \frac{\partial E[M^2]}{\partial \epsilon_2} &= 0 \\ \frac{\partial E[M^2]}{\partial \epsilon_3} &= 0 \end{aligned}\right\} \tag{4.23}$$

Substituting Eq.(4.22) into Eq.(4.23),

$$
\left.
\begin{aligned}
\frac{\partial E[M^2]}{\partial \epsilon_1} =& \epsilon_1 + \epsilon_2 E[\dot{z}] + \epsilon_3 E[z] + \frac{\xi c_T}{V} E[\dot{z}^2] \\
& - J\big(c_T E[\dot{z}] + k_T E[z] + mg\big) - \frac{T}{r_o} \\
=& 0 \\
\frac{\partial E[M^2]}{\partial \epsilon_2} =& \epsilon_1 E[\dot{z}] + \epsilon_2 E[\dot{z}^2] + \epsilon_3 E[z\dot{z}] + \frac{\xi c_T}{V} E[\dot{z}^3] \\
& - J\big(c_T E[\dot{z}^2] + k_T E[z\dot{z}] + mg E[\dot{z}]\big) - \frac{T}{r_o} E[\dot{z}] \\
=& 0 \\
\frac{\partial E[M^2]}{\partial \varepsilon_3} =& \epsilon_1 E[z] + \epsilon_2 E[z\dot{z}] + \epsilon_3 E[z^2] + \frac{\xi c_T}{V} E[z\dot{z}^2] \\
& - J\big(c_T E[\dot{z}z] + k_T E[z^2] + mg E[z]\big) - \frac{T}{r_o} E[z] \\
=& 0
\end{aligned}
\right\} \quad (4.24)
$$

Since the original surface profile is assumed to be a stationary Gaussian random process whose expected value is zero, the response, $z_{(t)}$, is also a stationary Gaussian random process having zero expected value and therefore,

$$
\begin{aligned}
E[z] &= 0 \\
E[\dot{z}] &= \frac{d}{dt} E[z] = 0 \\
E[\dot{z}z] &= R\dot{z}z(0) = \frac{d}{d\tau} Rzz(0) = 0 = E[z\dot{z}] \\
E[\dot{z}^3] &= \mu\, E[\dot{z}^2] + 2\sigma^2 E[\dot{z}] = 0
\end{aligned}
$$

where $R(\tau)$ = autocorrelation function

μ = $E[\dot{z}]$

σ^2 = standard deviation of $\dot{z}$

With regard to $E[z\dot{z}^2]$, the correlation coefficients between $z_{(t)}$ and $\dot{z}_{(t)}^2$ were investigated by applying random digit numbers generated by the computer since it is very complicated to analyze jointed random variables theoretically. Fig. 4.4.1 exhibits the results. Correlation coefficients, K, were computed twenty times with fifty random variables each. It was found that the coefficient lies in the range between $-0.2 < K < 0.2$. This means that the function, z, and the square of its derivative have little dependence. Thus, these two functions are assumed to be independent of each other. Then,

$$E[z\dot{z}^2] = E[z]\ E[\dot{z}^2] = 0$$

Therefore, Eqs.(4.24) can be simplified as:

$$\left.\begin{aligned}
\frac{\partial E[M^2]}{\partial \epsilon_1} &= \epsilon_1 + \frac{\xi c_T}{V} E[\dot{z}^2] - Jmg - \frac{T}{r_o} = 0 \\
\frac{\partial E[M^2]}{\partial \epsilon_2} &= \epsilon_2 E[\dot{z}^2] - Jc_T E[\dot{z}^2] = 0 \\
\frac{\partial E[M^2]}{\partial \epsilon_3} &= \epsilon_3 E[z^2] - Jk_T E[z^2] = 0
\end{aligned}\right\} \qquad (4.25)$$

Finally, the equivalence parameters, ϵ_i, are obtained as follows:

$$\left.\begin{aligned}
\epsilon_1 &= \frac{T}{r_o} + Jmg - \frac{\xi c_T}{V} E[\dot{z}^2] \\
\epsilon_2 &= Jc_T \\
\epsilon_3 &= Jk_T
\end{aligned}\right\} \qquad (4.26)$$

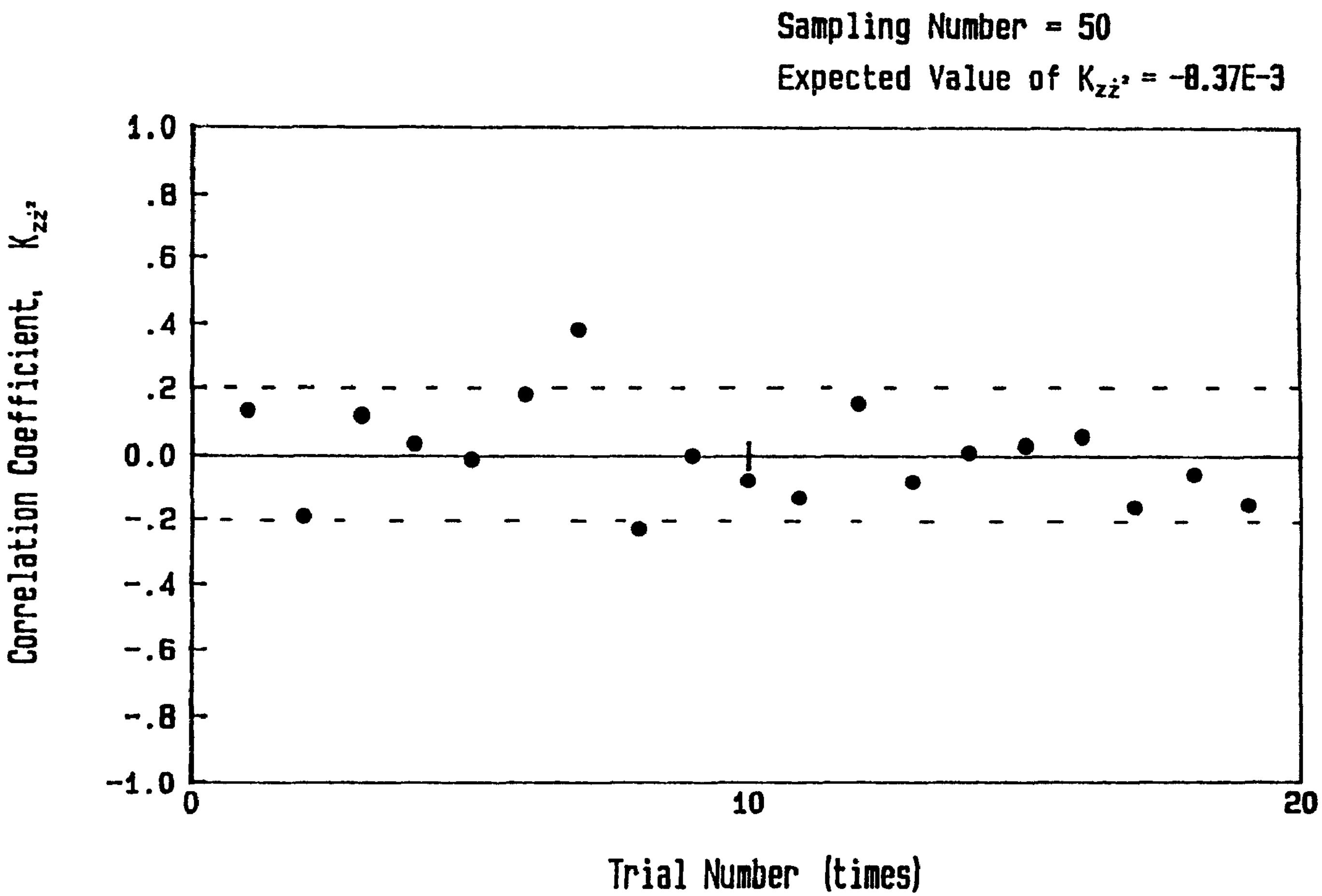

Fig. 4.4.1 Correlation coefficients between z and $(dz/dt)^2$

4.4.3 System Function

The system function representing a linearized relationship between the fluctuating component of the DBP and the original terrain surface irregularities ,y1, can be given by deriving the following individual transfer functions. That is,

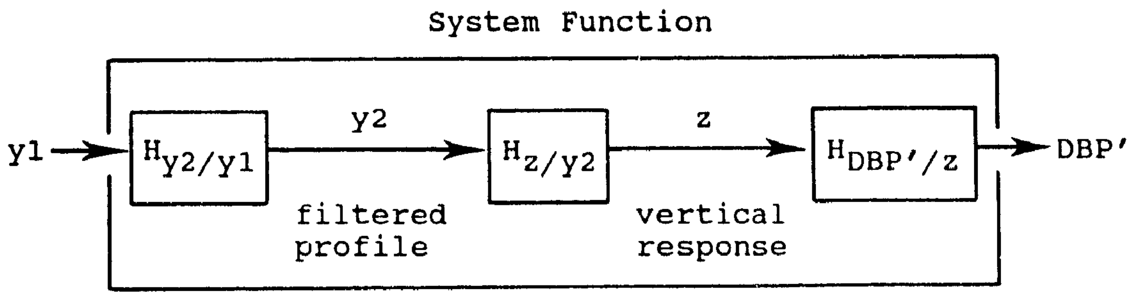

Fig. 4.4.2 Components of system function

(1) $H_{DBP'/z}$ (between variable DBP and vertical response of tyre axle)

Setting the second and third term in Eq.(4.21) as

$$DBP'_{(z(t))} = \epsilon_2 \dot{z} + \epsilon_3 z \qquad (4.27)$$

Performing the Laplace transform with the assumption that the initial values are zero, the transfer function between $DBP'_{(t)}$ and $z_{(t)}$ is obtained as follows.

$$H_{DBP'/z(s)} = \epsilon_2 s + \epsilon_3 \qquad (4.28)$$

where s is a Laplace operator and equal to $i2\pi f$.

(2) $H_{z/y2}$ (between the vertical response and filtered surface profile)

The transfer function will be derived by considering a simple one-degree-of-freedom vibration system shown in Fig. 4.4.3.

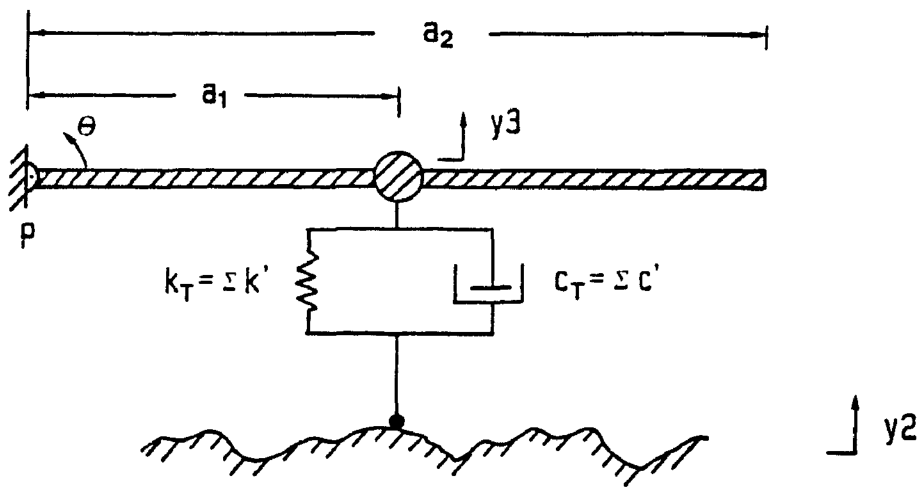

Fig. 4.4.3 Modeling of experimental rig

The equation of motion can be written as

$$I_o \ddot{\theta} + c_T a_1 (a_1 \dot{\theta} - \dot{y}2) + k_T a_1 (a_1 \theta - y2) = 0 \qquad (4.29)$$

where I_o is the moment of inertia about point P. Using the following relation, such that

$$\theta = y3/a_1$$

Eq.(4.29) can be rewritten as follows:

$$m_{eq} \ddot{y}3 + c_T(\dot{y}3 - \dot{y}2) + k_T(y3 - y2) = 0 \qquad (4.30)$$

where the equivalent tyre mass, m_{eq}, is

$$m_{eq} = I_o/a_1^2$$

Applying the Laplace transform to Eq.(4.30) in the same way,

$$(m_{eq}s^2 + c_T s + k_T)\ Y3_{(s)} = (c_T s + k_T)\ Y2_{(s)} \qquad (4.31)$$

Substituting

$$Z_{(s)} = Y2_{(s)} - Y3_{(s)}$$

into Eq.(4.31),

$$(m_{eq}s^2 + c_T s + k_T)\ Z_{(s)} = m_{eq}s^2\ Y2_{(s)} \qquad (4.32)$$

Thus, the transfer function between the tyre vertical response and the filtered terrain profile yields,

$$H_{z/y2(s)} = \frac{m_{eq}s^2}{m_{eq}s^2 + c_T s + k_T} \qquad (4.33)$$

(3) $H_{y2/y1}$ (between the filtered profile and the original terrain profile i.e. enveloping function)

As for the transfer function with regard to the tyre enveloping property, $H_{y2/y1(s)}$ is discussed in Chapter 3 and 7.

By multiplying these three transfer functions, the necessary system function can be finally obtained.

$$\left| H_{sy} \right| = \left| H_{DBP'/z} \cdot H_{z/y2} \cdot H_{y2/y1} \right| \qquad (4.34)$$

Fig. 4.4.4 compares the system functions for different translational velocity and tyre inflation pressure. Regarding the inflation pressure, it can be indicated that the lower inflated tyre generally exhibits the larger variation of the DBP because of a larger value of the system function. This is probably due to increased tyre flexibility. As for the effect of the translational velocity, a simple tendency cannot be derived from the Figure since its effect seems to be determined in combination with another factor's effect i.e. inflation pressure.

Note that this system function can only provide information of the variation of the DBP, not including the average value of the DBP. At natural frequencies, the system functions show their peak values in a lower range than 20 Hz although Fig. 4.4.4 shows only up to 10 Hz. When the excitation frequency from the ground meets with the natural frequency, the performance of the tyre is expected to be considerably reduced due to severe vertical vibration.

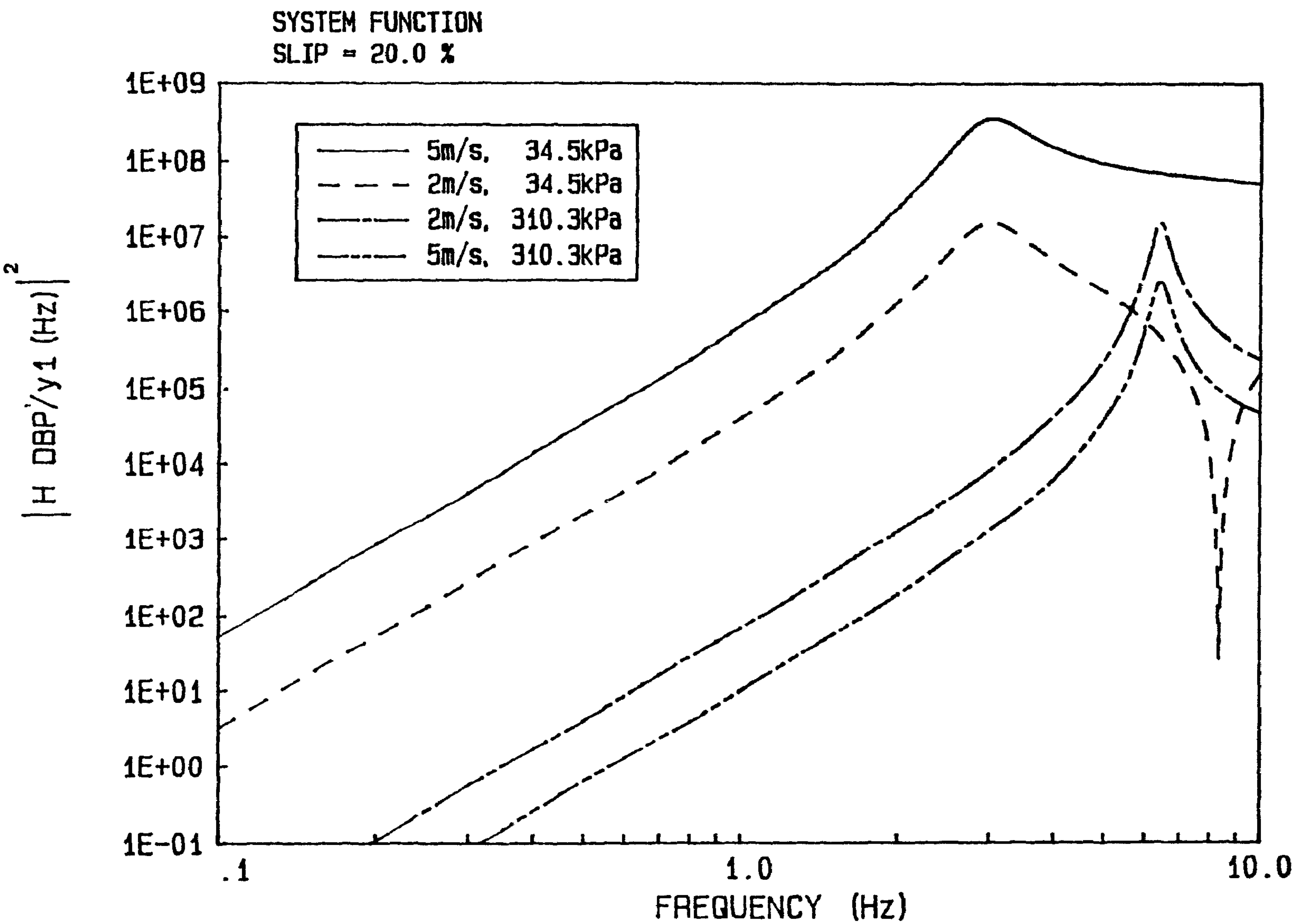

Fig. 4.4.4 Derived system functoins as a function of velocity and tyre inflation pressure

4.5 Nominal Tractive Efficiency

The tractive efficiency can represent vehicle tractive performance as a suitable evaluation index. It is, in general, expressed by the output/input power ratio as follows:

$$\eta = \frac{DBP \cdot V}{T \cdot \omega_T} \tag{4.35}$$

where DBP = drawbar-pull

V = translational velocity

T = input torque

ω_T = angular velocity of tyre

Under a static condition, this definition can be directly used without hesitation since all four parameters defining the efficiency are assumed to be constant. However, on a off-road terrain surface, whose surface is very rough compared with the on-road surface, it is expected that such variation of DBP becomes much larger. Therefore, it may be necessary to modify the equation slightly in order to compensate for the variation effect of the time-variant parameters in the case of dynamic operation situations on the rough roads, so that the practical evaluation of the off-road tyre performance can be made.

The DBP as a final output force can vary with time because of the continuous change of the power loss during motion, even though the input energy is controlled so that it is constant. Such time-dependent variable terms were shown in Eq.(4.19) in terms of tyre response, $z_{(t)}$. Fig. 4.5 demonstrates the comparison between the constant DBP developed on a theoretically flat and smooth ground surface and the fluctuating DBP developed on a rough terrain surface. It is found that the two different DBP curves illustrate the different tractive abilities of the tyre, even if their average values are the same. That is to say that curve B (variable DBP) produces randomly higher and lower values than its average DBP, whereas curve A (constant DBP) can consistently produce the effective DBP. This means that the potential performance expressed by the curve B is less than that by the curve A. In other words, curve B exhibits less efficiency than curve A.

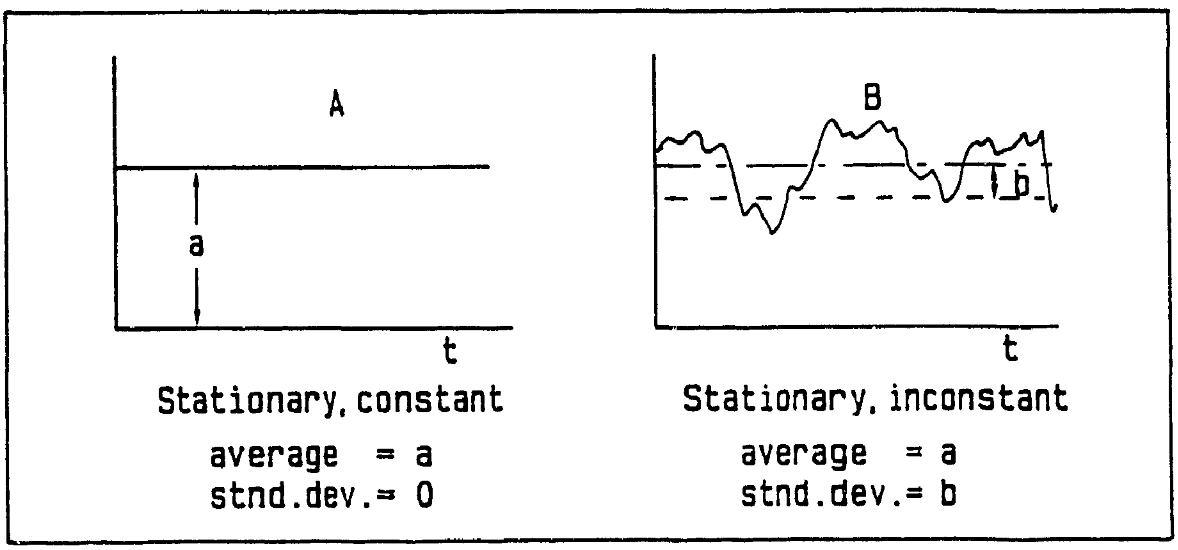

Fig. 4.5 Effect of constant DBP and variable DBP on vehicle performance

Therefore, in order to evaluate the tyre tractive performance on a rough road, a modification of the ordinary tractive efficiency is proposed in this study, by subtracting the standard deviation of the DBP from its average value. The nominal tractive efficiency is defined as follows:

$$\eta_n = \frac{(E[DBP] - \sigma_{DBP}) \cdot V}{T \cdot \omega_T} \tag{4.36}$$

where E[DBP] = mean DBP

σ_{DBP} = standard deviation of DBP

It should be noted that the average DBP can also be reduced by the increased tyre damping energy loss on rough ground, as shown in Eq.(4.26).

4.6 Summary

A predictive model which describes a flexible tyre moving on a rigid rough terrain was established. Using this model, the relationship between the resultant DBP and the terrain surface geometry was found, together with the energy conservation law. The effect of terrain roughness on tractive performance of tyre was expressed in terms of the system function in the frequency domain.

In order to evaluate the vehicle mobility on a rough road, the nominal tractive efficiency, which accounts for the variation of DBP, was proposed.

CHAPTER 5

PREDICTION OF NOMINAL TRACTIVE EFFICIENCY AS A FUNCTION OF SLIP FOR ROUGH NON-DEFORMABLE SURFACES

5.1 Introduction

The objective of this chapter is to illustrate the effect of slip rate on nominal tractive efficiency, using the system function. The effects of tyre inflation pressure, vehicle speed and terrain surface roughness are also introduced while further discussion about the effects of these parameters will be given in Chapter 7. Derivations of mean and standard deviation of DBP, which are required for the calculation of the nominal tractive efficiency, are shown in Appendix D.2.

Fig. 5.1.1 describes the classified terrain surfaces used in the computer simulation. Terrain surfaces are categorized as: i) deterministic rough surfaces and ii) non-deterministic (random) rough surfaces.

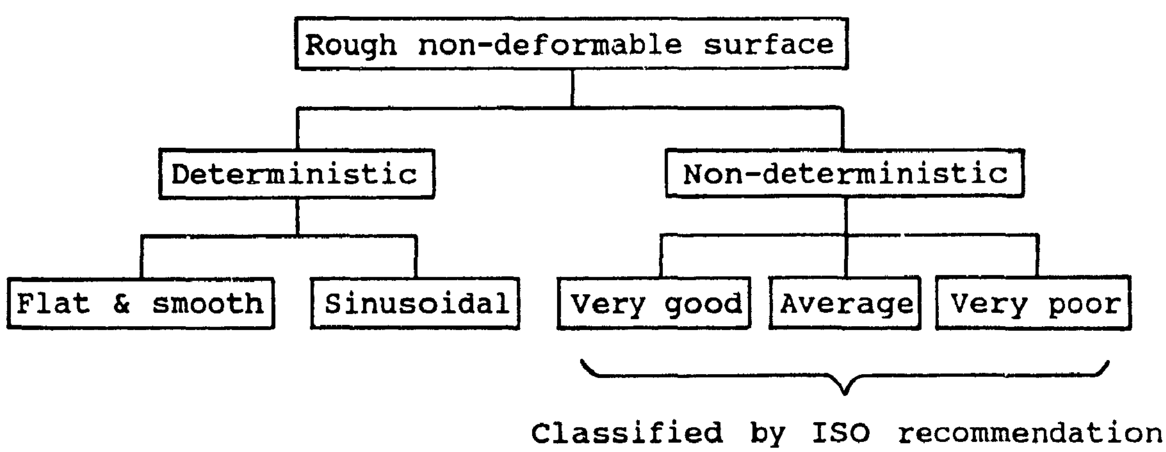

Fig. 5.1.1 Categorized surfaces for simulation

Fig. 5.1.2 illustrates the general flowchart for the simulation. The speed range in the computation was taken approximately between 1 m/s and 5 m/s (3.6km/h and 18km/h). This reflects the usual operational range of farm tractors. Here after, the term "tractive efficiency" or solely "efficiency" indicates the nominal tractive efficiency if no further explanation is given. In the simulation of this chapter, the following inputs are commonly used:

static load to the tyre axle	= 200.0 kg
tyre diameter	= 0.748 m
tyre section height	= 0.17 m
maximum input torque	= 330.0 N

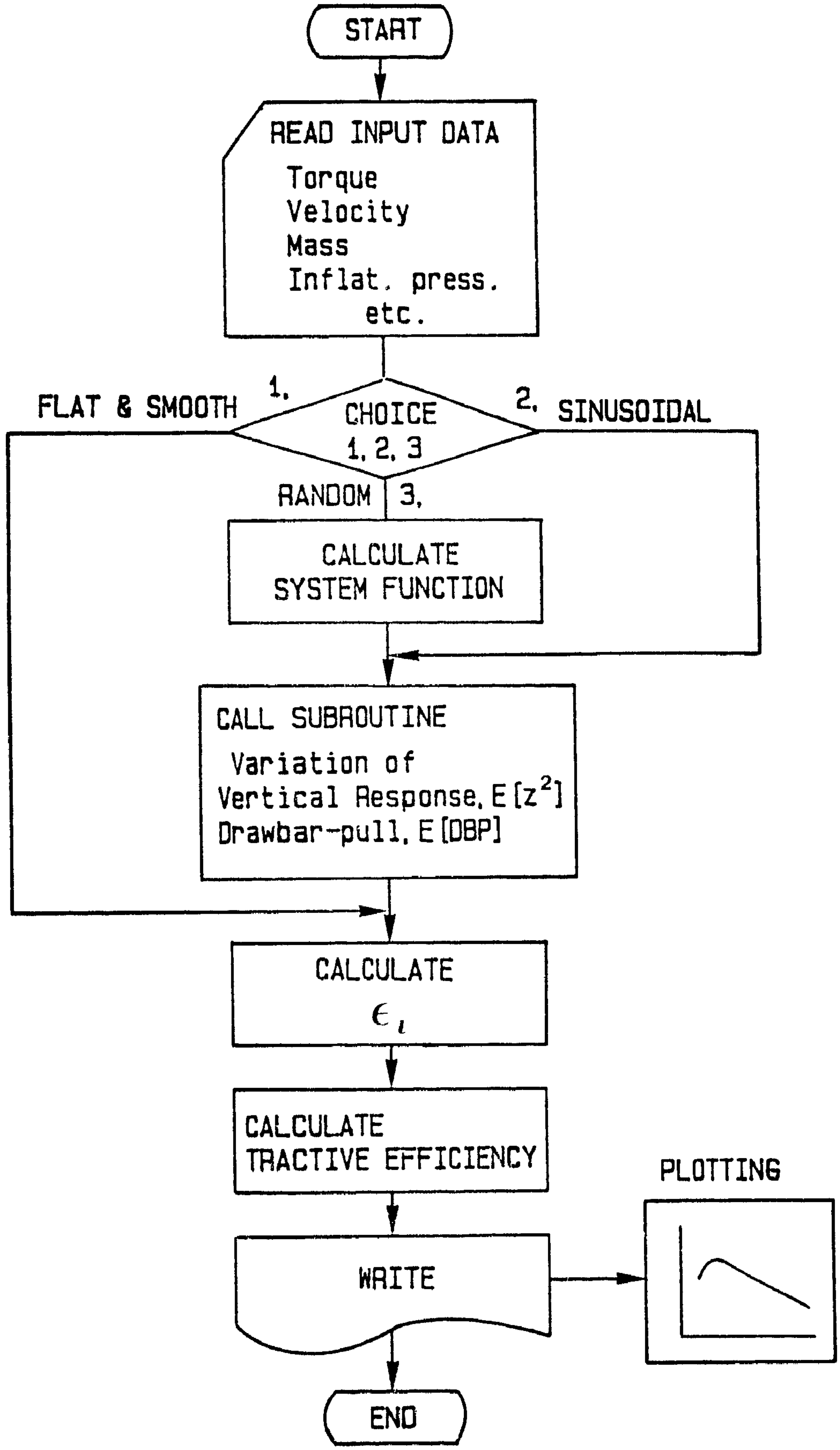

Fig. 5.1.2 General flow chart of computer simulation

5.2 Results for Deterministic Functioned Road Surfaces

5.2.1 Efficiency on a Flat and Smooth Road Surface

On this road surface, the average value of the DBP is immediately derived to be equal to ϵ_1 in Eq.4.26 since no vertical response of tyre, $z_{(t)}$, is theoretically expected.

$$E[\mathrm{DBP}] = \epsilon_1$$

$$= \frac{T}{r_o} + Jmg \tag{5.1}$$

where

$$J = \left(\frac{T}{8r_o^3} - \frac{\xi\, c_T\, \omega_T^2}{12V} \right) q^2$$

The standard deviation of the DBP is also zero.

$$\sigma_{\mathrm{DBP}} = 0 \tag{5.2}$$

The effect of slip rate on the tractive efficiency for a flat and smooth surface (F-surface) is demonstrated in Fig. 5.2.1 for different vehicle speeds (2 m/s and 5 m/s). Effect of three kinds of inflation pressures (310.3, 137.9 and 34.5 kPa) was also investigated. From Fig. 5.2.1, the following effects of each parameter can be briefly summarized.

For the slip rate, an optimum slip rate can be found to exist where the tyre can produce the highest tractive efficiency. The optimum slip rate tends to be increased when the tyre is deflated. The tractive efficiency is decreased with an increase of slip when it is greater than the optimum slip rate.

As for the effect of inflation pressure, a higher inflated tyre produces a higher tractive efficiency on a F-surface due to less rolling resistance. It is also indicated that the efficiency is significantly reduced as the tyre is deflated.

When a vehicle gains speed (comparison with Fig. 5.2.1a and b), the efficiency is decreased due to increased tyre deformation power loss. The reduction in efficiency is intensified with a decrease in inflation pressure. For the case of an extremely low inflation pressure (34.5 kPa), the efficiency is greatly decreased by the increased speed, as compared to other higher inflation pressures (310.3 and 137.9 kPa).

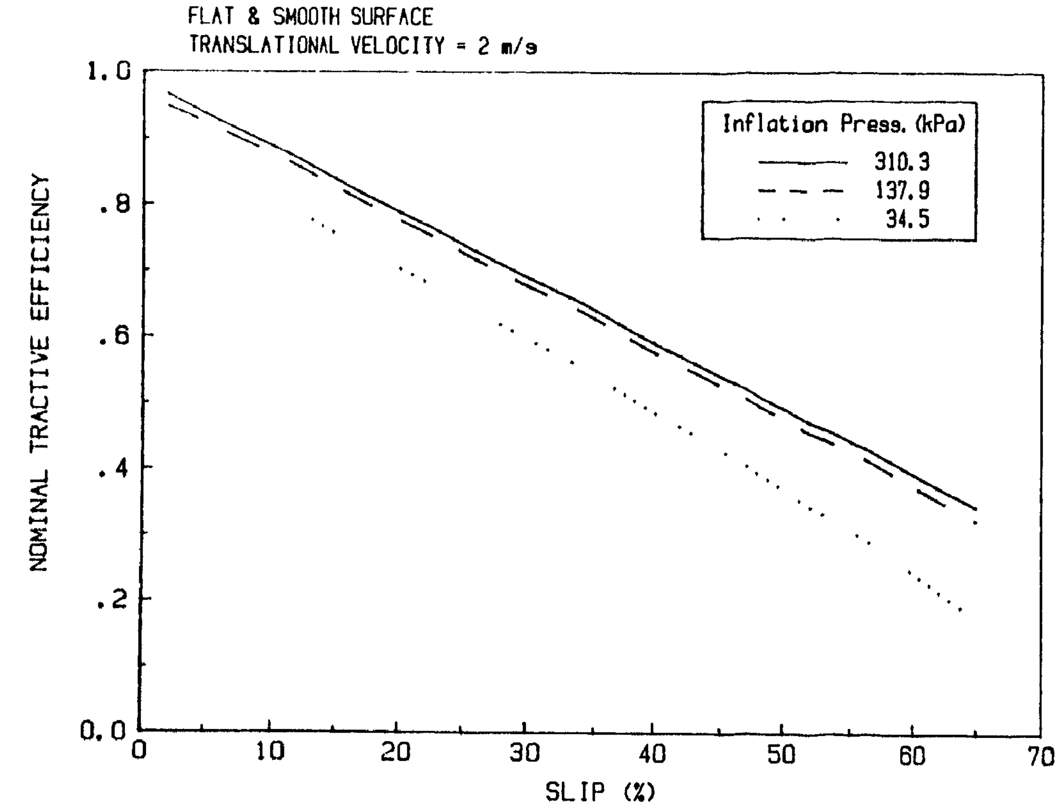

a. V=2 m/s

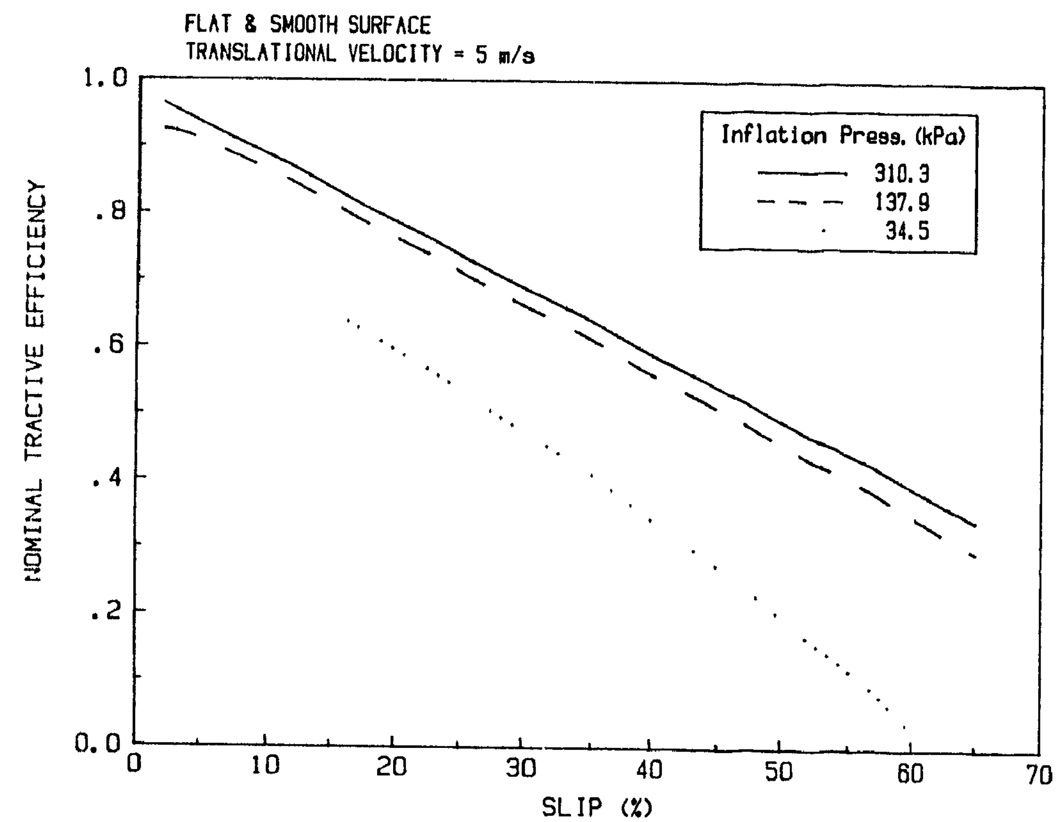

b. V=5 m/s

Fig. 5.2.1 Effect of slip rate on tractive efficiency for a flat and smooth road

5.2.2 Efficiency on a Sinusoidal Road Surface

The expected value and standard deviation of the DBP on a sinusoidal road surface (S-surface) is expressed as follows, respectively:

$$E[\mathrm{DBP}] = \frac{T}{r_o} + Jmg - \frac{\xi c_T}{V} E[\dot{z}^2] \tag{5.3}$$

$$\sigma_{\mathrm{DBP}} = \sqrt{\frac{1}{2}\ Z^2\ \{(\epsilon_2\omega)^2 + \epsilon_3^2\}} \tag{5.4}$$

where

$$Z = \frac{mh\omega^2}{\sqrt{(k_T - m\omega^2)^2 + (c_T\omega)^2}}$$

Fig. 5.2.2 depicts examples of the DBP variation with time, t, for three typical tyre inflation pressures on a S-surface. Peak-to-peak amplitude and the wavelength of the used S-surface were 0.04 m and 0.8 m respectively. The translational speed was 3 m/s (10.8 km/h) and the slip rate was set to 20%. As the tyre inflation pressure is deflated, variation of DBP is increased due to the increased tyre flexibility. Furthermore, it is indicated that the average value of the DBP is decreased. From this result, it is estimated that the tractive efficiency on a S-surface is more significantly decreased by reducing the tyre inflation pressure, compared to on a F-surface.

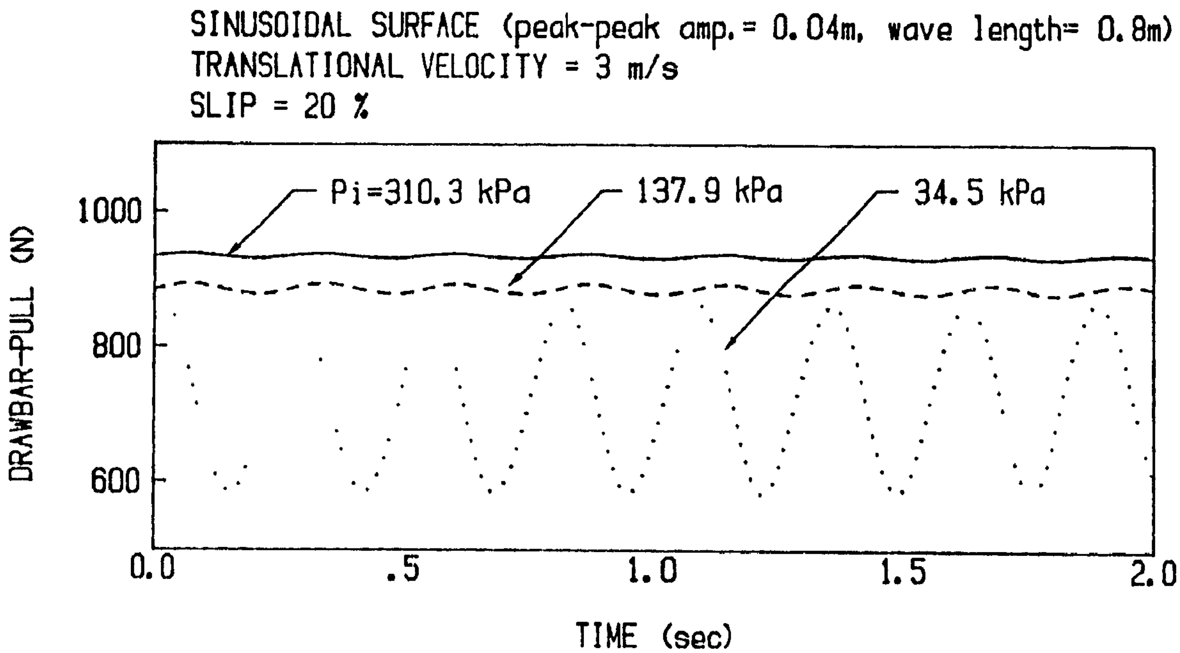

Fig. 5.2.2 Variation of DBP with time on a sinusoidal road surface

Fig. 5.2.3 shows the effect of slip rate on tractive efficiency on the same S-surface as before. The vehicle translational speeds are 2 m/s and 5 m/s. The effect of inflation pressure was also studied. From the results shown in Fig. 5.2.3, a similar trend in the effects of each parameter for the case of a flat and smooth surface is obtained. However the effects of inflation pressure and speed are more intensified on the sinusoidal surface.

As a general tendency, on a rigid S-surface, the optimum slip rate is slightly increased as compared to the slip rate on the F-surface, for both speeds. This may be explained by the requirement of larger input energy on a S-surface. On a sinusoidal waved ground surface, a marginally higher slip rate than that for an F-surface is preferable for achieving the effective work. The efficiency is decreased over a whole range of slip compared to an F-surface because of increased tyre deformation power loss due to vertical motion of the tyre. Increase in optimum slip rate is more conspicuous at a higher speed.

With regard to the inflation pressure, its effect is more evident on the S-surface than on the F-surface. Tractive efficiency is substantially decreased when the inflation pressure is 34.5 kPa.

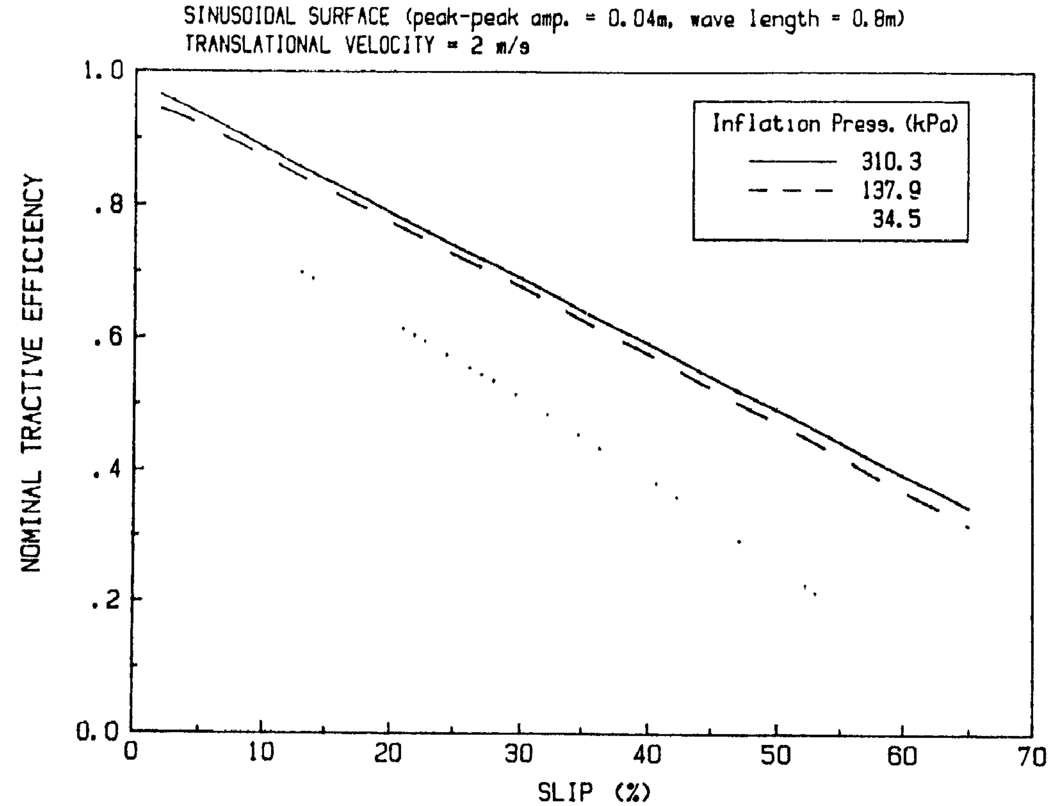

a. V=2 m/s

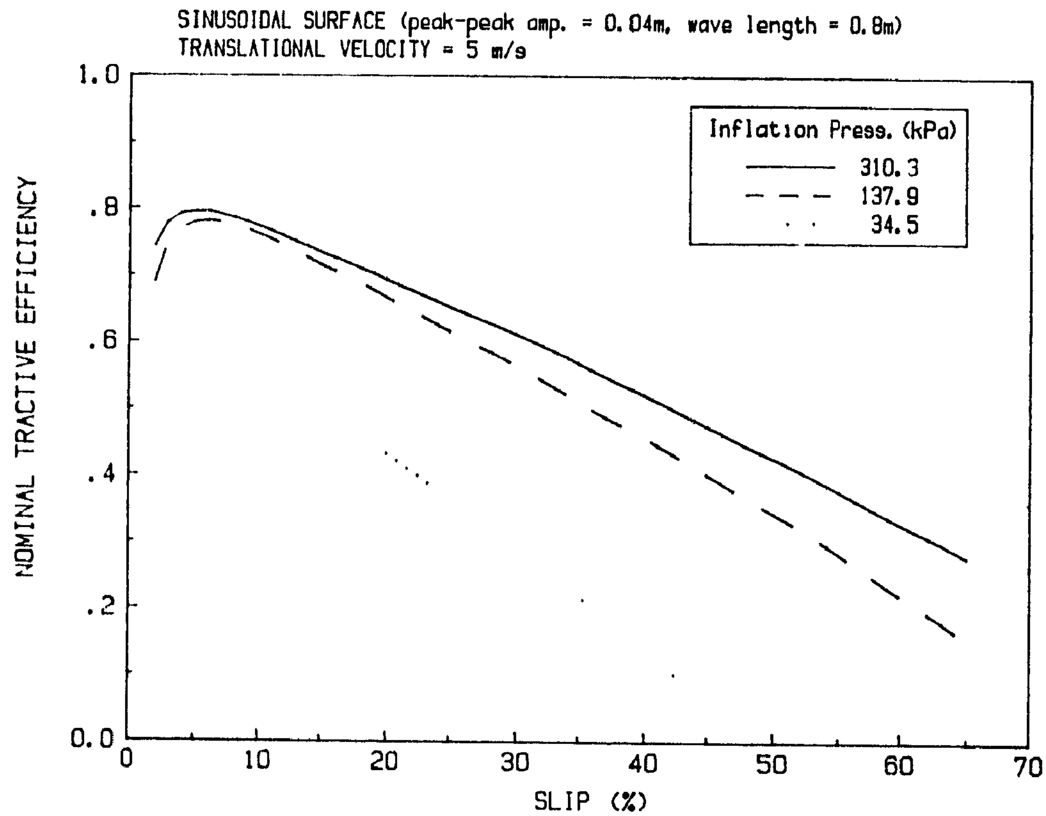

b. V=5 m/s

Fig. 5.2.3 Effect of slip rate on tractive efficiency for a sinusoidal road

5.3 Results for Non-deterministic Functioned Road Surfaces

5.3.1 Random Rough Road Surface used in the Simulation

Although an approximate expression for a random rough ground profile has been introduced with a combination of the sinusoidal waves considering their dominant amplitudes, wavelengths and frequencies included in that profile (Wendenborn,1966; Lesage and Yong,1987), the expression in the frequency domain will be used due to its simple handling and universality.

In the space domain, which is independent of the vehicle velocity, the PSD function of the ground surface profile can be expressed as follows:

$$S_{(\Omega)} = G_o \Omega^{-n} \tag{2.6}$$

where $S_{(\Omega)}$ = one-sided PSD function of ground surface

G_o = roughness constant

Ω = spatial frequency (c/m)

n = slope constant (normally $1.5<n<2.5$)

The values of Go and n vary for different road roughness. The slope constant is usually assumed in many studies to be n=2, as derived from measured elevation profiles of a number of grounds (Segel and Lu,1982; Beres̀,1987) though ISO recommended n as 1.5 over frequencies of more than $1/2\pi$ c/m (corresponding to the road profile wavelength of 6.3 m). As for the roughness constant, it varies from 1.27E-7 to 1.30E-4 ("very good" to "very poor"), according to ISO recommendations. Table 5.1 shows the range of Go values for various types of rough roads.

Table 5.1 Range of Go value by ISO (Ω >1/2π c/m) (after ISO draft)

Type of surface	Go
Very Good	1.27E-7 - 5.08E-7
Good	5.08E-7 - 2.03E-6
Average	2.03E-6 - 8.13E-6
Poor	8.13E-6 - 3.25E-5
Very Poor	3.25E-5 - 1.30E-4

Typical values of Go and n corresponding to several types of roads were suggested by Wendenborn (1966); Robson and Kammash (1977) and Van Deusen (1965) as shown in Table 5.2.

Table 5.2 Go and n values of various roads reported by several authors

Type of Road	Go	n
First Class Road Secondary Road Farm Road	Average 8E-6 Average 6E-5 Average 6E-4 after Wendenborn	N/A
Mortorway Principal Road Minor Road	3E-8 - 5E-7 3E-8 - 8E-6 5E-7 - 3E-5 after Robson and Kammash	2.5
Paved Road	1.2E-6	2.1
Unpaved, with gravel	1.1E-5	2.1
Unpaved, waved	3.7E-6	2.4
Unpaved, rough	2.0E-6	3.8
Virgin, cross-country	1.6E-3 after Van Deusen	2.0

Considering the above-noted results, three different rough road surfaces were selected in the computer simulation for the purpose of comparison of their roughness effect. They are classified as "very poor", "average" and "very good" surfaces according to their Go and n values. Fig. 5.3.1 shows the Go and n values of each surface and their PSD curves in the log-log scale. A rougher road has more power than does a smoother road. The larger contribution of the power lies normally in the lower frequency range.

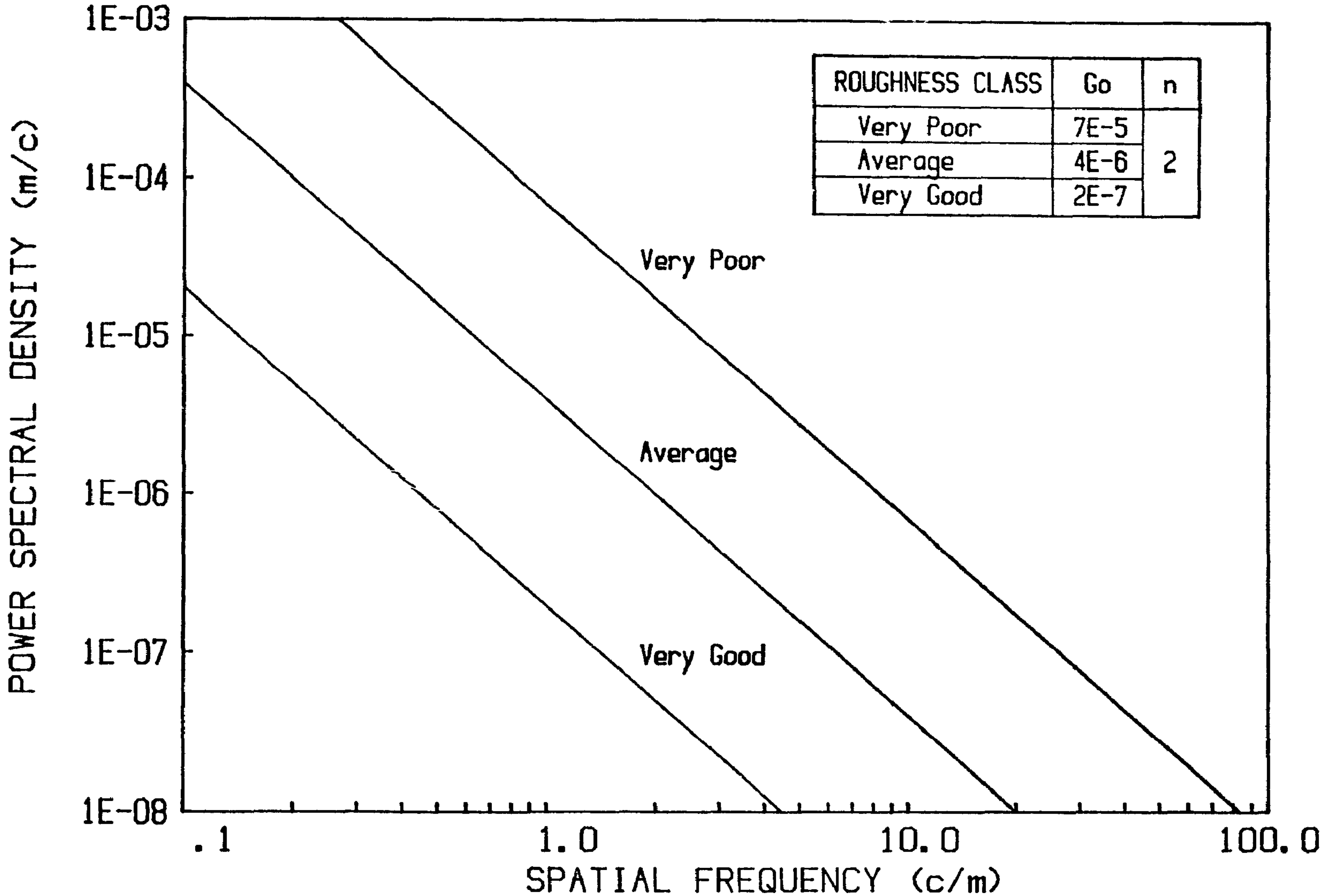

Fig. 5.3.1 PSD curves and Go, n values for three rough roads used in computer simulation

Although the amplitude PSD function of the ground surface was expressed in terms of the spatial frequency, it is preferable to convert it into an expression in terms of the time dependent frequency if the system response spectra are to be established over a fixed temporal frequency range. In the simulation, the range between 0.1 Hz and 20 Hz was determined to be the principal interest frequency range for off-road vehicle mobility dynamics, in reference to other studies (Robson and Kammash,1977; Wong,1970).

The PSD function of the original ground surface in terms of the spatial frequency can be converted into the PSD in terms of the temporal frequency, using the following relationships, previously mentioned in Chapter 2.

$$f = V\Omega \tag{2.3}$$

$$S_{(f)} = \frac{1}{V} S_{(\Omega)} \tag{2.4}$$

Consequently, the PSD function in terms of the temporal time-dependent frequency can be written in the following velocity-dependent manner.

$$S_{(f)} = G_o V^{n-1} f^{-n} \tag{5.5}$$

If n=2, Eq.(5.5) yields to

$$S_{(f)} = G_o V f^{-2} \tag{5.6}$$

Eq.(5.6) indicates an interesting relationship between the PSD function and the translational velocity. The level of the input to the system is directly proportional to vehicle speed. If the system is linear, it is expected that the dynamic response of the tyre will increase in direct proportion to the speed.

5.3.2 Efficiency on a Randomly Rough Road Surface

The mean value of the DBP on a randomly rough road surface is expressed using Eq.(D.2.15) as follows:

$$E[\mathrm{DBP}] = \frac{T}{r_o} + Jmg - \frac{\xi c_T}{V} \int_{f_1}^{f_2} S_{(z(f))} \quad df \tag{5.7}$$

where f_1 and f_2 are banded to 0.1 Hz and 20 Hz respectively in this study. The standard deviation of the fluctuated DBP is given by integrating the PSD over a bandwidth between f_1 and f_2.

$$\begin{aligned} \sigma_{\mathrm{DBP}} &= \sqrt{\int_{f_1}^{f_2} S_{\mathrm{DBP'}(f)} \quad df} \\ &= \sqrt{\int_{f_1}^{f_2} |H_{sy}|^2 \, S_{y1(f)} \quad df} \end{aligned} \tag{5.8}$$

The effect of slip rate on the tractive efficiency for different rough road surfaces is plotted in Fig. 5.3.2. The translational velocity is 5 m/s. Three different inflation pressures (310.3, 137.9 and 34.5 kPa), as well as the previously mentioned case, were applied for comparison of their effect. Comparing the predicted results, the following were obtained.

A clear difference in the efficiency between a "very good" surface and a "very poor" surface can be seen while very little difference is shown between a "very good" surface and an "average" surface. From this point of view, it is surmised that the tractive efficiency starts to decrease abruptly when road roughness exceeds a certain value. The efficiency, of course, becomes lower on a rougher ground surface.

Optimum slip rate increases when the ground surface condition becomes poorer. The optimum slip rate for a rougher surface and/or lower inflated tyre is larger than that for a smoother surface and/or higher inflated tyre. This is probably due to the need for a larger input energy on such conditions. It is also found that the optimum slip rate lies between 2% and 10% approximately, for a rough road within the range from a "very good" to a "very poor".

With regard to the inflation pressure, the low inflated tyre exhibited less tractive efficiency over the whole slip range. The effect of inflation pressure on efficiency is exponentially intensified by the roughness of the ground surface. This is significant when the tyre inflation pressure is low, in spite of the greater enveloping effect of a pneumatic tyre.

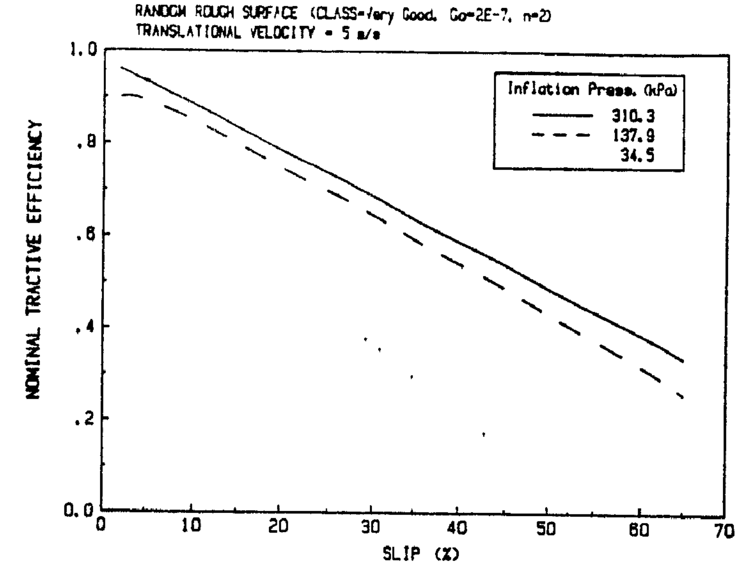

a. Very good surface

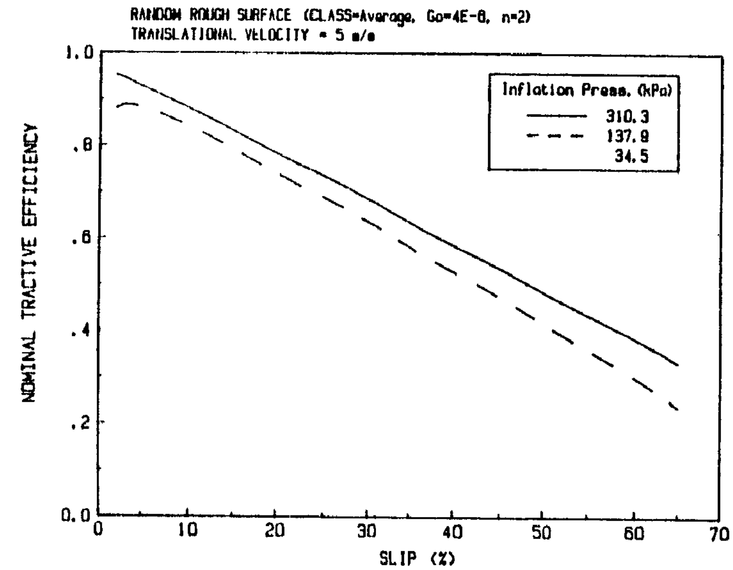

b. Average surface

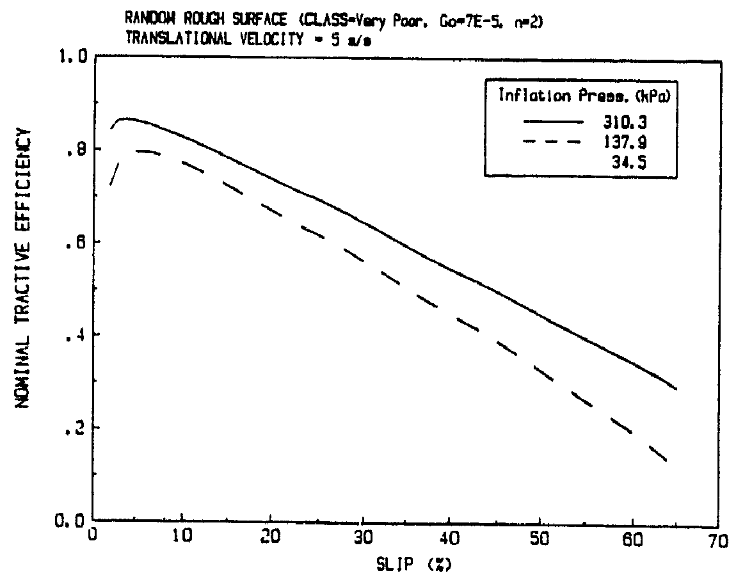

c. Very poor surface

Fig. 5.3.2 Effect of slip rate on tractive efficiency for a random rough road

5.4 Summary

Considering predicted results of tractive efficiency on deterministic and non-deterministic road surfaces, the following may be summarized as general effects of each parameter:

(1) slip rate

The tractive efficiency is reduced with an increase of tyre slip due to increased interfacial energy loss, although the highest efficiency is given at an optimum slip rate. Optimum slip rate tends to increase for a rougher surface, low inflated tyre and higher operational speed.

(2) inflation pressure

Higher efficiency is achieved with a highly inflated tyre. As inflation pressure is decreased, the efficiency is dramatically decreased by increased rolling resistance.

(3) vehicle speed

Vehicle speed considerably affects efficiency when the ground surface is rough or when the inflation pressure is low.

(4) ground roughness

Lower tractive efficiency is produced on a rougher ground. The nonlinear relationship between the efficiency and the ground roughness, vehicle speed and inflation pressure can be estimated.

PART II EXPERIMENTAL CONSIDERATIONS

CHAPTER 6

PNEUMATIC TYRE TESTS ON ROUGH NON-DEFORMABLE SURFACE

6.1 Introduction

The laboratory experiments performed in this study are directed towards the investigation of the effect of surface roughness on pneumatic tyre performance. Because of the nature of this study, some prior experimental results are necessary in order to develop a model which mimics pneumatic tyre performance. The correlation between theoretical and experimental analysis in this study is shown in Fig. 6.1. All the experiments performed were designed to serve the following objectives:

(1) To study the behavior of the pneumatic tyre under varying vertical dynamic loads and different inflation pressures,

(2) To investigate the tyre enveloping property together with the effect of inflation pressure,

(3) To evaluate the effect of traction surface roughness on the tractive efficiency through the change in amount of energy wasted in slip and deformation of the tyre, and

(4) To validate the proposed analytical model for predicting the tyre mobility performance on rough non-deformable terrain.

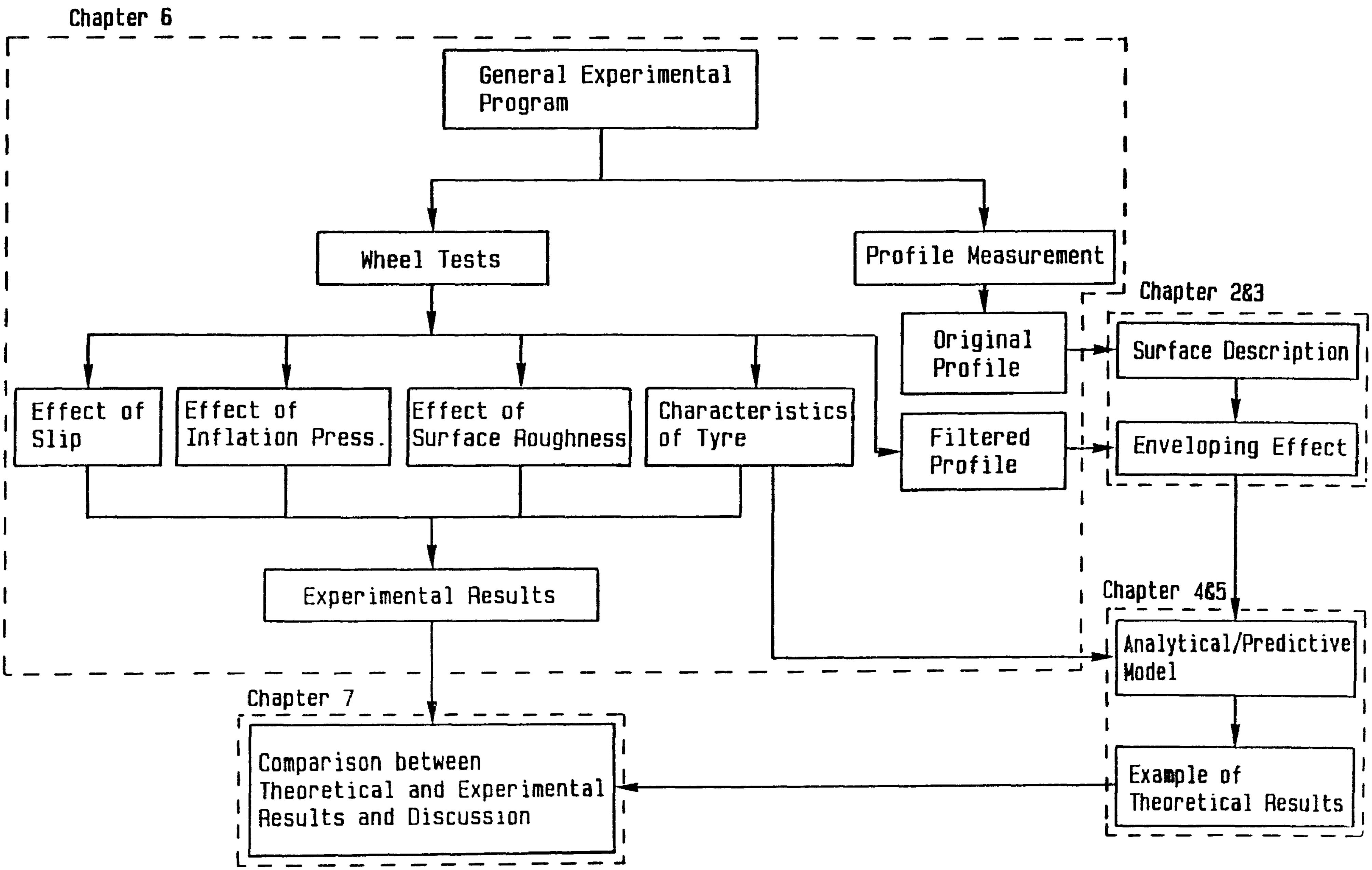

Fig. 6.1 Schematic representation of relationship between experimental and theoretical programs

6.2 Experimental Program

The outline of the experimental program of this study is illustrated in Fig. 6.2. The experiments can be categorized into three major divisions, namely:

(1) <u>Non-rolling tyre tests</u> (investigation of mechanical properties of a tyre)

The tyre is kept stationary without any rotational or translational motion, and it is further divided into:

a. static tests

The tested tyre is loaded through its axle by a compression machine with the tyre resting on top of a rigid unyielding surface. The mechanical properties such as tyre stiffness and contact length coefficient are found by investigating the load-deformation relationship and load-contact area relationship individually.

b. dynamic tests

The tyre having freedom of vertical motion is mounted on a hard unyielding flat surface. Its damping constant can then be calculated by measuring the decay of vertical vibration of the tyre axle after applying an impulse.

(2) <u>Terrain surface profile measurement</u>

In essence, this information is regarded as input data to the tyre-rough terrain system. An ultrasonic distance detector is used for the surface profile measurement in the laboratory.

(3) <u>Rolling tyre tests on rigid unyielding surfaces</u>

These tests are performed in order to consider (a) the tyre enveloping property and (b) the effect of rigid off-road surface profile on the tyre mobility performance, relative to the tractive efficiency.

The controlling parameters which are selected to be variable in the experiments are:

(1) Random profile of rigid traction surface (arbitrary amplitude from a reference plane)

(2) Tyre inflation pressure and angular velocity.

Specifications of the pneumatic tyre used in the test are shown in Table 6.1.

Table 6.1 Specifications of tyre used in laboratory test

Name of tyre	Michelin 7:00 R16 XCL
Diameter	0.748 m
Rim diameter	0.408 m
Section height	0.170 m
Width	0.114 m
Construction	Radial, 6ply
Surface condition	Buffed

The experimental results will be presented subsequently and analyzed where appropriate.

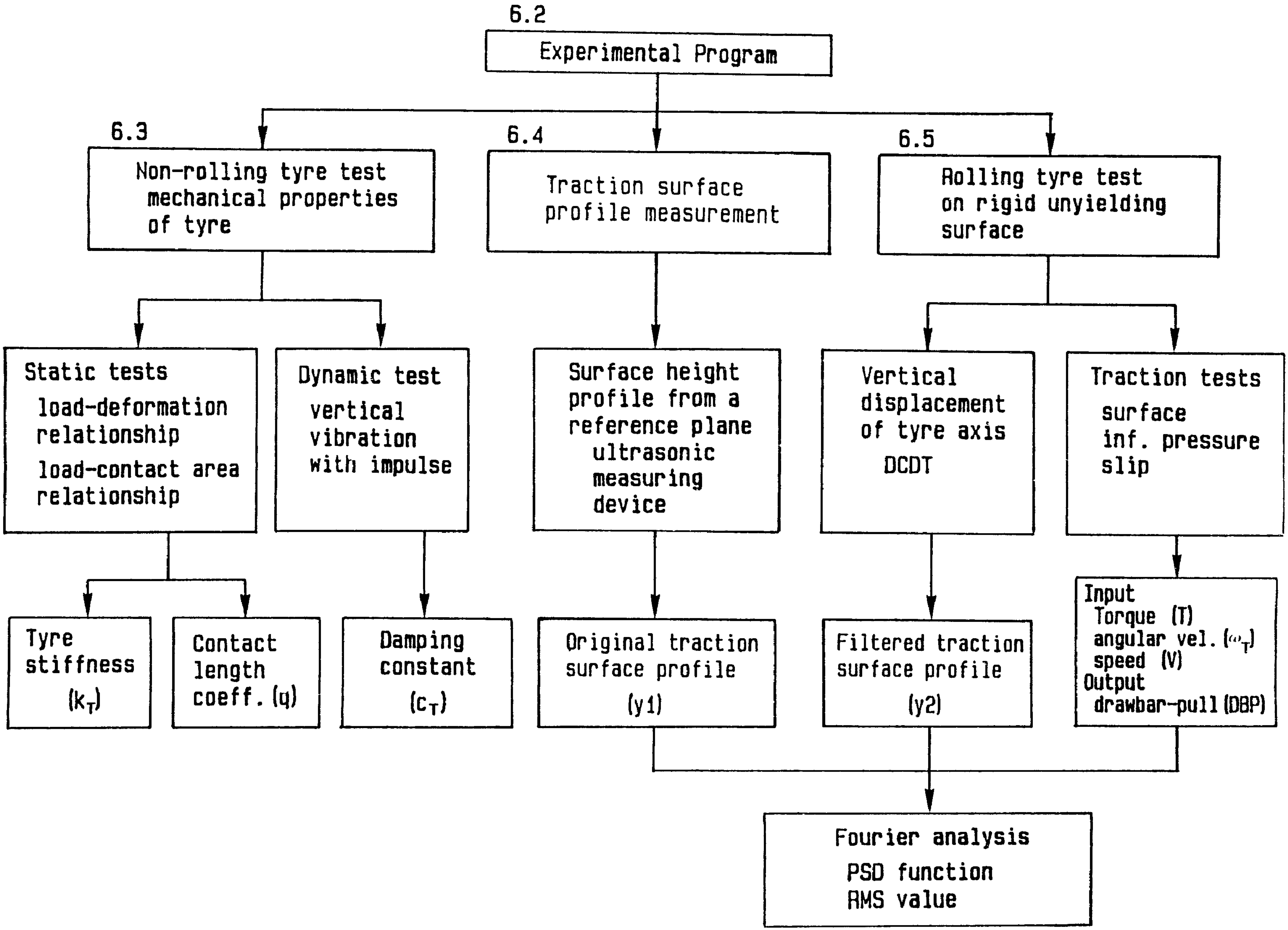

Fig. 6.2 Experimental program

6.3 Non-rolling Tyre Tests on a Smooth, Non-deformable Surface (Mechanical Properties of Pneumatic Tyre)

It is well known that a pneumatic tyre usually contains a variety of rubber compositions, fabric, beads and other components which contribute to overall tyre performance. It is difficult to know a tyre's properties precisely since the tyre exhibits complex combined mechanical and/or chemical characteristics. However it is important and necessary to investigate those properties since the difference in characteristics of tyres is expected to considerably affect the performance on a rough road as opposed to a flat, smooth road because of the dynamic vertical motion of a tyre. In this study, inflation pressure is selected as an indexing parameter for several kinds of mechanical properties of pneumatic tyres since it directly influences the response characteristics of the tyre.

Basic properties of tyre compounds, especially nonlinear characteristics of mechanical properties such as frequency, load or velocity dependence will be presented in Appendix C.

6.3.1 Static Tests for Tyre Stiffness and Contact Length Coefficient

The tyre stiffness and the contact length coefficient as a function of the tyre inflation pressure are investigated by the load-deformation test and load-contact area test, respectively.

(1) Load-deformation relationship

Depending upon the test conditions, three different types of tyre stiffness are generally defined.

a. Rolling dynamic stiffness

This stiffness may represent the most practical value of a rolling tyre in the actual operational condition (bumping). The rolling dynamic stiffness is a function of the rotating speed of the tyre and of the exciting trequency (see Fig. C.4 in Appendix C). The rolling dynamic stiffness is thus usually determined by measuring the response of a rolling tyre to a known harmonic excitation. The response is normally measured at the tyre hub and excitation is given at the tread band. Taking the ratio of output response to input excitation, the rolling dynamic stiffness is determined.

b. Non-rolling dynamic stiffness

Several methods are available for this stiffness. One of the simplest is the so-called "drop test".

In this test, a tyre with a certain load is allowed to fall freely from a height at which the tyre is just in contact with the ground, so that the tyre always remains in contact with the ground during the test. The trajectory of vertical displacement of the hub is recorded. Then the value of the non-rolling dynamic stiffness can be determined with its vibrational period of decay trace.

c. Static stiffness

In this study, the static stiffness is adopted as the tyre stiffness because of a limitation in test equipment and a comparatively small difference in the values (10-15%) between the dynamic and the static stiffness for a slowly rotating off-road tyre (Matthews and Talamo, 1965).

Experimental method

Both vertical deflection of a tyre and vertical loads are measured and plotted simultaneously. The static stiffness is determined from the slope of the derived curve. The test facility used is shown in Fig. 6.3.1. The vertical deflection of the pneumatic tyre and corresponding contact area together with applying load are measured separately by using the Instron loading machine.

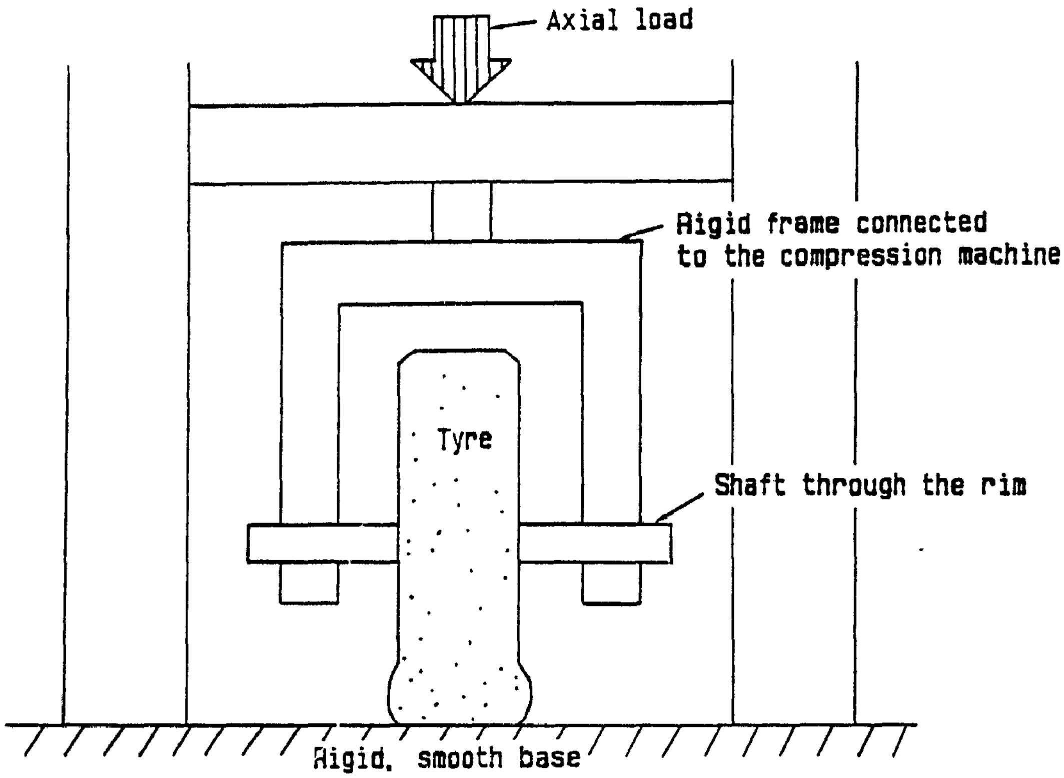

Fig. 6.3.1 Instron loading machine for investigation of deflection characteristics of tyre

In measuring tyre deformation and contact area under a vertical load, the tested tyre was loaded through the wheel axle by using a rigid frame connected to a loading machine. The inflation pressures of the tyre were measured by an electrical pressure gauge. The contact areas for different inflation pressures were measured with various loads.

Experimental results

Fig. 6.3.2 shows the experimental results for the static load-deformation characteristics. It is clear that the tyre deformation increases almost linearly with applied vertical load as reported elsewhere

(Clark, 1971), and curves for a highly inflated tyre indicate stiffer characteristics.

Several empirical equations for a nonlinear load-deflection relationship have been introduced (Ariano, 1933; Hadekel,1952). Although the nonlinear characteristics of tyre stiffness are still valid for a large deflection, linearity could be held for a relatively small deflection under the normal operation range of a tyre. Accordingly, the static tyre stiffness can be derived assuming a linear relationship between the applied vertical load and the tyre deflection. The equation indicating the load-deflection relationship can be expressed in the following simple form.

$$N = k_{T(Pi)} D \tag{6.1}$$

where $k_{T(Pi)}$ is the static tyre stiffness which is a function of inflation pressure, P_i (Pa), D is the vertical deflection of the tyre and N is the vertical load applied to the tyre axle.

The empirical relationship defining tyre stiffness for the specific tyre (Michelin 7:00 R16 XCL radial, buffed) can be determined from Fig. 6.3.3 as follows:

$$k_T = 30000 + 0.773\, P_i \qquad (N/m) \tag{6.2}$$

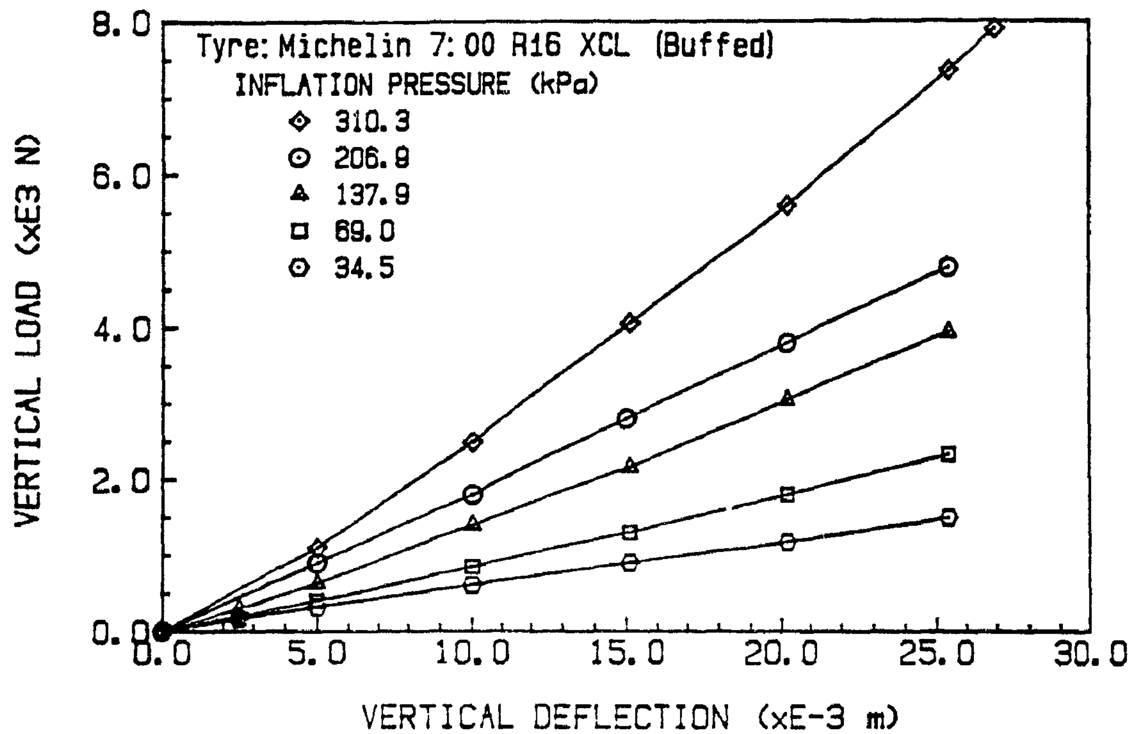

Fig. 6.3.2 Load-deflection curves for various inflation pressures

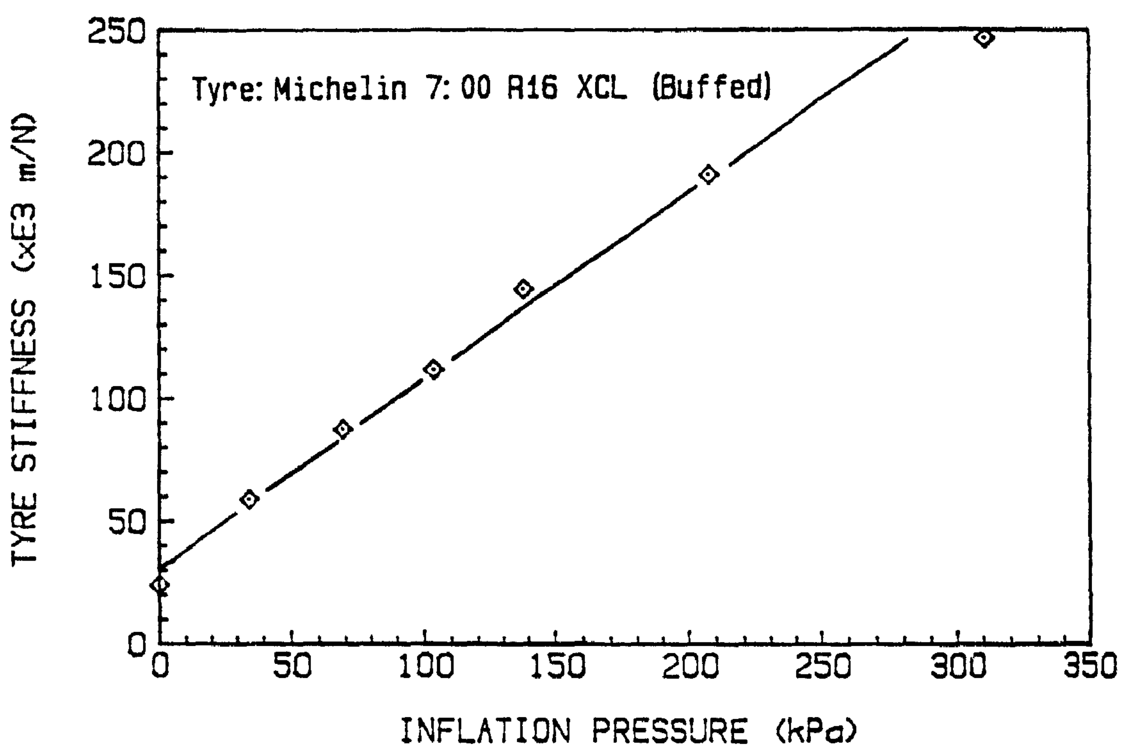

Fig. 6.3.3 Tyre stiffness as a function of inflation pressure

(2) Load-contact length relationship

Experimental method

The contact length,2d, between the tyre and the rigid flat smooth surface is derived based on an assumption of constancy of the width of contact area under varying loads. The measurement of contact area was performed by reading the size of the tyre foot print after spraying around the contact area under a specific load.

Experimental results

Fig. 6.3.4 compares the size of the foot prints for different inflation pressures under the same vertical load of 1.64 kN. Each foot print exhibits almost the same contact width and the lower inflated tyre has a longer contact length. Sets of experimental load-contact area curve are shown in Fig. 6.3.5. Since the contact length is expected to be a function of the tyre inflation pressure, the relationship between the contact length coefficient (defined in Chapter 4) and the inflation pressure is investigated. The contact length coefficient exhibits a nonlinear characteristic with respect to inflation pressure as shown in Fig. 6.3.6. This coefficient was also investigated for a different tyre (not shown here) and also showed a similar nonlinear tendency.

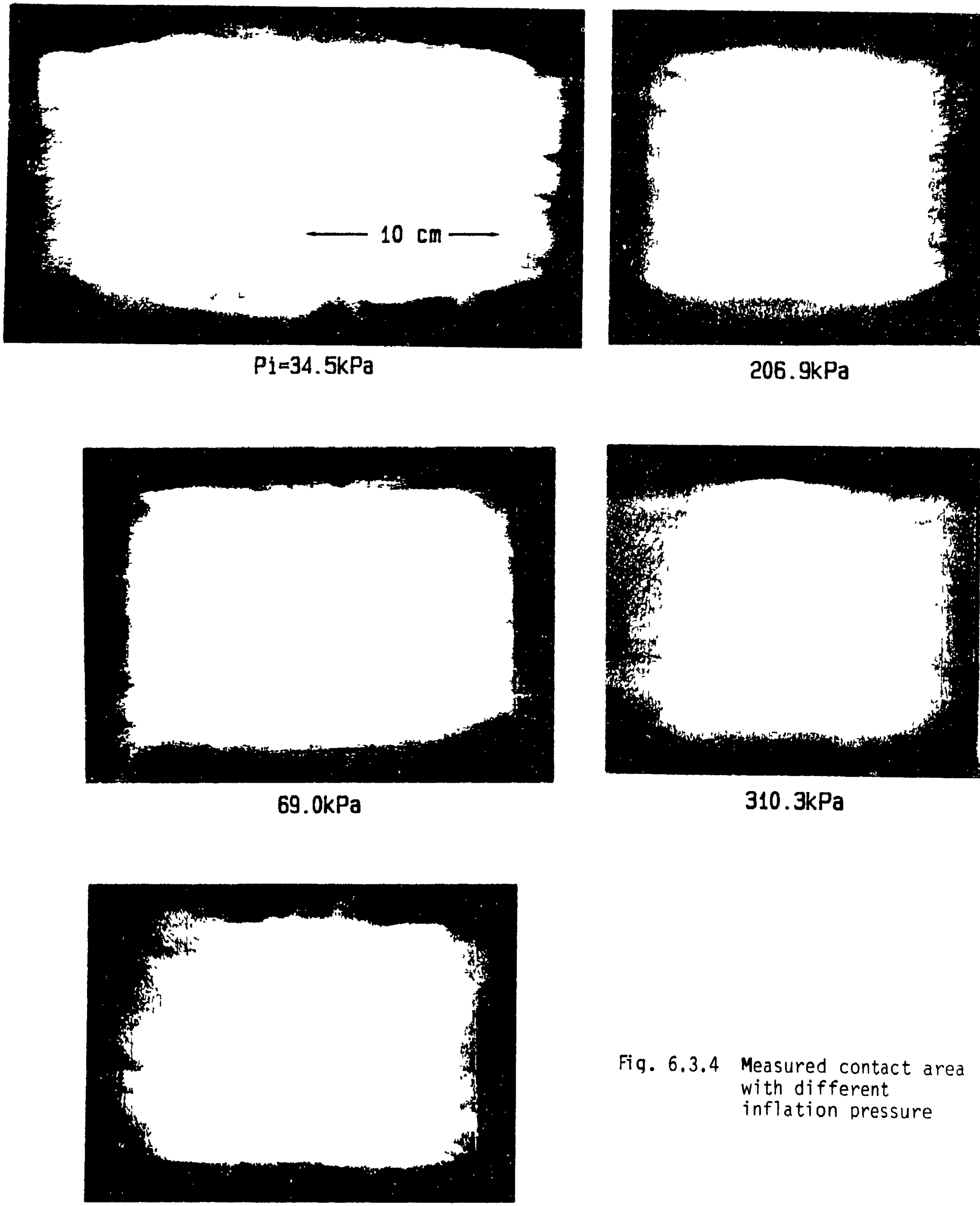

Fig. 6.3.4 Measured contact area with different inflation pressure

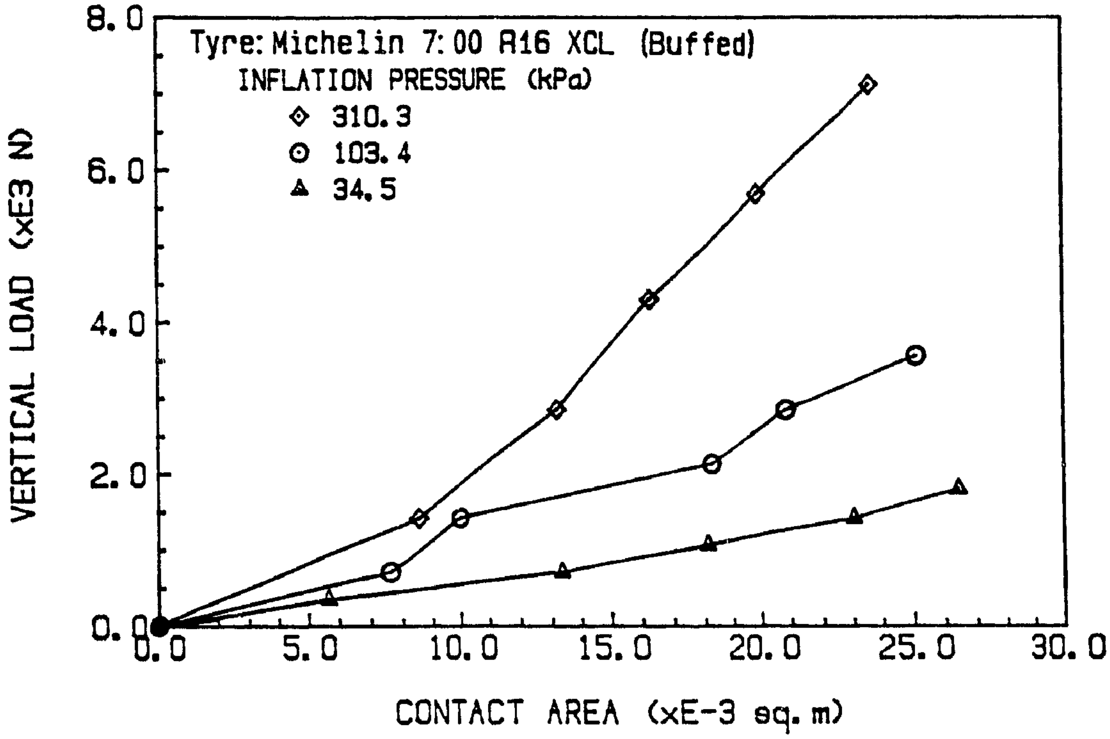

Fig. 6.3.5 Load-contact area curves for various inflation pressures

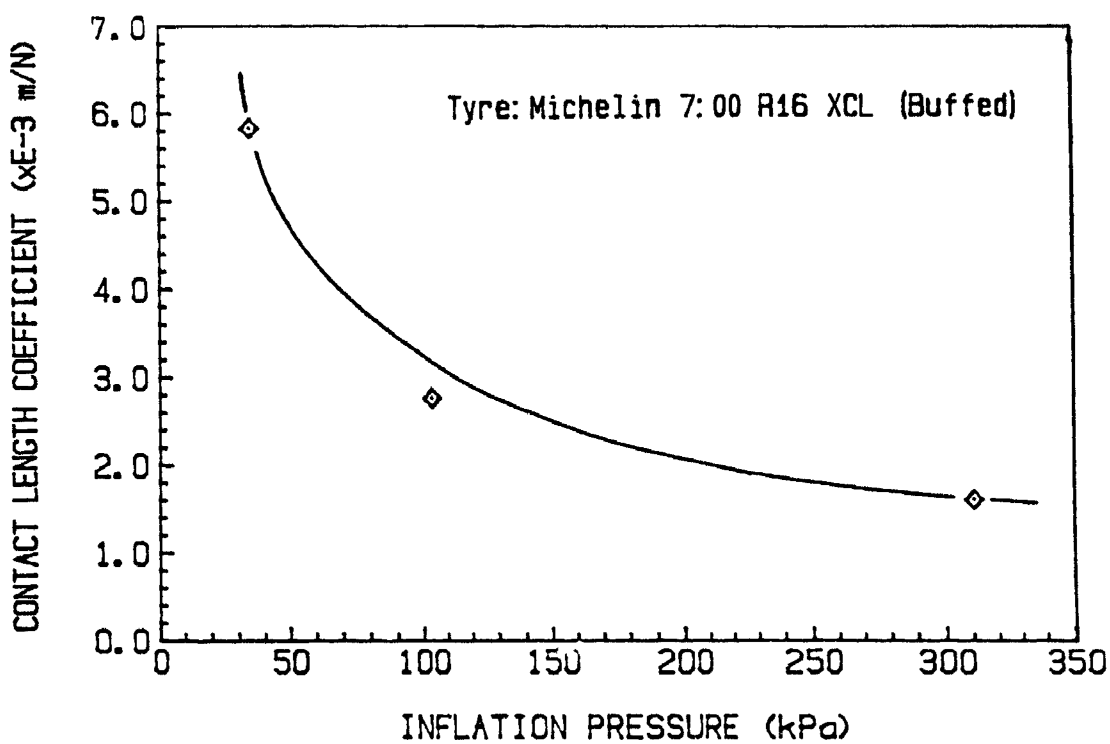

Fig. 6.3.6 Contact length coefficient as a function of inflation pressure

Based on the results exhibited in Fig. 6.3.6, an experimental relationship between the contact length coefficient and the tyre inflation pressure for the tyre 7:00 R16 XCL (buffed) is derived as follows:

$$q = (-4.61\, log\, P_t + 26.82) \cdot 10^{-3} \qquad (m/N) \qquad (6.3)$$

where log is the normal logarithm.

As a reference, the relationship between contact length and tyre radius shown in Fig. 6.3.7 (Clark, 1971) clearly indicates that the contact length decreases nonlinearly with an decrease of radius of the tyre.

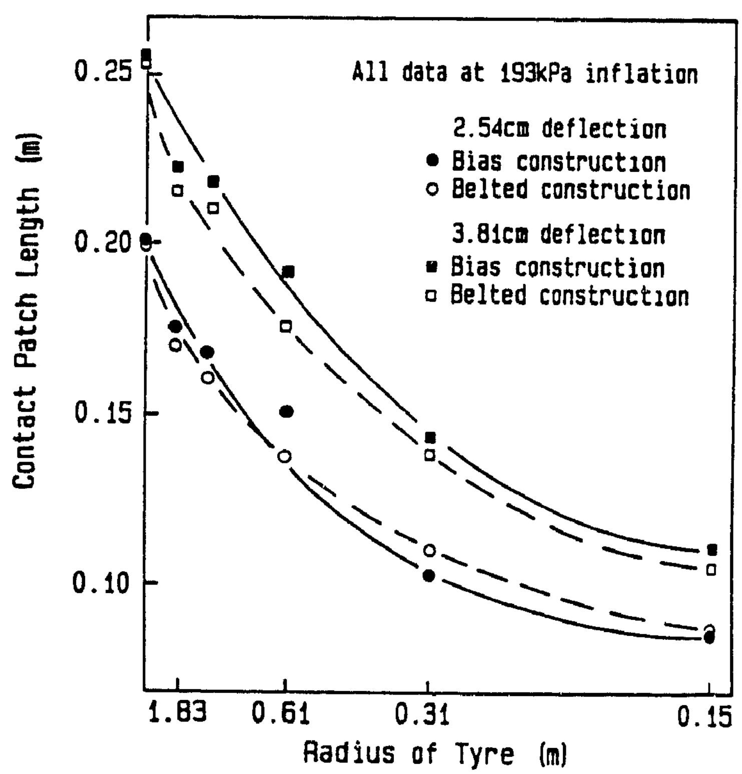

Fig. 6.3.7 Relationship between contact length and tyre radius (after Clark)

6.3.2 Dynamic Tests for Tyre Damping

In this section, the relationship between the damping factor and tyre inflation pressure will be investigated.

<u>Experimental method</u>

A simple and very popular drop test, which was explained in the previous section, was used for measurement of the damping factor of a tyre. Fig. 6.3.8 shows examples of the raw data for the test tyre inflated to 34.5 kPa or 310.3 kPa respectively. The damping ratio, ζ, is calculated from the decay rate of the response in amplitude.

<u>Experimental results</u>

The sophisticated characteristics of structure and rubber material of tyre viscoelasticity makes it difficult to focus on one factor alone, but for the purpose of this study, the effect of inflation pressure is chosen since it significantly influences the damping property as well as stiffness of the tyre. The test results are shown in Fig. 6.3.9. It is seen that the damping ratio of tyre compounds decreases exponentially with increasing inflation pressure.

The experimental equation for the tyre damping ratio is also derived as a function of the tyre inflation pressure, which is

$$\varsigma = -0.1363 \log P_t + 0.7884 \tag{6.4}$$

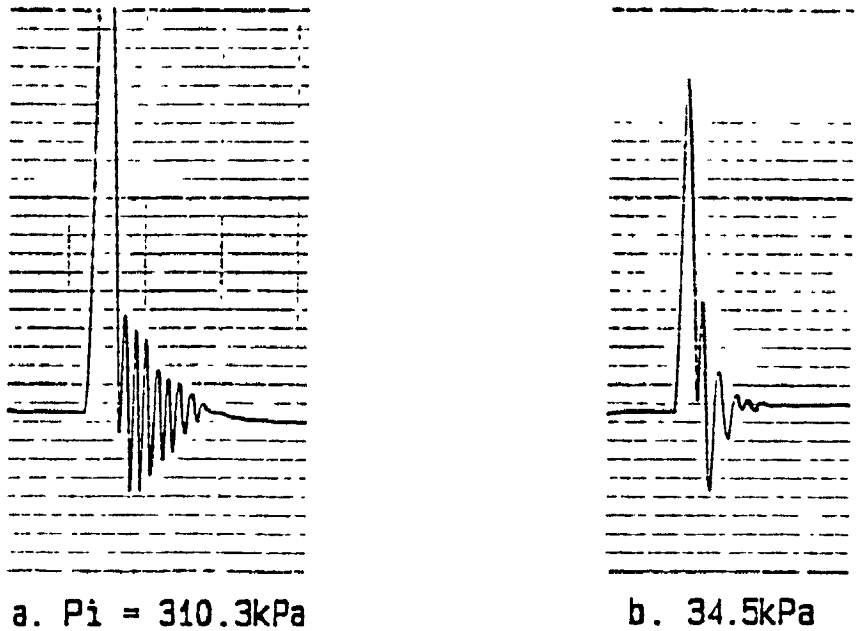

Fig. 6.3.8 Examples of tyre damping test results for different inflation pressure

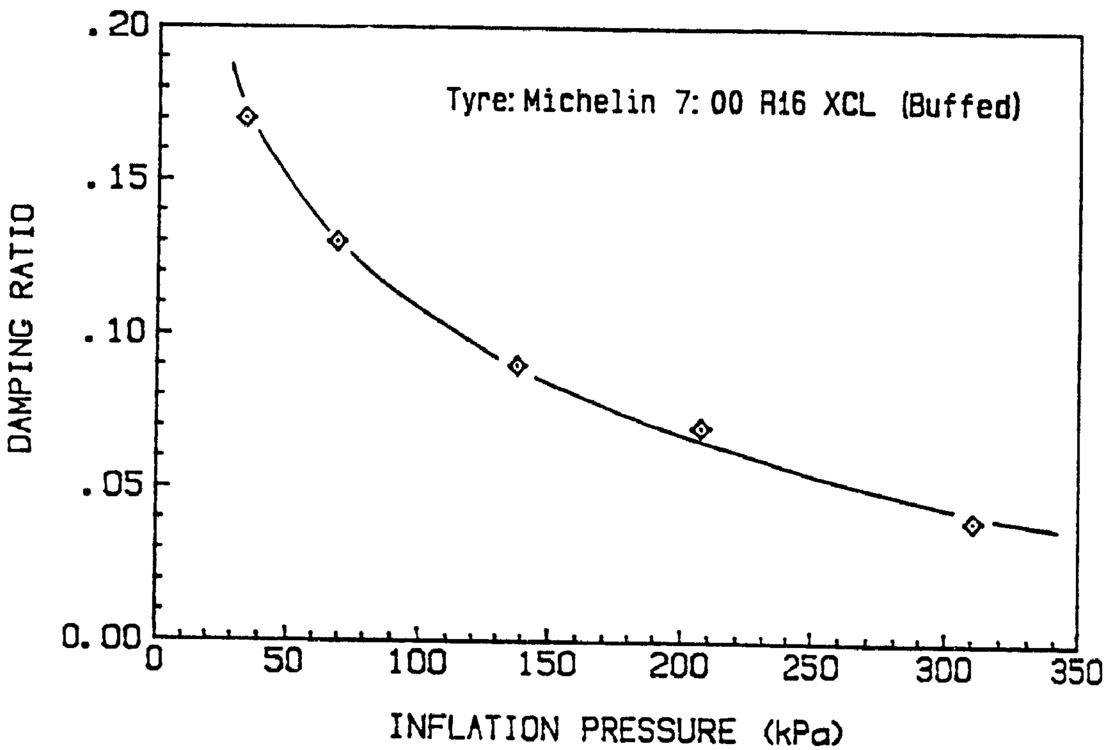

Fig. 6.3.9 Damping ratio as a function of inflation pressure

6.4 Traction Surface Profile Measurement

It is necessary to obtain information about the traction surface profile correctly in order to study the flexible tyre response to terrain surface geometry. By studying the characteristics of the random terrain surface geometry using statistical techniques, a theoretical input comprising the effect of surface roughness on tyre performance will be available for use with the developed model. Previous reports on surface profile measurement are introduced and discussed in Appendix B.

In our test, measurement of surface profiles was performed in the laboratory, using different rough surfaces. The measured data of traction surface profile were used for analysis of another important tyre characteristic i.e. the enveloping effect to the original road surface profile. The enveloping behavior will be measured in the following section (6.5 Rolling tyre tests).

6.4.1 Prepared Surfaces for Laboratory Test

In order to study the direct geometrical effect of traction surface profile, four rough non-deformable surfaces (including a flat and smooth surface) were used as test surfaces. They are shown in Fig. 6.4.1. As a flat and smooth surface (a), a flat wooden board was used. As randomly irregular surfaces, two surfaces having different profiles were considered (b and c).

a. Flat and smooth

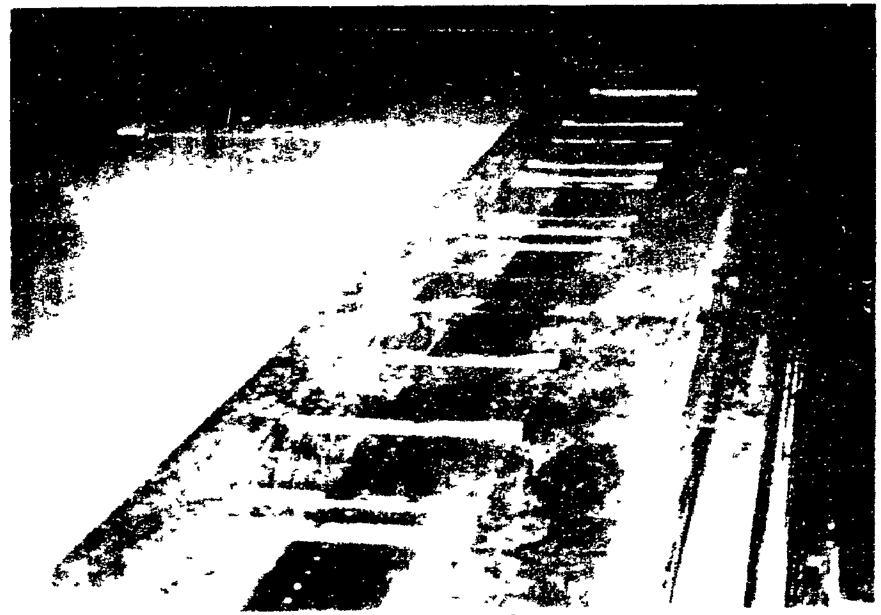

. Rough 1

The irregularity was created by arranging several rectangular ply-wood strips on a flat, rigid wooden board. For a sinusoidal surface (d), a ply-wood board was manufactured in the shape of a sinusoidal curve. The peak-to-peak amplitude was 0.04 m and its wavelength was taken as 0.8 m.

6.4.2 Apparatus for Surface Profile Measurement and Method

(1) Device for test surface profile measurement

Although several kinds of measuring methods and their devices used mainly in the field were considered, the ultrasonic wave apparatus (called ultrasonic distance detector here) was used. Fig. 6.4.2 shows the measuring equipment attached to a dynamometer carriage which sweeps horizontally over a test surface to collect profile data.

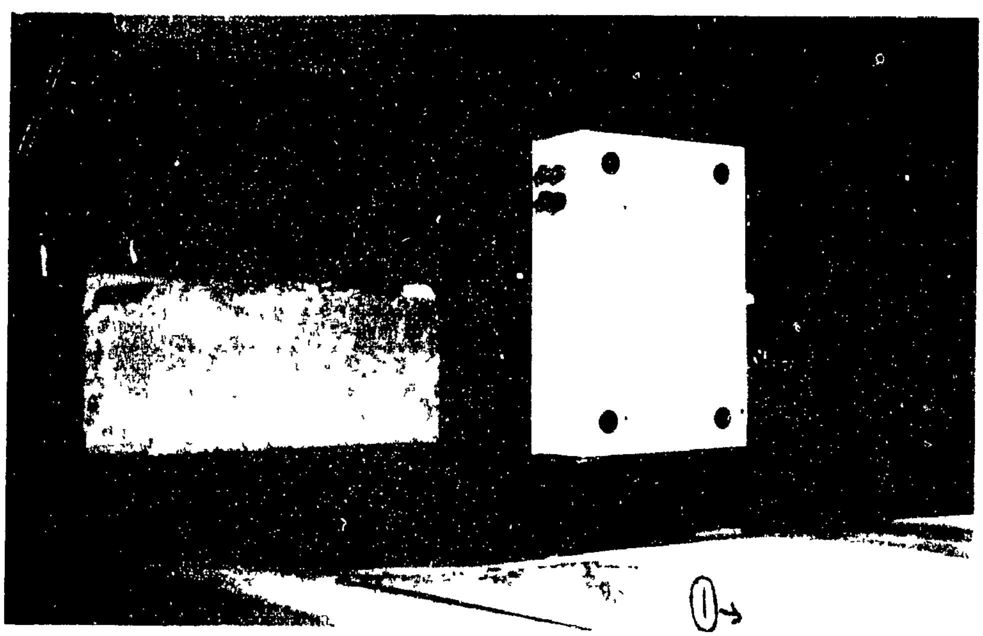

Fig. 6.4.2 Ultrasonic distance detector attached to dynamometer carriage

The fundamental principle of this equipment is illustrated in Fig. 6.4.3. The intermittent signal is applied to the transmitter of ultrasonic waves by an electrical switch, and the signal is regarded as S1. The reflected signal,S2, is picked up by the receiver. Both signals are sent to "flip-flop", then the difference of the two signals,S3, is converted into pulse-type signals,S4, through a counter.

Fig. 6.4.4 plots the characteristic curve of this detector. It shows a fairly good linear relationship between the output voltage and the measured distance. Its useful detectable range was found to be between about 6 cm and 15 cm. When beyond this range, the output signal often becomes unstable.

(2) Methods of measurement

In the measurement of traction surface profile, the following requirements are of major concern; i) setting the reference plane and ii) establishment of the horizontal base line in order to carry the measuring apparatus. As for the reference plane, any plane (point) can be regarded since the terrain surface roughness is evaluated as a variation from a descretionally fixed level or point i.e. mean or thereabouts.

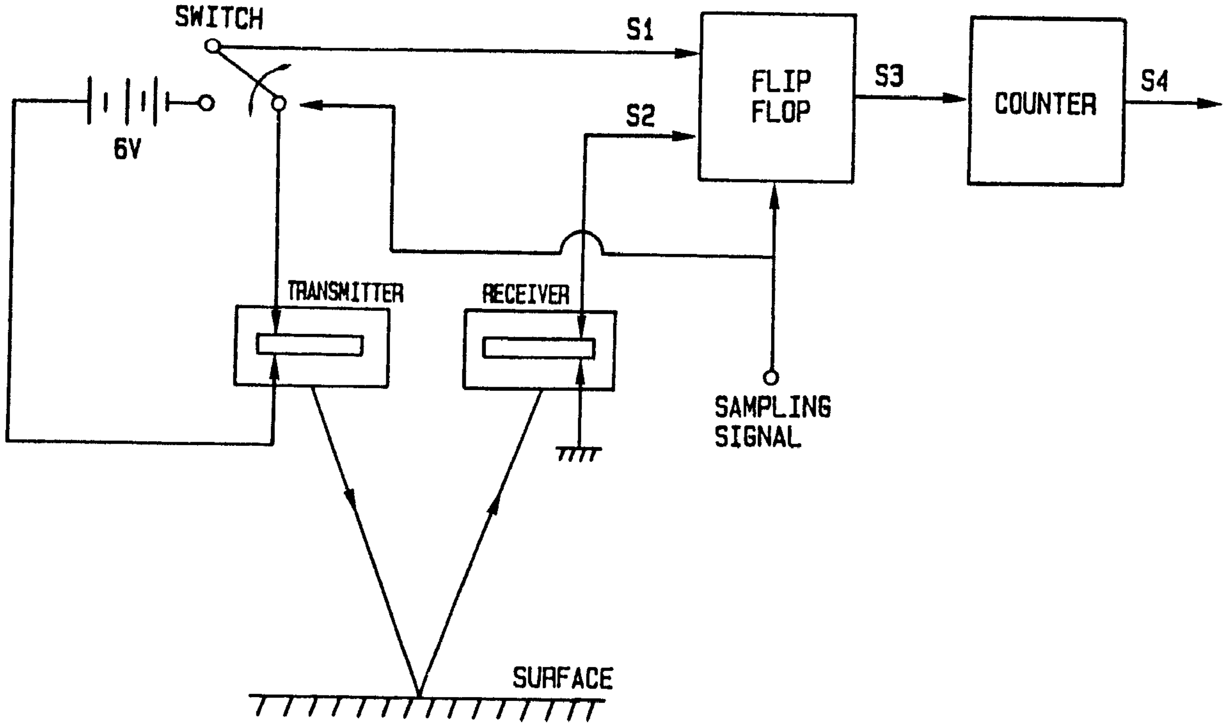

Fig. 6.4.3 Principle of contactless ultrasonic distance detector

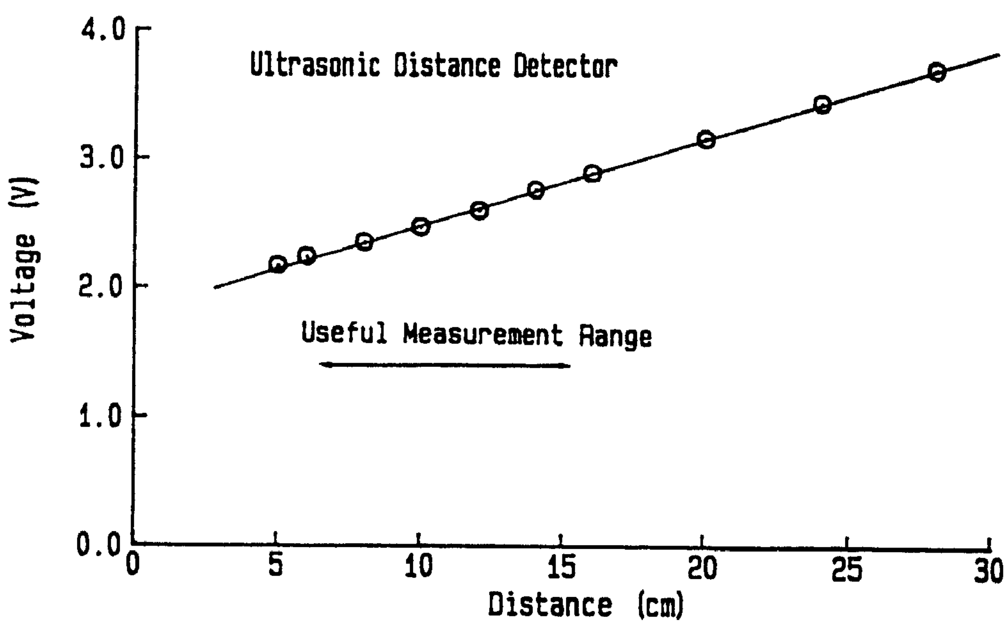

Fig. 6.4.4 Characteristic curve of ultrasonic distance detector

The need to establish a proper level baseline is paramount not only for reference determination of the irregularities but also for support of the moving carriage which contains the ultrasonic detector device. The difficulty in establishing this line may arise in the use of this method outdoors. The trend of ground surface roughness due to long wavelength components has to be considered, too. In the initial phase of development and testing, the use of the ultrasonic device and method has been restricted to laboratory tow bin trials.

Since the ultrasonic distance detector is horizontally swept over test surfaces at a constant speed (Fig. 6.4.5), a sweep line of the detector is regarded as both the reference plane and the base line (see also Fig. 6.5.2).

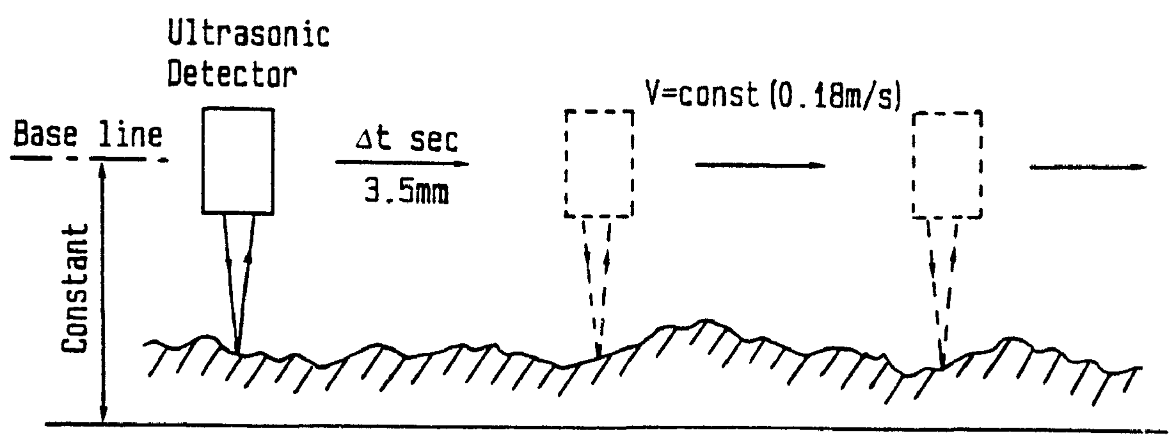

Fig. 6.4.5 Schematic diagram of surface profile measurement by ultrasonic distance detector

In order to deal with stochastic data, one analysis system was developed for this experiment (Fig. 6.4.6). All of the measured data were continuously recorded in a six-channeled tape recorder (Honeywell Model 5600) for about 30 seconds. The experimental data which were stored in a magnetic tape were transferred to a computer through GPIB interface while analogue signals were converted into 1024 points of digital signals by a digitizer 5B25N of Tektronix 5223 oscilloscope. These digitized experimental signals were also stored on a computer diskette, and Fourier analysis was performed by a personal computer (HP-85), using the digitized signals. The calculated data were stored on another diskette. The computer programs developed for transferring data through GPIB interface connecting between HP-85 and Tektronix 5223, and for calculating PSD using Fast Fourier Transform are given in Appendix G.

In the surface profile measurement, the sampling interval should be carefully determined. It must be large enough to take long distance data and must be small enough so as not to lose real information of surface geometry. The sampling interval of 3.5 mm (1024 points for 20 seconds, corresponding to 3.6 m surveyed length) seems to be sufficient enough for

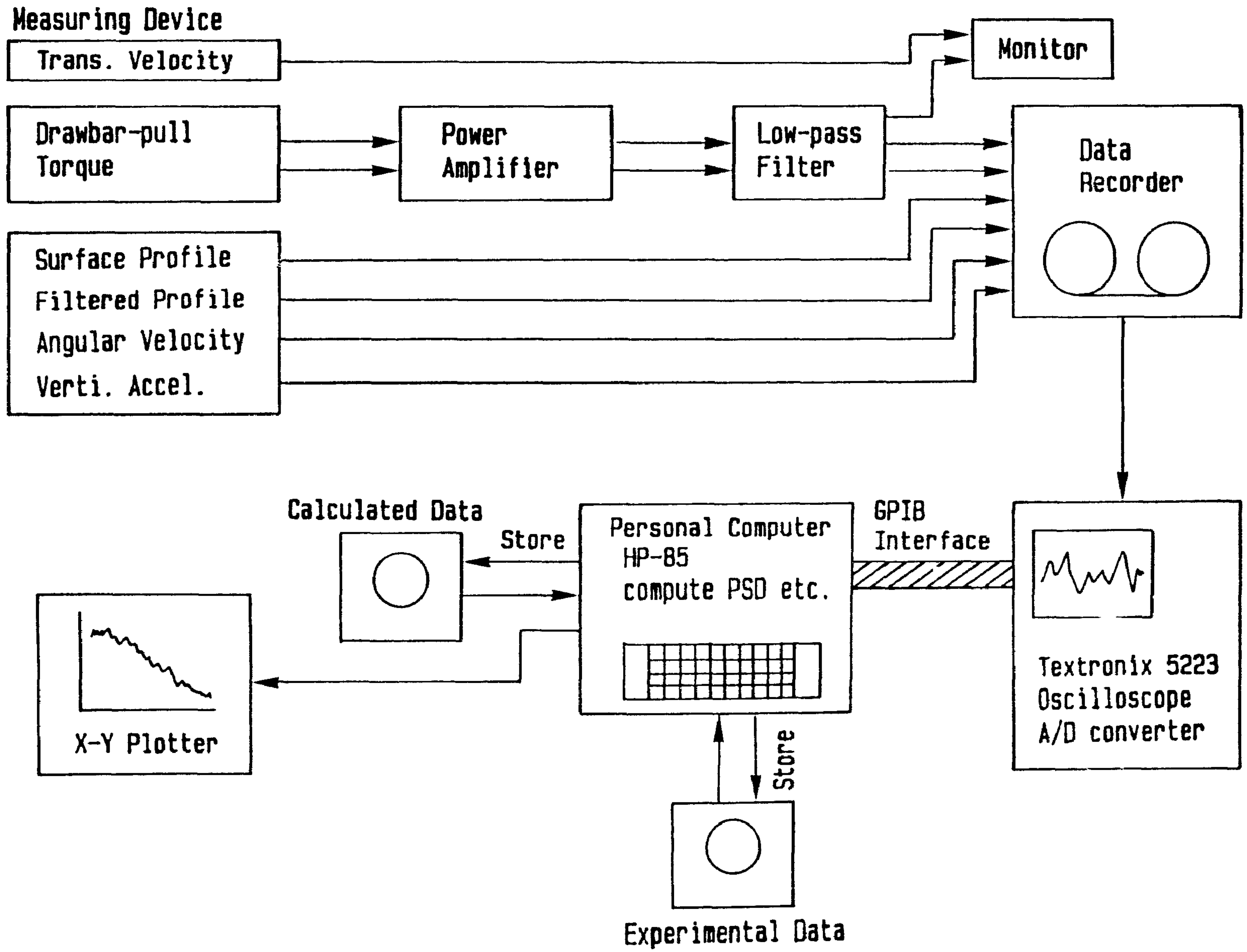

Fig. 6.4.6 Block schematic diagram of data process and analysis

off-road surface profile measurement. It is desirable to measure a longer distance of a surface in order to detect the components in the low frequency (long wavelength) range. A short period of measurement is the most disadvantageous to laboratory use. Ensemble averages of measured data are also employed for an achievement of higher reliability of data. Then measurement was repeated more than 10 times for each surface although little variation of results was observed.

6.4.3 Results of Test Surface Profile Measurements

Fig. 6.4.7 shows the measured surface profiles (upper) and their PSD curves (lower) of each surface individually. Both coordinates are expressed on a logarithmic scale so that a large scale of each parameter can be seen. Since the surface roughness is considered as a spatial disturbance rather than a temporal time dependent disturbance, the PSD curves were described in terms of the spatial frequency (cycle per meter). The spatial frequency is a particular concept in the space domain and it is therefore possible to express the PSD functions of various kinds of rough surfaces in a definite manner with no relation to vehicle speed.

(1) Surface profile measurement

In Fig. 6.4.7d, the characteristics of sinusoidal surface (peak-to-peak amplitude is 0.04 m, wavelength is 0.8 m) is described. As for the other surfaces, the difference in profile is clearly shown. The tiny and sharp irregularities in the measured profile are caused by the digitizing process of the analogue signal recorded in a magnetic tape, likely due to a noise produced in the measuring device itself or due to unexpected changes in reflection angle of the ultrasonic wave by rectangular shaped wooden pieces or surface contamination. Since these sharp irregularities provide larger PSD values than the expected true values in the higher frequency range, such irregularities should be eliminated by applying the averaging procedure or by multiplying by an adequate filter.

(2) PSD curves of surface profiles

Fig. 6.4.7c compares the PSD curves of rough2 surface profile obtained by the ultrasonic measuring method and by the optical measuring method. The curves show a good agreement of each other. Each PSD curve, except for the sinusoidal surface, shows a tendency of linear decline with spatial frequency in the logarithmic scale. This agrees with the results of previous researchers (Wendenborn,1966; Ohmiya,1986).

Comparing these PSD curves, it is also seen that the rougher the surface is, the larger the PSD values are at each frequency. Severe irregularities in PSD curves are plotted over 30 c/m. These are presumed to be a result of the noise in the measured profile data.

With regard to the slope of PSD curves, each curve shows a different decrement depending on the type of surface. The slope of the rough 2 surface is steeper than that of the flat and smooth surface. A steep slope means that the power included in a profile signal decreases rapidly with increasing of the spatial frequency. That is to say that the amplitude energy in the surface profile is contributed by the longer wavelength components (i.e. low spatial frequencies) rather than by the shorter wavelength ones. If the slope of a PSD curve is zero, such a random process is called the white noise giving the constant PSD values for all frequencies. As for the frequency component, the PSD curve can provide necessary information about frequencies. For instance, the bump can be clearly shown in the PSD plots of the sinusoidal surface at a spatial frequency of 1.25 c/m, which agrees with the wavelength (0.8 m) of that surface.

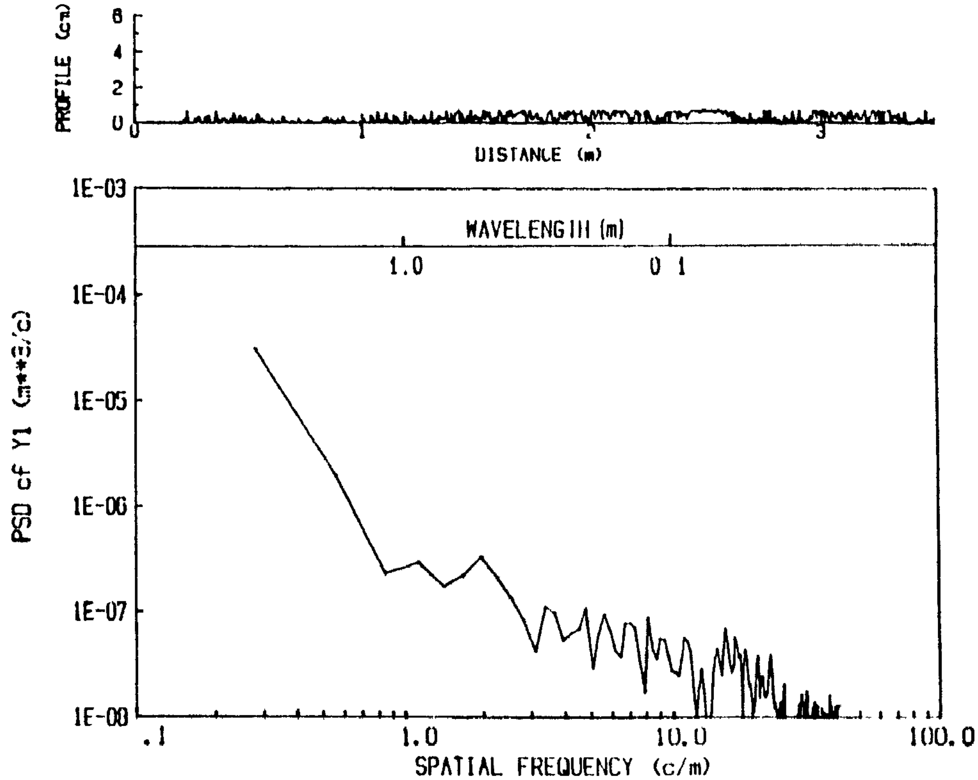

a. Flat and smooth surface

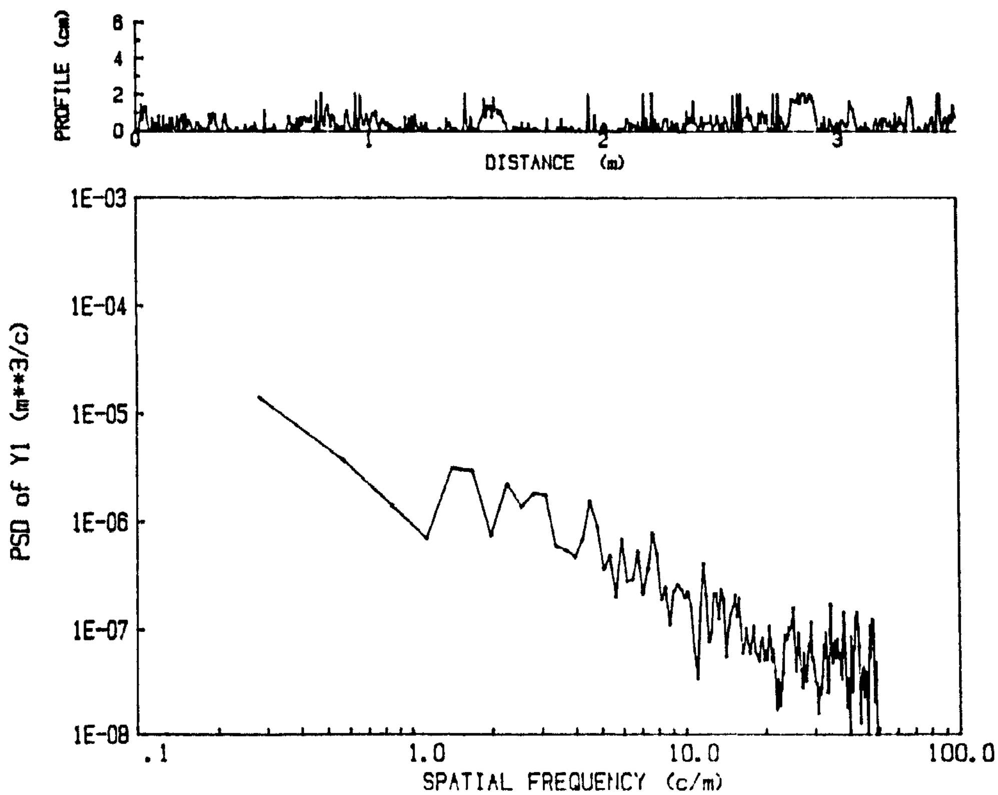

b. Rough1 surface

Fig. 6.4.7 Measured profiles of test surfaces and their PSD curves

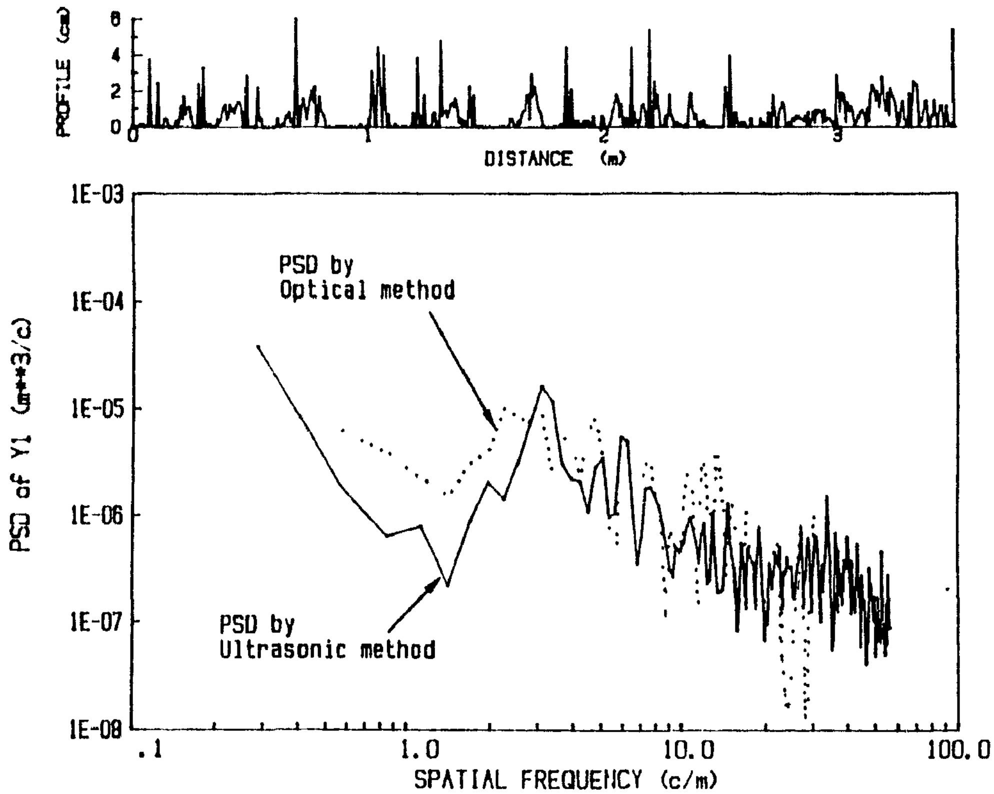

c. Rough2 surface

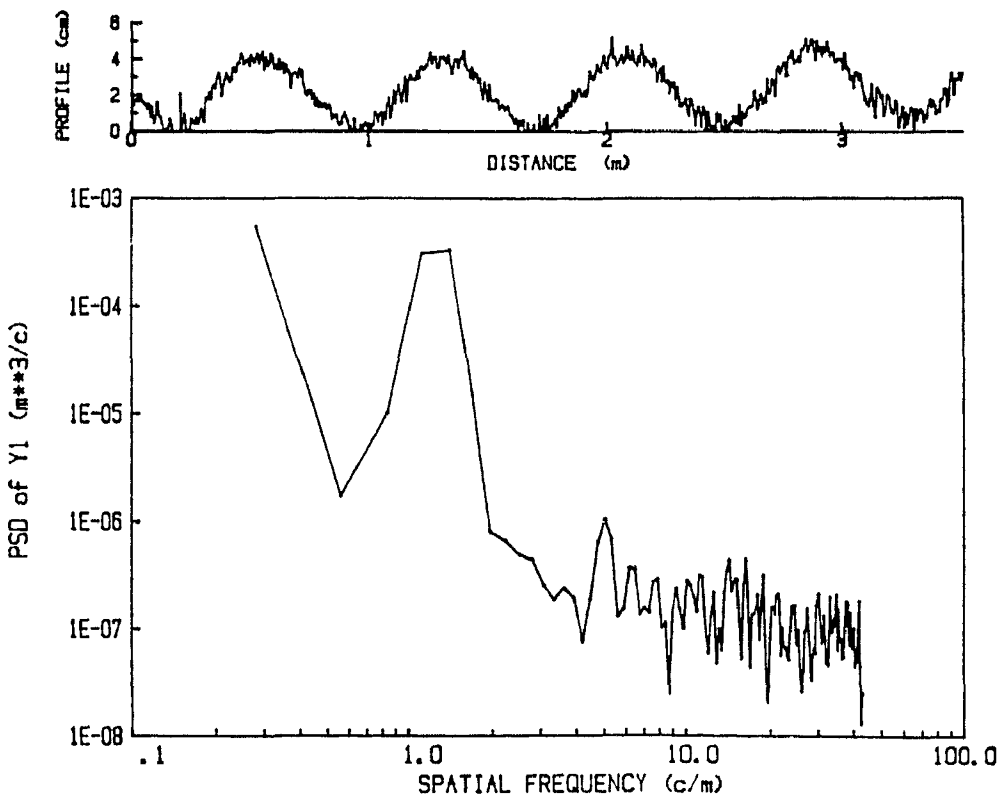

d. Sinusoidal surface

Fig. 6.4.7 Measured profiles of test surfaces and their PSD curves

Therefore, it can be said that the PSD function obtained from measured data supplies the important characteristic quantities (amplitude and frequency) of the road surface profile for the dynamic analysis.

The following are concluded for the measurement of surface profile.

Measurement of Traction Surface Profile

Surface profile measurement by the ultrasonic wave method gives fairly good results in spite of the short measuring distance. This ultrasonic measuring method is practically useful for laboratory use. However, it could also be available in the field if a reference plane is clearly defined, and if measuring equipment can sweep over a rough terrain surface maintaining a constant distance from the reference plane.

The advantages of this method are:

a. It is not influenced by the dimension of the measuring wheel contacting the road surface. In other words, the purely original geometry of the surface, which is not smoothed, can be surveyed since it is a non-contact type detector,

b. It is small, compact and cheap

The disadvantages are:

a. It includes electrical noise, which may be eliminated by applying a suitable filter,

b. It must be operated at a relatively slow sweep speed compared to the contact type method, since it generates unexpected peak values in the measurement for an abrupt change in surface height.

Expression of Surface Profile by PSD

The PSD function can describe the characteristics of random profile much better than other statistical expressions such as Root-Mean-Square (RMS) or probability density function, providing the energy and frequency information. It is possible to show any kind of surface roughness of mountains, hills or ball bearings by using the PSD function.

6.5 Rolling Tyre Tests on Rough Non-deformable Surfaces

Rolling tyre tests were performed in order to directly investigate the effect of rough surface profile on the tyre tractive performance, based on the concept of energy expenditure during its motion.

The other important objective of the rolling tyre test is to study the effect of tyre inflation pressure on the so-called tyre enveloping property of the pneumatic tyre.

Fig. 6.5.1 describes experimental facilities and recording devices available in the soil-mechanics laboratory of McGill Geotechnical Research Center. All the traction test data were processed in the same manner as explained in Section 6.4.

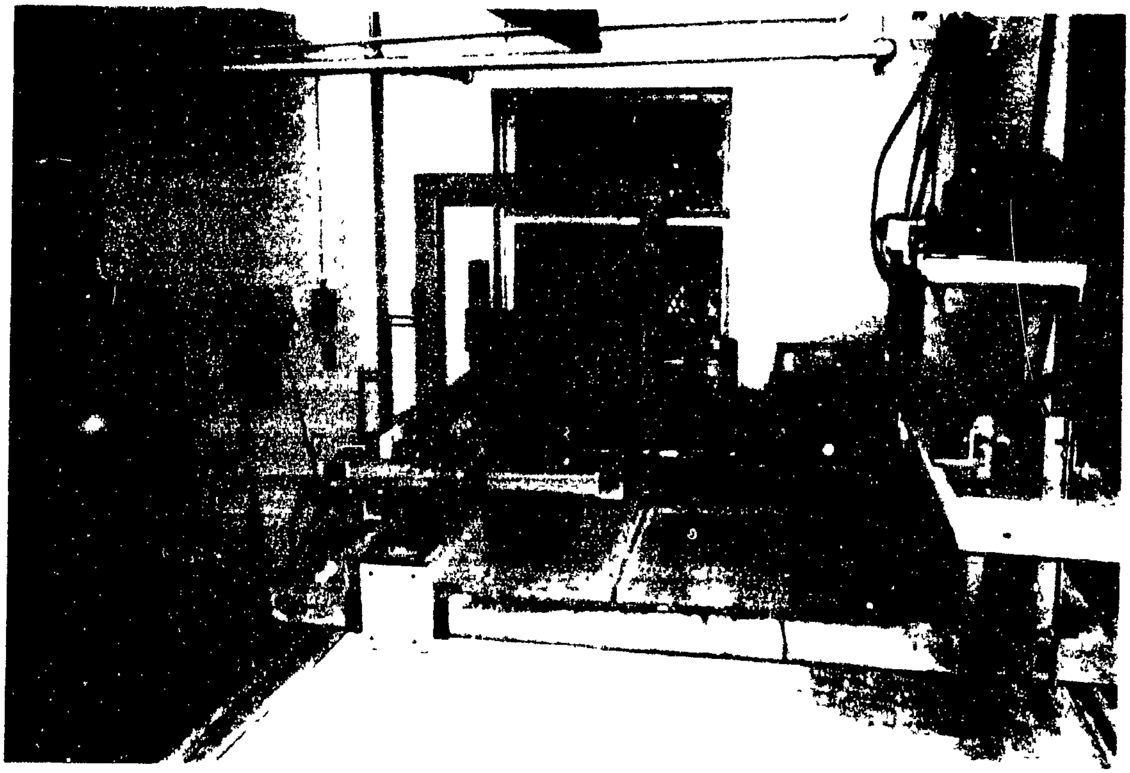

a. Experimental facilities

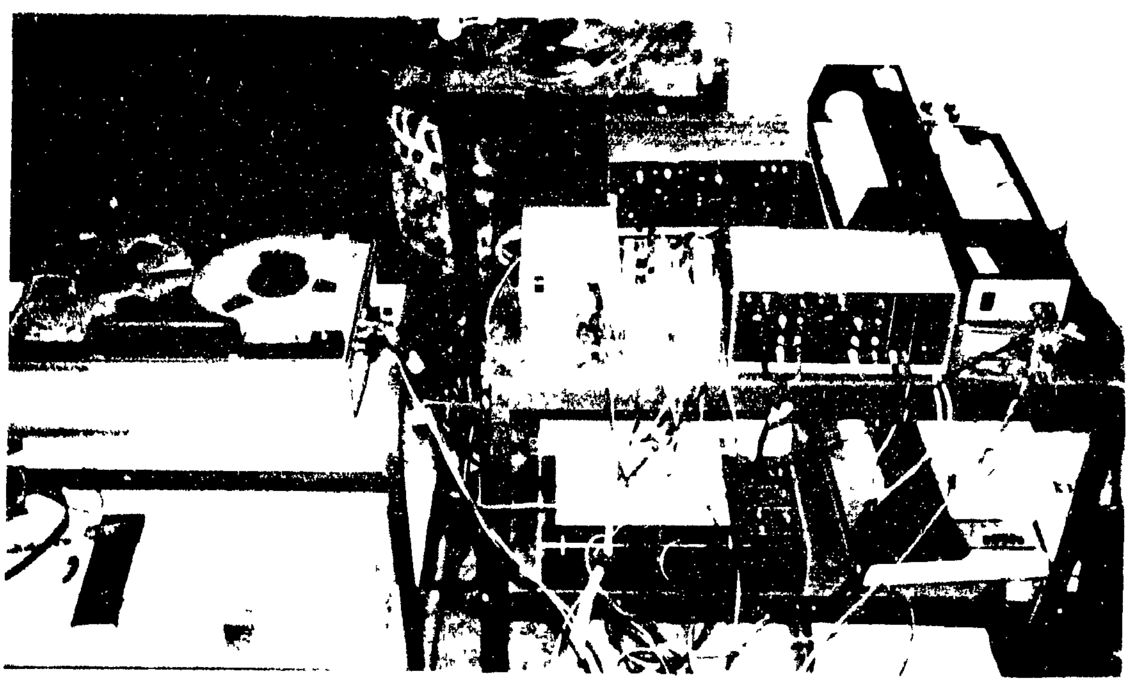

b. Recording devices

Fig. 6.5.1 Experimental facilities and recording devices for traction test

6.5.1 Investigation of Tyre Enveloping Property

As stated in Chapter 3, a pneumatic tyre has a capability of smoothing (enveloping) the original irregularities of road surface. Although it is clear that the size of contact length influences the enveloping property of a tyre, it is not easy to describe this characteristic with a mathematical expression since an original road surface normally has a random profile which cannot be simply expressed by a mathematical equation in the time domain. Therefore, one must depend upon the experimental results in order to investigate this special property.

In this study, the measurement of the tyre enveloping property is performed in order (a) to compare with the results of another study and (b) to derive a useful mathematical expression form for this so that it can be applied to theoretical consideration.

6.5.1.1 Test Apparatus and Method for the Investigation of Tyre Enveloping Property

<u>Test apparatus</u>

Fig. 6.5.2 illustrates the side view of the driven tyre test rig indicating measuring equipments for two types of surface profiles (the original rough traction surface profile and its filtered profile).

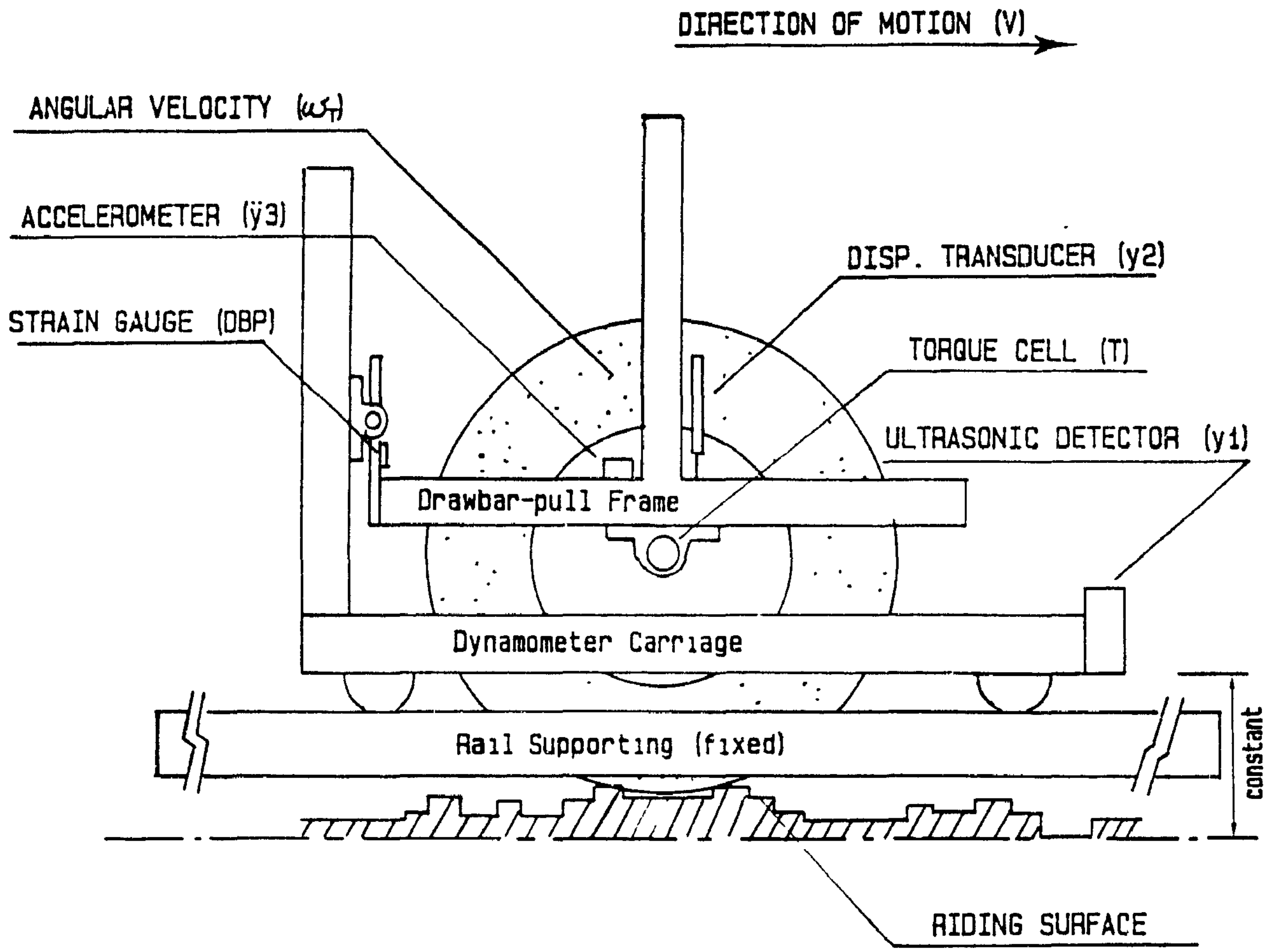

Fig. 6.5.2 Side view of driven tyre test rig and measured variables

The original surface profile was measured by the aforementioned ultrasonic distance detector which was attached at the front edge of the dynamometer carriage. A displacement transducer for the measurement of filtered profile was also fixed to the dynamometer carriage whilst its probe touched the "drawbar-pull frame" and moved freely with a vertical motion of the tyre axle. It was also set to a position as close to the vertical axis of tyre as possible to prevent a distortion of measured data.

Test method

Two kinds of methods are suggested in order to investigate the tyre enveloping property.

a. A method introduced by Beres (1987)

Sinusoidally rough surfaces whose amplitudes were fixed to 15 cm were used in his experiment. The surface was moved horizontally while the pneumatic tyre could move only in a vertical direction, with a certain weight applied on it (see Fig. 6.5.3a). Then the resultant response to a predetermined surface amplitude was derived by measuring the vertical displacement of the tyre axis. Several points were obtained by changing the wavelength of the sinusoidal surface. Results of his experiments are shown in Fig. 6.5.3b.

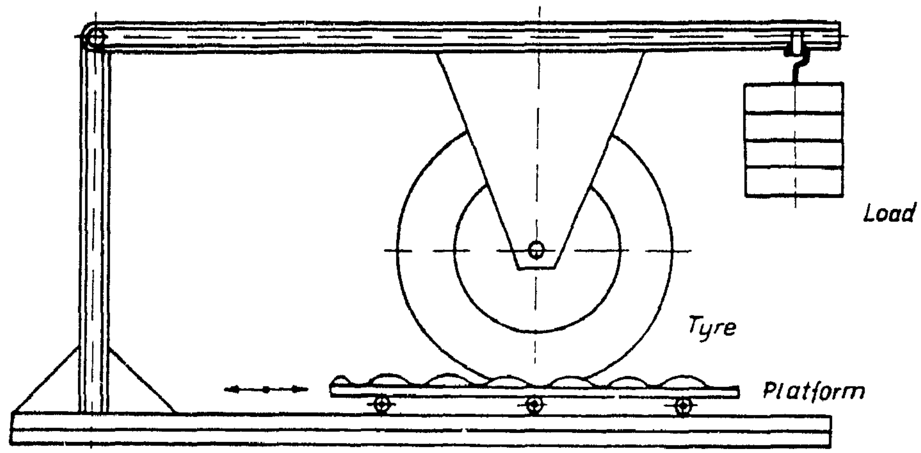

Fig. 6.5.3a Test rig used by Berés for the investigation of tyre enveloping property

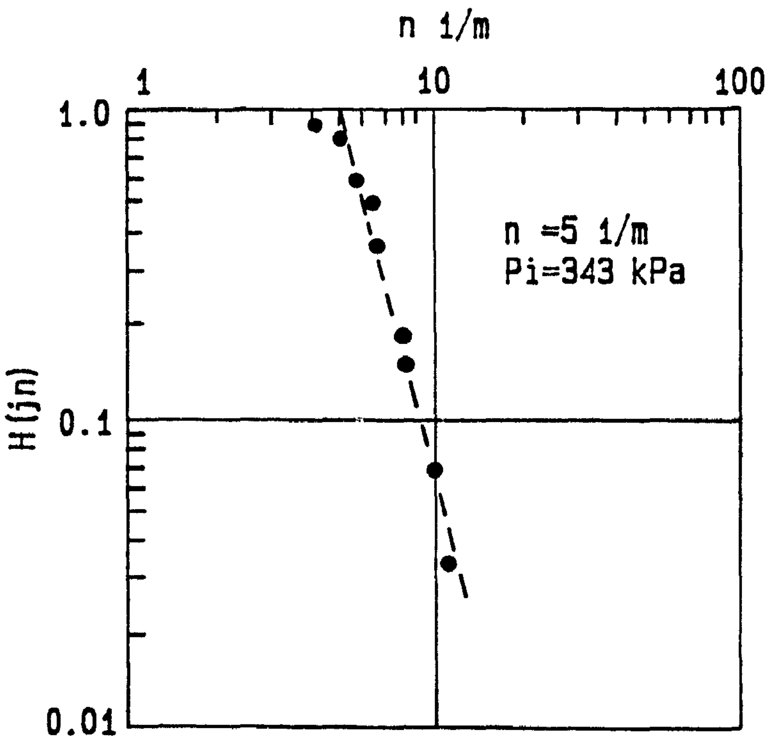

Fig. 6.5.3b Transfer function of tyre enveloping (after Berés)

b. A direct method (engaged in this study)

A bald (non-treaded) pneumatic tyre is operated on a randomly rough surface which include many frequency components. Then the original surface profile,y1, and the filtered profile,y2, are measured simultaneously. The transfer function of the tyre enveloping property can be found immediately by taking the ratio of two PSD functions of y1 and y2. The merit of this method is that the enveloping property is quickly predictable because it is not essential to prepare several different rough surfaces, as in the other method.

However, the difficulty of selecting an adequate rough surface should be noted to exist in both methods since the tyre enveloping property is a function of not only tyre dimensions such as diameter of a wheel but also of the terrain surface characteristics. To better understand this, two surfaces having the same wavelength but different amplitudes are shown below.

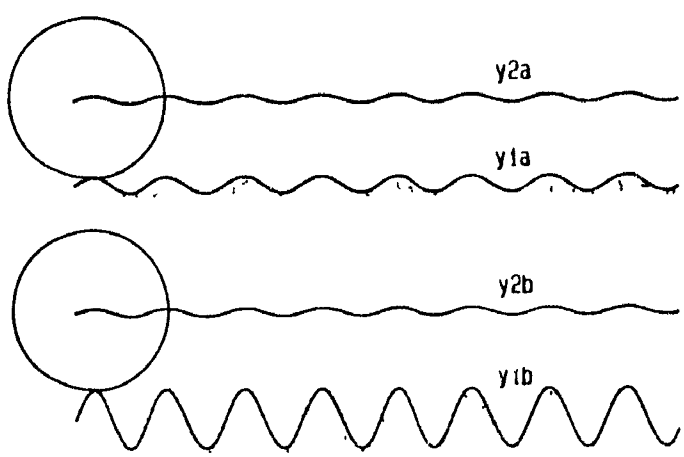

Fig. 6.5.4 Schematic diagram showing effect of original surface shape on tyre enveloping property

As shown in Fig. 6.5.4, one will see little difference in response (filtered profile) between y2a and y2b in spite of the clear difference in original surface. If the ratio,y2/y1, is taken, this may lead to a fatal error in prediction of this particular tyre property.

In this study, the latter method was taken because the effect of the difference by selection of road roughness was alleviated due to its randomness of amplitudes. Measurements were performed for each surface by alternating inflation pressures of tyre since this filtering effect seems to depend mainly on the size of contact length which is a function of inflation pressure. Only two kinds of inflation pressures (34.5 and 310.3 kPa) were considered in the experiment so that one may see their difference more clearly. The horizontal velocity of the moving tyre was set to a low velocity of 0.18 m/s so as not to produce a jumping phenomenon.

6.5.1.2 Measured Filtered Profile

A number of measurements were repeated with different inflation pressures and simulated rough traction surfaces. Fig. 6.5.5 compares filtered profiles with different inflation pressures. It is noted that both the original and filtered trajectories at each horizontal point do not correspond with each other because of different sampling portions in time.

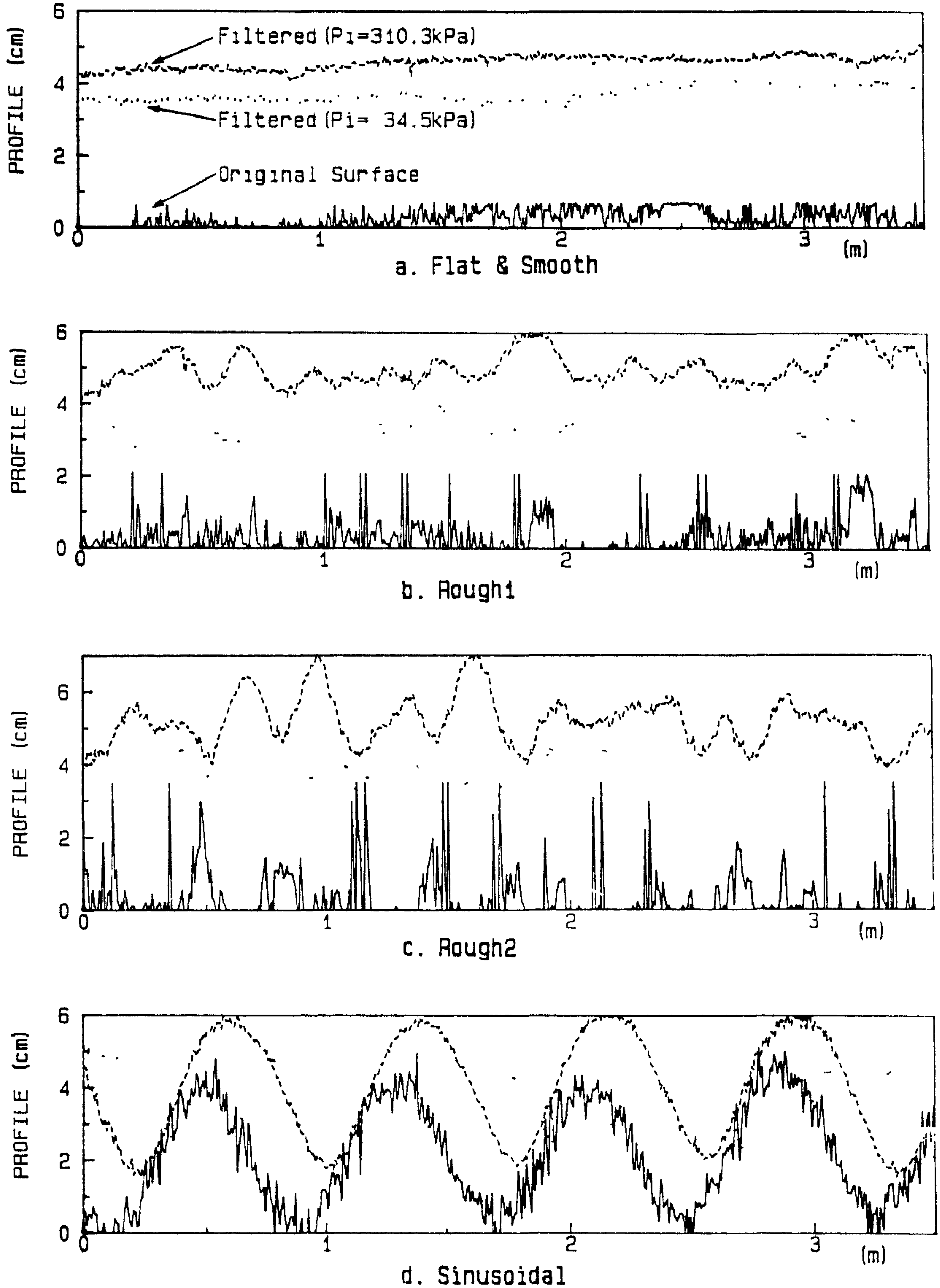

Fig. 6.5.5 Comparison of filtered profiles for various surfaces and inflation pressures

(1) Comparison of profiles by a change in surface type

a. In general, as the roughness increases (as shown in the upper Figures to the lower one), filtered profiles also gain their roughness.

b. On the flat and smooth surface, a clear statistical difference of the shape between the original and filtered profile cannot be seen although the original profile includes noise in the measurement. This means that there is little effect of tyre enveloping property for a relatively smooth track, as might be expected.

c. On randomly rough surfaces (rough1 and rough2), modifications of the original profiles have been achieved to some extent depending on tyre flexibility. It is also shown that both filtered profiles for rough2 surface have larger variations of height than the ones for rough1 surface because of its severe roughness.

d. As for a sinusoidal surface, both filtered profiles also exhibit the sinusoidal shape holding the same wavelength (0.8 m) as the original surface.

(2) Comparison of profiles by a change in inflation pressure

a. As for a flat and smooth surface, the effect of tyre inflation pressure on the enveloping property is almost nil.

b. Comparison of the filtered profiles for rough1 and rough2 surfaces respectively shows that a low inflated tyre can absorb peaky asperities on a original surface quite well although a highly inflated tyre does so to a lesser extent. Furthermore, one may find that filtered profile for 310.3 kPa dominates longer wavelength components in the trajectory. On the contrary, the profile for 34.5 kPa contains shorter wavelength components compared to other filtered profile. These phenomena may possibly be due to tyre vibration arising from its increased flexibility.

c. With regard to the sinusoidal surface, different amplitudes of filtered profile are observed by the inflation pressure. The profile for 310.3 kPa (very rigid) tyre indicates almost the same peak-to-peak amplitude as that of the original surface profile due to the tyre's rigidity. In contrast, a clear reduction in amplitude of filtered profile for the low inflated tyre is demonstrated. Its amplitude is 0.033 m which is about 80% of that of the original surface. This result shows that a greater enveloping effect is obtained by a lower inflated tyre.

Fig. 6.5.6 illustrates the RMS values of the original and filtered profiles, and the ratio of these RMS values (filtered/original profile). From the Figure, the following results are derived:

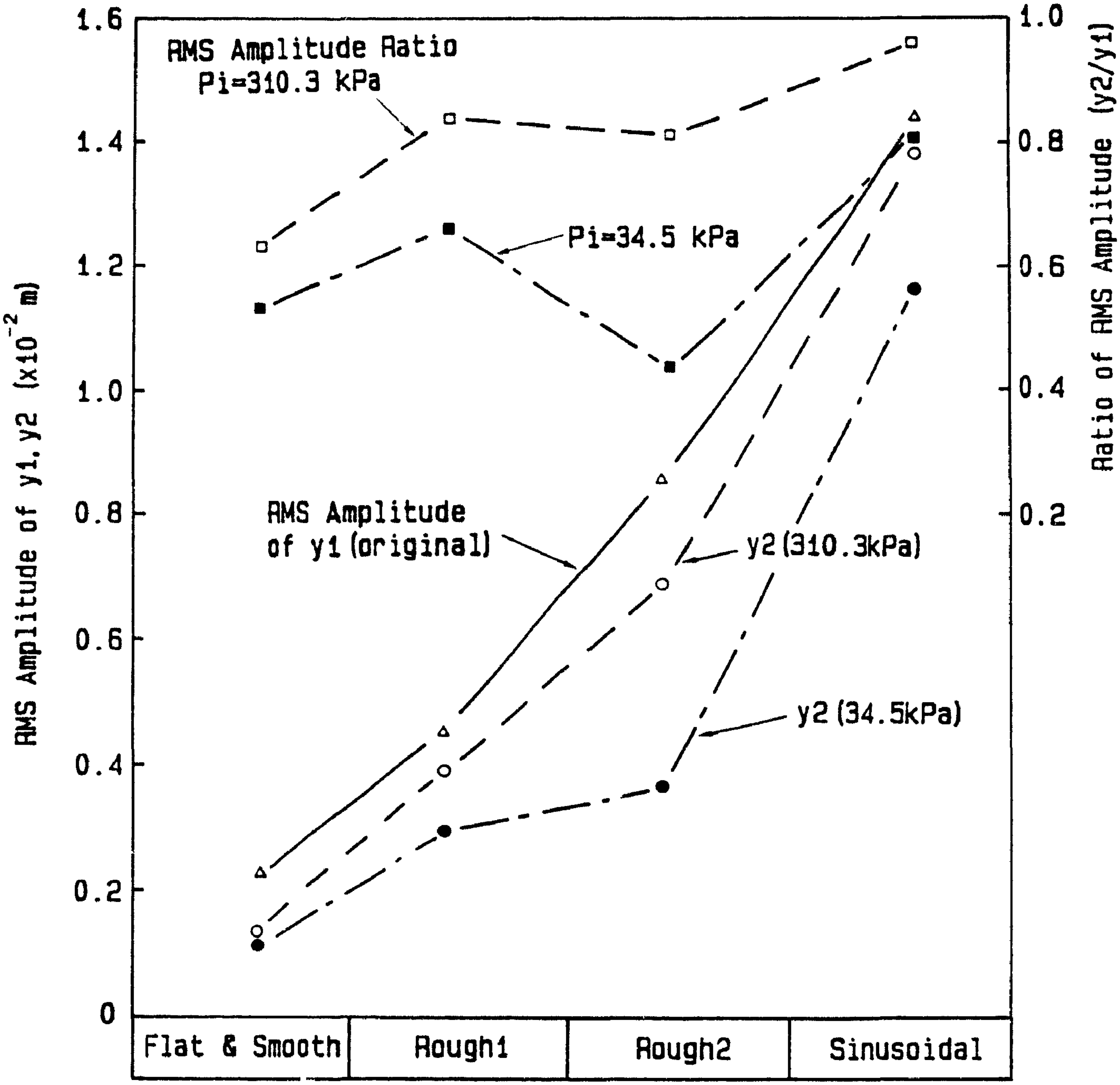

Fig. 6.5.6 RMS amplitude values and their ratio (y2/y1) for each test surface

(1) RMS values of the original and filtered profiles increase as surface type changes from flat and smooth to rough1, rough2 and sinusoidal surface.

(2) Secondly, a clear decrease in RMS value of the filtered profile is recognized, and the values for the low inflated tyre are smaller than those for the highly inflated tyre. For the flat and smooth surface, the RMS values of the filtered profiles for both the high and low inflated tyre are very close, indicating no distinctive effect of enveloping.

(3) Considering the ratios of RMS values of the filtered profiles to the original profiles, it can be said that about 80% of amplitude energy included in the original signal for 310.3 kPa tyre and only 60% for 34.5 kPa tyre are transmitted to the filtered signal respectively. This indicates the necessity of application of tyre enveloping function since a pneumatic tyre or vehicle would be given less excitation (energy) by the filtered profile rather than by the original surface.

(4) As for the filtered profile for rough2 surface in the case of 34.5 kPa, its RMS amplitude ratio is greatly decreased compared to other surfaces. This is surmised as follows:

The enveloping property of the pneumatic tyre is affected not only by the flexibility, size of tyre and load applied to tyre, but also by geometrical characteristics of a rough road. As previously mentioned, an incorrect estimate of the enveloping property often happens in the experiment if the vertical amplitudes are too large or wavelengths included in a off-road profile signal are too short (shown in Fig. 6.5.4).

6.5.2 Tyre Traction Tests on Rough Non-deformable Surface

Traction is the ability of the vehicle tractive element (wheel or track) to generate enough forces to overcome all types of vehicle resisting forces, and hence provides the vehicle horizontal motion. Although numerous investigations of vehicle tractive performance have been achieved for rigid/soft smooth level ground theoretically and experimentally, only a few limited experimental results were shown for the geometrical effect of ground surface due to complex mechanisms of traction on such a surface. Therefore, it was and is still very popular to simply apply a deterministic sinusoidal excitation to either rolling tyre or flat rubber plate in order to investigate the effect of exciting frequency and amplitude on tractive force, simulating the operational condition on a rough road. These attempts do not seem to represent the actual condition of a driven tyre on a rough surface, nor do they consider slip phenomena which is also an important parameter for off-road vehicle traction. Furthermore on a randomly rough terrain, a tyre would be excited not by a single frequency component but by a combined one, since a rough terrain normally contains an infinite number of frequency components. Therefore in this experiment, a pneumatic tyre is driven with a certain slip on a non-deformable, pseudo-random rough surface, assuming an actual operation of a vehicle on such a road.

The objectives of the traction test are:

(1) to evaluate the power dissipation during a rotation of tyre on a rough ground surface

(2) to investigate the effect of geometrical surface roughness on the DBP, which is the final useful output force of tyre, so that the established approach in predicting the traction in Chapter 4 can be verified

and finally,

(3) to consider how much vehicle nominal tractive efficiency is influenced by such a rough terrain geometry compared to a smooth road.

6.5.2.1 Method and Apparatus for Traction Test

Method

A schematic representation of the input-output relationship of the tyre traction test is shown in Fig. 6.5.7.

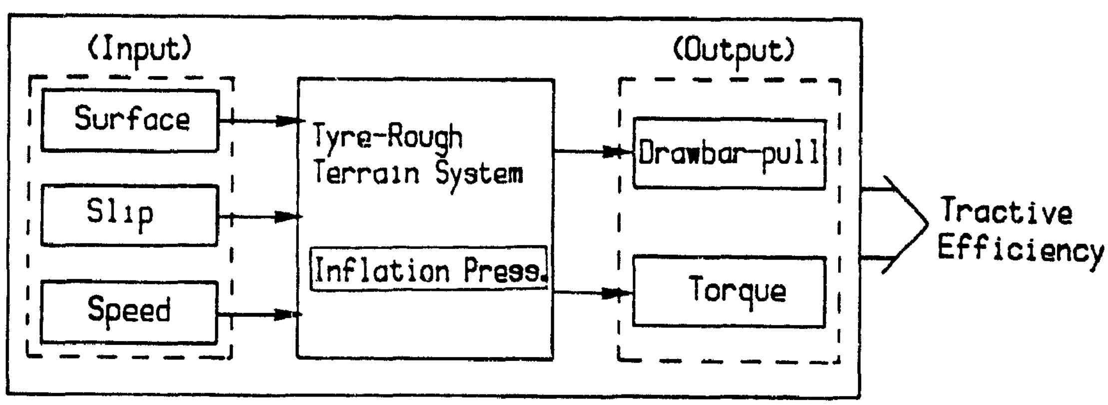

Fig. 6.5.7 Schematic representation of input-output relationship of traction test

In this test series, the bald pneumatic tyre (Michelin 7:00 R16 XCL) was controlled in such a way as to move over several types of rough, non-deformable surfaces made of plywood (Fig. 6.4.1). A very low translational velocity (0.18m/s) was applied through traction tests due to limited traction surface length while the velocity range of the agricultural tractor in normal operation ranged between about 1 and 5 m/s (18 km/h). The slip was produced by a differential speed between the rotating tyre and the dynamometer carriage. Rotational velocities of the tyre were changed to obtain different degree of slip. On the other hand, the translational velocity was maintained constant by a hydraulic motor. The range of slip was generally covered between 0 and 60% depending on the type of rough surface since it was difficult to produce a high slip, such as 60%, on a very rough surface. Two kinds of inflation pressure were selected. 310.3 kPa was the inflation pressure for normal operation for the tested tyre, and 34.5 kPa was chosen to be an extremely low pressure to clearly observe the effect of tyre inflation pressure.

For each slip rate and inflation pressure, the applied torque, DBP and vertical acceleration of tyre hub were measured. All of the experimental data, as well as the measurement data of traction surface profile and its filtered profile, were recorded in the magnetic tape.

Average values were computed for input torque and angular velocity respectively. Both average and standard deviation were computed for the measured data of DBP.

Apparatus

The measuring devices are shown in Fig. 6.5.2.

6.5.2.2 Results of Traction Test

A. Natural frequencies of experimental device

The machinery or structure normally forms the vibration system which has individual vibratory characteristics, depending on its shape, material characteristics or boundary condition of the attachment of pieces. The natural frequency is a particular property of the dynamical vibration system established by its mass and stiffness distribution. If the frequency of excitation coincides with one of the natural frequencies (generally structure etc. possess several vibration modes), a condition of resonance is encountered, and dangerously large oscillation may result.

Thus, it is helpful to know the natural frequencies of a pneumatic tyre so that one can see the effect of the difference of tyre construction on its vibrational characteristics. Although a tyre has several vibration modes, only the lowest natural frequency for the first mode is investigated due to the fact that the off-road vehicles generally meet with relatively low frequencies in the field compared to the on-road vehicle. Fig. 6.5.8 describes the natural frequencies of the testing system for the excitation in both vertical and longitudinal directions as a function of tyre inflation pressure. These vertical natural frequencies were calculated based on measured weight of traction gear and static stiffness of the tyre, and the longitudinal natural frequencies were determined by using the response PSD for impulse. The system's natural frequencies seem to be generally lower than those of the pneumatic tyre itself because of added mass of frame and tyre shaft. For vertical vibrations, the natural frequencies increase with an increase in tyre inflation pressure because of the increased vertical tyre stiffness.

On the contrary, any clear effect of tyre inflation pressure on the natural frequencies cannot be seen for the longitudinal excitation. It is found that the natural frequency in longitudinal direction lies around 4 Hz. This means that the longitudinal vibration characteristics of a tyre are affected by the structural and material properties of rubber composites themselves rather than by the air filling the tyre.

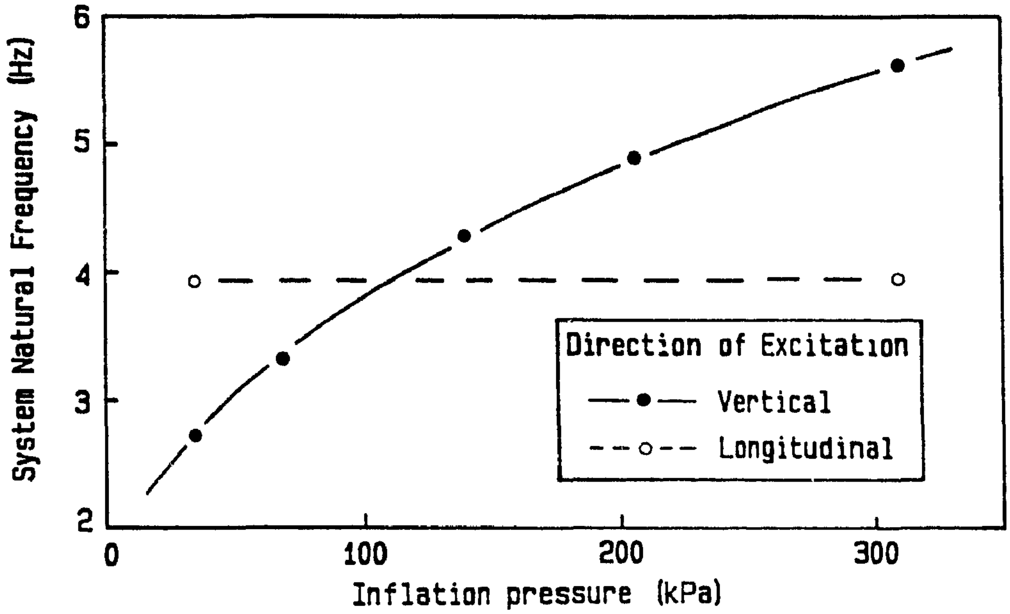

Fig. 6.5.8 Natural frequencies for vertical/longitudinal excitation as a function of tyre inflation pressure

These results may suggest selection of the inflation pressure to improve the off-road vehicle performance, i.e. ride comfort or operational speed etc. where the vehicle is operated on a rough harsh road. For instance, if the vehicle is driven on a typical regularly rough surface which is a "wash-board" road, the vehicle will suffer a severe excitation from this intolerable ground depending on the combination of traveling speed, tyre, suspension and/or vehicle structural characteristics and the nature of the ground. Looking at only the tyre property and off-road surface geometry, excluding other vehicle characteristics, if the dominant wavelength of this type of ground is 0.3 m and the vehicle speed is 5 m/s, the tyre will be shaken at about 17 Hz. The excitation amplitude of the tyre is not very large if the inflation pressure is 310.3 kPa since the excitation frequency (17 Hz) is much larger than the natural frequency (5.6 Hz) of the tyre at such an inflation pressure. However, if the wavelength is 1 m (everything else being equal), the rolling tyre is excited at 5 Hz which is very close to its natural frequency. Under this condition, the tyre may leave the ground surface due to the severe excitation and therefore lose the traction, which fails to maintain the controllability of the vehicle and finally allows it to fall into a very dangerous condition.

Furthermore, the natural frequency for vertical vibration matches the one for longitudinal vibration when the tyre is inflated to 120 kPa. If this system travels on such a ground which contains a dominant 4 Hz frequency component in surface geometrical pattern in relation to a vehicle speed, or if it is excited horizontally by this fiequency due to stick-slip phenomenon etc., this system will also be shaken hard. It is, therefore, very important to know the tyre dynamic characteristics and then to determine the most adequate combination of tyre parameters and running conditions in order to derive the effective tractive performance.

B. Tyre deformation energy

The power required for tyre deformation (say tyre deformation power), which is the main concern of this study, can be evaluated by rewriting Eq.(4.2) as follows:

$$\dot{E}_T = \dot{E}_{in} - \dot{E}_{out} - \dot{E}_s \tag{6.5}$$

where $\dot{E}_{in}$ = input power (Nm/s)

$= T\, \omega_T$

$\dot{E}_{out}$ = useful output power

$= DBP\ V$

$\dot{E}_s$ = interfacial power loss

$= T\, \omega_T S_i$

$\dot{E}_T$ = power loss by tyre deformation

where T = measured torque (Nm)

ω_T = rotational velocity of tyre (rad/s)

DBP = measured DBP (N)

V = translational velocity (m/s)

S_i = slip rate

With the knowledge of the average values of measured torque and DBP at each slip, the tyre deformation power can be calculated.

Figs. 6.5.9 and 6.5.10 demonstrate the comparison of tyre deformation power as a function of slip and tyre inflation pressure respectively for four different rough traction surfaces. As for Fig. 6.5.10, the powers were calculated by averaging the derived values at all measured slips. From these Figures, the following tendencies can be found.

(1) The tyre deformation power has little sensitivity to the change of the slip rate for both inflation pressures. This fact was observed by Boonsinsuk (1979), while only a flat and smooth traction surface was used.

(2) With regard to the effect of inflation pressure (Fig. 6.5.10), the low inflated tyre exhibits a larger amount of tyre deformation power due to its large deformation and hysteresis. A highly inflated tyre exhibited very little difference in tyre deformation power expenditure for different traction surfaces, excluding the rough2 surface. As the inflation pressure is decreased, the effect of road roughness on tyre deformation power becomes significant.

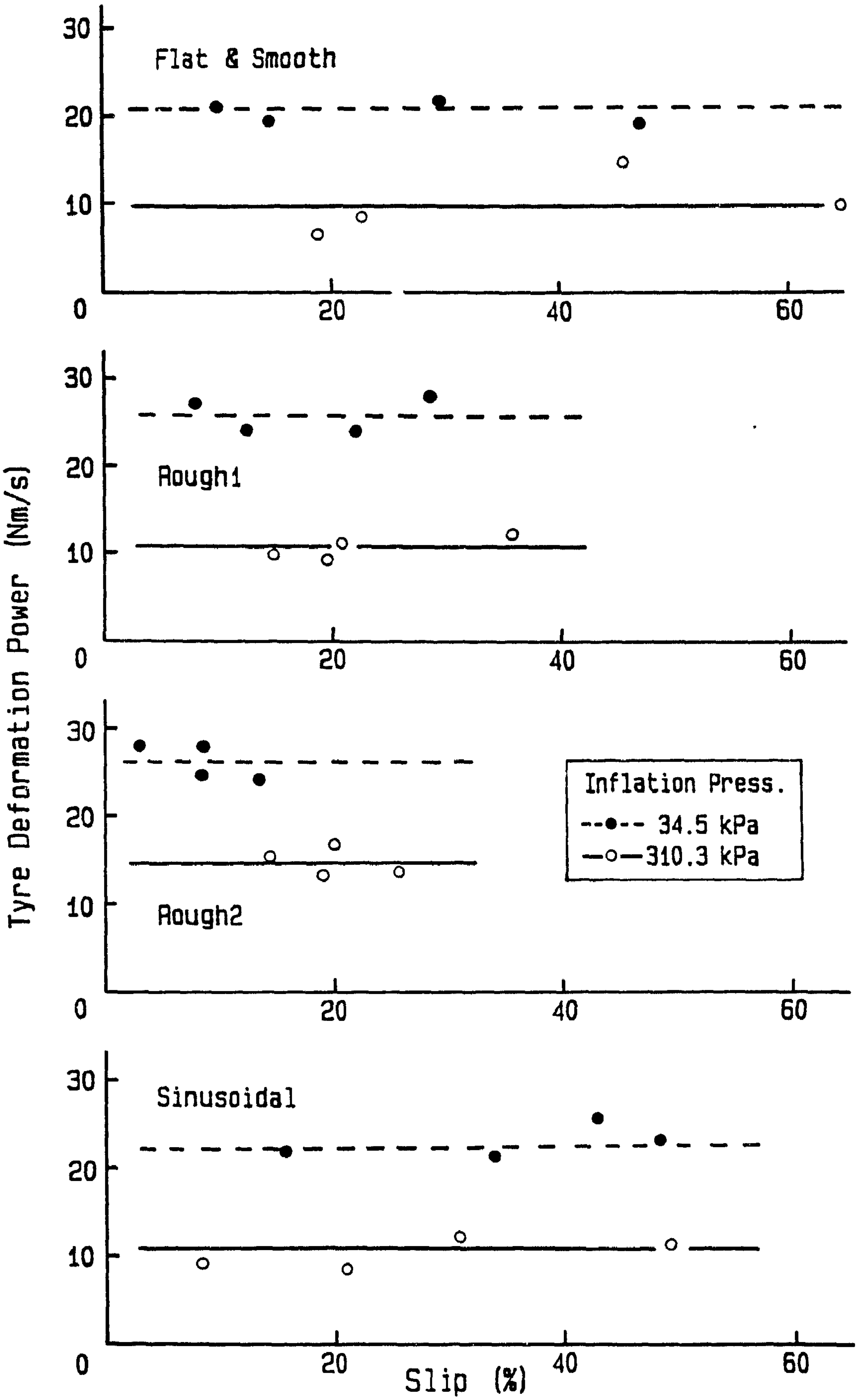

Fig. 6.5.9 Tyre deformation power for different surfaces as a function of slip

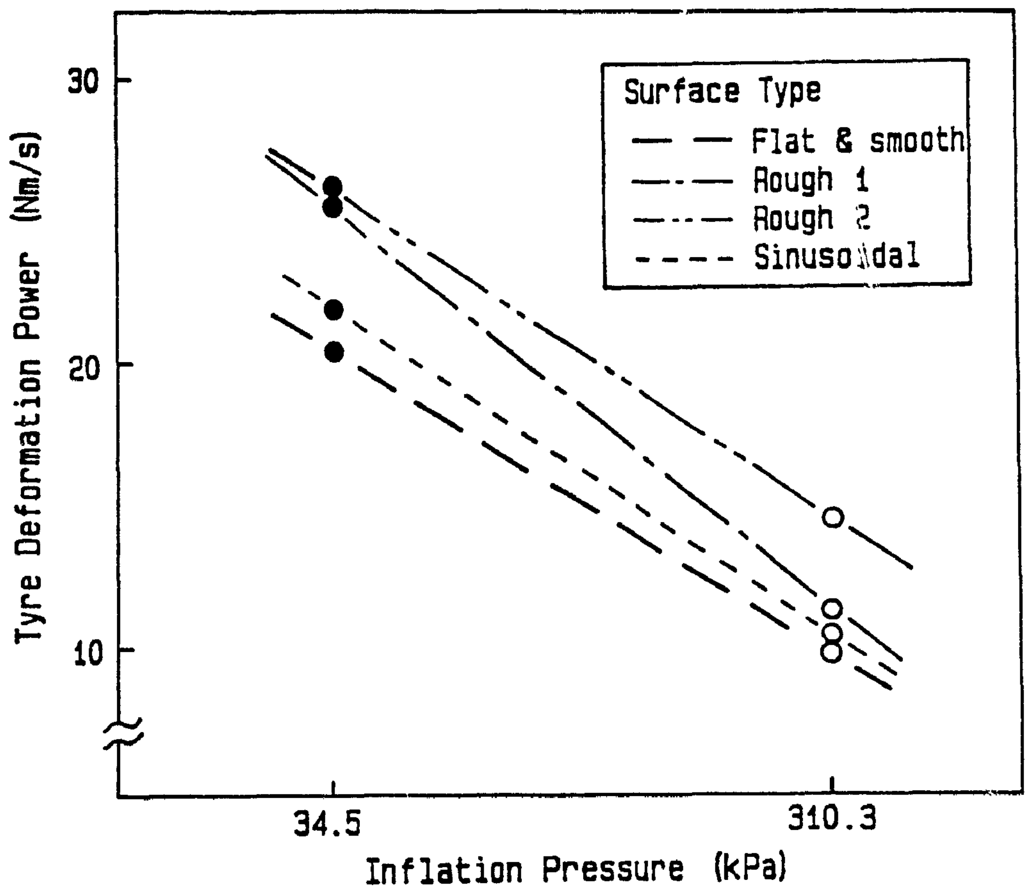

Fig. 6.5.10 Tyre deformation power for different surfaces as a function of inflation pressure

In Fig. 6.5.10, the inclined straight lines were simply drawn, although only two points were given. This was performed based on the results of Boonsinsuk. In his experiments, a linear relationship between tyre deformation power and inflation pressure was revealed. Theoretically the deformation power of the tyre should decrease asymptotically as inflation pressure increases, due to nonlinear material characteristics (Kamm, 1938). These nonlinear characteristics were not observed at very low speed regarding the power wasted in a tyre.

(3) On a rougher surface, a pneumatic tyre exhibits higher power dissipation for both high and low inflation pressures, which leads to less useful output work. Then the tyre will lose its efficiency.

A sinusoidal surface might be a particular surface compared with other randomly rough surfaces because of the unique frequency component included. While the sinusoidal test surface has a severe roughness according to its RMS amplitude, the surface cover itself may be said to be very smooth as well as a flat and smooth surface since a larger wavelength (0.8 m) than the tyre diameter (0.74 m) was used in order to conceal the tyre enveloping effect.

Comparing the flat/smooth surface and the sinusoidal surfaces, a clear difference of tyre deformation power, therefore, cannot be shown at a high inflation pressure due to the tyre's rigidity and low translational velocity in spite of the existence of excitation on such a wavy sinusoidal surface. On the other hand, more deformation power is dissipated when the tyre moves on that sinusoidal surface with very low inflation pressure. This is caused by the flexibility and large hysteresis of the tyre.

Thus, it is clear from the above results that there is a certain relationship between terrain surface roughness and the tyre deformation power resulting in resistance to motion. This will be further discussed relative to the degree of surface roughness in the following chapter.

C. DBP on various traction surfaces

a. Average of measured DBPs

Fig. 6.5.11 shows the average values of variable DBP produced by the test tyre moving on the four types of surfaces with the tyre inflation pressure of 310.3 kPa and 34.5 kPa, respectively. The averaged DBP exhibited insignificant change in their values with the slip rate over 20%. As for the effect of tyre inflation pressure, no distinct change of the DBP was observed. This means that the mean DBP is not significantly affected by the size of contact area on a non-deformable surface, although the contact area is the key concern to tyre performance on a soft deformable terrain.

With regard to the effect of surface roughness on the averaged DBP, the rough2 surface shows a little larger DBP than the rough1 surface does for both inflation pressures. It may be reasoned that the coefficient of friction of the rough2 surface is larger on average than the other due to severe geometrical roughness of rough2 surface. However, the difference of the averaged DBP by the change of surface roughness is quite small due probably to low operational speed and tyre enveloping effect. The enveloping property of a tyre reduces the efeect of the road roughness.

Moreover, it is noted that some compensation of data seem to be achieved in the testing system, causing insignificant effect of inflation pressure and surface roughness. For example, if a traction surface is rough, a larger torque may be required for the same output DBP or a smaller DBP may be obtained for the same input torque. Since both torque and DBP are output in this experiment (i.e. cannot be fully controlled), it is necessary that these two quantities have to be taken into account simultaneously for the evaluation of vehicle performance. In other words, it is questionable to evaluate the effect of surface roughness by simply considering the average DBP. Therefore, the ratio of averaged output force (DBP) to input torque was investigated to observe the effect of surface roughness. The results were normalized by setting the ratio of results for smooth and flat surface (310.3 kPa) to unity. The results are plotted in Fig. 6.5.12. It is shown from this Figure that the ratio (DBP/torque) is decreased on a rough surface and it is also affected by the inflation pressure of a tyre.

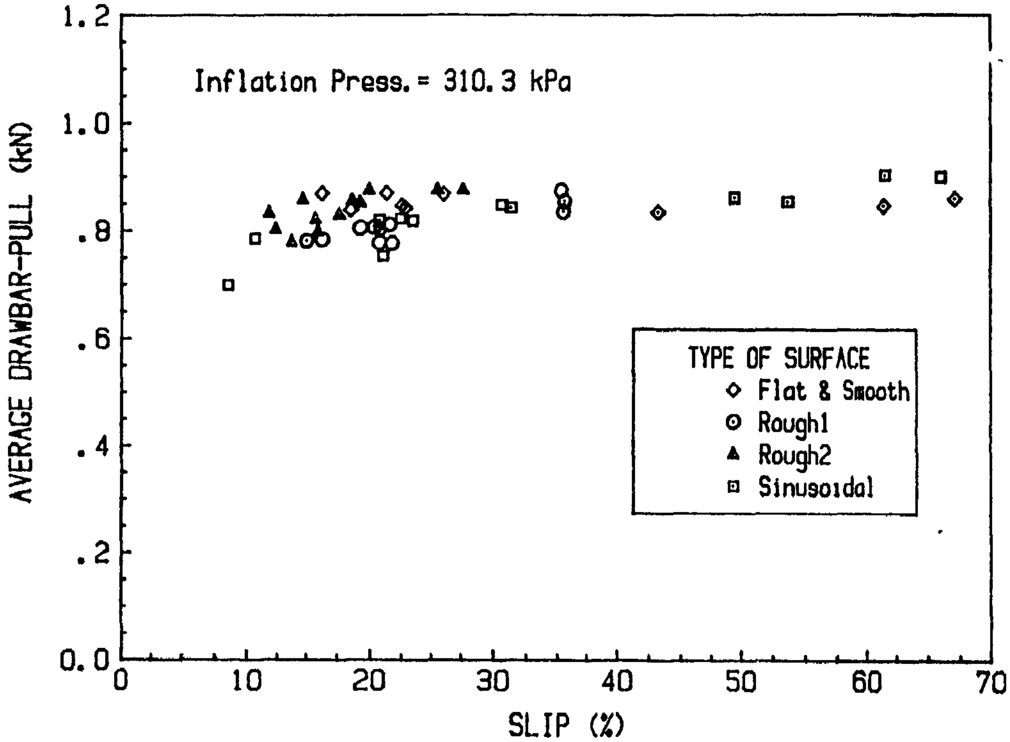

a. Inflation pressure=310.3 kPa

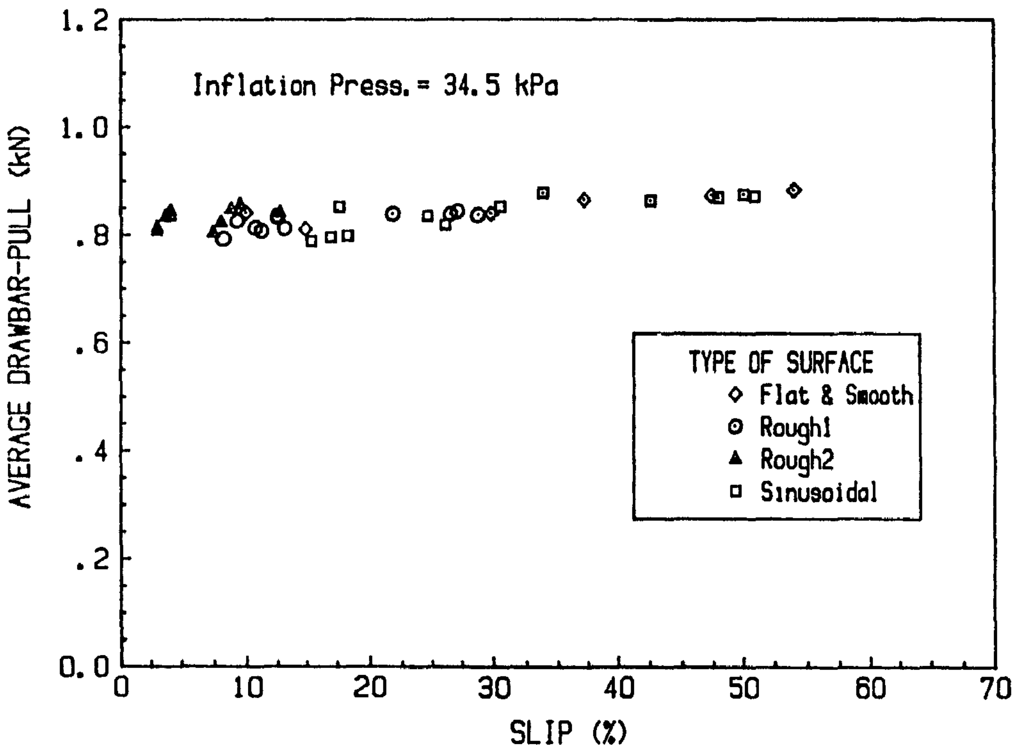

b. Inflation pressure=34.5 kPa

Fig. 6.5.11 Averaged DBP measured on each surface

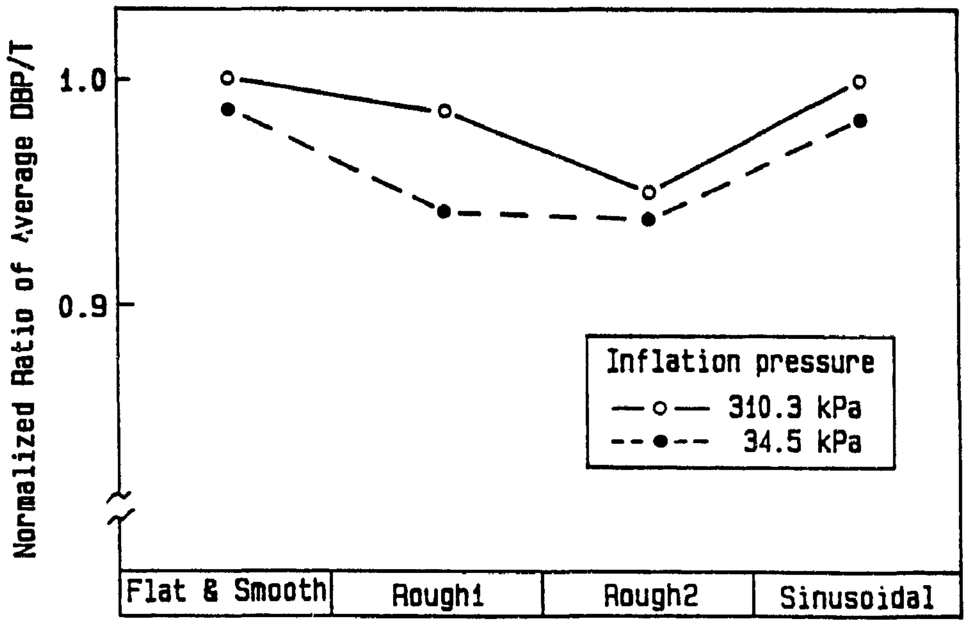

Fig. 6.5.12 Ratio of DBP to torque normalized by the ratio for flat and smooth surface at 310.3kPa

b. Variation in DBP

In fact, measured DBPs exhibit a different fluctuation phenomenon even if averaged values of DBP are similar or almost the same. Therefore, some additional consideration has to be added for the true evaluation of off-road vehicle performance on a rough terrain as explained in Chapter 4.

With a view to achieve the true evaluation of vehicle performance and to clarify the effect of surface roughness on that performance, the raw experimental data are next evaluated in the time domain. Fig.

6.5.13 shows the fluctuation (AC) component of measured DBP on each traction surface for two kinds of inflation pressure individually. The full scale for the horizontal axis is 20 seconds, and 1200 N for the vertical axis. The slip rate was chosen to be about 20% since an unexpected vibration phenomenon was observed at a high slip rate due to the non-steady state rotation of tyre. The input torque showed much a smaller variation in each measurement.

Difference in magnitude of the DBP fluctuation can be seen, depending on the type of traction surface. A larger variation of data is observed in the case of rougher surface for both inflation pressures, as might be expected. The peak-to-peak variation of measured DBP for the rough2 surface is about 1000 N for the case of 310.3 kPa (Fig. 6.5.13a(c)). On the other hand, it is about 200 N for the smoothest, flat surface. On a rough road, the tangential (frictional) force at the contact area varies every instant of time due to the continuous change of vertical load to the tyre axis and frictional characteristics. In addition, the non-uniformity of tyre properties such as radius, mass distribution, material non-uniformity or contamination of the road surface may cause the variation of DBP with a vibration of the testing machine as experienced even on the flat and smooth surface.

A lower inflation pressure generally reduces the variation of DBP. This result is related to the tyre enveloping property. When the tyre is inflated to 310.3 kPa, this pneumatic tyre acts like a rigid wheel. The difference of surface roughness is thus directly reflected in the variation of DBP. On the other hand, when the tyre is deflated to 34.5 kPa, the pneumatic tyre functions as a low-pass filter with elongated contact length between tyre and traction surface. Therefore, the surface profile is significantly modified as shown in Fig. 6.5.5 and the difference of surface roughness would not be intensified on DBP showing less variation. Thus, it is important to establish the relationship between surface roughness and the tyre enveloping property as well as the surface roughness characterization, so that one can estimate the DBP on a rough terrain.

Fig. 6.5.14 illustrates the RMS values of DBP fluctuation for each surface with different inflation pressures as a function of slip rate. A larger RMS value of DBP is observed on a rougher traction surface for both inflation pressures. The larger value of RMS decreases the true vehicle performance because of its fluctuation. Therefore, the tractive efficiency is estimated to be reduced on a rough road compared to on a flat and smooth surface. Each RMS value does not show any distinctive change with the slip.

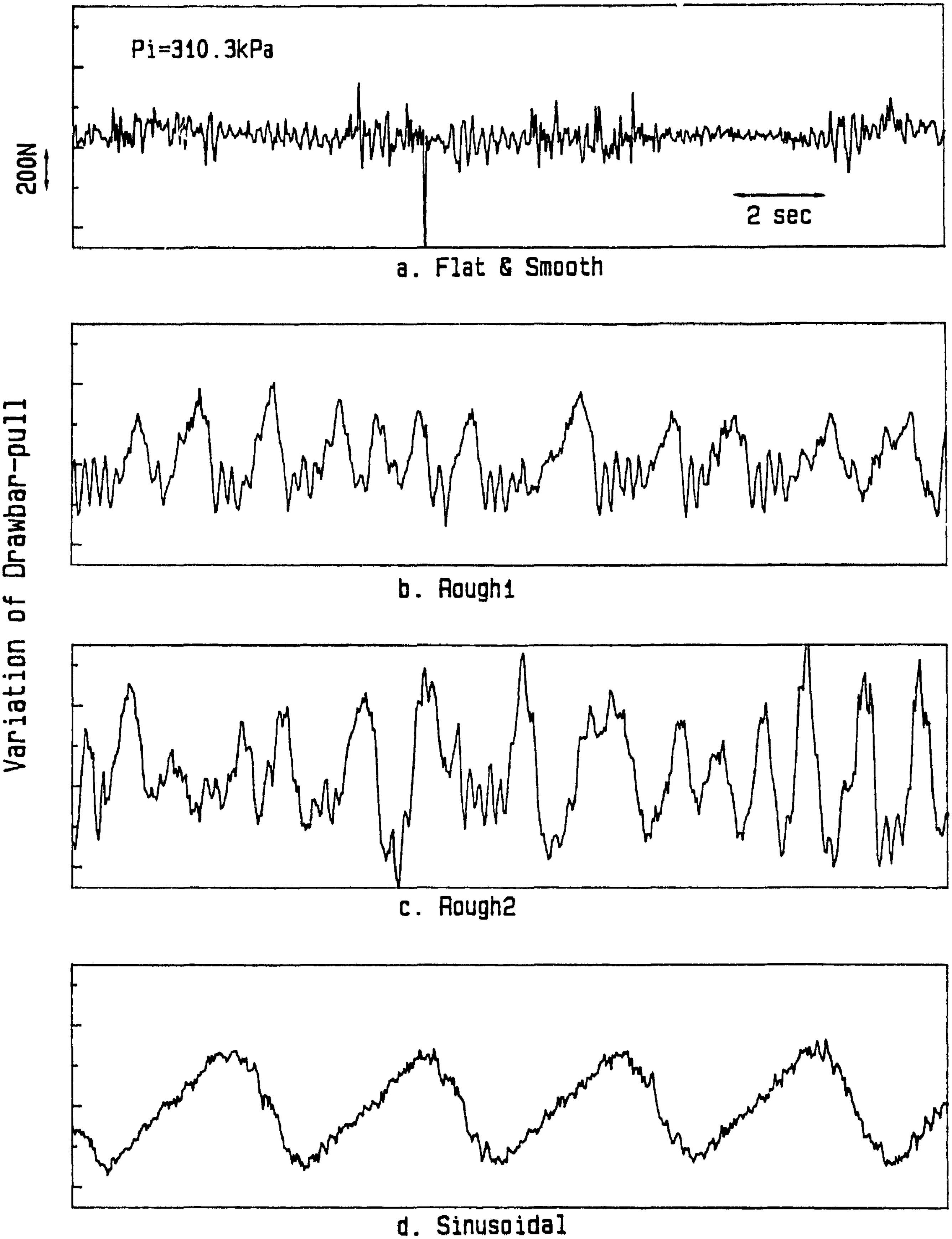

Fig. 6.5.13a Variation in DBP on various surfaces (inflation pressure=310.3 kPa)

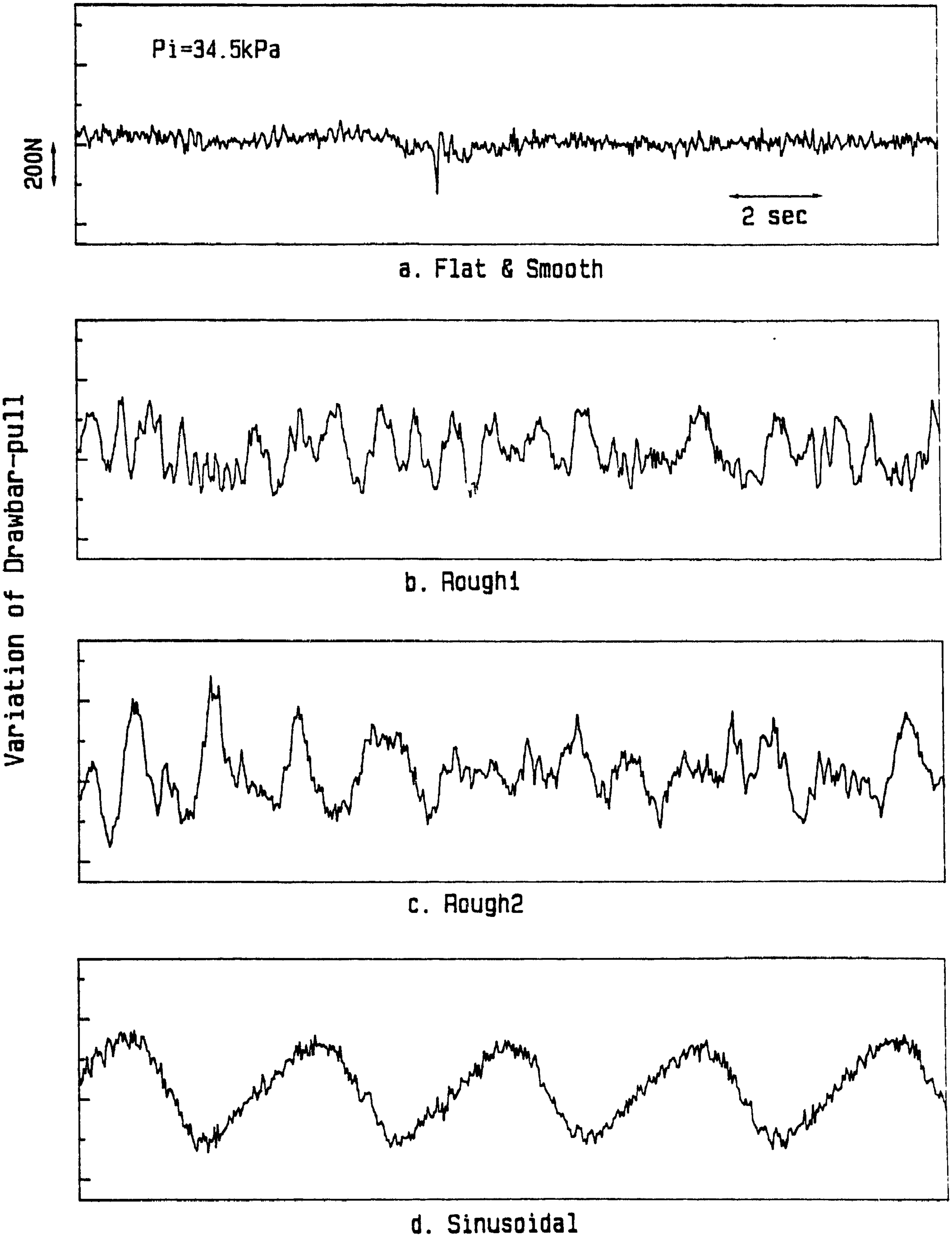

Fig. 6.5.13b Variation in DBP on various surfaces (inflation pressure=34.5 kPa)

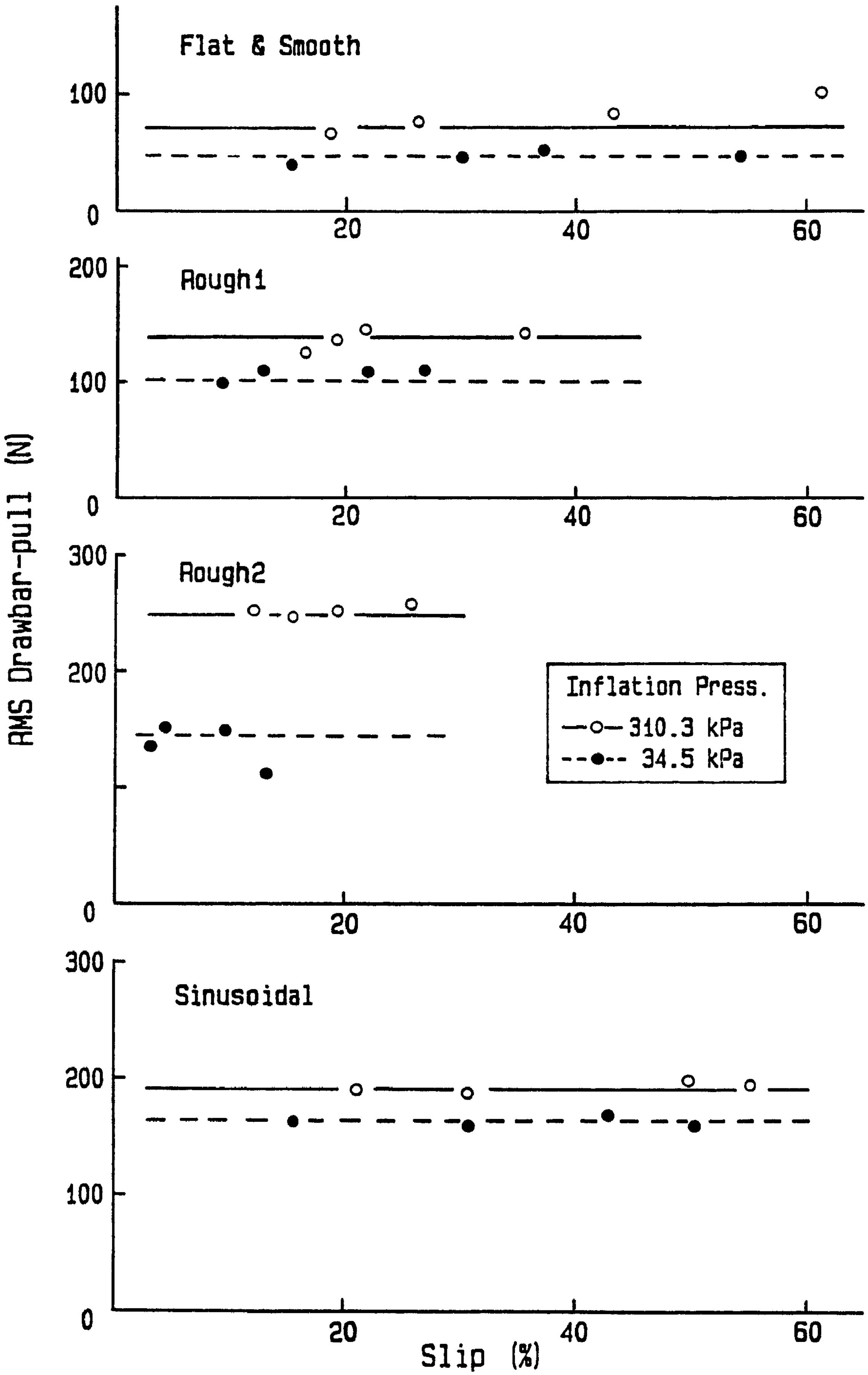

Fig. 6.5.14 RMS values of DBP over various surfaces as a function of slip

c. PSD of measured DBP

Fig. 6.5.15 displays the PSD curves of measured DBPs over each rough surface, indicating the effect of surface geometry (wavelength) on DBP variation. The translational velocity is 0.18 m/s and slip rate is set to about 20%. The frequency range is taken between 0.1 and 20 Hz (shown only up to 10 Hz in Figures). From the comparison of these four Figures, the following remarks can be derived in terms of frequency contribution.

On the sinusoidal surface (Fig. 6.5.15d), the peak value of DBP PSD is observed at 0.22 Hz. Since the temporal frequency, f, can be altered by the following relationship with the wavelength, λ,

$$\lambda = V/f \qquad V : \text{velocity } (0.18 m/s)$$

this frequency corresponds to the particular wavelength (0.8 m) of the test sinusoidal surface. That is to say that the fluctuation of tractive force is directly influenced by the terrain surface geometry. The second peak is the harmonic component of this distorted sinusoidal DBP signal.

As for random rough traction surfaces (Fig. 6.5.15b,c), the PSD curves of the DBP demonstrate, in general, larger values in the lower frequency range, especially between 0.2 Hz and 1.0Hz. The corresponding wavelength range for this frequency range is between 0.18 m and 0.9 m. A large part of the fluctuation in DBP is caused by these wavelength components of traction surface, and in this range, more tractive power is dissipated by these low vibration frequencies.

However, on a flat and smooth surface, their PSD curves do not show any particular characteristics such as mentioned above but display the white noise-like characteristics, since this surface does not possess the conspicuous irregularities on it. Therefore, it can be said that the fluctuation of DBP is related to the traction surface geometry.

The effect of inflation pressure is also seen in the PSD curves of the DBP. On a rough surface, a low inflated tyre shows less PSD i.e. less variation of DBP for a whole frequency range. Especially, the dominant fluctuation component between 0.2 Hz and 1.0 Hz of DBP is largely diminished by the reduced inflation pressure of 34.5 kPa. By contrast, there is little effect of inflation pressure in DBP PSD for the flat and smooth surface.

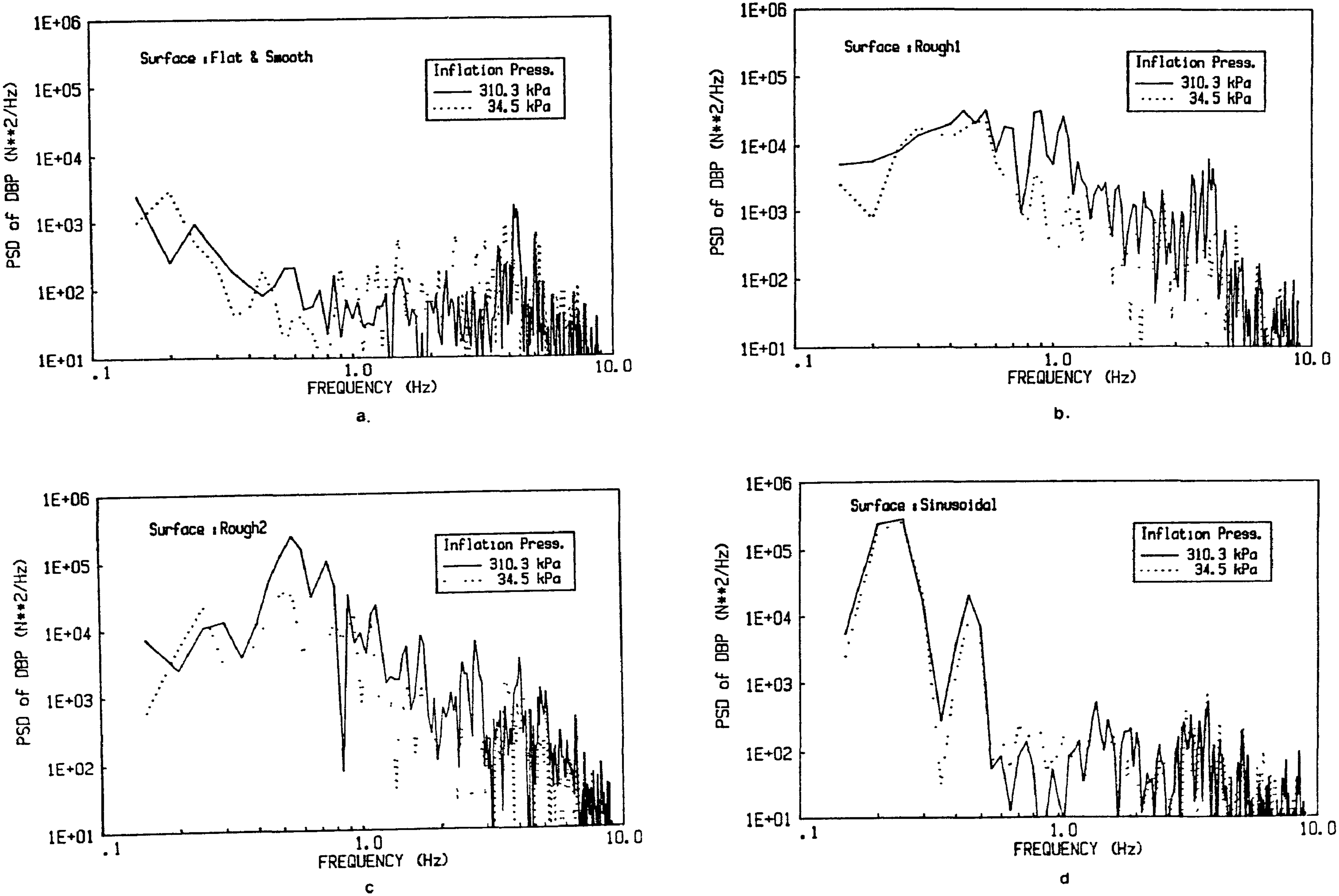

Fig. 6.5.15 PSD curves of measured drawbar-pull for various traction surfaces

6.6 Summary

(1) The stiffness, contact length coefficient and damping ratio of the pneumatic tyre were obtained as a function of tyre inflation pressure.

(2) The roughness of pseudo-random rough traction surfaces were measured in the laboratory using an ultrasonic distance detector. The measurement by this equipment would be more effective by improving some defects.

(3) Smoothed (enveloped) surface profiles were directly measured by rolling a tyre freely on the test surfaces. A low inflated tyre exhibited a large effect of surface enveloping.

(4) A larger tyre deformation power loss was observed on a rougher surface or for a low inflated tyre. Tyre deformation power was not affected by the slip.

(5) While a clear difference in the average DBP was not shown for different traction surface, larger input torque was required on a rougher traction surface, indicating the effect of road roughness.

(6) Rougher surface and highly inflated tyre exhibited a larger variation of the DBP.

(7) Traction surface geometry affects the manner of the variation of DBP. The range of traction surface wavelengths, between 0.18 m and 0.9 m approximately, contributes to the fluctuation of the DBP.

PART III GENERAL DISCUSSION AND CONCLUDING REMARKS

In Part III, the following two components are studied.

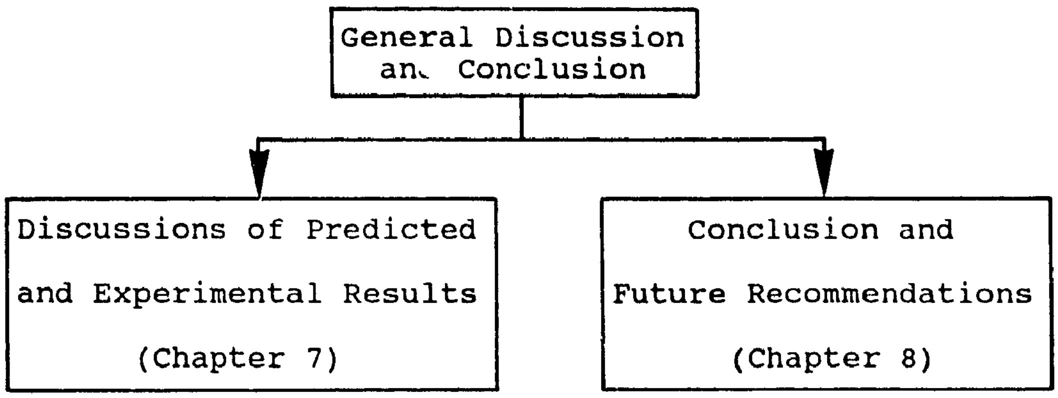

CHAPTER 7

DISCUSSIONS OF PREDICTED AND EXPERIMENTAL RESULTS

7.1 Introduction

Both theoretical (Part I) and experimental (Part II) investigations were attempted in order to study the effect of ground surface roughness on tyre performance. In this chapter, three major components of this study (surface roughness characterization, tyre enveloping property and tyre tractive performance) are discussed separately.

Section 7.2 presents a discussion on the measured test traction surfaces and classification of their surface roughness by ISO recommendations. The enveloping function of the specified tyre (Michelin 7:00 R16 XCL) is determined by using the experimental results in Section 7.3. Section 7.4 provides the discussion of surface roughness effect through traction test results and shows a comparison of experimental results and theoretical results. Section 7.5 presents a parametric investigation using computer simulation regarding the effect of road roughness, tyre inflation pressure and speed on the nominal tractive efficiency of a pneumatic tyre.

7.2 Comparison and Classification of Test Surface Roughness

Our prime interest in this section is the classification and evaluation of the roughness of measured test surface profiles.

7.2.1 RMS Value of Surface Height Profile

RMS amplitude value is frequently used as an index representing the degree of road roughness. The RMS value is obtained by calculating the area under the PSD curves of the test surface profile. The results are shown in Table 7.1.

Table 7.1 Calculated RMS amplitude values for each test surface

Surface	Flat/smooth	Rough1	Rough2	Sinusoidal
RMS(E-3 m)	2.19	4.52	8.54	14.38

Table 7.1 depicts the "degree" of roughness in the order of sinusoidal, rough2, rough1 and flat and smooth surface. RMS value may provide a certain basis for the evaluation of road roughness. However, the "condition" of road roughness cannot be fully described by information from the RMS values only. For instance, the variances of sinusoidal surfaces which have the same amplitude, are consistent even if their wavelengths are different. Thus, the description of road surface roughness using RMS is insufficient since the road wavelength determines the dynamic excitation frequency, in relation to the vehicle speed.

7.2.2 Classification of Test Surface Roughness

Fig. 7.2 compares the PSD curves of four types of test surfaces and the classification boundaries of surface roughness, as proposed by ISO. The PSD representation gives information about both amplitude energies and frequencies included in a stochastic process. These two quantities are required for the analysis of dynamic behavior. The representation by PSD is based on the assumption that the road surface profile is the stationary random process.

The PSD curve may be approximated by a straight line inclined at a certain angle on a log-log plot, as suggested by ISO. Vertical shifting of the lines occurs for different road amplitudes that have similar distributions of wavelengths. Different PSD values show differences in dimensions of surface amplitudes, and changes in slope explain different amplitude-frequency (wavelength) distributions.

The approximation of the PSD curve by a straight line demonstrates the possibility of using a simple mathematical expression for a random signal. The simplified mathematical form representing road roughness was given previously as follows:

$$S_{(\Omega)} = G_o \Omega^{-n} \tag{2.6}$$

where Ω is the spatial frequency. The roughness constant,Go, and slope constant,n, for each road surface,

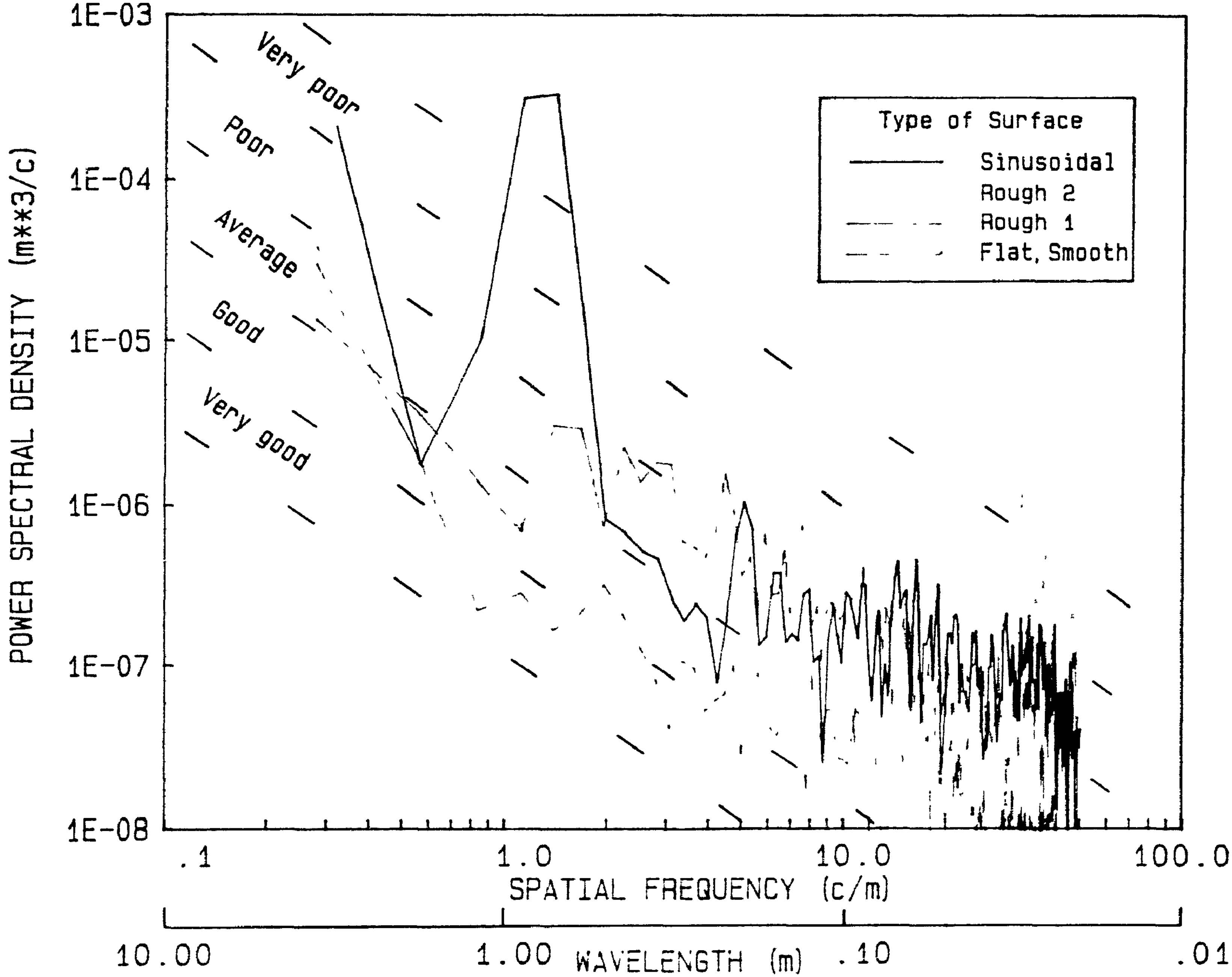

Fig. 7.2 Comparison of PSD curves for four types of test surfaces

except for the sinusoidal surface, are determined from averaged PSD curves (Table 7.2). Large Go and small n values generally correspond to a rough road due to large power components over a wide range of frequencies. These experimental constants take different values depending on the type of road roughness. However it was reported by other researchers (Dodds and Robson,1973; Ohmiya,1986) that the slope constant lies between 1.0 and 2.5 in most cases. Considering the PSD curves and their experimental constants, the test surfaces can be individually categorized based on the proposed classification method by ISO (Table 7.2).

Finally, the roughness of the test traction surfaces used in our laboratory are found to correspond to the following types of actual road surfaces, as shown in Table 7.2.

Table 7.2 Measurement of test surface profile-summary

Test Surface	Go	n	Roughness	Actual Road Surface
Flat & smooth	6E-7	1.5	Very Good-Good	Good paved runway
Rough1	6E-6	1.6	Average	Poorly paved road
Rough2	5E-5	1.8	Poor	Country road
Sinusoidal	N/A			

7.3 Analysis of Tyre Enveloping Property

In Chapter 3, two types of theoretical enveloping functions (rectangular type and exponential type) were introduced. In this section, these two tyre enveloping functions are compared by using the experimental results.

7.3.1 Effect of Speed on Tyre Enveloping

A relationship between the enveloping effect and the translational velocity has not been experimentally confirmed. It can be estimated that the filtering effect would be intensified if the translational speed is fast, since a tyre does not follow a ground profile, but jumps (Fig. 7.3.1).

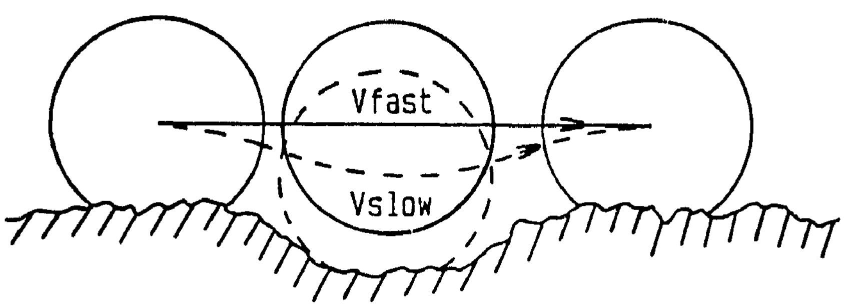

Fig. 7.3.1 Effect of speed on tyre enveloping

However, since the jumping phenomenon is assumed to be negligible because of the relatively heavy weight and slow operational speed of the off-road vehicle, it is reasonable to assume the enveloping property of the tyre to be a function of contact dimension only in the space domain, excluding the effect of speed. Under this assumption, the derived experimental data can be used for the analysis of the tyre enveloping effect.

7.3.2 Empirical Derivation of Enveloping Function

Fig. 7.3.2a shows the plots of PSD curves for a filtered test surface profile,y2, for tyre inflation pressures of 310.3 kPa and 34.5 kPa respectively. A clear distinction between the two amplitude PSD curves can be seen over the spatial frequency range between 1 c/m and 4 c/m. The total power of amplitude PSD for 34.5 kPa is clearly less than for 310.3 kPa. This indicates that a greater amplitude energy from the original surface is absorbed by the low inflated tyre as compared to the high inflated one, as a result of a large enveloping effect. As for the range over 4 c/m, no difference between the two curves is exhibited due to a difficulty in detecting small road surface asperities with the current equipment.

The frequency response function of the tyre enveloping property can be directly derived by calculating the ratio of PSD functions of two surfaces, i.e. the filtered profile and the original ground surface profile. Thus,

$$H_{E(\Omega)} = \sqrt{\frac{\text{PSD of filtered profile}}{\text{PSD of original profile}}} \qquad (7.1)$$

Fig. 7.3.2b describes the tyre enveloping function derived from the experimental data obtained by running tyre tests with two different inflation pressures. It is indicated that the tyre enveloping function works over the spatial frequency of 1 c/m for this system. Since this spatial frequency (1 c/m) corresponds to a wavelength of 1 m, it is estimated that wavelengths shorter than 1 m will be filtered somewhat by this flexible tyre, depending on the wavelength of the ground surface and the inflation pressure of the tyre. The wavelengths which start to exhibit the enveloping property are approximately 1 m for both inflation pressures, though the contact lengths on a flat and smooth test surface are different from each other by the inflation pressure.

A difference in the enveloping effect of tyre inflation pressure is clearly exhibited in the results. A lower inflated tyre is found to show a larger effect of attenuation. Although several improvements are still required for precise measurement, it was confirmed that a tyre acts like a low-pass filter, i.e. the shorter the wavelengths are, the more intensively an original road surface amplitude power is reduced by the enveloping property of a flexible tyre.

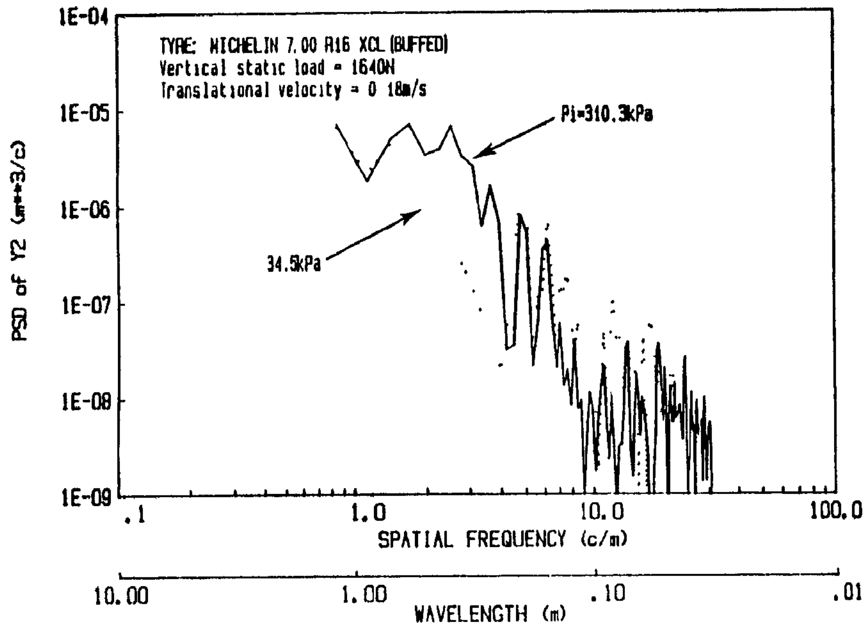

Fig. 7.3.2a PSD curves of filtered profile showing effect of tyre inflation pressure

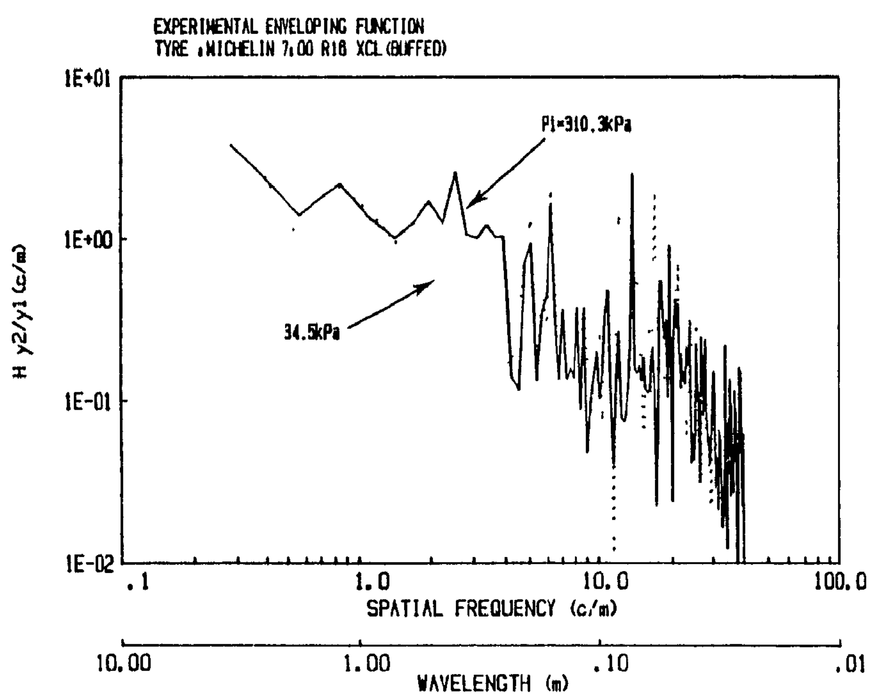

Fig. 7.3.2b Tyre enveloping functions derived from experimental results

7.3.3 Comparison of Rectangular Type and Exponential Type Enveloping Function

Fig. 7.3.3. shows theoretical curves of the rectangular type (R-type) enveloping function and exponential type (E-type) enveloping function individually, exhibiting the effect of the tyre inflation pressure (310.3 kPa and 34.5 kPa). Curves for the R-type function (Fig. 7.3.3a) are derived using the experimental relationship between the contact length and the vertical static load on the tyre axle. It is seen that a low inflated tyre has a larger enveloping effect to shorter wavelengths because of its flexibility. Gibb's phenomenon (ripple components) can be seen over 2 c/m. However, the "enveloping" lines of the rippled curves give a general decay rate in the response function with increasing frequency.

For the effect of the tyre inflation pressure, these theoretical curves agree with the experimental results, up to a spatial frequency of approximately 4 c/m, while the slopes of the theoretical curves are slightly smaller than those derived from experiments. One of the advantages of this function is the convenience in defining the function by simply knowing the load-contact length relationship of a tyre.

The E-type enveloping function can provide better fitting curves to the experimental results, as seen in Fig. 7.3.3b, because it relies totally on the experimental

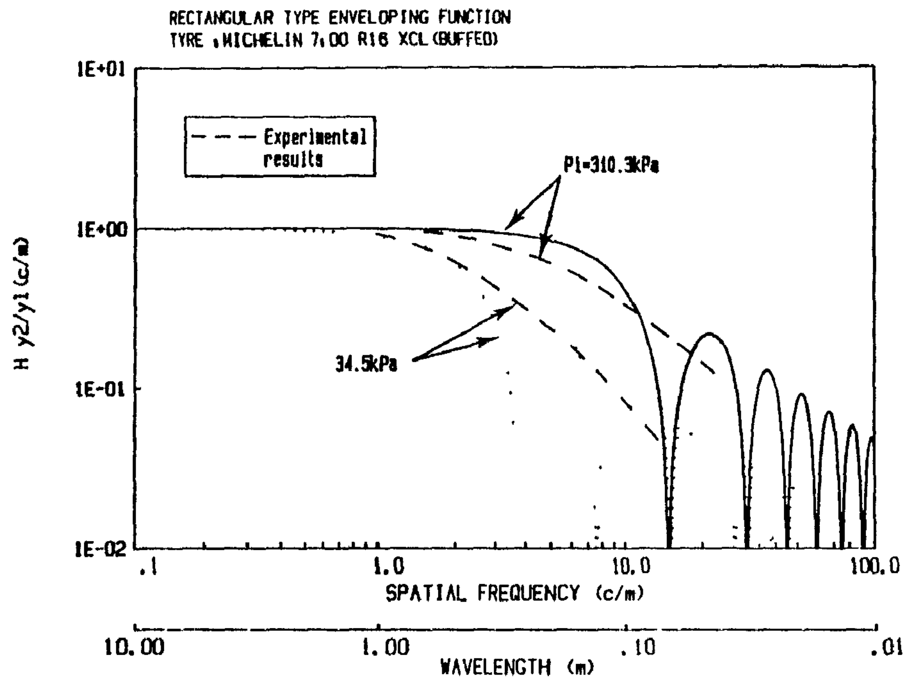

Fig. 7.3.3a Theoretical curves of a rectangular type of enveloping function for different inflation pressure

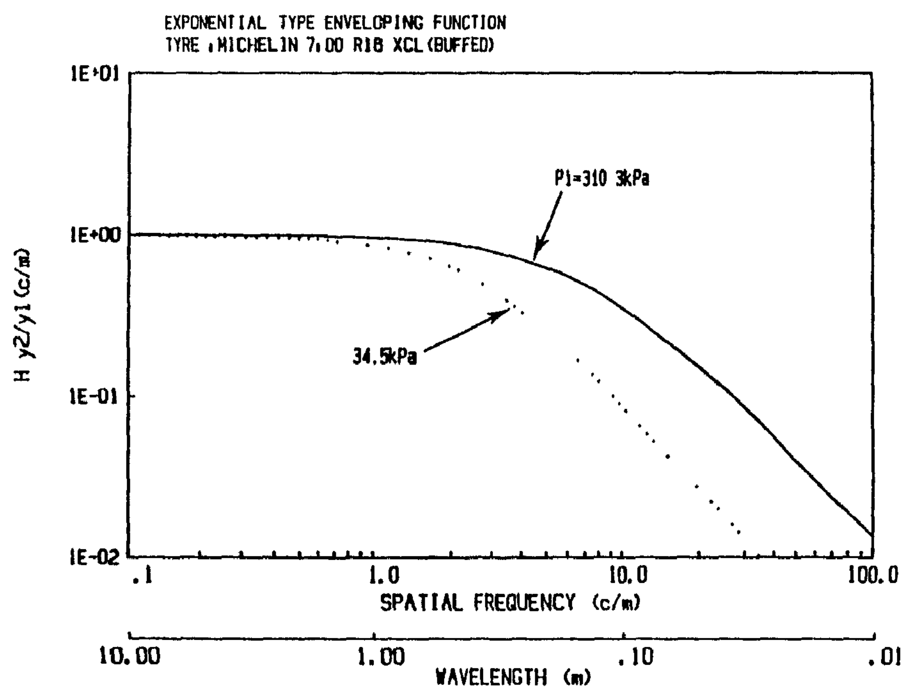

Fig. 7.3.3b Theoretical curves of an exponential type of enveloping function for different inflation pressure

results. This enveloping function decays smoothly with an increase of spatial frequency, without exhibiting any ripples as shown in the R-type enveloping function. Table 7.3 indicates the experimental constants, a and b in Eq. (3.6), for the derived E-type function.

Table 7.3 Constants for exponential type enveloping function (tyre:Michelin 7:00 R16 XCL)

Inflation pressure	a	b
310.3 kPa	6.8	1.6
34.5 kPa	2.7	1.8

This function is more empirical than the R-type enveloping function, since no characteristic parameters of the tyre are included. Therefore, a number of tests are required to define this frequency response function. Furthermore the derived function is not universally determined, but is limited in its application to a specific type of tyre inflated to a specific pressure. The advantages and disadvantages of each enveloping function are compared and are summarized in Table 7.4.

Table 7.4 Comparison of advantages and disadvantages of two enveloping functions

Enveloping function	advantage	disadvantage
Rectangular type	includes tyre parameter (contact length) simply determined	not very accurate displays Gibb's phenomenon (not smoothly decayed)
Exponential type	smooth filtering accurate	needs numbers of experiments

In conclusion, the rectangular type of tyre enveloping function is chosen in this study because:

(1) it shows relatively good agreement with experimental results, and

(2) it is determined in a simple manner, using load-deflection relationship.

7.4 Discussion of Surface Roughness Effect through Traction Test Results

7.4.1 Vertical Acceleration, Tyre Deformation Power and DBP Variation

Fig. 7.4.1 compares the RMS value of vertical acceleration at the tyre axle, average tyre deformation power and RMS value of DBP variation as a function of the roughness constant. Each result is normalized by setting the value for a flat and smooth test surface (310.3 kPa) to be unity. The classification range of road surface roughness by ISO and derived roughness constants of test traction surfaces are also indicated at the bottom of the Figure. The following results may be found by a comparison of the three sets of experimental curves.

Effect of traction surface roughness

A larger vertical acceleration is produced on a poorer (rougher) surface. Under a high speed operation, a larger vertical acceleration would be expected. This produces a condition similar to rougher road operation. This may result in a reduction of average DBP because of increased tyre deformation power.

The tyre deformation power loss is increased with an increase in the test surface roughness. This power loss may have a limited value under the same velocity and load, because a tyre does not recognize the difference in road roughness when the roughness exceeds a certain level, as previously exhibited in Fig. 6.5.4 (pg.156).

As for the variance in measured DBP, the effect of road roughness is evident. It can be estimated that not only vertical vibration but also horizontal vibration arises when a tyre is operated on a rough road. That is, the change in vertical dynamic load due to road roughness causes the change in the horizontal frictional force at the wheel-ground interface, resulting in a horizontal vibration with a variation of DBP. Since the tractive efficiency is estimated to decrease with an increased variation of the DBP, it is important to design a proper suspension or tyre rigidity to reduce the vertical vibration, as well as to improve ride comfort and vehicle controllability or steerability.

Effect of tyre inflation pressure

A highly inflated tyre exhibits a larger acceleration on a rough traction surface. This is probably due to high restitution of the tyre. With regard to the tyre deformation power loss, larger power loss is obtained for a low inflated tyre.

For the RMS value of DBP, a low inflated tyre exhibits a small variance of DBP. In fact, the smooth rotating motion of a soft tyre was observed during laboratory tests. The flexibility has the function of reducing the horizontal vibration, in addition to magnifying the enveloping effect, while tyre deformation power loss is increased.

Thus, in order to achieve high tractive efficiency, it is necessary to accomplish the two conflicting demands i.e. less tyre deformation power loss by high inflation pressure, and less horizontal vibration by low inflation pressure, since the efficiency is defined by both the mean and variance of DBP. From the results, it was reconfirmed that the tyre inflation pressure was one of the most important parameters controlling not only the vertical acceleration but also the tractive efficiency on a rigid rough road, as well as on a soft deformable terrain.

As for the sinusoidal test surface, the vertical accelerations for each inflation pressure are nearly equal to those for the flat and smooth surface i.e. very small, since that test surface cover is smooth and test speed is quite slow (0.18 m/s). For the tyre deformation power, the effect of surface roughness is observed at a low inflation pressure in spite of the low translational velocity. RMS DBP becomes unexpectedly large on this sinusoidal surface because of "up and down motion" due to a large amplitude wave form.

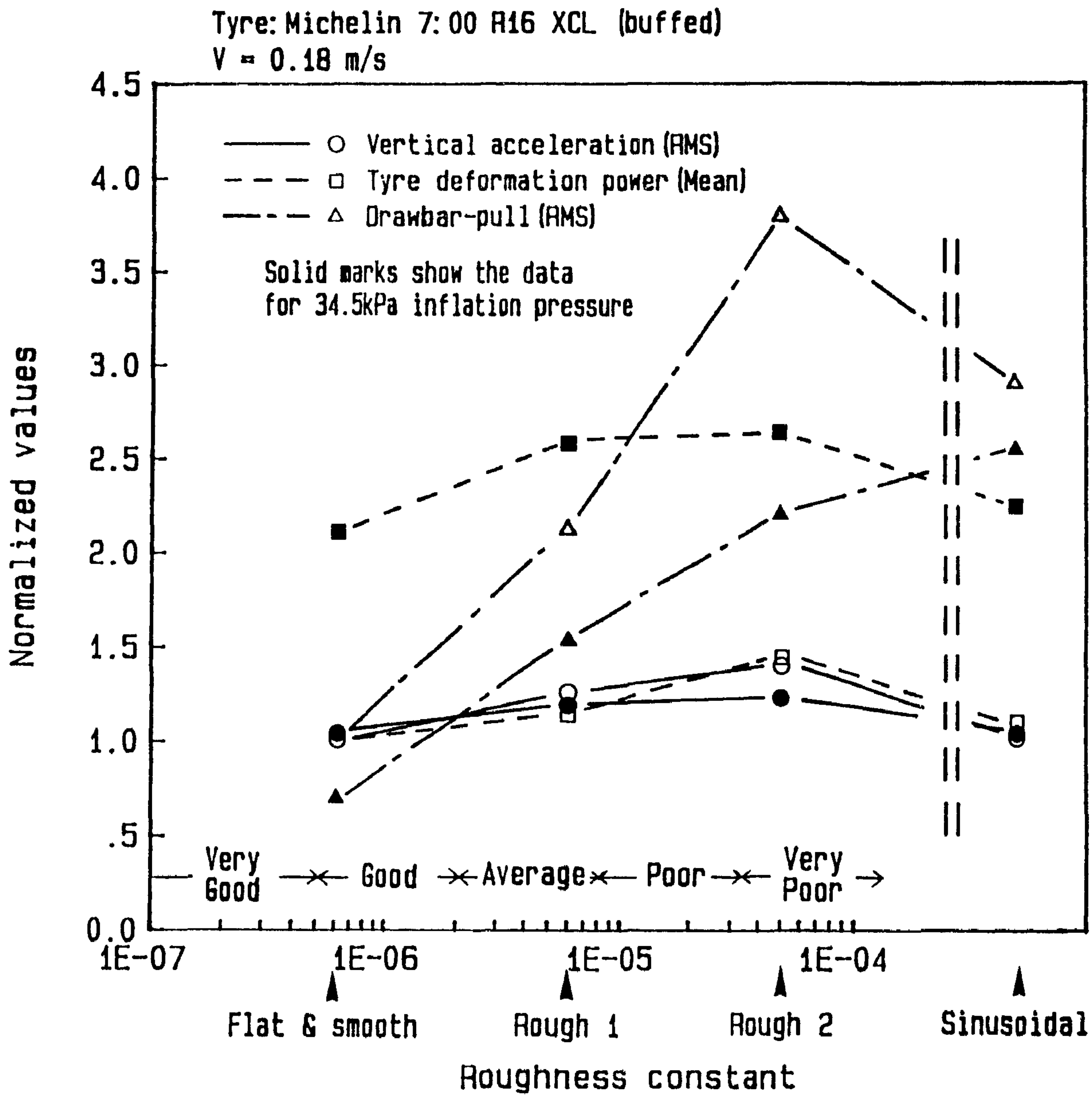

Fig. 7.4.1 Effect of surface roughness on RMS vertical acceleration, average tyre deformation power and RMS DBP

7.4.2 Nominal Tractive Efficiency obtained by Experiments

Fig. 7.4.2 displays the experimental results of nominal tractive efficiency for various rough traction surfaces for the inflation pressures of 310.3 kPa and 34.5 kPa, respectively. It is well understood that efficiency is decreased with an increase of tyre slip due to an increased interfacial (slip) power loss. The following trends are found from the experimental results:

Effect of traction surface on tractive efficiency

The efficiency on a smoother traction surface is greater than that on a rougher surface over a whole slip range and, therefore, the efficiency at the same slip rate is reduced in the following order: flat and smooth, rough1, sinusoidal and rough2 surface. However, an overly large effect seems to be exhibited by surface roughness in the experimental results, despite very low translational speed. Although these results could be due to a slight change in horizontal velocity, the effect of traction surface roughness on tyre performance can still be recognized by considering the increased input power on a rougher surface, as previously shown in Fig. 6.5.12 (pg.179).

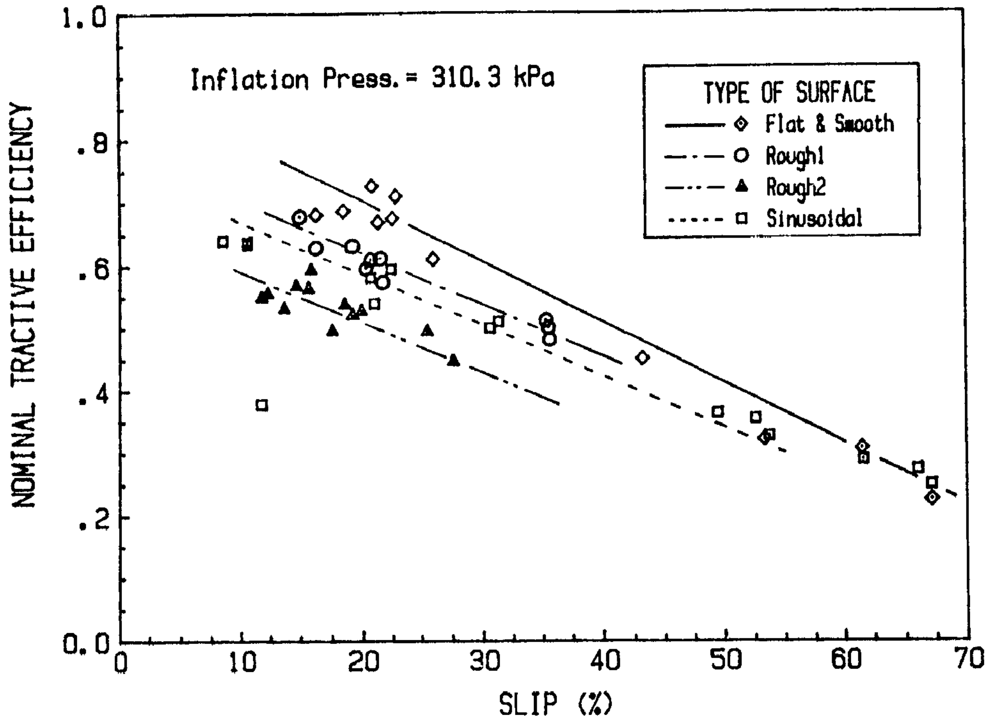

a. Inflation pressure=310.3 kPa

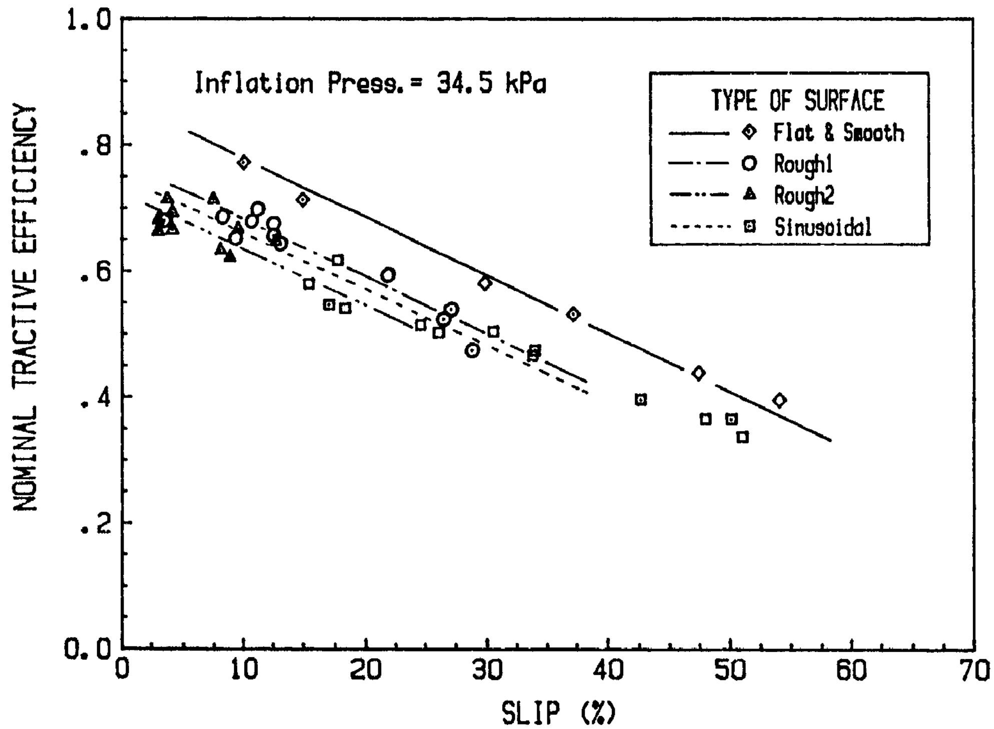

b. Inflation pressure=34.5 kPa

Fig. 7.4.2 Experimental results of nominal tractive efficiency for each traction surface as a function of wheel slip

Effect of inflation pressure on tractive efficiency

In general, a highly inflated tyre can produce a higher efficiency because of a smaller power loss by tyre deformation. However, the reverse effect is exhibited only for the case of the rough2 surface. The efficiency for 310.3 kPa pressured tyre is marginally lower than for 34.5 kPa tyre on this surface. This can be due to intensified variation of DBP resulting from the horizontal vibration (a slight stop and go motion). This is caused by the high rigidity of the tyre and insufficient dynamometer carriage power. As a result, the tractive efficiency of a high inflated tyre becomes smaller than that of a low inflated tyre, in spite of small tyre deformation power loss.

7.4.3 Comparison of Experimental Results with Prediction

Fig. 7.4.3 shows the comparison between predicted results and experimental results using the flat and smooth road surface. Vehicle speed is 0.18 m/s and inflation pressures are 310.3 kPa and 34.5 kPa. It is found that approximately 7% lower tractive efficiency is obtained in the experimental results. This is assumed to be due to too much DBP variance during the running test, as explained earlier. For instance, 50-70 N of variation (RMS) of DBP is observed in the experiments, even on a flat and smooth surface. This value corresponds to 6-8% of average DBP (about 830 N). The variance of DBP reduces the nominal tractive efficiency.

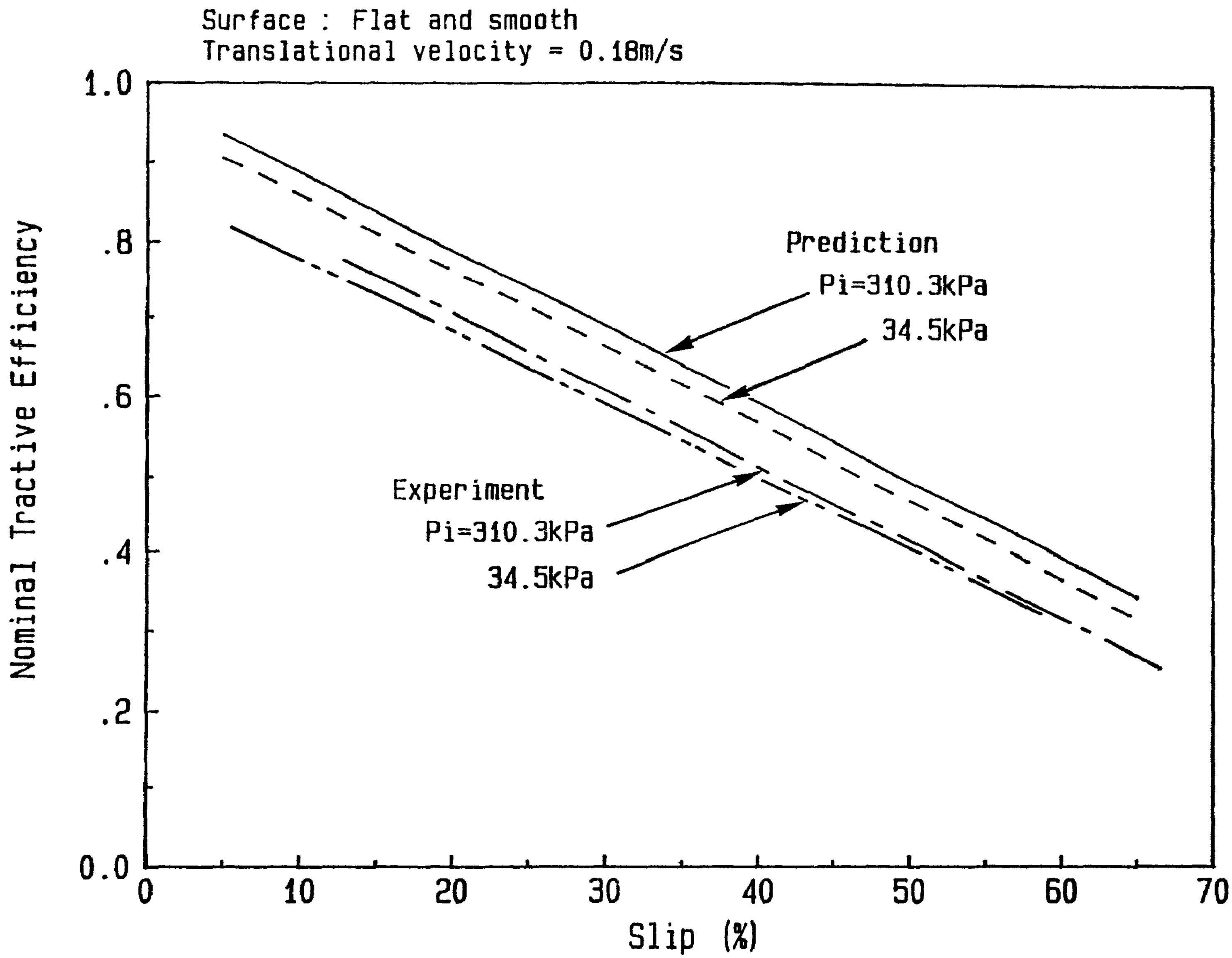

Fig. 7.4.3 Comparison of predicted and experimental nominal tractive efficiency

However, a completely constant velocity was assumed in the prediction. Thus the efficiency is larger than that given in the experimental results because of a lesser variation in DBP. Fig. 7.4.4 exhibits the set of typical curves of tractive efficiency measured on various grounds (Mckyes, 1985). While the effect of terrain roughness is not shown here, our predicted result for the flat and smooth surface shows a good agreement with the results for a smooth concrete road surface in Fig. 7.4.4.

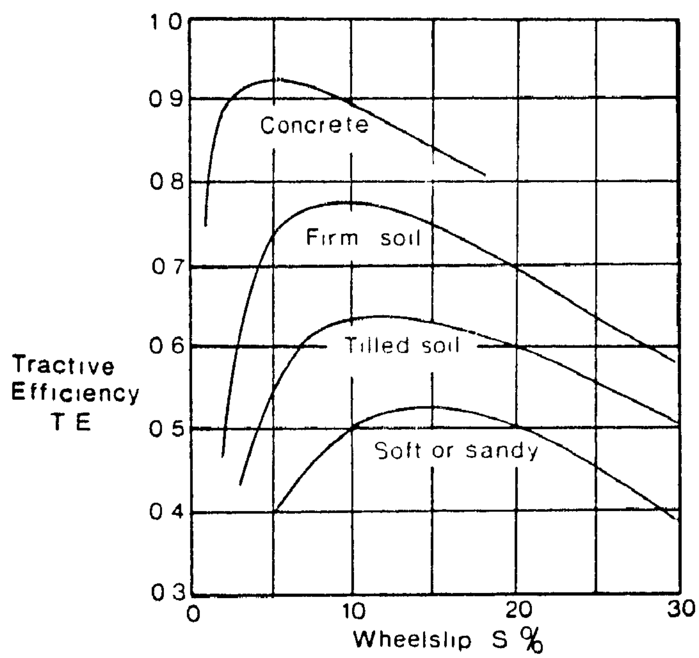

Fig. 7.4.4 Tractive efficiency curves versus wheel slip for different grounds (after Mckyes)

7.5 Investigation of Tractive Efficiency by Predicted Results

With the objective of obtaining further information regarding the effect of the principal parameters for vehicle mobility on road roughness, several investigations have been attempted, based on the predicted results. Three parameters, which are the vehicle translational velocity, the tyre inflation pressure and the road surface roughness, are taken into account for the analysis. Two assorted rough surfaces, i.e. the deterministic sinusoidal road surface and the non-deterministic random rough road surfaces, are employed in the analytical prediction.

7.5.1 Efficiency on a Sinusoidal Road Surface

(1) Effect of vehicle velocity on tractive efficiency

Fig. 7.5.1 shows a plot of the nominal tractive efficiency curves against the translational vehicle velocity for different tyre inflation pressure. The sinusoidal road surface used in the analysis has a peak-to-peak amplitude of 0.02 m and its wavelength is 0.8 m. The roughness of this surface is relatively severe according to its RMS amplitude (7.07E-3 m). 20% of slip was chosen as the value at which to quote the coefficient of traction because this value is commonly used by other authors and is usually close to the highest value at which an off-road vehicle can work continuously at reasonable efficiency.

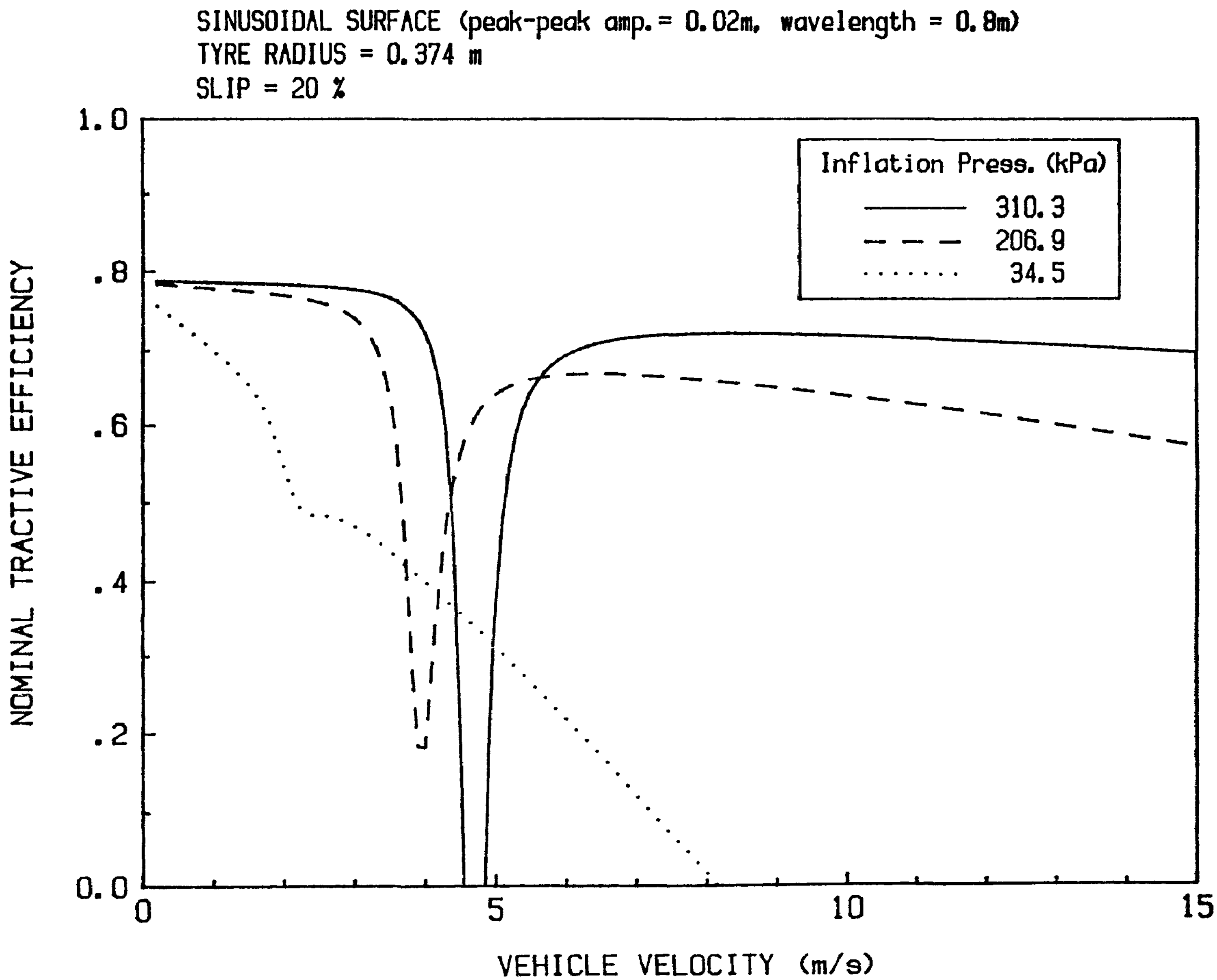

Fig. 7.5.1 Predicted nominal tractive efficiency as a function of vehicle velocity on a sinusoidal surface

An unstable operating speed range is found to exist between 2 m/s and 5 m/s, depending on the tyre inflation pressure, which alters the natural frequency of a system. This unpleasant speed range includes two significant effects; one is the sudden drop in the tractive efficiency due to a decrease in tractive force (DBP) and the other one is the occurrence of a dangerous condition of operation (jumping) due to resonance. The phenomenon of more severe resonance of a tyre will occur at a higher inflation pressure.

A decrease in tractive force under an oscillatory tyre motion was also reported by Wong (1970, 1972) and Cap and Wambold (1984). Orlandi and Matassa (1986) found an abrupt reduction of friction at the resonant frequency under sinusoidal excitation, though the excitation amplitude, which could give additional insight into the phenomena, was not shown. Their test facility and experimental results are shown in Fig. 7.5.2. The vertical exciting load was controlled by the eccentricity of the rotor. F_E and F are the measured tractions with/without vibration, respectively. The result exhibits a good agreement with our prediction that the tractive force drops drastically where the excitation frequency matches the natural frequency of the system. The effect of inflation pressure was not shown in their study.

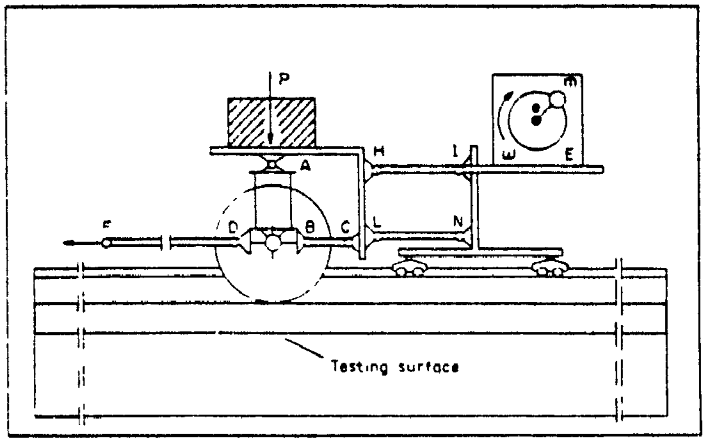

a. Test rig (after Orlandi and Matassa)

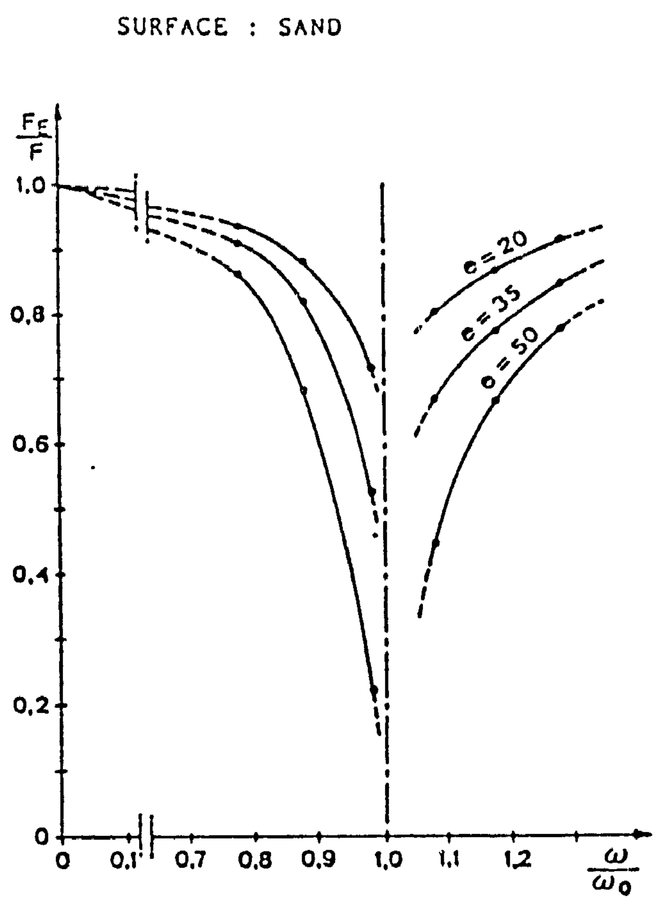

b. Relative force (F_E/F) vs. frequency ratio

Fig. 7.5.2 Testing facility and results by Orlandi and Matassa

(2) Effect of inflation pressure on tractive efficiency

The effect of inflation pressure on the tractive efficiency is plotted in Fig. 7.5.3, for different vehicle velocities. The same sinusoidal surface as before was used for the analysis. Since all three investigated parameters interact, the effect of inflation pressure cannot be simply described. However, in general, a higher inflated tyre exhibits a higher tractive efficiency and the tendency is intensified by the increased vehicle speed. An insignificant effect of the inflation pressure is displayed at a low speed.

It is interesting to note that the efficiency changes drastically by changing inflation pressure when this system is operated at a speed of 3 m/s. At 100 kPa of inflation pressure, the efficiency drops sharply. As previously shown in Fig. 7.5.1, this speed lies in the undesirable speed range. It is found that there is an undesirable inflation pressure range which shows an abrupt change of efficiency, as well as an undesirable speed range, since the vibrational response is determined by the combination of these quantities in addition to the road surface geometrical characteristics.

Therefore, for the tyre to be vertically excited under a resonant condition, the inflation pressure has to be carefully considered in order to prevent this phenomenon. Selection of the adequate inflation pressure also

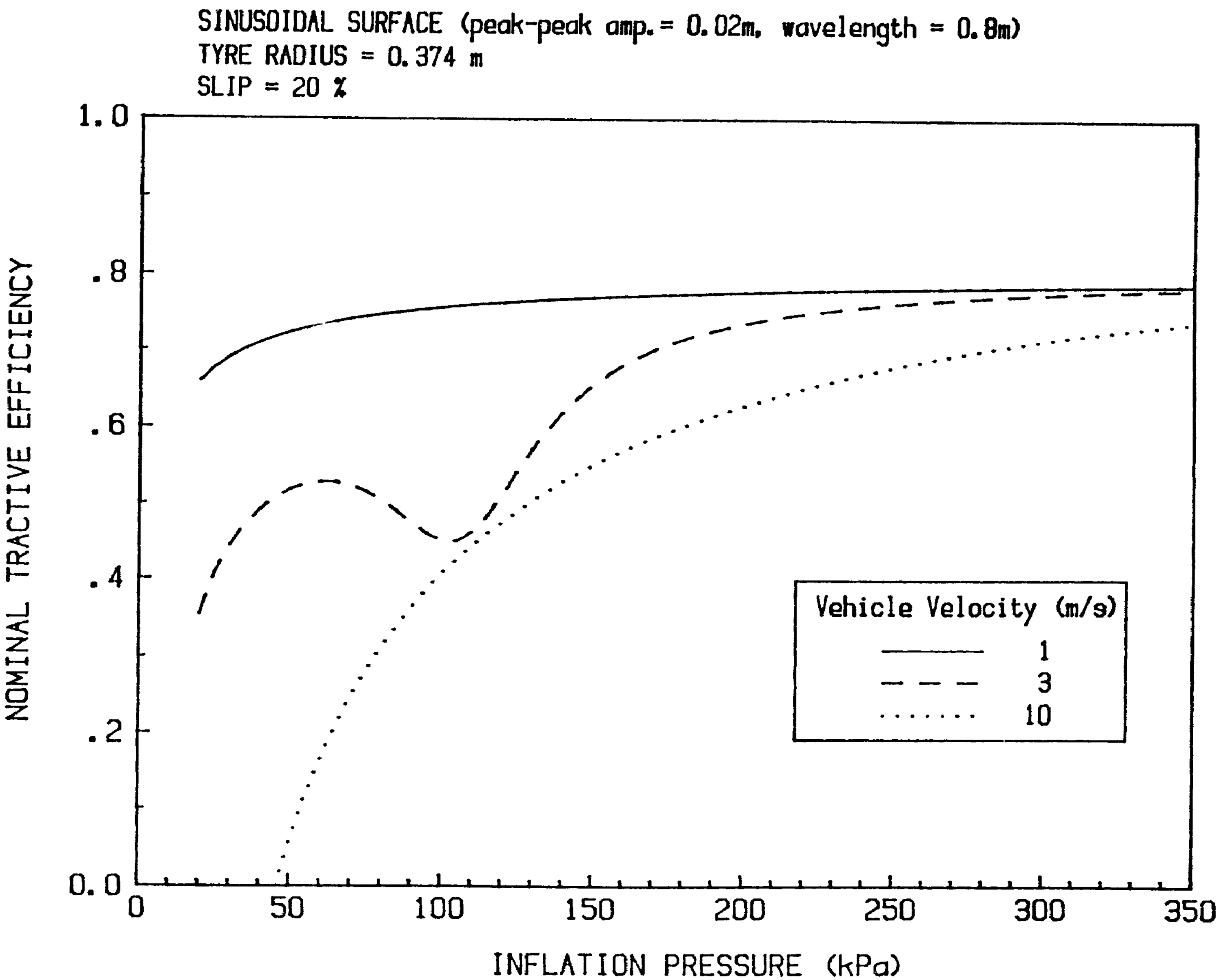

Fig. 7.5.3 Predicted nominal tractive efficiency as a function of tyre inflation pressure on a sinusoidal surface

contributes to an improvement in the ride quality and steerability or controllability of a vehicle.

(3) <u>Effect of surface amplitude on tractive efficiency</u>

Fig. 7.5.4 demonstrates the effect of sinusoidal road surface amplitude on the tractive efficiency, showing also the effect of vehicle speed. The wavelength was kept constant (0.8 m), while the inflation pressure and slip were assigned as 310.3 kPa and 20%, respectively for the analysis. When a tyre is operated at a very low speed, such as 1 m/s, no clear decrease in the tractive efficiency can be given by the increased amplitude of the sinusoidal road surface. However, the effect of road roughness is dramatically intensified at a higher speed. It can be estimated that this tendency is emphasized for low inflation pressures, because large amounts of tyre deformation power would be dissipated at these pressures.

The definition of negative efficiency is immobilization, i.e. more input torque is required to maintain the vehicle motion in order to overcome the resistance to motion. In addition, a jumping phenomenon of the tyre can be expected under a high speed operation over a very rough road. For such an extreme case, the ride quality or controllability rather than the tractive efficiency should be taken into account for.

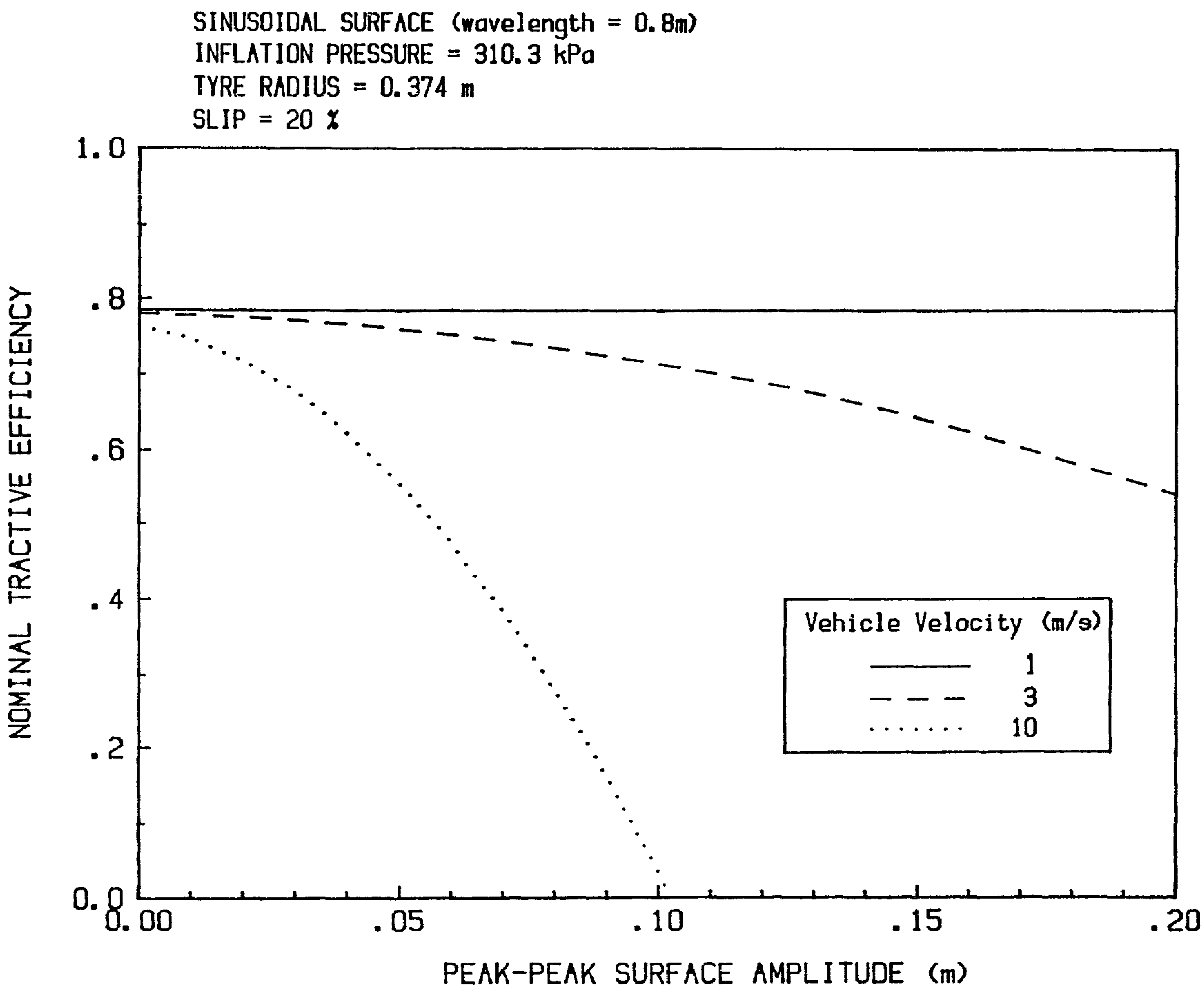

Fig. Predicted nominal tractive efficiency as a function of surface amplitude on a sinusoidal surface

7.5.2 Efficiency on a Random Rough Road Surface

In calculating the tractive efficiency on a random rough road, the three different roads, which were classified as "very good", "average" and "very poor" as described in Chapter 5, were considered.

(1) <u>Effect of vehicle velocity on tractive efficiency</u>

Fig. 7.5.5 depicts the nominal tractive efficiency curves plotted against changing vehicle translational velocity for three randomly rough road surfaces. The tyre inflation pressure and slip rate were specified as 250 kPa and 20%, individually. As an effect of velocity, it is indicated that the tractive efficiency gradually decreases as the velocity increases. This can be understood by considering the fact that rolling resistance is increased with speed (Fig. c.2), which is amplified when the ground surface is rough. For example, when the speed is increased from 2 m/s (7.2 km/h) up to 15 m/s (54 km/h), as much as a 10% reduction of efficiency for the "very poor" surface is observed, while only a 4% decrease in efficiency is seen for the "average" surface. On the "very good" surface, speed has little effect on efficiency since the tyre deformation power loss is quite small in the total power balance.

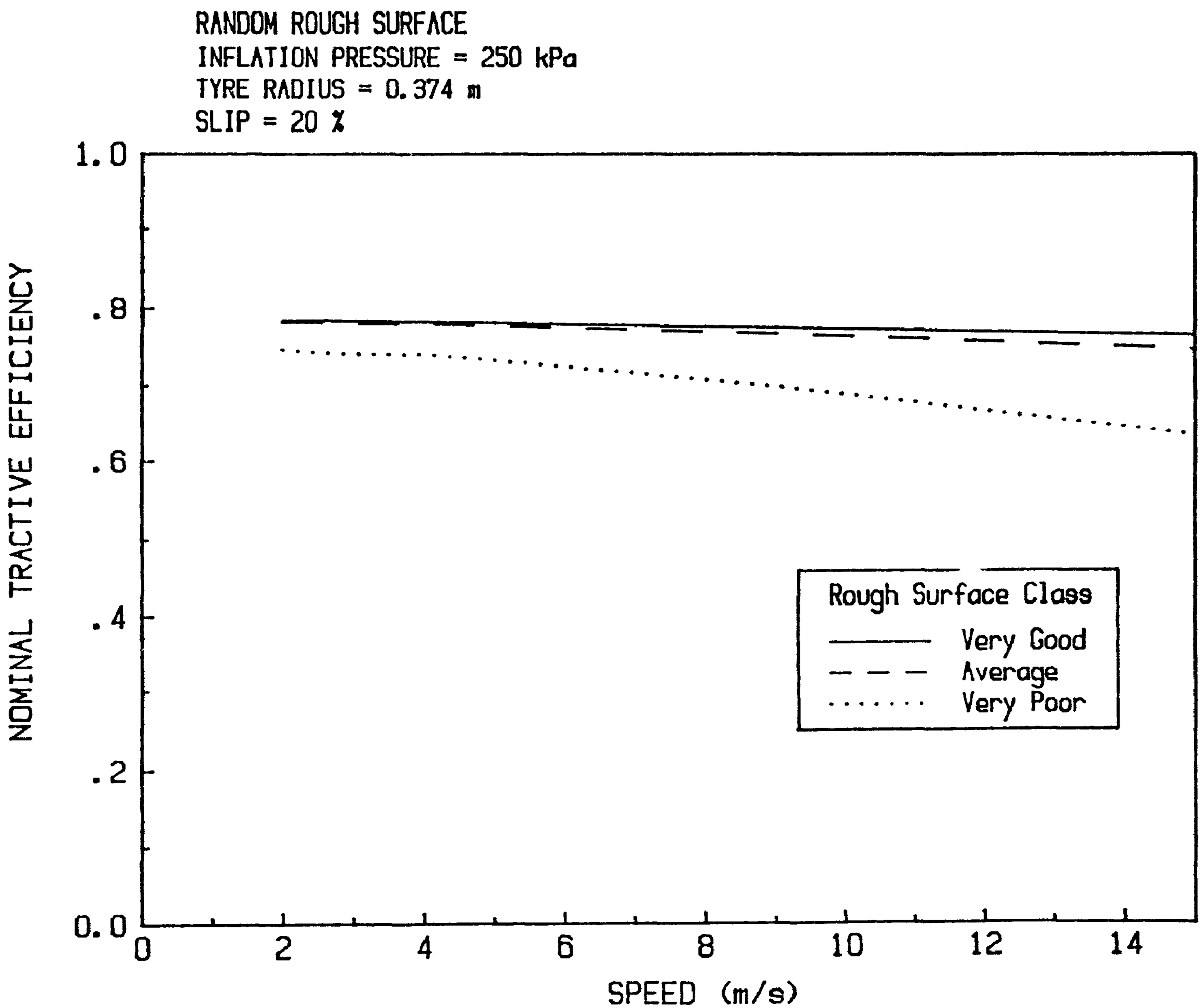

Fig. 7.5.5 Predicted nominal tractive efficiency as a function of vehicle velocity on a random rough surface

In addition, the steep drop in efficiency, as exhibited on a sinusoidal surface, is not shown because no specific dominant frequency is included in a surface profile of a randomly rough road.

(2) Effect of inflation pressure on tractive efficiency

Fig. 7.5.6 shows the effect of tyre inflation pressure on the nominal tractive efficiency for the three random rough roads. A nonlinear relationship between the tractive efficiency and the tyre inflation pressure is demonstrated. The efficiency increases asymptotically with an increase in inflation pressure. A notable effect of inflation pressure can be recognized at values under 150 kPa. This indicates that the internal energy expenditure due to tyre hysteresis increases exponentially as the inflation pressure is reduced.

The most important factor influencing the power consumption in the rolling tyre is the hysteresis of the material, representing 90-95% of the total tyre deformation power loss (Clark, 1971). A decrease in tyre deformation during rotation and vibration will help to minimize the power loss, as well as optimize the tyre structure and rubber compound to lower hysteresis. It is no surprise that the higher the inflation pressure the smaller the rolling resistance. Thus, on a hard smooth ground, the inflation pressure goes up. However, if the ground is rock-strewn or uneven, the effect of inflation pressure is great: in the

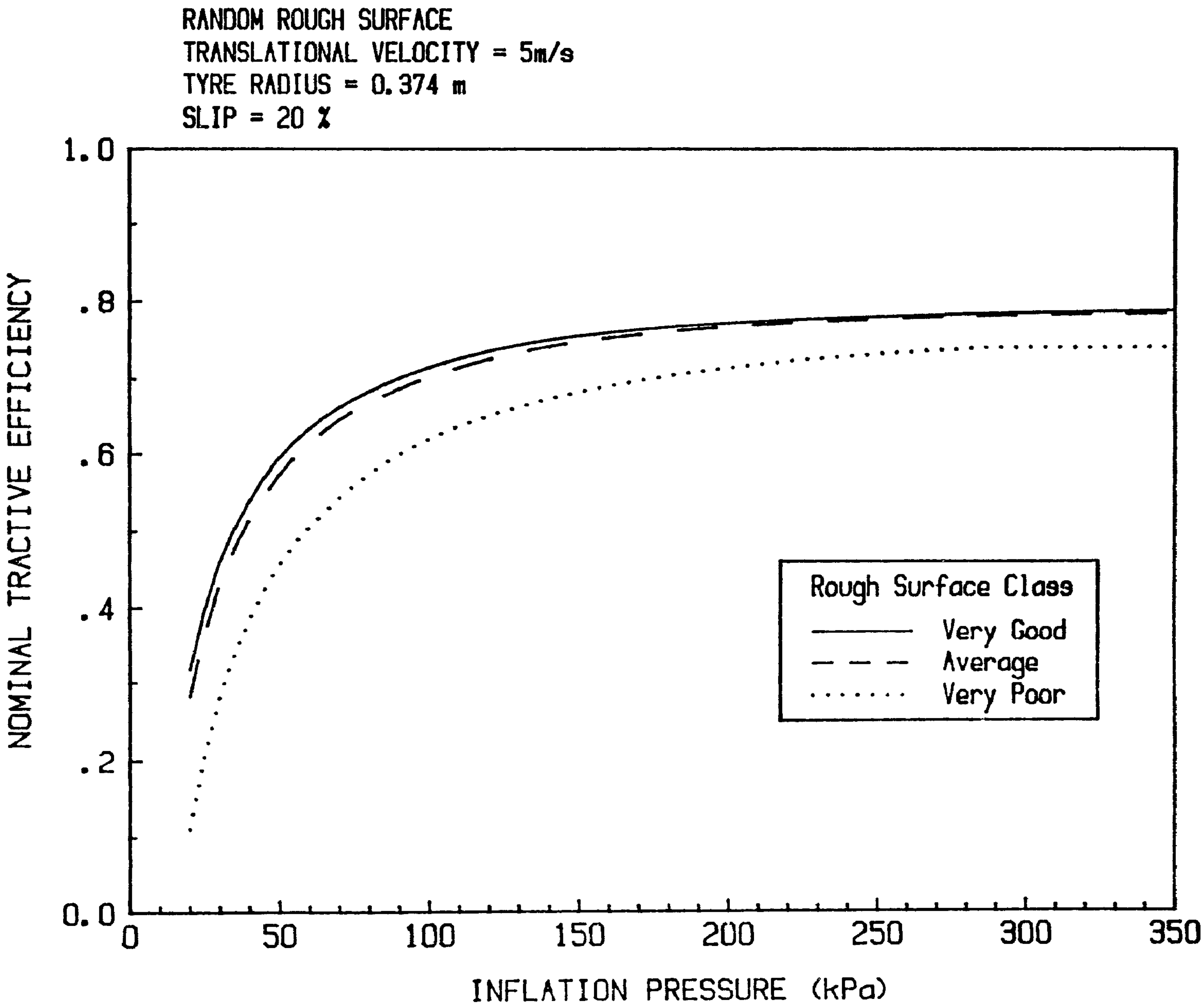

Fig. 7.5.6 Predicted nominal tractive efficiency as a function of tyre inflation pressure on a random rough surface

first case, the tractive efficiency is strongly affected by the tyre inflation pressure; in the second, bruising and wear of the tyre are accelerated by the reduced pressure; and in the third, the dynamic reacting load may dangerously exceed the static load by the increased inflation pressure.

Furthermore, since on-road tyres are usually used at inflation pressures greater than 200 kPa, the effect of extremely low inflation pressure may not have to be seriously considered from the viewpoint of tractive efficiency. However, it becomes an inevitable and important problem for off-road tyres because they are used over a wide range of inflation pressures, covering very low pressures, - e.g. a terra tyre. Hence, optimization of tyre pressure is imperative and must consider several conflicting factors, i.e. high tractive efficiency accomplished by using high inflation pressure and high soft terrain crossing capability or good ride quality accomplished by using low inflated tyre, - depending on the type of supporting ground surface.

(3) Effect of road roughness on tractive efficiency

Fig. 7.5.7 shows the effect of road roughness on the mean and standard deviation of the predicted DBP, as well as the effect of inflation pressure. Vehicle speed is 3 m/s (10.8 km/h). At this speed, a clear effect of road roughness on mean DBP cannot be exhibited for the range up to "average" rough road. However, comparison between the "average" road and the "very poor" road shows a decrease of about 5% of mean DBP for both inflation pressures.

A low inflated tyre produces a low average DBP under the same amount of input torque. In other words, more torque is required to produce the same DBP for the case of low inflation pressure.

The road roughness shows a significant effect on standard deviation of the DBP, with a drastic increase as road roughness is gained, and this tendency is intensified when the tyre is deflated. It can be surmised that the effect of inflation pressure on the standard deviation of DBP is determined by the complex combined effect of the energy recovery factor, tyre damping, tyre stiffness and the excitation frequency (speed). A highly inflated tyre exhibits large mean DBP and less standard deviation of DBP. From these results, a high inflated tyre seems to provide effective traction on a rigid terrain and is recommended, unless the riding quality is a concern.

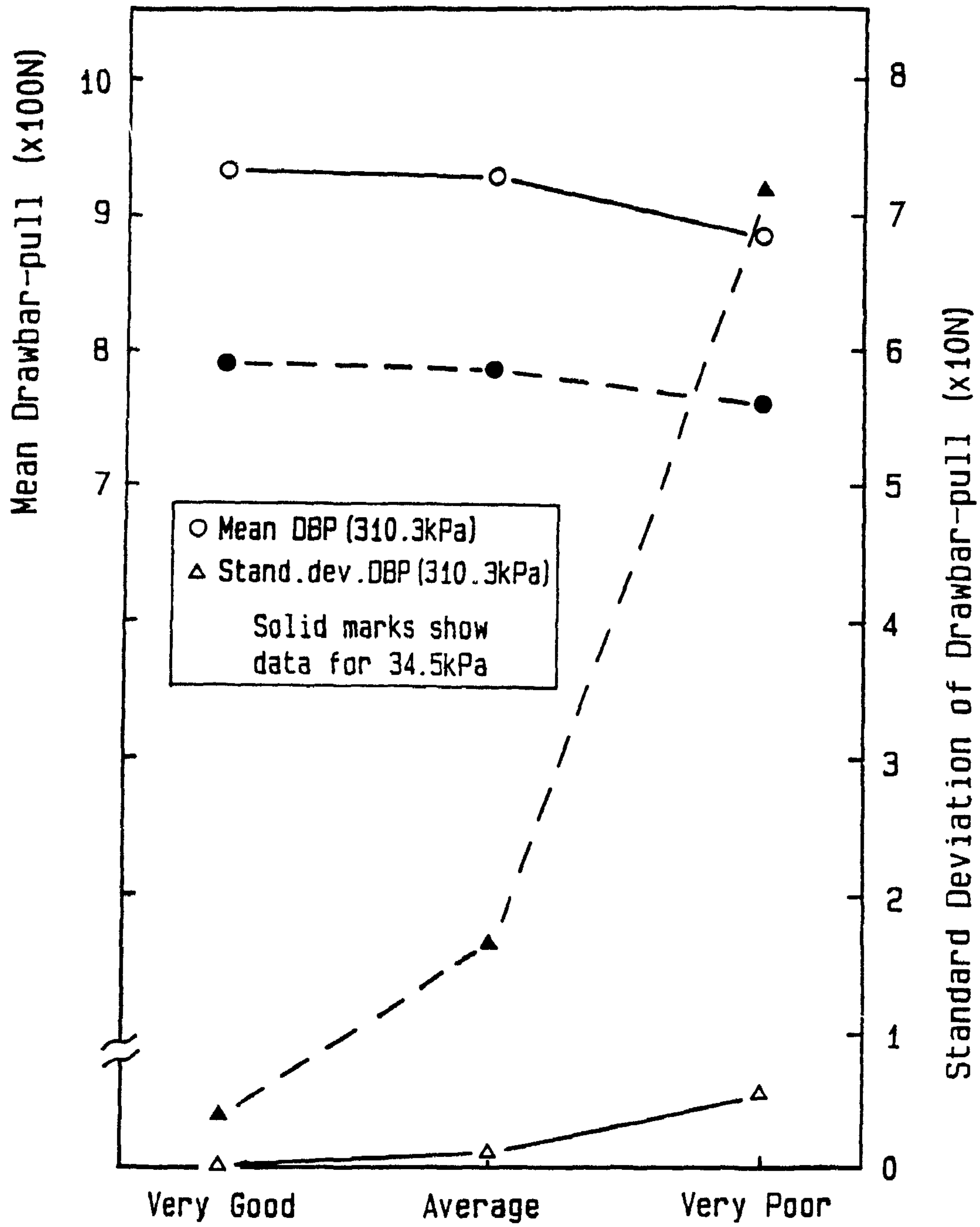

Fig. 7.5.7 Predictive investigation of the road roughness effect on mean and standard deviation of DBP (V = 3 m/s)

Recognizing these results, nominal tractive efficiency on a random rough road surface is investigated. Fig. 7.5.8 shows the effect of road roughness on tractive efficiency. The range of roughness classification is associated with the roughness constant,Go. Vehicle speed and slip rate are 5 m/s (18 km/h) and 20%, respectively. A substantial decrease in tractive efficiency due to increased motion resistance is obtained, when the condition of the road surface becomes sufficiently rough that the road would be classified as "poor" or "very poor" under the ISO proposal. Since an off-road surface is normally classified as "average" or rougher than that, the effect of road roughness on the tractive efficiency should be taken into vehicle mobility consideration. It is also noted that the efficiency is decreased by several percent on a very rough road, even if the inflation pressure is high, such as 310.3 kPa. This is a major concern in fuel economy.

Although no studies have been reported for the investigation of the off-road surface roughness effect on the tractive efficiency, the effect of road roughness on the motion (rolling) resistance of a tyre was investigated by Segel and Lu (1982) (see Fig. 7.5.9).

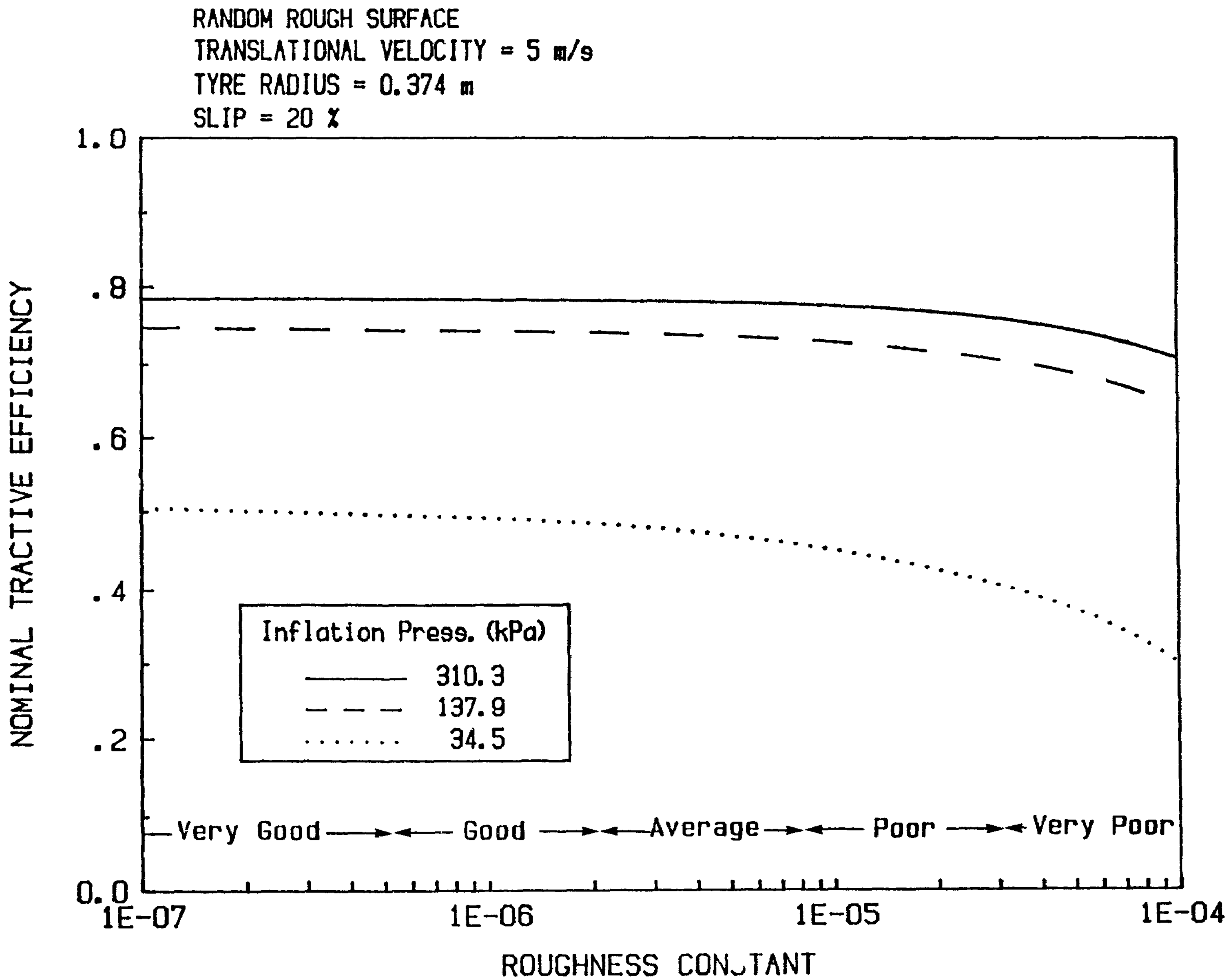

Fig. 7.5.8 Predicted nominal tractive efficiency as a function of roughness constant on a random rough surface

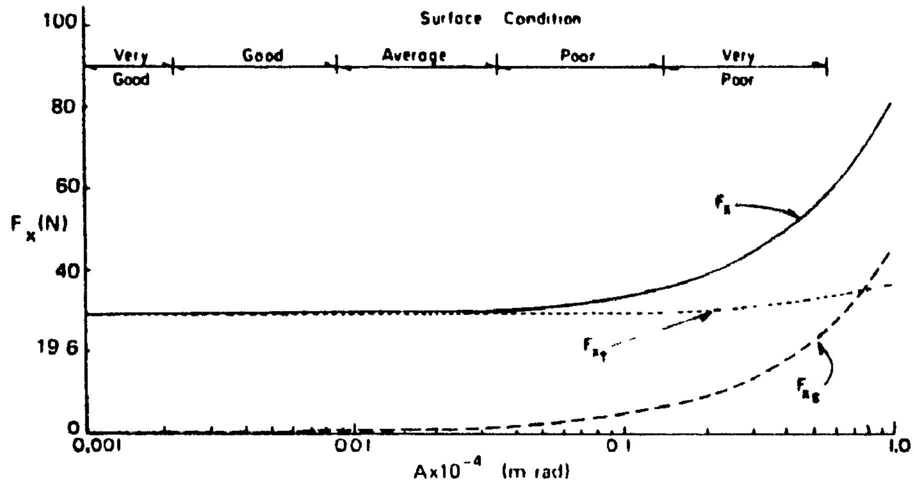

Fig.7.5.9 Motion resistance influenced by road roughness (after Segel and Lu)

The vehicle speed is 15 m/s (54 km/h). F_{xt} is the motion resistance which can be attributed to tyre hysteresis and F_{xs} is that attributed to suspension. F_x is a total motion resistance. The rolling resistance, which directly affects the vehicle tractive efficiency, starts to increase when the road roughness is beyond "poor". Although different input values were used in their analysis, our prediction obtained in Fig. 7.5.8 shows a good agreement with their result on a qualitative basis.

7.6 Summary

In this chapter, surface profile measurement, tyre enveloping property and the effect of several parameters on tyre tractive efficiency were discussed.

As a concluding remark, interesting and useful information for the achievement of not only high tractive efficiency, but also better ride quality, was obtained from the experiments and analytical predictions. Nevertheless, many of the assumptions established in the analytical analysis are likely to be violated when the road becomes very rough or a very high speed is employed.

In addition, further investigation of software (human response to the excitation) is needed because the study on human tolerance to applied vibration is inevitable to the study on vehicle mobility on a rough road, while only hardware (tyre) was the focus of the analysis of tractive efficiency. To do this, one has to recognize the vibrational characteristics of the human body. For example, Murphy and Ahlvin (1976) specified the maximum power which a human can absorb as 6 watts and the maximum tolerable vertical acceleration as 2.5 g, based on this absorbed power criteria. There are other criteria, such as ISO 2631, for evaluating human tolerance to vibration, which are shown in Appendix E.

CHAPTER 8

CONCLUDING REMARKS, CONTRIBUTIONS AND SUGGESTIONS FOR FURTHER STUDIES

8.1 Concluding Remarks

The effect of geometrical road surface roughness on the nominal tractive efficiency of the driven tyre was investigated. This research program was centered on (A) the characterization of road surface roughness, (B) the investigation of tyre enveloping property and (C) the analysis of tyre tractive performance on a rough non-deformable road, although it can be argued that the results will be highly dependent on the tyre used. This study may be regarded as an essential step in dealing with the actual off-the-road situation. The following observations and conclusions are drawn:

A. <u>Measurement and Evaluation of Road Surface Roughness</u>

(1) For the measurement of traction surface profile, a non-contact type of measuring equipment using the ultrasonic wave was used. Measurement was easily and quickly performed on the four different rough test surfaces in the laboratory. Satisfactory accurate data of surface profile were obtained.

(2) The roughness of road surface is uniquely expressed in the spatial frequency domain by means of the PSD

function. It was confirmed that the mathematical equation for a rough road surface profile is given in a simple form.

(3) Classification and evaluation of road roughness was performed based on the ISO proposal augmented by a PSD correlation scheme.

B. Investigation of the Tyre Enveloping Property

(1) The enveloping function of a tyre is directly determined by calculating the ratio of two profile PSD functions (the PSD of the filtered surface profile and the PSD of the original ground surface profile).

(2) The rectangular type enveloping function, compared to the exponential type enveloping function, was found to be suitable as a enveloping function for the specific tyre (Michelin 7:00 R16 XCL).

C. Analysis of Tyre Tractive Performance

In the theoretical investigation:

(1) A relationship between the drawbar-pull and the ground surface irregularities was developed in the form of a system function in the frequency domain, associated with the principle of energy conservation.

(2) The nominal tractive efficiency produced by a driven tyre on a rough terrain is obtained from the system

function and the PSD of terrain surface geometry.

(3) The tractive efficiency is decreased with increasing road roughness. The effect of terrain surface roughness is emphasized when the tyre inflation pressure is low or the operational speed is high.

(4) As the inflation pressure becomes low, the tractive efficiency is significantly decreased. On a sinusoidal road, it is found that there are undesirable inflation pressure and speed ranges which exhibit an abrupt decrease in the tractive efficiency.

(5) The tractive efficiency is gradually decreased with increasing traveling speed.

(6) In general, tractive efficiency is decreased with slip rate. However, there is an optimum slip rate which can produce the highest efficiency, - between 2% and 10% approximately. The optimum slip rate is likely to increase with a rougher ground surface, lower inflated tyre, or higher operational speed.

(7) Nominal tractive efficiency, which is defined by the mean and standard deviation of the DBP, is proposed to evaluate the tractive performance of off-road tyre traveling on a rough terrain.

From the traction tests:

(8) An increase in tyre deformation power due to road roughness was observed. This results in a loss of tractive effort of a tyre i.e. less drawbar-pull and less tractive efficiency.

(9) Tyre deformation power is not dependent on the slip rate of a tyre, but on the road surface roughness and tyre inflation pressure.

(10) A larger input torque is required on a rougher traction surface to obtain the same DBP.

(11) The PSD of measured DBP shows that the fluctuation in DBP is directly affected by the traction surface geometry, and a large part of the fluctuation is caused mainly by the range of wavelength (0.18 m - 0.9 m) of the traction surface.

8.2 Contributions

The main contributions achieved herein are as follows:

(1) Establishment of an analytical and predictive system function that can estimate the tractive efficiency of a pneumatic tyre on various random rough roads,

(2) Establishment of several test techniques to determine the road surface roughness and tyre enveloping property,

(3) Determination of the tyre enveloping function from experimental results,

(4) Prediction of the motion resistance of a pneumatic tyre traveling on a rigid rough ground at various operational conditions based on the energy expenditure due to tyre deformation and interfacial slip,

(5) A better understanding of the influences of the ground surface roughness, tyre inflation pressure, operational speed and slip rate for the overall tyre-rough terrain mobility performance,

(6) Proposal of the nominal tractive efficiency accounting for the time-variant DBP, and

(7) Presentation of the necessity for further engineering study of tyre performance on a rough terrain.

8.3 Suggestions for Further Studies

In order to extend the capability of the predictive model established in this study, so that it can be available for an actual tyre-rough terrain situation, the following considerations should be investigated and modification should be made, if necessary.

A. Measurement of Road Surface Profile

With regard to the ultrasonic distance detector, further improvement of reduction of measurement noise, faster sweep speed and wider survey range of vertical distance are needed.

B. Investigation of Tyre Enveloping Function

(1) A more predictive and/or analytical model which can more accurately describe the tyre enveloping property has to be proposed. Considerations should be associated not only with geometrical characteristics of the tyre but also with dynamic motion, tyre stiffness, tyre structural properties and terrain surface features etc.

(2) The change in contact length during vertical motion should be considered for a precise analysis of the tyre enveloping effect.

C. Analysis of Tyre Tractive Performance

The following should be concerns in the theoretical modeling of the tyre (vehicle)-rough terrain system:

(1) Investigation of jumping phenomena is needed for a mobility study of high speed off-road vehicles.

(2) Tribology at the tyre-rough ground interface should be investigated, including the "shape effect" of surface asperities (harshness or roundness etc.).

(3) The mechanism of the reduction of adhesion (friction) force under the vertical excitation on a flat, smooth surface has to be studied in parallel with the investigation of the traction mechanism of a driven tyre over a rough terrain.

(4) Deformability of supporting ground needs to be taken into account together with the dynamic property of the soil, although too much deformability reduces the effect of ground surface roughness. For this investigation, another type of frequency response function defining the soil deformability should be considered.

(5) Change in the slip rate due to road roughness should be studied in relation to the vertical load, traveling speed and tyre characteristics.

With regard to the traction tests,

(1) A thorough investigation and understanding of the dynamic mechanical properties of pneumatic tyres is necessary for the evaluation of tyre performance.

(2) In the laboratory, higher speed tests are desired in order to investigate the dynamic behavior of the pneumatic tyre. It is recommended to use a rough soil surface instead of the wooden surface for the evaluation of practical performance of the tyre. The difficulty in obtaining repeatability of results poses a particular problem.

(3) Fulfillment of outdoor high speed and long distanced traction tests on various rough roads are required for the comparison and the evaluation of predicted results, despite the high cost and time consumption involved in conducting these experiments.

In conclusion, in order to evaluate the total off-road vehicle mobility, a theoretical model that can synthetically describe the whole driver-vehicle system in terms of agility, maximum speed, fuel consumption, maximum drawbar-pull or human fatigue needs to be established.

REFERENCES

Ahmed, N., and Natarajan, T. (1983)
"Discrete-Time Signals and Systems" Printice-Hall

Al-Deen, H.H., Liljedahl, J.B., and Soedel, W. (1978)
"Jumping Phenomena of Tractors" proc. 6th Int. ISTVS Conf. Vol.1 pp.403-436

Anderson, R.A. (1967)
"Fundamentals of Vibrations" N.Y. Macmillan

Ariano, R. (1931)
"Strada e Traffico" Hoepli, 1931 French translation "La Route et les Transports Routiers" Leon Eyrolles (1933)

Aseltine, J.A. (1958)
"Transform Method in Linear System Analysis - Electrical and Electronic Engineering Series" McGraw-Hill

Bailey, A.C. and Burt E.C. (1976)
"An Analysis of Tractive Efficiency on Selected Pneumatic Tires" paper submitted to the 1976 winter Meeting, ASAE Chicago

Barson, C.W., James, D.H. and Morlombe, A.W. (1967-68)
"Some Aspects of Tire and Vehicle Vibration Testing" proc. IME 182, 3B pp.32

Bekker, M.G. (1955)
"Theory of Land Locomotion" The University of Michigan Press

Bekker, M.G. (1969)
"Introduction to Terrain - Vehicle Systems" The University of Michigan Press

Bekker, M.G. (1960)
"Off-The-Road Locomotion" The University of Michigan Press

Bekker, M.G. (1983)
"Prediction of Design and Performance parameters in Agro-forestry Vehicles" Division of Energy NRC Ottawa Dec. NRCC 22880

Bendat, J.S. and Piersol, A.G. (1986)
"Random Data : Analysis and Measurement Procedures, 2nd Edition" Wiley Interscience

Bender, E.K. and Karnopp, D.C. (1967)
"On the Optimization of Vehicle Suspension Using Random Process Theory" ASME paper67 Trans.12 pp.28-30

Berés, W. (1986)
"Modification of Terrain Power Spectra by the Rolling Tyre" ISTVS Chap.4 pp.16-24

Beres, W. (1987)
"Linear Models of Tyre Developing Properties" Int. J. of Veh. Des. Vol.8 No.4 pp485-503

Blackman, R.B. and Tukey, J.W. (1958)
"The Measurement of Power Spectra" N.Y.Dover Publications

Boonsinsuk, P. (1979)
"Analysis and Prediction of Tyre-soil Interaction and Mobility Performance" PH.D. Thesis McGill University

Bowden, F.P. and Tabor, D. (1954)
"The Friction and Lubrication of Solids - Part 1, 2" Oxford Clarendon Press

Bradley, J. and Allen, R.F. (1930-31)
"Factors Affecting Behavior of Rubber Tyred Wheels an Road Surfaces" proc. Inst. Auto. Engrs. Vol.25 pp.63

Butknnas, A.A. (1967)
"Power Spectral Density and Ride Evaluation" SAE Trans. paper 660138 Vol.75

Cap, J.S. and Wambold, J.C. (1984)
"Traction Loss of a Suspended Tire on a Sinusoidal Road" Transportation Research Record No.1000 pp.33-38

Captain, K.M., Boghani, A.B. and Wormley, D.N. (1979)
"Analytical Tire Models for Dynamic Vehicle Simulation" Vehicle System Dynamics Vol.8 pp.1-32

Chiesa, A. (1962)
"Vehicle Vertical Vibration and Tire Performance" SAE paper No.490C pp.14

Chiesa, A. and Tangora, G. (1959)
"The Dynamic Stiffness of Tyres" Revue Gen du Caoutchouc Vol.36 No.10 pp.1321

Chong, G.J. and Phang, W.A. (1973)
"PCA Road Meter Measuring Road Roughness at 50mph" Highway Res. Board -Pavement Evaluation using Road Meters Special Rep.133 pp.51-65

Clark, S.K. (1971)
"Mechanics of Pneumatic Tires" National Bureau of Standards Monograph 122

Clark, S.K. (1984)
"Tire Rolling Resistance and Vehicle Fuel Economy" Fuel Economy in Road Vehicles Powered by Spark Ignition Engines Prenum Press

Cote, L.J., Kozin F. and Bogdonoff, J.L. (1966)
"Introduction to a Statistical Theory of Land Locomotion-4, Effects of Vibration on the Contents of the Vehicle and Conclusions" J. Terramech. Vol.3 No.4 pp.47-51

Craighead, I.A., Loo Y.W., Storey A., et al. (1986)
"Validation Tests on Computer Simulation Programs Modelling of Off-road Vehicles" J. Terramech. Vol.23 No.1 pp.13-22

Crandall, S.H. (1963)
"Random Vibration Volume2" The MIT Press

Crolla, D.A. (1981)
"Off-road Vehicle Dynamics" Vehicle System Dynamics Vol.10 pp.253-266

Crolla, D.A. and Maclaurin, E.B. (1986)
"Theoretical and Practical Aspects of the Ride Dynamics of Off-road Vehicles- Part2" J. Terramech. Vol.23 No.1 pp.1-12

Curtiss, W.W. (1969)
"Low Power Loss Tires" SAE paper 690108

Czako, T.F. (1970)
"The Influence of the Inflation Pressure on Cross-country Performance" proc. ISTVS-TRW Off-road mobility symposium pp.327-349

Davisson, J.A. (1969)
"Design and Application of Commercial Type Tires" SAE paper 690001

Deitchman, S.J. (1964)
"Limited War and American Defense Policy" The MIT Press. Cambridge

DeRaad, L.W. (1977)
"The Influence of Road Surface Texture on Tire Rolling Resistance" Tire Rolling Losses and Fuel Economy-an R&D Planning Workshop p-74 pp.143-149

Devinney, W. (1967)
"Factors Affecting Tire Traction" SAE paper 670461

Dodds, C.J. and Robson, J.D. (1973)
"The Description of Road Surface Roughness" J. Sound and Vibration Vol.31 No.2 pp.175-183

Dugoff, H., Fancher, P.S. and Segel, L. (1970)
"An Analysis of Tire Traction Properties and their Influence on Vehicle Dynamic Performance" SAE paper 700377

Dwyer, M.J., Comely, D.R. and Evernden, D.W. (1975)
"The Development of a Handbook of Agricultural Tyre Performance" proc. 5th Int. Conf. ISTVS Vol.3 pp.679-699

Dzielski, J.E. and Hedrick, J.K. (1984)
"Energy Dissipation due to Vehicle/Track Interaction" VSD Vol.13 pp.315-337

Eiyo, F. and Yong, R.N. (1990)
"Measurement of Road Surface Roughness by Ultrasonic Detector" 10th Int. Conf. ISTVS Japan (Accepted)

Fekete, A. (1986)
"Effect of the Variance of Plough Resistance on the Tractive Performance" proc. 3rd European ISTVS Conf. Chap.2 pp.200011-200016

Freitag, D.R. (1965)
"A Dimensional Analysis of the Performance of Pneumatic Tyres on Soft Soils" US Army WES Tech. Rep. 3-688

Fujimoto, Y. (1983)
"Spectrum Analysis of Road Roughness for Earthmoving Machinery" J. Terramech. Vol.20 No.1 pp.43-60

Gee-Clough, D. (1980)
"Selection of Tyre Sizes for Agricultural Vehicles" J. Agric. Engng. Res. Vol.25 pp.261-278

Gillespie, T.D. and Sayers, M. (1981)
"Role of Road Roughness in Vehicle Ride" Transportation Research Record No.835 pp.15-20

Gough, V.E. (1963)
"Tyres and Air Suspension, Advances in Automobile Engineering-Vehicle Ride" Pergamon Press. Oxford

Gray, G.G. and Johnson, K.L. (1972)
"The Dynamic Response of Elastic Bodies in Rolling Contact to Random Roughness of their Surfaces" J. Sound and Vibration Vol.22 No.3 pp.323-342

Grosch, K.A. (1963)
"The Relation between the Friction and Viscoelastic Properties of Rubber" proc. Royal Soc.(London) Vol.274 Ser.A. pp.21-39

Hać, A. (1987)
"Adaptive Control of Vehicle Suspension" VSD Vol.10 pp.57-89

Hadekel, R. (1952)
"The Mechanical Characteristics of Pneumatic Tyres" S&T memo No.10/52

Harris, J. and Stevenson, A. (1987)
"On the Role of Non-linearity in the Dynamic Behavior of Rubber Components" Int. J. Veh. Des. Vol.8 No.4 pp.553-557

Hedrick, J.K. and Wormley, D.N. (1975)
"Active Suspensions for Ground Transport Vehicles-A State of the Art Review" ASME-Mechanics of Transportation Suspension Systems AMD-Vol.15 pp. 21-40

Horne, W.B. (1969)
"Results from Studies of Highway Grooving and Texturing at NASA Wallops Station" NASA SP-5073 pp.465

Hudson,W.R., Halbach,D., Zaniewski,J.P. and Moser,L. (1985)
"Root-Mean-Square Vertical Acceleration as a Summary Roughness Statistic" ASTM STP-884 pp.3-24

Hughes, P.C. (1973)
"Evaluation of the PCA Road Meter - Pavement using Road Meters" Highway Research Board Special Report 133

Hullender, D.A. and Bartley, T.M. (1975)
"Defining Guideway Irregularity Power Spectra in terms of Construction Tolerances and Constraints" High Speed Ground Transportation Journal Vol.9 No.1 pp.355-368

ISO/TC108/SC2/WG4 N57 (1982)
"Reporting Vertical Road Surface Irregularities"

ISO 2631 (1974,78,82)
"Guide for the Evaluation of Human Response to Whole-body Vibration"

Kamash, K.M.A. and Robson, J.D. (1977)
"Implication of Isotropy in Random Surfaces" J. Sound Vib. Vol.54 No.1 pp.131-145

Karnopp, D. (1978)
"Power Requirement for Traversing Uneven Roads" VSD Vol.7 No.3 pp.135-152

Koeppel, W. and Grabau, W. (1987)
"Terrain Description for Mobility Prediction" proc. 9th Int. Conf. ISTVS Vol.1 pp.160-175

Komandi, G. (1975)
"Determination of the Peripheral Force for Pneumatic Tires Rolling on Concrete Surfaces" proc. 5th Int. ISTVS Conf. Vol.2 pp.567-588

Korst, H.H. and Funfsinn, M.A. (1977)
"Determination of Effective Rolling Resistance by Coastdown Experiments on Smooth and Rough Roads" Tyre Rolling Losses and Fuel Economy an R&D planning workshop P-74 pp.133-141

Kozin, F. and Bogdonoff, J.L. (1960)
"On the Statistical Analysis of the Motion of Some Simple Two-Dimensional Linear Vehicles Moving on a Random Track" Int. J. Mech. Scie. Vol.2 pp.168-178

Kozin, F., Bogdonoff, J.L. and Cote, L.J. (1966)
"Introduction to a Statistical Theory of Land Locomotion-3 Vehicle Dynamics" J. Terramech. Vol.3 No.3 pp.69-81

Krylov, N. and Bogoliubov, N. (1937)
"Introduction a la Mechanique Nonlineaire: les Methodes Approchees et Asymptotiques" Ukr. akad. nauk. Inst. de la Mechanique, chaire de Phys. math. Ann., t. 1-2 ; translated by S. Lefshetz in Annals of Mathematical Studies No.11 Princeton N.J. 1947

Kutzbach , H.D. and Schrogl, H. (1987)
"Dynamic Behavior of Rolling Tractor Tyres" proc. 9th Int. Conf. ISTVS Vol.2 pp.457-464

Laib, L. (1975)
"On the Problem of the Dynamics of Wheeled Cross-country Vehicles, in view of the Relationship between the Vertical Motion of the Tires and Peripheral Force" proc. 5th Int. ISTVS Conf. pp.513-531

Laib, L. (1977)
"Measurement and Mathematical Analysis of Agricultural Terrain and Road Profiles" J. Terramech. Vol.14 No.2 pp.83-97

Laib, L. (1978)
"A Vibration Analysis of Agricultural tyres" proc. 6th Int. Conf. ISTVS Vol.1 No.3 pp.1317-1341

Lesage, B.C. and Yong, R.N. (1987)
"Optimization of Vehicle Suspension Components to Maximize the Mobility of a Vehicle in Off-road travel" proc. 9th Int. Conf. ISTVS Vol.2 pp.515-522

Lippman, S.A., Piccin, W.A. and Baker, T.P. (1965)
"Enveloping Properties of Tires" SAE SP260 N.Y.

Lu, X-P. (1985)
"Effects of Road Roughness on Vehicular Rolling Resistance" ASTM STP-884 pp.143-161

Lu, X-p. and Segel, L. (1984)
"Design Procedure for Vehicle Suspension Optimization" Int. J. Vehicle Design Vol.15 No.1/2 pp.129-142

Manor G. and Nir D. (1987)
"Accuracy of Performance of Farm Machinery" J. Terramech. Vol.24 No.1 pp.87-94

Melzer, J. and Hellwich, H. (1975)
"Efficiency-A Parameter for Judging the Performance of Running Gear ?" proc. 5th Int. ISTVS Conf. Vol.3 pp.731-749

Martin, F.R. (1969)
"Pavement Surface Treatments at Airports in Great Britain" NASA SP-5073 pp.235

Matthews, J. (1966)
"Ride Comfort for Tractor Operations 4: Assessment of the Ride Quality of Seats" J. Agric. Eng. Res. Vol.11 No.1 pp.44-57

Matthews, J. and Talamo, J.D.C. (1965)
"Ride Comfort for Tractor Operators:3-Investigation of Tractor Dynamics by Analogue Computer Simulation" J. Agric. Engng. Res. Vol.10 No.2 pp.93-108

Mckyes, E. (1985)
"Soil Cutting and Tillage" Elsevier

Meirovitch, L. (1985)
"Introduction to Dynamics and Control" John Wiley & Sons

Meyer, W.E. and kummer, H.W. (1968)
"Pavement Friction and Temperature Effects" NRC H.R.B.-Control of Pavement Slipperiness SP-101 pp.47-55

Michelberger, P. and Szoke, D. (1985)
"Speed-Dependent 'ertical Vibrations of Elastic Vehicle Bodies" Int. J. Vehicle design Vol.8 No.1 pp.87-95

Moore, D.F. (1975)
"Principles and Applications of Tribology" Pergamon Press

Moyer, R.A. (1951)
"Recent Development in the Measurement of Road Roughness and Skid Resistance" proc. Assoc. Asphalt Paving Tech. Vol.20 pp.42

Murphy, N.R. and Ahlvin R.B. (1976)
"AMC-74 Vehicle Dynamics Module" Tech. Rep. M-76-1 WES

Muth, E.J. (1977)
"Transform Methods with Applications to Engineering and Operations Research" Printice-Hall

Nigam, N.C. (1983)
"Introduction to Random Vibrations" The MIT Press.

Ohmiya, K. and Matsui, K. (1982)
"Studies on Agricultural Terrain Profiles (1) -A Measuring Apparatus for Agricultural Profiles (in Japanese)" J. Agric. Eng. Vol.44 No.1 pp.17-22

Ohmiya, K. and Matsui, K. (1982)
"Studies on Agricultural Terrain Profiles (2) - Measurements and Evaluations of Agricultural Terrain Profiles (in Japanese)" J. Agric. Eng. Vol.44 No.2 pp.293-297

Ohmiya, K. (1986)
"Studies on Agricultural Terrain Profiles (3)-Roughness of Agricultural Terrain (in Japanese)" J. of Agric. Eng. Vol.47 No.4 pp.469-474

Ohmiya, K. (1986)
"Characteristics of Farm Field Profiles as Sources of Tractor Vibration" J. Terramech. Vol.23 No.1 pp.23-36

Orlandi, A. and Matassa, M. (1987)
"Effects of Vibration on Rolling Resistance" proc. 9th Int. ISTVS Conf. Vol.2 pp.523-530

Orlandi, A. and Matassa, M. (1986)
"Wheel-Ground Contact Phenomena in the Presence of Vibrations" proc. 3rd European ISTVS Conf. pp.400075-400086

Phillips, A.V. (1972)
"A Study of Road Noise Vibration and Noise in Motor Vehicles" IME pp.70-81

Pottinger, M.G. and Yager, T.J. (1986)
"The Tire Pavement Interface" ASTM STP-929

Priestley, M.B. (1981)
"Spectral Analysis and Time Series" Academic Press

Pugh, B. (1973)
"Friction and Wear" Newnes-Butterworths

Robson, J.D. (1963)
"Random Vibrations" London:Edinburgh University Press

Robson, J.D. and Kamash, K.M.A. (1977)
"Road Surface Description to Vehicle Response" proc. 5th VSD and 2nd IUTAM symp. pp.222-228

Rossi, C.E. (1984)
"Energy Aspects of Road Transport" Int. J. Vehicle Design Vol.5 No.5 pp.548-566

Sattaripour, A. (1977)
"The Effect of Road Roughness on Vehicle Behavior" proc. 5th VSD and 2nd IUATM symp. pp.229-236

Sattinger, I.J. and Sternick, S. (1961)
"An Instrumentation System for the Measurement of Terrain Geometry" proc. 1st. Int. Conf. ISTVS N.23 pp.362-370

Sawyer, R.H. and Kolnick, J.J. (1959)
"Tire-to-Surface Friction Coefficient Measurements with AC-123B Airplane on Various Runway Surfaces" NASA Tech. Rep. R-20

Sayers, M. (1985)
"Development, Implementation and Application of the Reference Quarter-car Simulation" ASTM STP-884 Measuring Road Roughness and Its Effect on User Cost and Comfort

Segel, L. and Lu, X-P. (1982)
"Vehicular Resistance to Motion as Influenced by Road Roughness and Highway Alignment" Aust. Road Res. Vol.12 No.4 pp.211-222

Schuring, D. (1966)
"The Energy Loss of a Wheel" proc. 2nd Int. Conf. ISTVS pp.391-424

Sireteanu, T. (1984)
"The Effect of Sequential Damping on Ride Comfort Improvement" IME Vehicle Noise and Vibration C145/84

Spangler, E.B. and Kelly, W.J. (1962)
"Servo-seismic Method of Measuring Road Profile" Highway Research Board Bulletin 328 pp.33-41

Sugg, R.A. (1969)
"Skid Correlation Study results from British Vehicles" NASA SP-5073

Thomas, T.R. (1982)
"Rough Surfaces" Longman, London and Newyork

Thompson, W.E. (1958)
"Measurements and Power Spectra of Runway Roughness at Airports in Countries of North Atlantic Treaty Organization" NACA TN4303

Thomson, W.T. (1981)
"Theory of Vibration with Applications" Prentice-Hall

Van Deusen, B.D. (1967)
"Analytical Techniques for Designing Riding Quality into Automotive Vehicles" SAE paper 670021

Van Deusen, B.D. (1966)
"A Statistical Technique for the Dynamic Analysis of Vehicles Traversing Rough Yielding and Non-yielding Surfaces" NASA Contract Reports CR-659

Velinsky, S.A. and White, R.A. (1980)
"Vehicle Energy Dissipation due to Road Roughness" VSD Vol.9 pp.359-384

Walls, J.H., Houbolt, J.C. and Press, H. (1954)
"Some Measurements and Power Spectra of Runway Roughness" NACA TN3305 pp.1-29

Wambold, J.C. (1985)
"Road Roughness Effects on Vehicle Dynamics" ASTM STP-884 pp.179-196

Wehage, R.A. (1987)
"Vehicle Dynamics" J. Terramech. Vol.24 No.4 pp.295-312

Weissm R.A. (1981)
"Terrain Microroughness and the Dynamic Response of Vehicles" Conference of Army Mathematics, Trans. of 27th West Point, U.S.Army W.E.S.

Wendenborn J.G. (1966)
"The Irregularities of Farm Roads and Fields as Sources of Farm Vehicle Vibrations" J. Terramech. Vol.3 No.3 pp.9-40

Whitehouse, D.J. and Archard, J.F. (1970)
"The Properties of Random Surfaces of Significance in their Contact" proc. of the Royal Soc,. A316 pp.97-121

Williams, T. (1975)
"Power Consumption of Tires" TRRL Supp. Rep. SR192UC

Wismer, R.D. and Luth, H.J. (1973)
"Off-road Traction Prediction for Wheeled Vehicles" J. Terramech. Vol.10 No.2 pp.49-61

Wolfson, B.P. (1987)
"Wheel Slip Phenomena" Int. J. Vehicle Design Vol.8 No.2 pp.177-191

Wong, J.Y. (1970)
"The Effect of Vibrations on the Performance of Terrain-vehicle Systems" J. Terramech. Vol.7 No.3 pp.11-21

Wong, J.Y. (1972)
"Effect of Vibration on the Performance of Off-road Vehicles" J. of Terramech. Vol.8 No.4 pp.25-42

Wong, J.Y. (1978)
"Theory of Ground Vehicles" John Wiley & Sons

Yong, R.N., Boonsinsuk, P. and Fattah, E.A. (1980) "Tyre Load Capacity and Energy Loss with respect to varying Soil Support Stiffness" J. Terramech. Vol.17 No.3 pp.131-147

Yong, R.N. and Fattah, E.A. (1976) "Prediction of Wheel-soil Interaction and Performance using the Finite Element Method" J. Terramech. Vol.13 No.4 pp.227-240

Yong, R.N., Fattah, E.A. and Boonsinsuk, P. (1978) "Analysis and Prediction of Tyre-soil Interaction and Performance using Finite Elements" J. Terramech. Vol.15 No.1 pp.43-63

Yong, R.N., Fattah, E.A. and Skiadas, N. (1984) "Vehicle Traction Mechanics" Elsevier

Yong, R.N. and Muro, T. (1981) "Prediction of Drawbar-pull of Tracked Over-snow Vehicle" proc. 7th Int. ISTVS Conf. Vol.3 pp.1119-1149

Yong, R.N. and Eiyo, F. (1990) "Effect of Traction Surface Roughness on Tyre Performance" 10th Int. Conf. ISTVS Japan (Accepted)

APPENDIX A

POWER SPECTRAL DENSITY FUNCTION

The Power Spectral Density (PSD) function of the random process describes the general frequency composition of the data in terms of the spectral density of its mean square values.

A.1 Derivation of PSD Function

1. Derivation associated with autocorrelation function

The autocorrelation function, $R_{(\tau)}$ of the function, $y_{(t)}$ is given by

$$R_{(\tau)} = E\left[\, y_{(t)} \cdot y_{(t+\tau)} \,\right]$$

$$= \lim_{T \to \infty} \frac{1}{T} \int_{-\frac{T}{2}}^{\frac{T}{2}} y_{(t)} \cdot y_{(t+\tau)} \quad dt \tag{A.1}$$

One-sided PSD function, $S_{(f)}$ is given by the Fourier transform of the autocorrelation function of $y_{(t)}$ (Wiener-Khintchine's theorem).

$$S_{(f)} = 2 \int_{-\infty}^{\infty} R_{(\tau)}\, e^{-i2\pi f\tau} \quad d\tau \tag{A.2}$$

which will exist if $R_{(\tau)}$ exists and if

$$\int_{-\infty}^{\infty} |\, R_{(\tau)}|\ d\tau \ < \infty$$

The inverse Fourier transform of $S_{(f)}$ gives the autocorrelation function conversely.

$$R_{(\tau)} = \frac{1}{2} \int_{-\infty}^{\infty} S_{(f)}\, e^{i2\pi f\tau} \quad df \tag{A.3}$$

The Eq.(A.2) may be simplified to

$$S_{(f)} = 2\int_{-\infty}^{\infty} R_{(\tau)} \cos 2\pi f\tau \quad d\tau$$

$$= 4\int_{0}^{\infty} R_{(\tau)} \cos 2\pi f\tau \quad d\tau \tag{A.4}$$

2. Direct derivation of PSD function

Instead of Eq.(A.1), the autocorrelation function, $R_{(\tau)}$ is defined, in order to avoid complexity of the integration period.

$$R_{(\tau)} = \lim_{T\to\infty} \frac{1}{T} \int_{-\infty}^{\infty} z_{(t)} \cdot z_{(t+\tau)} \quad dt \tag{A.5}$$

where

$$z_{(t)} = y_{(t)} \qquad |\,t\,| \le \frac{T}{2}$$

$$= 0 \qquad |\,t\,| > \frac{T}{2}$$

Let

$$Z_{(f)} = \int_{-\infty}^{\infty} z_{(t)}\, e^{-i2\pi f t} \quad dt \tag{A.6}$$

so that

$$z_{(t)} = \int_{-\infty}^{\infty} Z_{(f)}\, e^{i2\pi f t} \quad df$$

Then

$$R_{(\tau)} = \lim_{T\to\infty} \frac{1}{T} \int_{-\infty}^{\infty} z_{(t)} \int_{-\infty}^{\infty} Z_{(f)}\, e^{\imath 2\pi f(t+\tau)} \quad df\, dt$$

$$= \lim_{T\to\infty} \frac{1}{T} \int_{-\infty}^{\infty} Z_{(f)} e^{\imath 2\pi f\tau} \int_{-\infty}^{\infty} z_{(t)}\, e^{\imath 2\pi f t} \quad dt\, df$$

$$= \lim_{T\to\infty} \frac{1}{T} \int_{-\infty}^{\infty} Z_{(f)} \cdot Z_{(-f)}\, e^{\imath 2\pi f\tau} \quad df \tag{A.7}$$

We now let

$$R_{(\tau)} = \frac{1}{2} \int_{-\infty}^{\infty} S_{(f)}\, e^{\imath 2\pi f\tau} \quad df \tag{A.8}$$

Comparing Eq.(A.7) with Eq.(A.8), we get

$$S_{(f)} = \lim_{T\to\infty} \frac{2}{T}\, |\, Z_{(f)}\,|^2$$

$$= \lim_{T\to\infty} \frac{2}{T} \left| \int_{-\infty}^{\infty} z_{(t)}\, e^{-\imath 2\pi f t} \quad dt \right|^2$$

$$= \lim_{T\to\infty} \frac{2}{T} \left| \int_{-\frac{T}{2}}^{\frac{T}{2}} y_{(t)}\, e^{-\imath 2\pi f t} \quad dt \right|^2 \tag{A.9}$$

A.2 Discrete Form of PSD

1. Blackman-Tukey method

This digital computation method of PSD was established by Blackman and Tukey in 1958 and is obtained by calculating the autocorrelation of the sampled data, followed by its Fourier transform. The discrete form of the autocorrelation function is given by

$$R_k = \frac{1}{N-k}\sum_{i=1}^{N-k} y_i \cdot y_{i+k} \qquad (k = 0, 1, 2 \cdot \cdot m) \tag{A.10}$$

where m is called the lug number and must be much smaller than the data sampling number. y_i is a deviation from an expected value of y, i.e. $y_i = y - \mu$. y is the original data and μ is its expected value. Then PSD is computed with Eq.(A.4)

$$S_{(f)} = 4\int_0^\infty R_{(\tau)} \cos 2\pi f\tau \quad d\tau \tag{A.4}$$

The integration is performed using Simpson's rule. Therefore,

$$S_k = \frac{1}{f_c}\left[r_o + 2\sum_{i=1}^{m-1} r_i \cos(\frac{\pi i f}{f_c}) + r_m \cos(\frac{\pi m f}{f_c})\right] \tag{A.11}$$

where k is the harmonic number, f_c is Nyquist frequency and f is the frequency, equal to kf_c/m

2. Cooley-Tukey method

In order to make the Fourier calculation faster, FFT (Fast Fourier Transform) was developed in the late 1960's, and it can be used for the computation of PSD. PSD have been widely accepted in accordance with the development of the digital computer (Hullender and Bartley, 1975). Application of the FFT for computing PSD can be explained using Parseval's theorem for computing the average power associated with a function, y(t). The average power is

$$E[y_{(t)}^2] = \frac{1}{T}\int_0^T y_{(t)}^2 \quad dt$$

$$= \frac{1}{T}\int_{-\infty}^{\infty} Y_{(f)} \cdot Y^*_{(f)} \quad df \qquad \text{(A.12)}$$

where $Y_{(f)}$ is the Fourier transform of $y_{(t)}$ and $Y_{(f)}^*$ is a conjugate of $Y_{(f)}$. The discrete form of $Y_{(f)}$ yields:

$$Y_n = \sum_{k=0}^{N-1} y_k \cdot e^{-i2\pi f_n k\Delta t}$$

$$= \sum_{k=}^{N-1} y_k \cdot e^{\frac{-i2\pi nk}{N}} \qquad (n = 0, 1, 2 \cdots N-1) \qquad \text{(A.13)}$$

since $N \cdot \Delta t = T$ and $f_n = n \cdot \Delta f = n/T$. The FFT is simply an effective tool for numerically computing the digital equivalent of the above equation.

A raw estimate of the PSD function at any frequency, f, is given by the definition of

$$S_{(f)} = \frac{2}{T} \mid Y_{(f)} \mid^2 \qquad \text{(A.14)}$$

Therefore,

$$S_n = \frac{2}{T} \mid Y_n \mid^2 \cdot \Delta t^2$$

$$= \frac{2\Delta t}{N} \mid Y_n \mid^2 \qquad \text{(A.15)}$$

APPENDIX B

REVIEW OF SURFACE ROUGHNESS MEASUREMENT

B.1 Measurement Methods of Road Surface Profile

For the measurement of the road surface height profile, several methods have been considered depending on certain objectives. After the Second World War, many road surface profiles were investigated. One of the most interesting surfaces was the runway of an airport because an airplane undergoes severe vibration on the runway before taking off and especially after landing. These surface profile data are required for the vibration analysis. These data are also used to evaluate the repair time of a paved road. Many different measurement methods were then developed in order to get data for surface profiles. They are classified roughly as follows:

(1) Conventional (optical) method

(2) Servo-seismic method

(3) Profilometer method

(4) Slope integration method

(5) Artificial satellite method

(6) Fifth wheel method

(1)-(5) are generally called direct methods, while (6) is an indirect method.

(1) The conventional method (Fig. B.1a) is the most primitive one, since it uses a level and staffs. It is cheap and simple, and does not require any expensive equipment. However this method is very tedious and requires long measurement time, depending on the user's skill. Therefore, other methods were conceived for the measurement of terrain profiles.

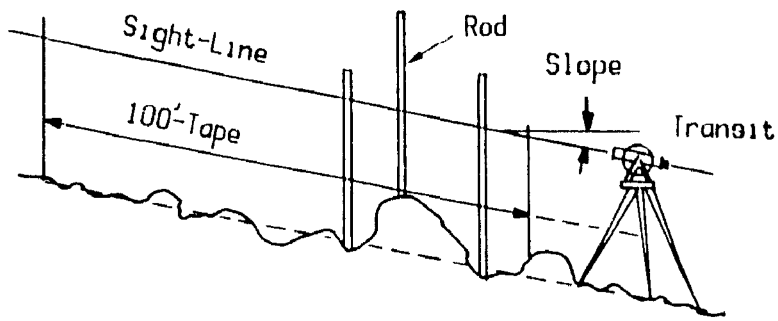

Fig. B.1a Measurement of surface profile by conventional method

(2) The servo-seismic method (Fig. B.1b) has a more complicated mechanism, described as follows. For example, as the wheel goes up the bump, the wheel, actuator and accelerometer are accelerated upward. This accelerometer signal is integrated twice to determine the upward displacement of these components. This displacement signal is used to create an oil flow in the electrohydraulic valve. The signal is scaled so that the oil flow into the top chamber of the actuator, and the exhausted oil out of the bottom chamber, cause a relative movement of the

actuator cylinder and ram, exactly equal to the upward movement of the actuator cylinder, thus causing the ram to remain stationary. The road profile can be obtained by measuring the displacement of the actuator cylinder with respect to the ram.

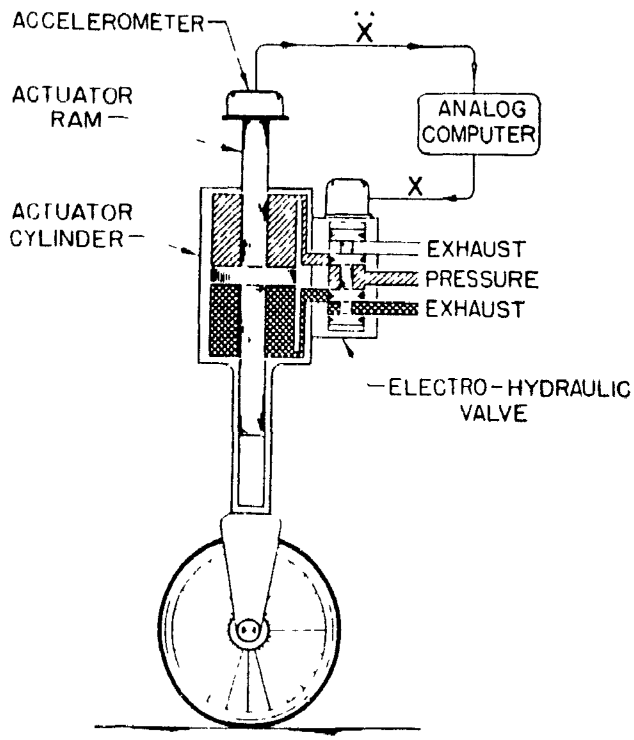

Fig. B.1b Schematic diagram of servo-seismic road profile recording device (after Spangler and Kelly,1962)

(3) The profilometer (Fig. B.1c) is basically a 16-wheeled articulated carriage that supports a detecting and recording device at a constant height above the main level of the road surface. The 16 wheels and their axles support four 4-wheeled bogies that cover a total width of 1.2 m (4 ft.) and 6.4 m

(21 ft.) long wheel base. The tyres of the wheels are made of soft rubber and are inflated to a low pressure to ensure that very small irregularities in the road surface are not introduced into the measurement. Due to the large span of the device, it may not be suitable for the measurement of off-road surface profiles whose wavelength is relatively short.

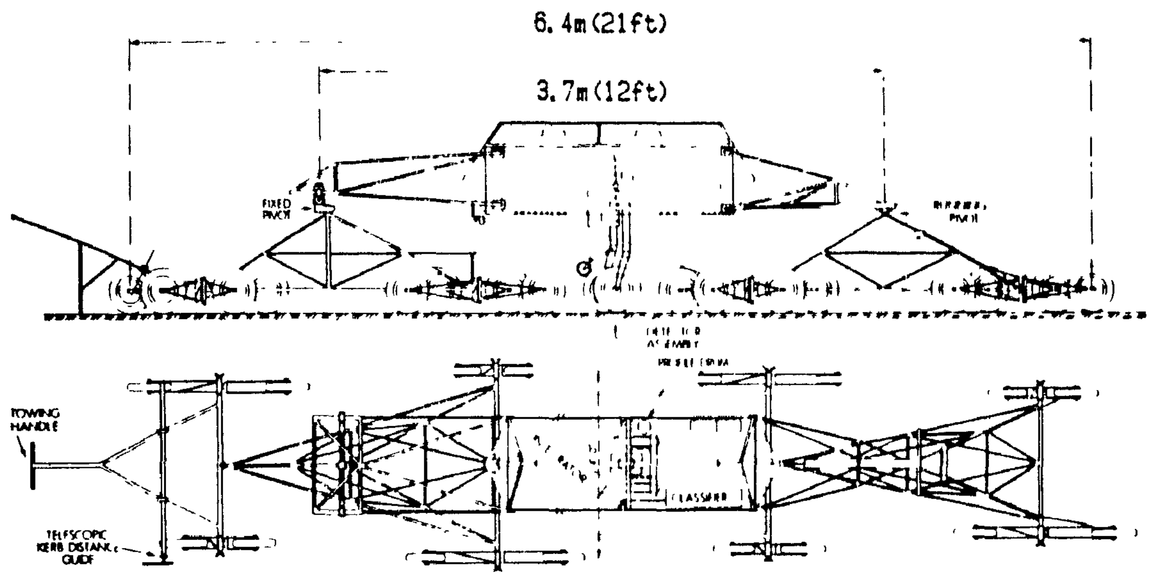

Fig. B.1c The Ontario Department of highways profilometer (after Chong and Phang, 1973)

(4) In order to overcome the disadvantage of the preceeding method, the slope integration method was developed by the University of Michigan and the Land Locomotion Research Laboratory (Sattinger and Sternick, 1961). In this method, the terrain surface

profile is derived by a continuous measurement of two quantities, i.e. distance traveled by the vehicle and the slope angle of the ground points. In 1982, Ohmiya and Matsui manufactured a three wheeled surface height detector using this method (Fig. B.1d), and agricultural farm profiles were obtained with fairly good accuracy.

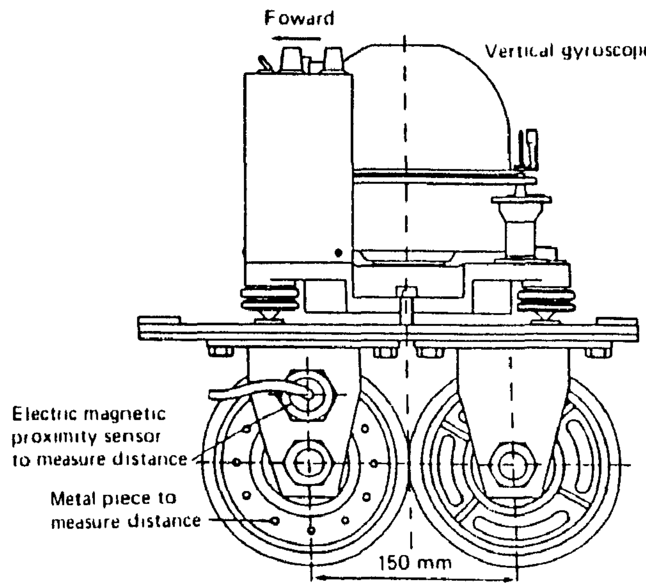

Fig. B.1d Side view of measuring system using slope integration method (after Ohmiya and Matsui)

(5) The artificial satellite method can be used for mapping the distribution of obstacles, slope or vegetation. Sample measured data is shown in Fig.B.1e.

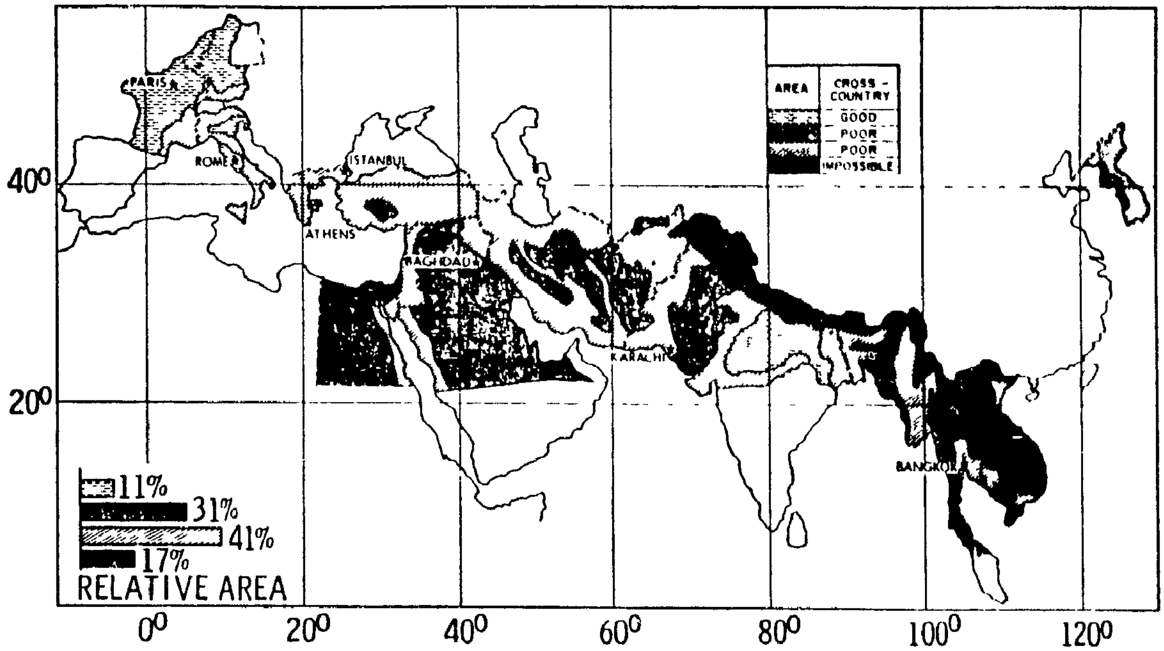

Fig. B.1e Global trafficability map
(after Deitchman, 1964)

The maps were prepared primarily for strategic and tactical planning. Since the accuracy of this method has been improved over the last two decades, and it can survey a large area in a short time, it could be expected to be widely used for surveying terrain roughness in the near future, unless the cost becomes exorbitant.

(6) The fifth wheel method as an indirect measurement (Fig. B.1f) was introduced by Fujimoto in 1983. The fifth wheel, whose transfer function is known, is attached to the tail of a vehicle. The vehicle is

then driven at a constant speed on a terrain, while an accelerometer attached to the fifth wheel measures the vertical vibration (response). Surface profile as an input can be determined from a relationship between the response and transfer function.

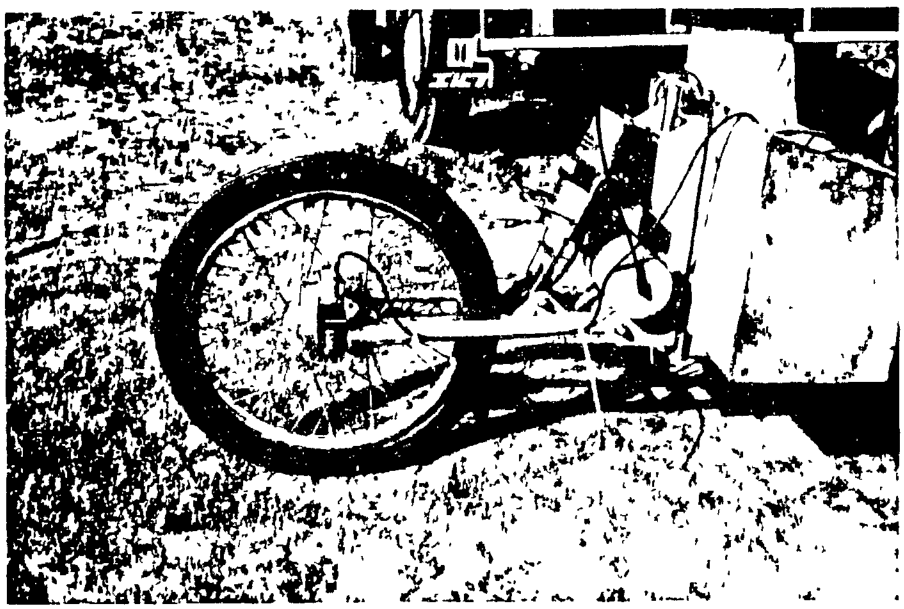

a.

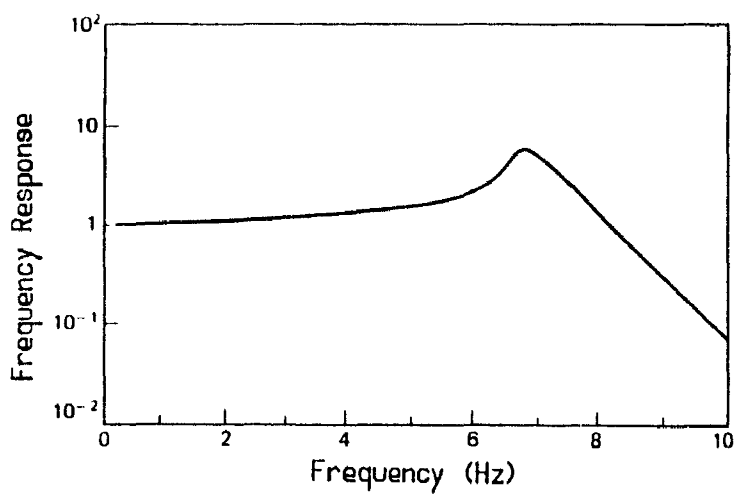

b.

Fig. B.1f Fifth wheel for indirect method and its frequency response curve (after Fujimoto)

B.2 Measured Surface Profiles and Description of Roughness

A relatively large number of road profile measurements have been performed. Several indices for a description of roughness are introduced. They are Root-Mean-Square vertical acceleration (RMSVA), quarter-car index (QI) or riding comfort index (RCI) etc.. Moyer (1951) suggested the use of the roughness index (RI). Two sets of bogie wheels nine meters apart (Fig. B.2a) provide reference points from which vertical displacement is measured by a recording wheel at the midpoint. The cumulative vertical displacement per mile is termed tne roughness index. This index is correlated with another index, such as RMSVA or QI. However, it cannot provide useful information for a dynamic analysis.

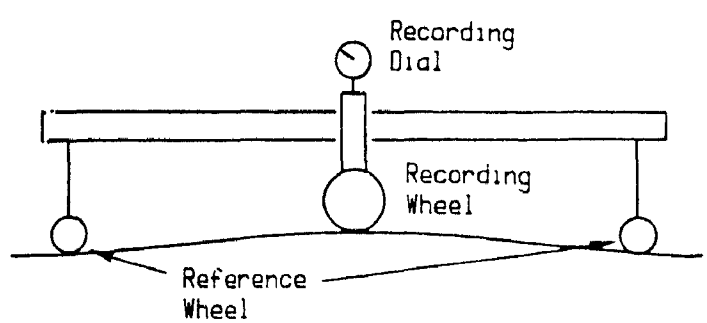

Fig. B.2a Profile measurement by common straightedge

Manor and Nir (1987) investigated the effect of span,l, of the straightedge, and the measuring point,r, on the accuracy of the surface roughness measurement (Fig. B.2b). The standard deviation of y was calculated. It was mentioned that the minimum deviations were found at the wheels, the deviations increased at the middle of the machine's span and rose steeply outside the span. Higher accuracy was found on a smoother surface, especially in the case of the machines with longer wheel spans.

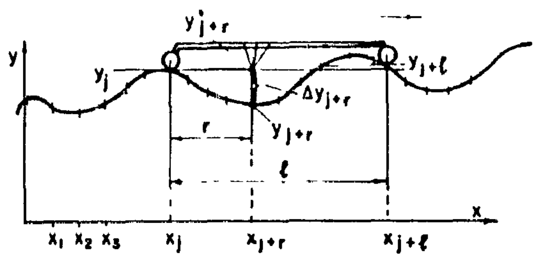

a.

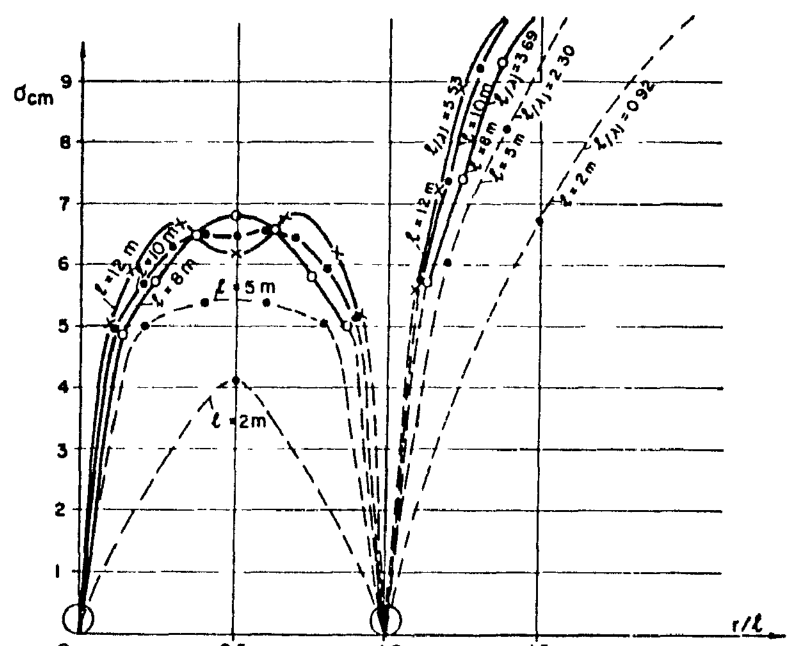

b.

Fig. B.2b Straightedge on a ground and effect of measuring point on height deviations using different wheelbases (after Manor and Nir)

Wendenborn (1966) investigated the surface profile from on-road surface to agricultural fields. Fig. B.2c shows various profiles of the ground surfaces. The simplest, conventional step by step method was employed for the measurement because of the smaller error in data processing. Sampling was performed at every 0.15 m. The PSD function was calculated from the measured profile, and it was generally expressed in the following form for most of the naturally formed surfaces.

$$S_{(F)} = b\,F^{-2\,3} \tag{B.1}$$

where b is an experimental constant and F is frequer.cy (rad/m).

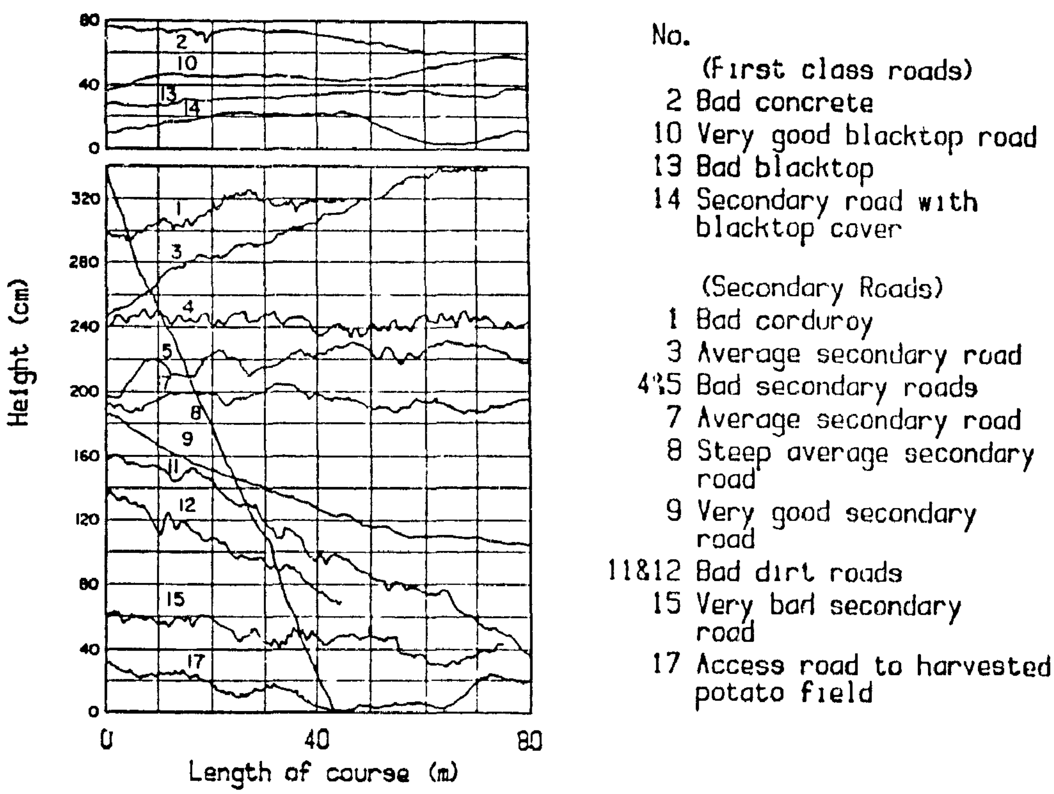

Fig. B.2c Measured surface profiles (after Wendenborn)

Gray and Johnson (1972) measured the micro surface roughness of elastic disk surface, to study the dynamic response of these bodies in rolling contact. Differing from the case of off-road surfaces, a very wide range of frequency, including high frequencies, was investigated (Fig. B.2d). White noise PSD can be seen for wavelengths shorter than 2.5 mm. By using the measured PSD and the system transfer function, the acceleration PSD was obtained as an output and compared with the measured acceleration PSD.

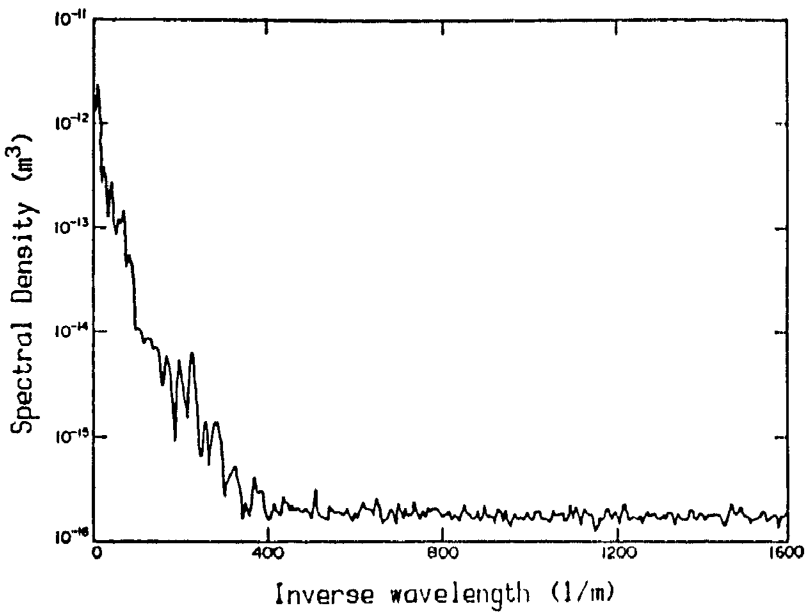

Fig. B.2d Roughness spectrum of aluminium-alloy lathe -turned disc (after Gray and Johnson)

Kozin and Bogdonoff (1960, 1966) described the surface roughness using the variance of profile. A form of PSD was introduced for the surface description.

$$S_{(\lambda)} = \frac{2\sigma^2}{\lambda_o\sqrt{2\pi}} e^{-\frac{\lambda^2}{2\lambda_o^2}} \tag{B.2}$$

where σ^2 = variance

λ_o = constant

λ = frequency (1/wavelength)

A smaller λ_o means that most of the power is concentrated in the low frequency region, while conversely, a large λ_o means that most of the power is distributed in the high frequency region.

Hullender and Bartley (1975) numerically generated spectra using a random number generator by an ideal sampler, which provided uncorrelated data with variance, σ^2. It was found that their PSD curves dropped significantly for the wavelengths below approximately 66 m (200 ft). Then another PSD function was expressed in terms of variance and section length, h of of the road. It was suggested that the following expression for PSD could be applicable for very short wavelengths. The equation yields

$$S_{(\Omega)} = \frac{4\sigma^2}{h^3\Omega^4}(1 - \cos\Omega h) \tag{B.3}$$

where the spatial frequency has units of radian/ft. For relatively long wavelengths compared to h, Eq.(B.3) simplifies to the form of $G_o\Omega^{-2}$ where $G_o = 2\sigma^2/h$.

A realistic description of road surface roughness has to be achieved by two-dimensional spectral densities, since the surface height points z are determined in the x-y plane, not only along the x axis, as shown in Fig. B.2e. Such an expression becomes very complicated because of the joint probability.

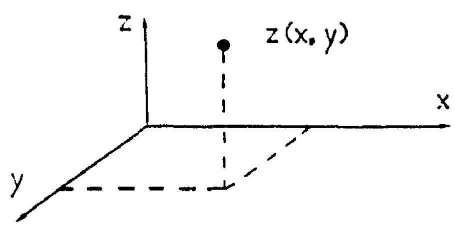

Fig. B.2e Height of surface as measured from the x-y plane

Dodds and Robson (1973), Kamash and Robson (1977) made a considerable simplification by assuming that the surface concerned is isotropic i.e. independent of the direction of the vector separating the two points (x,y), in addition to the stationarity. As a result of this, the complete probabilistic description of the surface was inferred from the probabilistic description of a one-dimensional profile. Note that PSD should essentially be defined for all the frequencies because of the use of the Fourier transform. However, it is only necessary that the mathematical expression of PSD be valid within the range of frequency over which response is to be expected. A bounded PSD form was proposed as follows, assuming fixed values beyond the range of interest.

$$
\begin{cases}
S_{(\Omega_a)} & |\Omega| \leq \Omega_a \\
S_{(\Omega_a)}|\Omega/\Omega_a|^{-n_1} & \Omega_a \leq |\Omega| \leq \Omega_o \\
S_{(\Omega_a)}(\Omega_o/\Omega_a)^{-n_1}\,|\Omega/\Omega_o|^{-n_2} & \Omega_o \leq |\Omega| \leq \Omega_b \\
0 & |\Omega| > \Omega_b
\end{cases}
\tag{B.4}
$$

The values of Ω_a, Ω_b and Ω_o are suitably chosen.

Ohmiya (1986) measured profiles of meadows and roads with a three wheeled machine using the slope integration method. Its running speed was 0.3 m/s. Fig. B.2f exhibits the measured profiles.

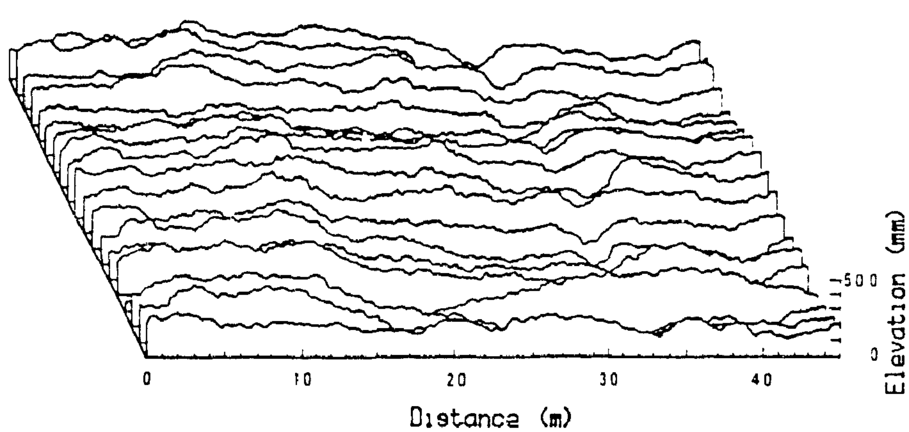

Fig. B.2f Measured profiles of meadow (after Ohmiya)

It was concluded from the PSD curves that the slope integration method was suitable for the measurement of agricultural fields, the ground surfaces were geometrically random, including no periodic undulations, and an approximate form of PSD could be employed for a dynamic analysis. The PSD was given by

$$S_{(\Omega)} = G_{(\Omega_o)} \left(\frac{\Omega}{\Omega_o} \right)^{-n} \tag{B.5}$$

The value of n was found to be 2.3 and Ω was taken from 0.1 c/m to 4 c/m. The coherence functions were calculated in order to investigate the correlation between two parallel tracks, spaced at 1.5 m. The values of coherency functions were small over 0.2 c/m and, therefore, it was suggested that the two parallel profiles were independent of each other. With regard to the evaluation of roughness, it was useful to apply the recommended classification by ISO.

While many surface profile PSDs showed a linear decrease with increasing frequency, Hać (1987) took notice of the bump in the PSD curves as plotted in Fig. B.2g.

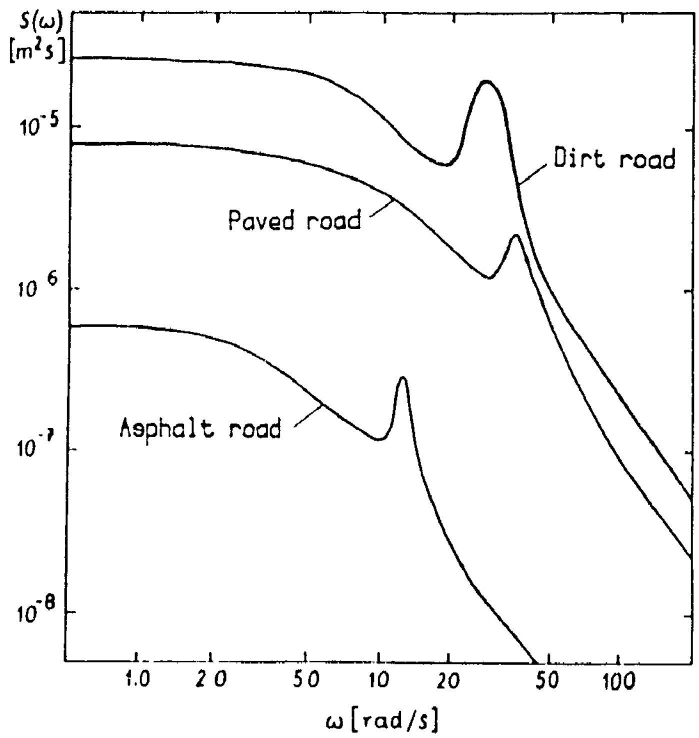

Fig. B.2g PSD curves for three types of roads (after Haćʹ)

A slightly complicated mathematical form of PSD was determined as follows:

$$S_{(\omega)} = (s_1{}^2/\tau)[k_1V/(\omega^2+k_1{}^2V^2)]+$$
$$(s_2{}^2/\tau)[k_2V(\omega^2+k_2{}^2V^2+k_3{}^2V^2)]/[(\omega^2+k_2{}^2V^2-k_3{}^2V^2)^2+4(k_2k_3)^2V^4] \qquad (B.6)$$

where ω = angular frequency

V = vehicle velocity

k_1, k_2, k_3, s_1, s_2 = coefficients depending on type of surface

The sum, $s_1{}^2+s_2{}^2$, gives the variance of road surface irregularities. Values of each parameter for the surface shown in Fig. B.2g are shown in Table B.1.

Table B.1 Values of parameters describing three road spectrums (after Hać)

Type of road	k_1 (1/m)	k_2 (1/m)	k_3 (1/m)	s_1^2 (m^2)	s_2^2 (m^2)
Asphalt	0.2	0.05	0.6	7.65E-6	1.35E-6
Paved	0.5	0.2	2.0	2.55E-4	4.50E-3
Dirt	0.8	0.5	1.1	7.50E-4	2.50E-4

B.3 Detrend of the Measured Profile

As a preliminary to the power spectrum calculations, it appeared desirable to make some modifications to the actual measured profiles. The process of detrending the terrain record was discussed by Van Deusen (1965) and Walls et al. (1954). This process is necessary in order to eliminate the characteristic of non-stationarity included in the measured data. Non-stationarity is the sub-product of trend by low frequency (long wavelength) components (Fig. B.3a).

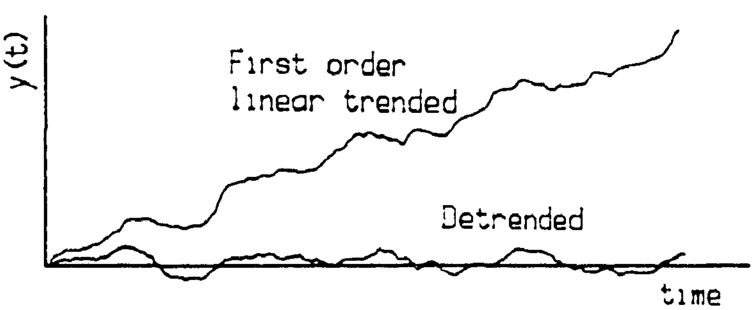

Fig. B.3a Trended and detrended data

The effect of this trend is to raise the estimate of the surface roughness at each frequency, as shown in Fig. B.3b. In order to cope with this problem, a linear moving average associated with the exponential weighting function was adopted (Fig. B.3c). This exponentially weighted average appears similar to the effect derived from an electrical high-pass filter. The mathematical expression for computing the detrend is given in the following manner:

$$y_{d(x)} = y_{(x)} - \frac{1}{2\lambda} \int_{a=0}^{a=\infty} \left[y_{(x+a)} - y_{(x-a)} \right] e^{-\frac{a}{\lambda}} \, da \qquad \text{(B.7)}$$

where $y_{d(x)}$ is the detrended filtered function, $y_{(x)}$ is the the original function and λ is the exponential weighting constant.

Since the test surfaces were prepared by distributing the wooden pieces on a flat and level surface in our laboratory, the detrending process of the measured surface profiles was not considered in this study under the assumption of stationarity of the profiles.

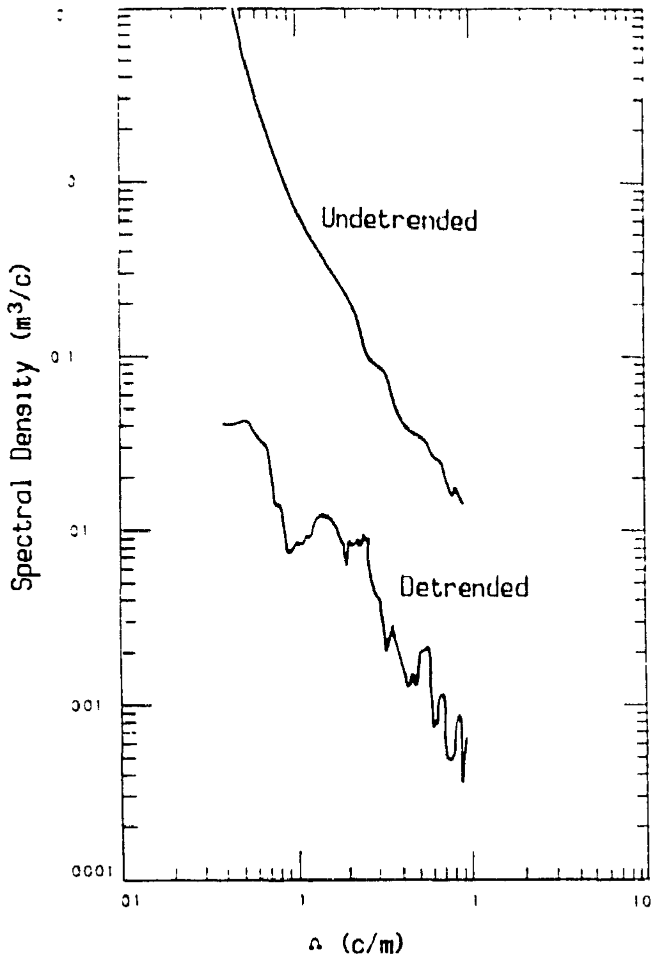

Fig. B.3b Comparison of detrended and undetrended PSD (after Van Deusen)

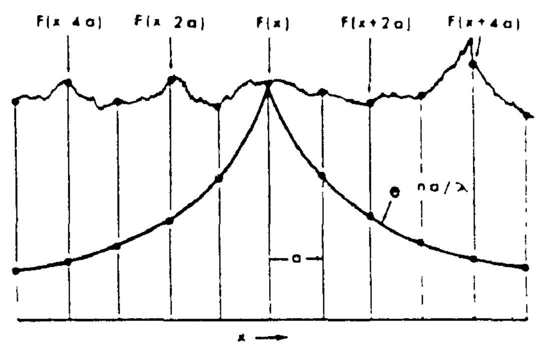

Fig. B.3c Moving average with exponential weighting function (after Van Deusen)

APPENDIX C

MECHANICAL PROPERTIES OF PNEUMATIC TYRE

C.1 Tyre Carcass Construction

The modern automobile tyre is classified as bias-ply or radial-ply, depending on its carcass construction, which is made up of a number of layers of flexible cords of high modulus of elasticity, encased in a low modulus of rubber. The carcass is the most important part of the tyre structure, and it affects the mechanical properties of a pneumatic tyre. The conventional bias-ply tyre (Fig. C.1a) is made by fabricating several plies of cord material in a definite angle with respect to the direction of tyre rotation. Half of the layers have the cords at a positive angle and half at a negative angle. The radial-ply tyre (Fig. C.1b) has been produced for several decades. The difference from the cross-bias tyre is the angle of cord, which is disposed in a radial or substantially radial direction in relation to the axis of rotation of the tyre.

The crown angle is the angle between the cord and the circumferential centerline of the tyre. Recent technology placed several belts on top of the radial tyre. When the cords have a small crown angle, the tyre will have good cornering characteristics, but a poor ride. On the contrary, for right angled cords, the opposite effect occurs.

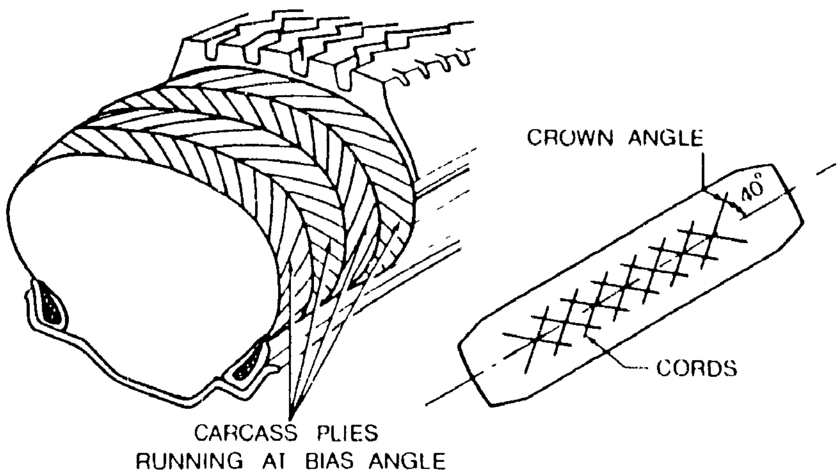

(a) Bias-ply tyre

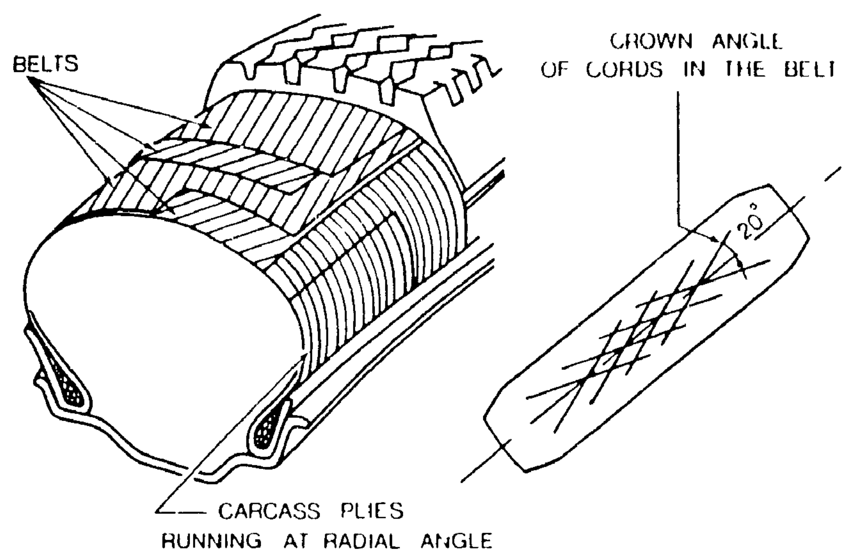

(b) Radial-ply tyre

Fig. C.1 Comparison of tyre construction between (a) bias-ply and (b) radial-ply tyre (after Wong, 1978)

Fig. C.2 shows the coefficient of rolling resistance as a function of speed, for bias-ply and a radial-ply tyre. Rolling resistance increases with an increased speed. As can be seen, the radial-ply tyre has an advantage when it is new i.e. less resistance than the bias-ply tyre. However it displays the opposite characteristic in behavior when the tread is lost.

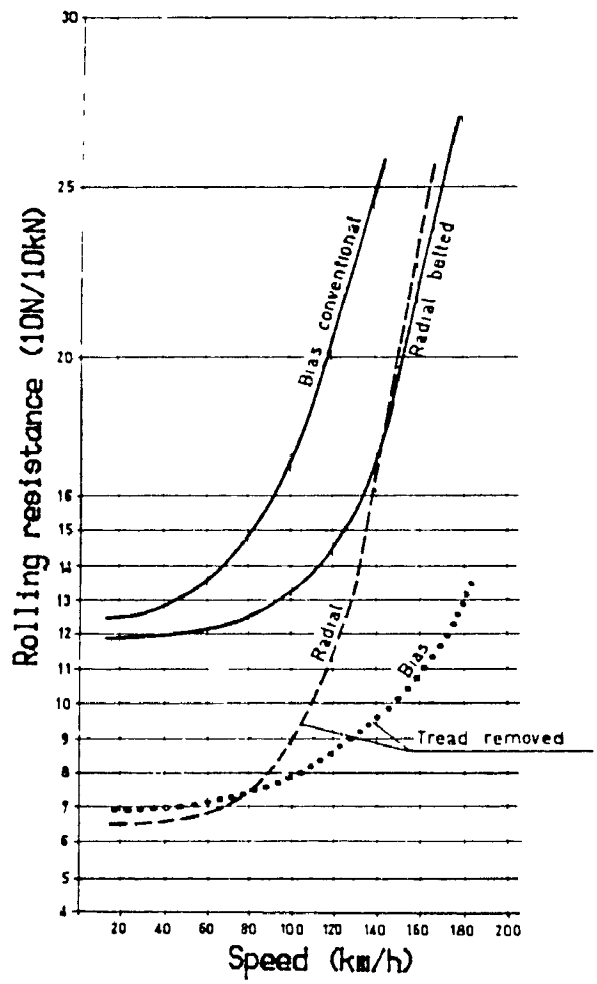

Fig. C.2 Variation of coefficient of rolling resistance for bias/radial-ply tyre (after Clark, 1971)

C.2 Frequency Range of Interest for Various Types of Noise and Vibration Problems

When the noise and vibration problem caused by terrain/road surface roughness or tyre peripheral surface roughness is considered, the frequency induced by these kinds of roughness has a dominant role in the response of the tyre. Several frequency ranges, depending on the type of problem, are presented in Fig. C.3. It is generally said that high frequency, above approximately 100 Hz, is important for the tyre noise problem and relatively low frequency is vital for a vertical and horizontal vibration problem. As described in this Figure, the tyre response as a spring-mass-damper system is influenced by very low frequencies, below 20 Hz.

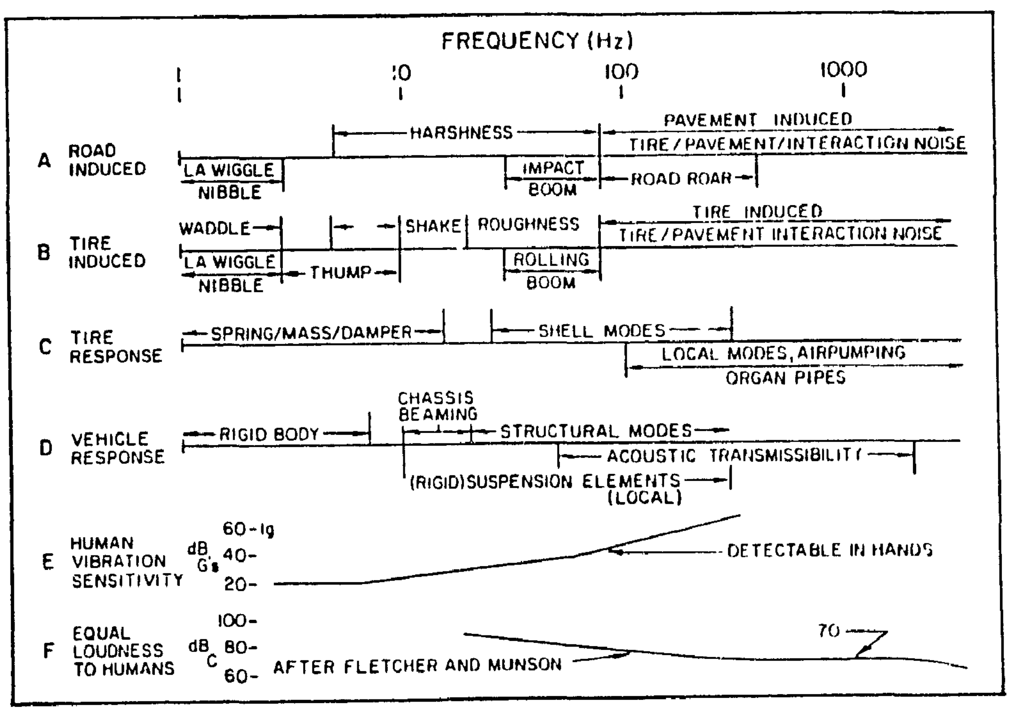

Fig. C.3 Frequency range of noise/vibration problem (after Pottinger and Yager, 1986)

C.3 Nonlinear Characteristics of a Pneumatic Tyre

1. Tyre stiffness

   a. frequency dependence

The effect of exciting frequency, which is also related to vehicle speed, on the tyre stiffness is indicated in Fig. C.4a. The stiffness increases nonlinearly with an increase in frequency. However, since the vertical spring rate at low frequencies is not very frequency dependent, the use of a constant stiffness is a reasonable approximation, especially for a off-road vehicle's tyre vibration problem arising from terrain surface roughness. Hardening of the tyre by higher frequencies is supposedly due to a molecular process of the rubber composite (Laib, 1978).

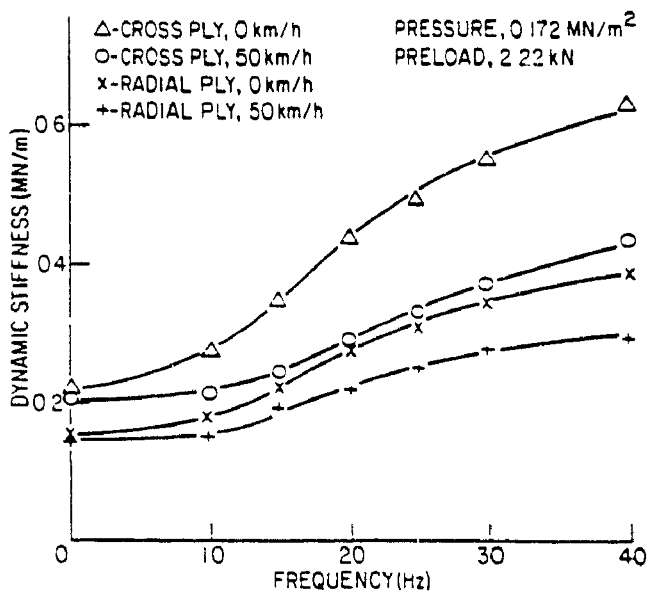

Fig. C.4a Frequency dependency of tyre stiffness (after Phillips, 1972)

b. velocity dependence

Although it has been reported by many authors that the tyre stiffness varies with the operational velocity of a vehicle, a definite conclusion may not be derived. For example, Matthews and Talamo (1965) indicated that the stiffness increases with velocity, although Chiesa and Tangora (1959) showed the opposite results. Furthermore, Gough (1963) concluded that pneumatic tyre stiffness was unlikely to vary by more than 1-2% between the static mode and the dynamic mode. These differences may result from the testing method, equipment or consideration of heat generation inside a tyre.

However, the stiffness is generally considered to increase with velocity due to the centrifugal force and the increase in inflation pressure by heating during the rotation (see Fig. C.4b).

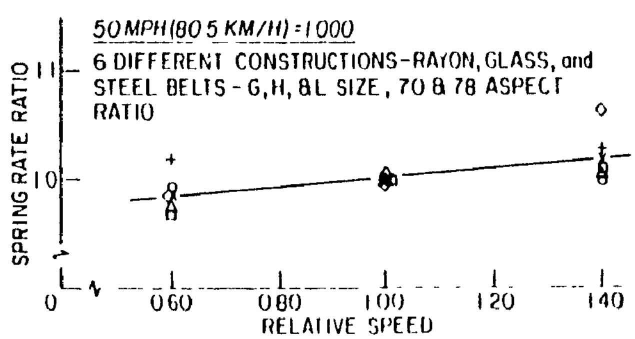

Fig. C.4b Velocity dependency of tyre stiffness (after Pottinger and Yager, 1986)

c. load dependence

Effect of load on vertical stiffness of the tyre is also shown in Fig. C.4c. The stiffness increases slightly with an increase in load (deflection), but the degree of increase depends highl on the type of tyre. Although it seems to be due to an increased inflation pressure, this mechanism has not been proved theoretically due to the complexity of the tyre structure, since some tyres show the opposite tendency from that described above.

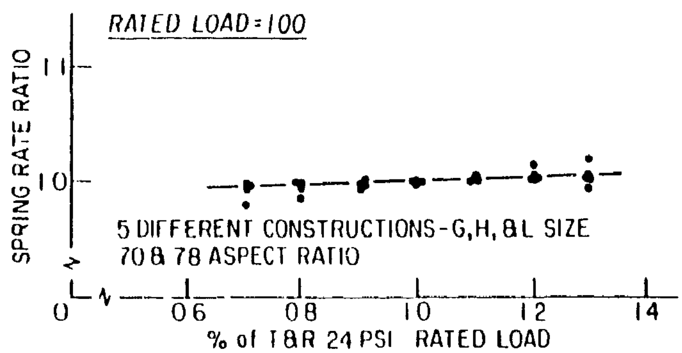

Fig. C.4c Load dependency of tyre stiffness (after Pottinger and Yager, 1986)

2. <u>Tyre damping</u>

Damping is expected to have a dependency on the above-mentioned factors since it is directly related to stiffness.

a. frequency dependence

The effect of exciting frequency on damping of a rubber composite specimen was investigated by Laib (1978) and Weiner and Gogos (1961). Damping characteristics were studied by creating a sinusoidal excitation in bending of a rubber specimen (6.4mm thick). The results are shown in Fig. C.5. It was found that damping of the rubber specimen was caused by the energy loss in shear, and that the damping ratio increases markedly with the frequency range above 100 Hz.

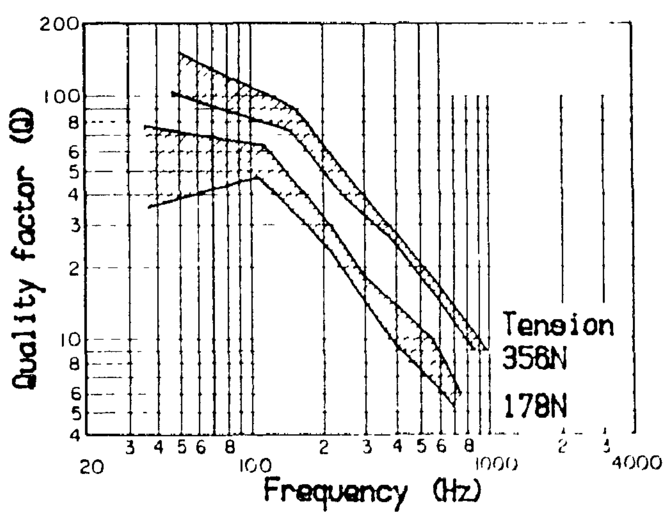

Fig. C.5 Effect of excitation frequency on quality factor ($Q = 1/2\zeta$) (after Weiner et al.)

b. Velocity dependence

The tyre damping is inferred to be decreased by an increased rolling speed because the tyre stiffness is hardened by the inflation pressure rise and centrifugal force under a high speed operation. It may include the effect of chemical reaction due to heat generation in the tyre.

c. Exciting amplitude dependence

Amplitude dependency of the tyre damping was indicated by Matthews (1965). The damping ratio was decreased with an increased exciting amplitude. It was reported that about 50% of the decrease in damping ratio was observed over the excitation amplitude range between 0.0127 m and 0.0508 m (0.5 in. and 2 in.), (peak-to-peak), which, in most cases, an off-road vehicle receives from the rough ground.

Up until now, the effect of several factors on tyre stiffness and damping have been mentioned. These, however, merely show the general tendencies of the mechanical properties of a tyre. Some of them may exhibit different characteristics. Unfortunately, since there is a lack of information about these properties in spite of their importance, especially for vehicle dynamics, no rational explanation, except empirical results, has been given for these phenomena.

C.4 High Frequency Behavior of a Tyre

On the highway, the tyre is expected to vibrate at high frequencies, compared to the off-the-road operation. Barson et al. (1967-68) investigated the transmissibility and acceleration level of a tyre, which is excited at high frequencies, using a vibrator and slatted drum. Fig. C.6 shows the result for longitudinal excitation. Tyre A and B are radial/bias-ply tyres, respectively. The Figure describes the vibration mode and actual acceleration level and the author thus concluded that both tests are necessary to obtain useful information for tyre dynamics.

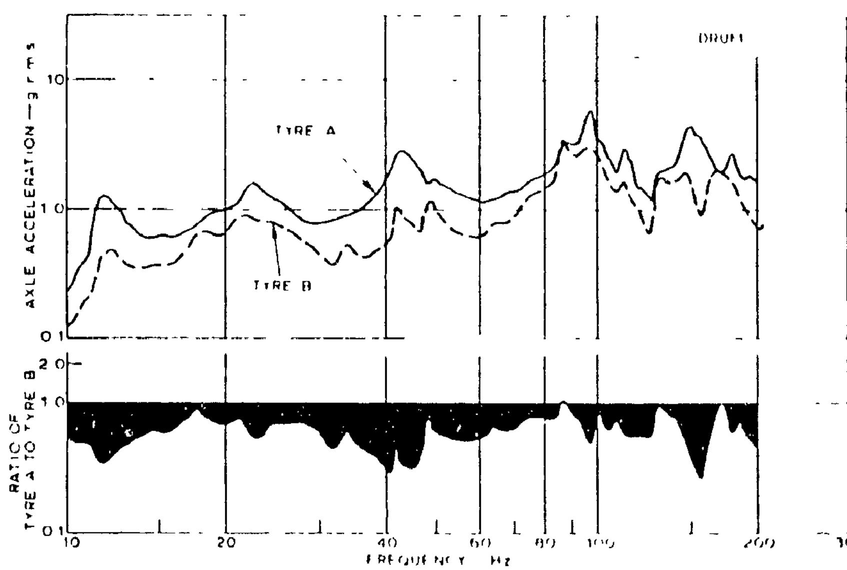

Fig C.6 High frequency behavior of a tyre (after Barson et al.)

APPENDIX D

DERIVATION OF ROLLING RESISTANCE AND STANDARD DEVIATION OF DRAWBAR-PULL ON VARIOUS ROUGH SURFACES

D.1 Rolling Resistance on a Rough, Non-deformable Terrain

Fig. D.1 shows a schematic diagram of a rotating tyre on a rough, non-deformable terrain moving at a horizontal velocity of V. There are tyre vertical motions due to terrain surface and constant rotational motion. During the motion, several powers are dissipated by tyre deformation. For the first part, power is spent by the vertical motion due to ground roughness, namely $\dot{E}_{V1}$. If the tyre contacting the ground surface is not in point contact, other forms of power expenditure, $\dot{E}_{V2}$, will be given by the rotational motion of a tyre. This power is contributed by the tyre deflection due to static wheel loading in contrast to dynamic loading. These two power components result in the rolling resistance of a pneumatic tyre on a rough terrain.

<u>Power Loss due to Vertical Excitation</u> ($\dot{E}_{V1}$)

When a tyre is excited vertically at a velocity of V_1, the energy spent per unit time is

$$\dot{E}_{V_1} = \int_{-d}^{d} c' \, dx \cdot V_1^2$$

$$= c_T \, V_1^2 \qquad (Nm/s) \qquad \text{(D.1.1)}$$

where c' and c_T are the distributed and total damping of the tyre, respectively. It is assumed that the tyre is always touching the ground surface.

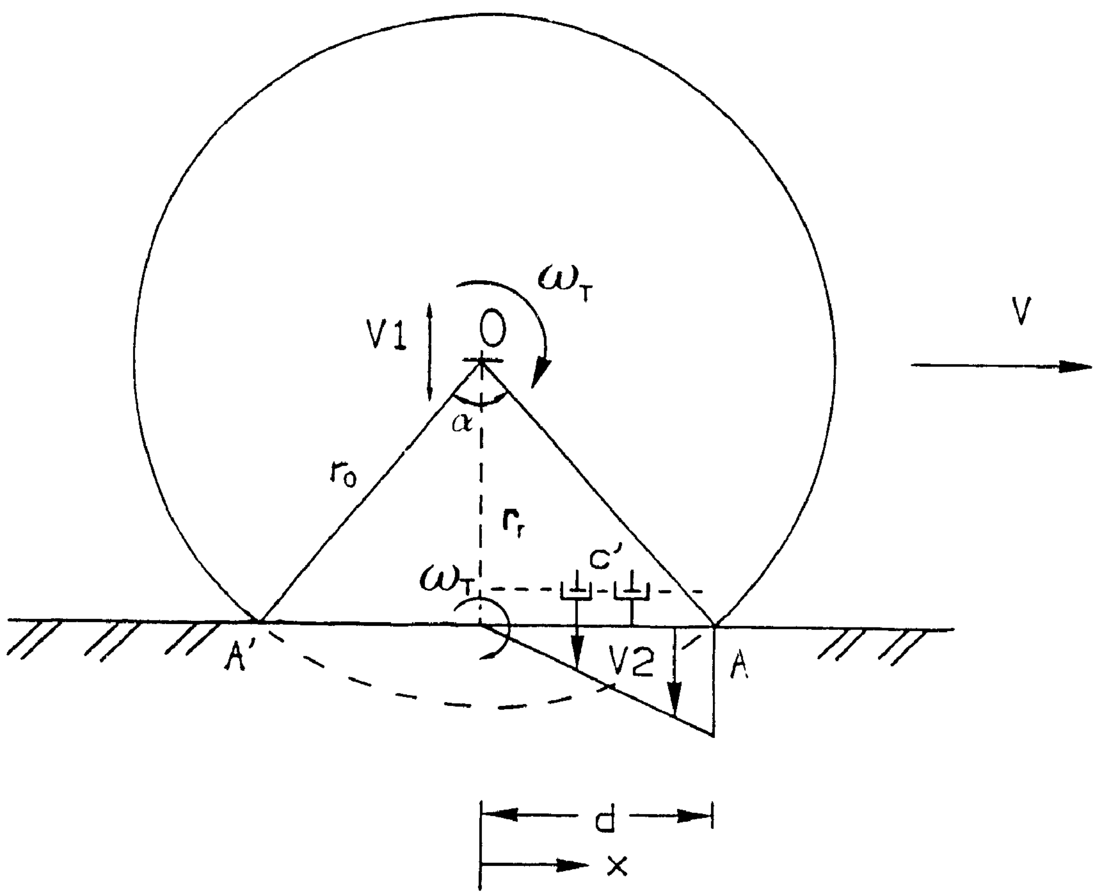

Fig. D.1 Schematic diagram of rolling tyre with vertical excitation

Power Loss due to Tyre Rotation ($\dot{E}_{v2}$)

Since each point along the contact region obtains a vertical impacting velocity, V_2, which is dependent on both rotational velocity and the distance from the center of the contact region, the following work will be achieved while a distributed damping element of tyre is being compressed between point A and A'.

$$W_{V_2} = c' V_2^2 \cdot \Delta t \qquad (Nm/m) \tag{D.1.2}$$

where Δt is the time required for a point to move from A to A', and is given by

$$\Delta t = \frac{\alpha}{\omega_T} \tag{D.1.3}$$

where α is an angle $\angle$AOA' due to tyre deflection.

The total work performed by whole damping elements along the chord A to A' can be given by integrating the energy, W_{V2} through that region.

$$W'_{V_2} = \int_{-d}^{d} W_{V_2} \quad dx \qquad (Nm) \tag{D.1.4}$$

Since the work W'_{V2} is performed $2\pi/\alpha$ times in one revolution of the wheel travel, the work per revolution is

$$W''_{V_2} = W'_{V_2} \frac{2\pi}{\alpha} \qquad (Nm) \tag{D.1.5}$$

The number of revolutions of the wheel per second is $\omega_T / 2\pi$, because the rotational (angular) velocity is rad/sec. Therefore, the power which will be dissipated by the tyre rotation is,

$$\dot{E}_{V_2} = W''_{V_2} \frac{\omega_T}{2\pi}$$

$$= \frac{2c' \omega_T^2 d^3}{3} \qquad (Nm/s) \tag{D.1.6}$$

Since the total damping factor, c_T is expressed as follows,

$$c_T = 2\,d\,c' \tag{D.1.7}$$

the power dissipation can be finally rewritten as

$$E_{V_2} = \frac{1}{3} c_T (\omega_T d)^2 \tag{D.1.8}$$

Therefore, the total tyre deformation power of a tyre traveling on a rough road is

$$\dot{E}'_T = \dot{E}_{V_1} + \dot{E}_{V_2}$$

$$= c_T \left\{ V_1^2 + \frac{1}{3} (\omega_T d)^2 \right\} \tag{D.1.9}$$

As pointed out by Bekker (1983), it is preferable to apply the energy recovery factor in the computation of tyre deformation power. Thus,

$$\dot{E}_T = \xi E'_T$$

$$= \xi c_T \left\{ V_1^2 + \frac{1}{3} (\omega_T d)^2 \right\} \tag{D.1.10}$$

where ξ = energy recovery factor

$= 1 - e^{-AD/H}$

A : constant

(7.0/radial, 15.0/bias tyre; Bekker,1983)

D : tyre deflection

H : tyre carcass height

D.2 Standard deviation of Vertical Response and DBP

D.2.1 On a Sinusoidal Surface

(1) $E[\dot{z}^2]$ (Variance of vertical response of a tyre)

When a wheel rotates on a rigid, sinusoidal wavy road (wavelength= λ) at a certain translational velocity, the wheel axle moves up and down due to a base excitation from the ground. The steady-state response of the wheel axle, $z_{(t)}$, is given by solving a well-known differential equation for a one degree-of-freedom vibration system. That is

$$mz + c_T z + k_T z = -my \tag{D.2.1}$$

where z is a relative displacement (response) between the ground and the wheel axle elevation. y is a sinusoidal ground surface profile which is assumed to be

$$y = h \sin \omega t \tag{D.2.2}$$

where h is an amplitude of the road wave (half of peak-to-peak amplitude), and ω is an excitation frequency ($=2\pi V/\lambda$). Assuming the particular solution for steady-state motion in the form of

$$z = Z \sin(\omega t - \phi) \tag{D.2.3}$$

The derivative of the response is simply expressed as

$$\dot{z} = Z\omega \cos(\omega t - \phi) \tag{D.2.4}$$

Substituting Eq.(D.2.2) into Eq.(D.2.1), the response is given as:

$$Z = \frac{mh\omega^2}{\sqrt{(k_T - m\omega^2)^2 + (c_T\omega)^2}} \tag{D.2.5}$$

The phase angle is

$$\phi = \tan^{-1} \frac{c_T\omega}{k_T - m\omega^2}$$

Thus, the variance of $\dot{z}$ on a sinusoidal road is obtained from Eq.(D.2.4).

$$\sigma_{\dot{z}}^2 = E[\dot{z}^2] = \frac{1}{2} Z^2\omega^2 \tag{D.2.6}$$

(2) σ_{DBP} (standard deviation of DBP)

Substituting Eq.(D.2.3) and (D.2.4) into Eq.(4.21), the drawbar-pull (DBP) on a sinusoidal road is obtained as follows:

$$\begin{aligned}
\mathrm{DBP}_{(t)} &= \epsilon_1 + \epsilon_2\dot{z} + \epsilon_3 z \\
&= \epsilon_1 + \epsilon_2 Z\omega\cos(\omega t - \phi) + \epsilon_3 Z \sin(\omega t - \phi) \\
&= \epsilon_1 + Z\sqrt{(\epsilon_2\omega)^2 + \epsilon_3^2}\,\sin(\omega t - \phi + \psi)
\end{aligned}$$

$$\phi = \tan^{-1} \frac{c_T\omega}{k_T - m\omega^2}$$

$$\psi = \tan^{-1} \frac{\epsilon_2\omega}{\epsilon_3} \tag{D.2.7}$$

The expected value of the DBP is expressed as

$$E[\mathrm{DBP}] = \epsilon_1$$

$$= \frac{T}{r_o} + Jmg - \frac{\xi\, c_T\, E[\dot{z}^2]}{V} \qquad \text{(D.2.8)}$$

where

$$J = \left(\frac{T}{8r_o^3} - \frac{\xi\, c_T\, \omega_T^2}{12V} \right) q^2$$

The standard deviation of the DBP on a sinusoidal road is given from Eq.(D.2.7).

$$\sigma_{DBP} = \sqrt{\frac{1}{2}\, Z^2\, \{(\epsilon_2 \omega)^2 + \epsilon_3{}^2\}} \qquad \text{(D.2.9)}$$

D.2.2 On a Randomly Rough Surface

(1) $E[\dot{z}^2]$

The autocorrelation function of $z_{(t)}$ is obtained from its PSD function with the well-known Wiener-Khinchine relation. That is,

$$R_{z(\tau)} = \int_0^{\infty} S_{z(f)}\, e^{i2\pi f\tau} \quad df \qquad \text{(D.2.10)}$$

where $R_{z(\tau)}$ is the autocorrelation function, and $S_{z(f)}$ is the one-sided PSD function of $z_{(t)}$.

If the random process of $z_{(t)}$ is stationary, the autocorrelation function of the derivative of $z_{(t)}$ is given by

$$R_{z(\tau)} = -\frac{d^2}{d\tau^2}\, R_{z(\tau)} \qquad \text{(D.2.11)}$$

Substituting Eq.(D.2.11) into Eq.(D.2.10),

$$R_{z(\tau)} = -\frac{d^2}{d\tau^2}\left[\int_0^{\infty} S_{z(f)}\, e^{i2\pi f\tau} \quad df\right]$$

$$= \int_0^{\infty} (2\pi f)^2 \; S_{z(f)}\, e^{i2\pi f\tau} \quad df \qquad \text{(D.2.12)}$$

Since $\dot{z}_{(t)}$ is also a stationary random process,

$$R_{\dot{z}(\tau)} = \int_0^{\infty} S_{\dot{z}(f)}\, e^{i2\pi f\tau} \quad df \qquad \text{(D.2.13)}$$

Comparing Eq.(D.2.12) with Eq.(D.2.13), the following relation is obtained.

$$S_{z(f)} = (2\pi f)^2 \; S_{z(f)} \qquad \text{(D.2.14)}$$

Since E[z] = E[$\dot{z}$] = 0,

$$\sigma_z^2 = \int_0^{\infty} S_{z(f)} \quad df$$

$$= \int_0^{\infty} (2\pi f)^2 \; S_{z(f)} \quad df$$

$$= E[\dot{z}^2] \qquad \text{(D.2.15)}$$

(2) σ_{DBP}

Standard deviation of random DBP can be calculated by integrating the PSD function of the DBP with frequency.

$$\sigma_{\mathrm{DBP}} = \sqrt{\int_0^{\infty} S_{\mathrm{DBP'}(f)} \quad df} \tag{D.2.16}$$

The PSD function of DBP'$_{(t)}$ which is the variable component of DBP is given by using the linear relationship between surface geometry and the DBP, together with a system function.

$$S_{\mathrm{DBP'}(f)} = |H_{sy(f)}|^2 \quad S_{y1(f)} \tag{4.20}$$

The system function is expressed as follows:

$$|H_{sy(f)}| = |H_{DBP'/z} \cdot H_{z/y2} \cdot H_{y2/y1(f)}|$$

$$= \left| \left(\frac{f}{f_n}\right)^2 \sqrt{\frac{\epsilon_3^2 + (\epsilon_2 \, 2\pi f)^2}{\left\{1 - \left(\frac{f}{f_n}\right)^2\right\}^2 + \left(2\varsigma \frac{f}{f_n}\right)^2}} \frac{\sin \frac{2\pi f d}{V}}{\frac{2\pi f d}{V}} \right| \tag{D.2.17}$$

where f_n is the natural frequency of a system and ζ is the damping ratio.

APPENDIX E

RECOMMENDED VIBRATION CRITERIA FOR RIDE DYNAMICS

In order to improve the vehicle traction on a rough terrain, human response or sensitivity to the vibration must also be considered because the problems of human sensitivity and vehicle traction are inseparable. For example, a higher operation speed may be required as one of the superior mobility factors. However, it is out of discussion if the driver or passengers cannot stand the severe shaking inside the vehicle hull. Therefore a coordination of these two factors is necessary in designing a high-performance off-road vehicle. In this Appendix, two criteria from the view point of ride dynamics will be introduced.

E.1 Factors to be Considered for Ride Comfort

(1) Vehicle factors

Considering the off-road vehicle performance, the following two factors may be important in relation to ride dynamics criteria.

a. maximum speed

b. maximum permissible vibration level

(2) Human factors

Considering the human sensitivity for vibration due to surface roughness of the ground, the following considerations are suggested.

a. frequency and amplitude

b. exposure time of vibration

c. method of excitation (continuously, discretely or mixed)

d. individuality of human

e. position and direction of vibration

E.2 Recommended Criteria

(1) ISO 2631 criteria

This criteria was proposed by ISO in 1978. For three directions of vibration (x axis= back-to-chest, y axis= right-to-left side and z axis = foot-to-head), the criteria is described in terms of maximum permissible RMS acceleration as a function of frequency and exposure time (Fig. E.1). According to the criteria, humans are most sensitive to the frequency range between 4 and 8Hz for vertical, and between 1 and 2Hz for horizontal and lateral directions (not shown here), respectively.

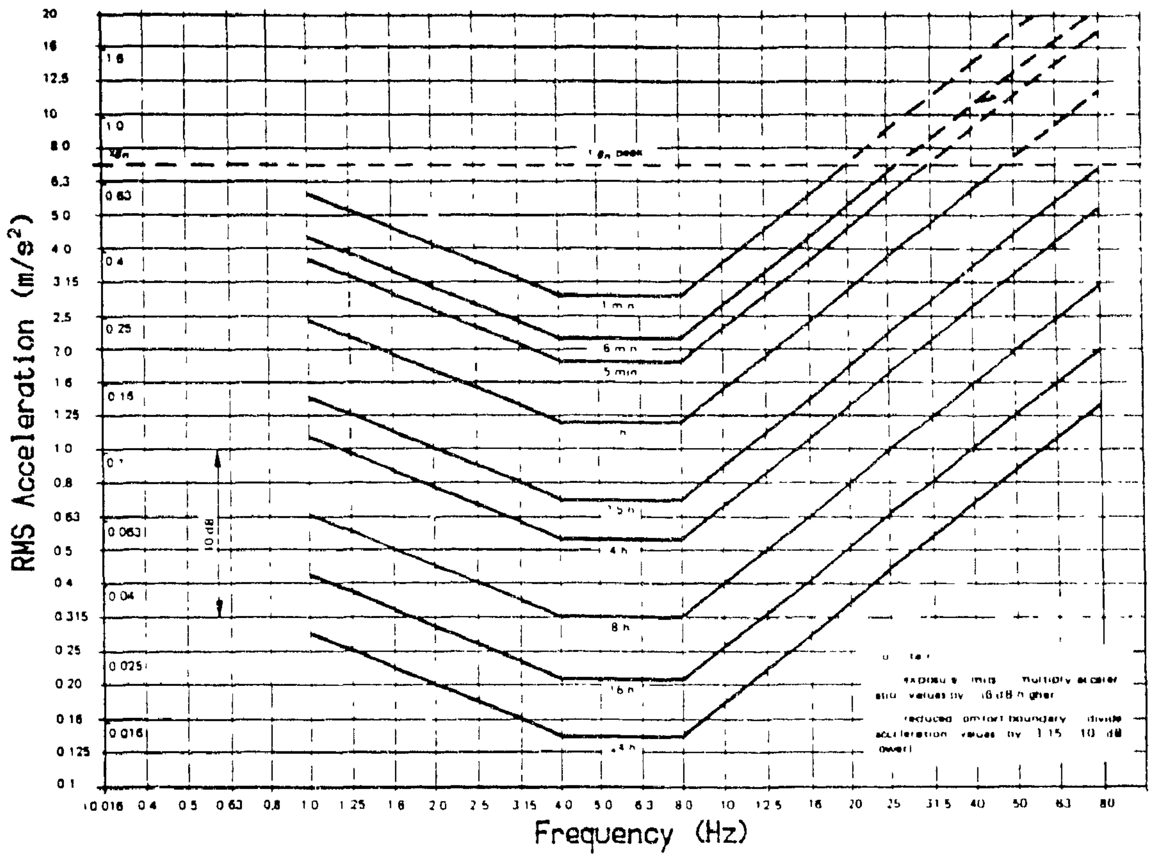

Fig. E.1 Vertical acceleration limits as a function of frequency and exposure time (ISO 2631)

(2) Absorbed power criteria

Marphy and Ahlvin (1976) suggested another criteria based on the assumption that there should be a maximum absorbable vibrational energy to the human body. Absorbed power is the measure of the rate at which vibrational energy is absorbed at the man/seat interface by an average man under vibration conditions of different frequency and severity. It is the quantity used to determine human tolerance to vibration when a vehicle is traveling on a rough terrain. The absorbed power is computed from the product of force and velocity vectors, both of which are computed from an input acceleration. The absorbed power corresponds to mean square acceleration rather than RMS acceleration. In a series of experiments, the maximum power which a human being can stand was found to be, on average, 6 watts. This criteria is used in part of the NATO Reference Model for predicting vehicle limiting speeds. Fig. E.2a schematically shows the ride limiting speed (RS) for a particular terrain profile having a certain RMS surface roughness, based on the 6 watt criteria.

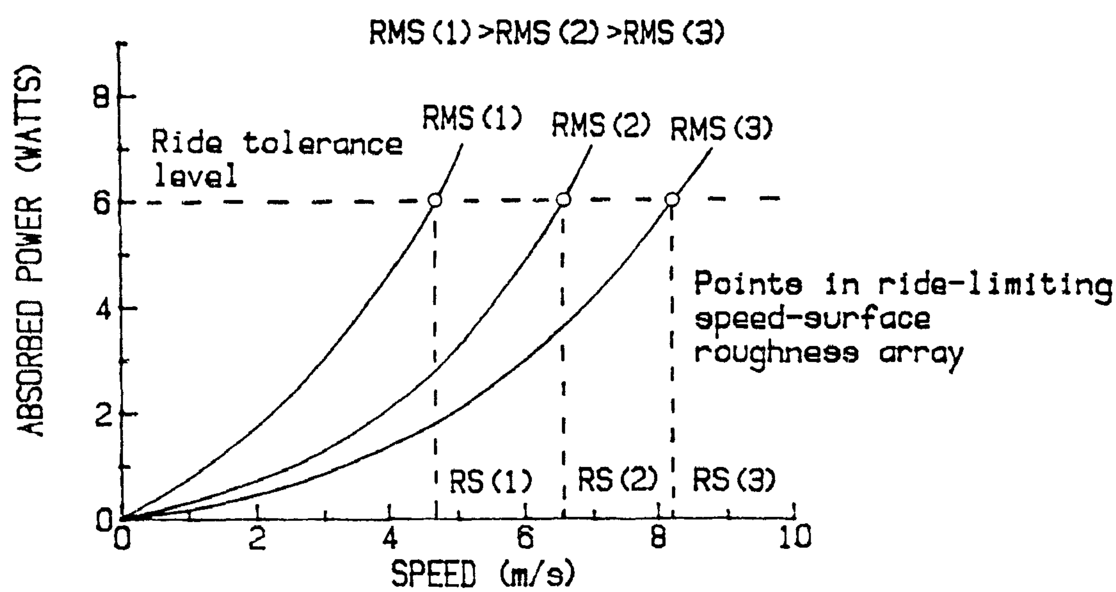

Fig. E.2a Ride limiting speed and absorbed power (after Marphy and Ahlvin)

Fig. E.2b illustrates the relationship between frequency and tolerable maximum acceleration when the power of 6 watts is applied to the human body. It is found that humans are most sensitive when vehicle vibrations are predominant at low frequencies such as 4 or 5 Hz, according to this criteria.

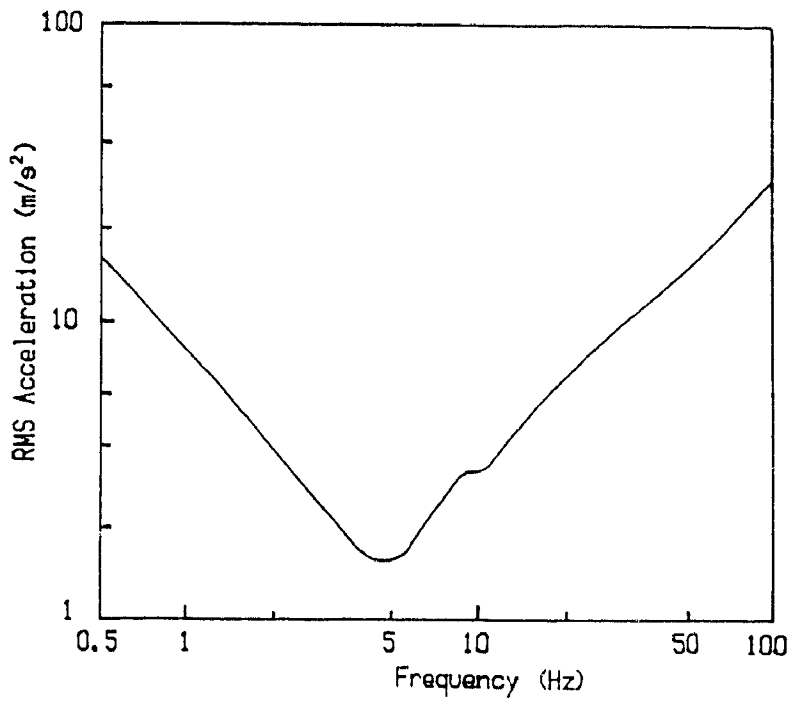

Fig. E.2b Relationship between acceleration and frequency for constant 6-watt absorbed power level (after Marphy and Ahlvin)

Although these ISO 2631 and absorbed power criteria may serve as initial limits for a ride dynamics study, further investigation is required in order to improve precision, and therefore usefulness, of these criteria since the human factors for vibration described in B.2 have not yet been fully explained quantitatively.

APPENDIX F

EXPERIMENTAL DATA

Table F.1 Test Surface Measurement

Type of Surface	RMS of Y1 $\times 10^{-3}$ m	G_0 $\times 10^{-6}$	n	RMS of Y2 $\times 10^{-3}$ m	Vertical Acceleration m/s^2	Roughness Classification
Flat & Smooth	2.19	0.6	1.5	1.36 / 1.18	0.229 / 0.241	very good / good
Rough 1	4.52	6.0	1.6	3.80 / 2.96	0.289 / 0.274	average
Rough 2	8.54	50.0	1.8	6.94 / 3.69	0.323 / 0.284	poor
Sinusoidal	14.38	N/A	N/A	13.86 / 11.64	0.237 / 0.241	N/A
				P_1 = 310.3 / 34.5 kPa		

RMS = Root-Mean-Square

P_1 - Inflation pressure of tyre

Table F.2.1 Traction Test Data on Flat and Smooth Surface

ω rad/s	Slip %	Torque Nm	$\overline{DBP}$ N	σ_{DBP} N	$\dot{E}_T$ Nm/s	Pull Coeff.	Tractive Efficiency	Nominal Tractive Efficiency
0.57	16.3	361.2	870.8	68.6	12.2	0.531	0.740	0.682
0.625	22.8	323.0	843.1	63.3	6.2	0.514	0.693	0.641
0.849	43.2	344.5	834.6	83.5	15.4	0.509	0.502	0.451
1.033	53.3	338.8	813.6	172.4	15.1	0.496	0.408	0.322
1.457	67.1	326.0	859.6	251.8	10.0	0.524	0.318	0.225

a. P_i = 310.3 kPa

0.594	14.9	319.3	810.6	37.9	19.5	0.494	0.747	0.713
0.720	29.8	334.2	839.5	41.4	22.0	0.512	0.610	0.580
0.805	37.2	332.6	865.7	52.2	16.6	0.528	0.565	0.531
0.962	47.4	339.7	873.2	53.9	19.1	0.532	0.467	0.438
1.105	54.0	337.0	883.4	45.9	24.7	0.539	0.417	0.395

b. P_i = 34.5 kPa

$\overline{DBP}$ = average of DBP

$\dot{E}_T$ = tyre deformation power

Pull Coefficient = $\overline{DBP}$/Static Load

Table F.2.2 Traction Test Data on Rough 1 Surface

ω rad/s	Slip %	Torque Nm	$\overline{DBP}$ N	σ_{DBP} N	$\dot{E}_T$ Nm/s	Pull Coeff.	Tractive Efficiency	Nominal Tractive Efficiency
0.551	15.0	306.7	782.4	114.8	9.1	0.477	0.790	0.679
0.580	19.2	314.8	806.2	135.8	8.8	0.492	0.753	0.632
0.588	20.3	330.6	808.1	134.2	14.9	0.493	0.709	0.596
0.599	21.7	320.0	777.6	191.2	16.0	0.474	0.693	0.574
0.728	35.6	339.6	854.8	162.8	12.2	0.521	0.589	0.481

a. P_i = 310.3 kPa

0.533	11.2	323.0	807.2	72.9	21.4	0.492	0.762	0.698
0.551	12.5	334.5	835.2	90.5	23.1	0.509	0.751	0.675
0.555	13.1	334.4	811.6	95.6	27.5	0.495	0.723	0.643
0.654	21.8	333.0	839.2	109.8	23.1	0.512	0.677	0.593
0.707	28.8	345.3	837.0	170.8	28.2	0.510	0.591	0.474

b. P_i = 34.5 kPa

Table F.2.3 Traction Test Data on Rough 2 Surface

ω rad/s	Slip %	Torque Nm	$\overline{DBP}$ N	σ_{DBP} N	$\dot{E}_T$ Nm/s	Pull Coeff.	Tractive Efficiency	Nominal Tractive Efficiency
0.547	11.8	342.3	833.4	251.1	17.6	0.508	0.782	0.550
0.562	14.7	348.1	859.2	231.6	15.6	0.524	0.771	0.568
0.576	18.6	341.8	856.2	258.1	13.0	0.522	0.742	0.538
0.585	19.9	355.9	876.2	254.9	16.1	0.534	0.718	0.528
0.629	25.5	344.9	876.2	256.2	13.4	0.534	0.679	0.492

a. P_1 = 310.3 kPa

0.531	3.7	343.2	834.2	132.8	27.8	0.509	0.804	0.681
0.533	4.1	333.3	844.6	150.3	20.9	0.515	0.835	0.692
0.556	8.0	340.8	822.3	144.5	28.8	0.501	0.762	0.633
0.558	8.8	342.2	847.5	174.1	24.9	0.517	0.775	0.621
0.566	12.7	340.6	840.7	111.4	24.5	0.513	0.740	0.647

b. P_1 = 34.5 kPa

Table F.2.4 Traction Test Data on Sinusoidal Surface

ω rad/s	Slip %	Torque Nm	$\overline{DBP}$ N	σ_{DBP} N	$\dot{E}_T$ Nm/s	Pull Coeff.	Tractive Efficiency	Nominal Tractive Efficiency
0.527	8.5	276.6	700.4	172.5	9.4	0.427	0.850	0.641
0.608	20.7	303.3	820.9	171.3	8.8	0.500	0.788	0.624
0.700	30.6	335.1	848.6	185.4	12.6	0.517	0.640	0.490
0.955	49.5	338.2	862.6	198.7	10.4	0.526	0.472	0.364
1.020	52.6	349.8	909.6	193.1	8.1	0.555	0.451	0.355

a. P_1 = 310.3 kPa

0.605	15.4	315.4	788.1	163.8	21.9	0.481	0.731	0.579
0.678	24.6	332.4	835.4	181.1	22.1	0.509	0.647	0.514
0.772	33.8	345.2	877.9	175.9	21.0	0.535	0.579	0.466
0.891	42.6	348.4	863.7	168.6	25.3	0.527	0.492	0.396
0.984	48.0	346.4	869.5	166.7	23.4	0.530	0.452	0.365

b. P_1 = 34.5 kPa

APPENDIX G

COMPUTER PROGRAMS

G.1 Transfer of Analogue Signal to Digital Computer by Digitizer of Tektronix 5B25N

```
10 ! ***************************
20 ! * PROG  FOR TRANSFERRING *
30 ! * DATA FROM OSCIL TO HP85*
40 ! *    sampling No =1024    *
50 ! ***************************
60 X=0 @ X9=0 @ M7= 1373
70 DISP "DATA FILE NAME?"
80 INPUT F$
90 N9=1016
100 CREATE F$,N9+8,8
110 ASSIGN# 1 TO F$
120 REMOTE 710
130 GOSUB 480
140 ON INTR 7 GOSUB 490
150 DISP " ENTER DESIRED ACCESS
    CODE?" @ INPUT Q$
160 DISP "ENTER VOLT/DIV" @ INPU
    T V
170 DISP "CONVERSION RATE FOR RE
    AL VOLT (MAX )?" @ INPUT V9
180 R$="ASCII,ACCESS "&Q$
190 OUTPUT 710 ,R$
200 GOSUB 510
210 OUTPUT 710 ,"CURVE?"
220 DIM B(1024),W$[50]
230 K9$=CHR$(44)&CHR$(10)
240 CONVERT IN 710 PAIRS , K9$
250 CLEAR
260 BEEP 100,100
270 ! ------------------------
280 DISP "PLEASE WAIT      "
290 DISP "DATA ARE BEING TRANSFE
    RRED"
300 FOR N=0 TO N9-1
310 ENTER 710 , B$
320 IF N<=T THEN 650
330 B(N)=VAL(B$)/100*V*V9
340 PRINT# 1,N+1 , B(N)
350 X9=X9+B(N)
360 NEXT N
370 FOR N3=N9 TO N9+8
380 B(N3)=0
390 PRINT# 1,N3 , B(N3)
400 NEXT N3
410 ASSIGN# 1 TO *
420 OUTPUT 710 ,"SET DISP L,DISP
    R"
430 X8=X9*M7/1024
440 DISP "MEAN VALUE=",X8
450 DISP "TRANSFERED COMPLETELY"
460 GOSUB 730
470 END
480 REM SERIAL POLL ROUTINE --
490 S=SPOLL(710)
500 RETURN
510 OUTPUT 710 ,"SELECT SAVE L,S
    AVE R,WFMPRE?"
520 ENTER 710 , W$
530 A1=POS(W$,"NR PT ")+6
540 A2=A1+3
550 L$=W$[A1,A2]
560 L=VAL(L$)-1
570 DISP "POINTS RECORDED BY OSC
    ILLOSCOPE",L
580 A3=POS(W$,"PT OFF ")+7
590 A4=A3+3
600 T$=W$[34]
610 T=VAL(T$)
620 DISP "TRIGGER POSITION",T
630 DISP "PRESS [CONT]" @ PAUSE
640 RETURN
650 REM SUB------------------
660 ! B(N)=0
670 IF N=0 THEN X=VAL(B$[7])
680 B(0)=X*V*V9/100
690 IF N=0 THEN GOTO 340
700 X=(VAL(B$)+X)/2
710 GOTO 340
720 ! PLOTTING --------------
730 CLEAR @ GCLEAR
740 BEEP 100,100
750 DISP "PLOTTING ROUTINE" @ DI
    SP
760 PLOTTER IS 1
770 DISP "MIN Y,MAX Y"
780 INPUT M8,M9
790 LORG 5
800 GCLEAR
810 LOCATE 10,120,10,90
820 FXD 0,1
830 FRAME
840 SCALE 0,N9,M8,M9
850 LAXES -100, 1,0,0,2,2
860 FOR I=0 TO N9
870 IF I=0 THEN MOVE I,B(I)
880 PLOT I,B(I)
890 NEXT I
900 FOR I=10 TO 50 STEP 10
910 BEEP I,100
920 NEXT I
930 RETURN
```

G.2 Computation of PSD by Fast Fourier Transform

```
10  ! **************************
20  ! *POWER SPEC DENSITY (log)*
30  ! *  COMPUTE "PSD" WITH    *
40  ! *  DIGITIZED DATA BY THE *
50  ! *  OSCILLOSCOPE          *
60  ! *  sampling No =512      *
70  ! **************************
80  !   $ N1/L)=20 $
90  ! This program is for [TIME
    DOMAIN] data  Not [SPACE DOM
    AIN]
100 ! For ROAD ROUGHNESS, modifi
    cation is needed
110 ! It is done in "PSD-PLOT"
120 !  DCDT        0 025 m/Volt
130 !  ULTRA      13 78 cm/Volt
140 !  OMEGA       3 60 rad/sec/V
150 !  TORQUE    762 0 N m/Volt
160 !  DBP      1860 0 N/Volt
170 !  ACC   1 004316 ms/Volt
180 !
190 M9= 1378
200 V1= 177
210 N1=512
220 N5=N1/2
230 C1=8/3
240 GCLEAR
250 OPTION BASE 1
260 DIM X(512),R(256),I(256),S(2
    56)
270 L=20
280 N3=200 @ ! COMPUTATION CYCLE

290 T=L/N1 @ ! delta t
300 F5=1/L @ ! delta freq
310 F6=2*T/N1
320 ! --- print ---------------
330 PRINT "ESTIMATION OF POWER S
    PECTRAL DENSITY (PSD)"
340 PRINT "--------------------"
350 PRINT @ PRINT
360 PRINT "NO  OF DATA POINTS=",
    N1
370 PRINT USING 380 , L
380 IMAGE "DATA LENGTH=",3D D,2X
    , "sec"
390 PRINT "COMPUTATION CYCLES=",
    N3
400 PRINT "  DELTA t= ",T
410 PRINT "  DELTA f= ",F5
420 PRINT @ PRINT
430 LDIR 0
440 GOSUB 830
450 DISP "REPLACE DISK OF D 701"
460 DISP "PRESS CONTINUE WHEN RE
    ADY"
470 PAUSE @ BEEP 450,200
480 REM
490 ! *   COMPUTE POWER        *
500 ! --- assign file ---------
510 DISP "PSD FILE NAME?"
520 INPUT F$
530 ! PRINT "PSD FILE NAME= ",F$
540 CREATE F$&" D701",N3,16
550 ASSIGN# 1 TO F$&" D701"
560 PRINT# 1,1 , N3
570 ! --- compute PSD ---------
580 GOSUB 1180
590 PRINT
600 PRINT "      No    FREQ(Hz)
      PSD(m*2/Hz)"
610 M1=0
620 S1=S(1)^2*F6*F5*C1
630 S2=S(2)^2*F6*F5*C1
640 FOR K1=1 TO N3
650 F1=(K1-1)/T/N1+ 00000001
660 IF F1> 5/T THEN 790
670 G1=S(K1)^2*F6*C1
680 A1=G1*F5
690 M1=M1+A1
700 PRINT# 1,K1+1 , F1,G1
710 NEXT K1
720 M1=M1-S1-S2
730 M5=X5^2+M1
740 M2=SQR(M1) @ ! STANDARD DEVI
    ATION
750 PRINT "   STND  DEVIA= ",M2
760 PRINT "   MEAN SQUARE= ",M5
770 PRINT# 1,N3+2 , M2
780 ASSIGN# 1 TO *
790 STOP
800 END

830 ! ************************
840 ! *     READING  DATA     *
850 ! *  REDUCTION OF DATA    *
860 ! *     APPLY HANNING     *
870 ! ************************
880 DISP "RAW DATA FILE NAME?" @
     INPUT D$
890 PRINT "DATA FILE NAME= ",D$
900 ASSIGN# 1 TO D$&" D701"
910 ! -- reduction of data ---
920 X5=0
930 FOR I=1 TO N1
940 I5=2*I-1
950 READ# 1,I5 , X(I)
960 X(I)=X(I)*M9 @ ! "m"
970 T5=(I-1)*T*V1
980 X5=X5+X(I)
990 NEXT I
1000 X5=X5/N1
1010 PRINT "MEAN VALUE (m) = ",X
     5
1020 ! -- rearrangement of data-
1030 ! -- Hanning -----------
1040 FOR I1=1 TO N5
1050 I8=2*I1-1
1060 I9=2*I1
1070 W1= 5*(1-COS(2*PI*I8/N1))
1080 W2= 5*(1-COS(2*PI*I9/N1))
1090 R(I1)=X(I8)*W1
1100 I(I1)=X(I9)*W2
1110 NEXT I1
1120 ASSIGN# 1 TO *
1130 RETURN
```

```
1140 ! ************************
1150 ! *     SUBROUTINE FFT     *
1160 ! *       # MAX=1024       *
1170 ! ************************
1180 F=1
1190 N=512
1200 DISP " PERFORMING FFT NOW!"
1210 DISP " WAIT FOR 2 MIN ++++"
1220 GOSUB 1270
1230 N2=N/2
1240 GOSUB 1340
1250 RETURN
1260 ! -- Perform  FFT ---------
1270 F=1
1280 FOR I=1 TO 10
1290 P=P*2
1300 IF P=N THEN 1320
1310 NEXT I
1320 P1=I
1330 RETURN
1340 GOSUB 1470
1350 M=R(1)/N2
1360 I1=I(1)/N2
1370 S(1)=SQR(R(1)^2+I(1)^2)
1380 PRINT @ PRINT "DC TERM=",M
1390 PRINT "MAX FREQUENCY=",I1
1400 PRINT "FREQ       REAL        I
     MAGINERY     ABSOLUTE"
1410 FOR I=2 TO N2
1420 S(I)=SQR(R(I)^2+I(I)^2)
1430 PRINT USING 1170 , I-1,R(I)
     ,I(I),S(I)
1440 IMAGE DDD,  3X,MZ 3De,2X,MZ
      3De,2X,MZ 3De
1450 NEXT I
1460 RETURN
1470 B=N2<=0 OR F<>1 AND F<>-1 O
     R P1<=0
1480 IF B=0 THEN 1520
1490 PRINT "ERROR IN SUBROUTINE"
1500 PRINT "CHECK INPUTS"
1510 PAUSE @ GOTO 1470
1520 RAD
1530 IF F=-1 THEN 1770
1540 K=0
1550 FOR J=1 TO N2-1
1560 I=2
1570 IF K<N2/I THEN 1590
1580 K=K-N2/I @ I=I+I @ GOTO 157
     0
1590 K=K+N2/I
1600 IF K<=J THEN 1630
1610 A=R(J+1) @ R(J+1)=R(K+1) @
     R(K+1)=A @ A=I(J+1)
1620 I(J+1)=I(K+1) @ I(K+1)=A
1630 NEXT J
1640 G= 5 @ P2=1
1650 FOR I=1 TO P1-1
1660 G=G+G @ C=1 @ E=0 @ Q=SQR((
     1-P2)/2)*F
1670 P2=(1-2*(I=1))*SQR((1+P2)/2
     )
1680 FOR R=1 TO G
1690 FOR J=R TO N2 STEP G+G
1700 K=J+G @ A=C*R(K)+E*I(K) @ B
     =E*R(K)-C*I(K) @ R(K)=R(J)-
     A
1710 I(K)=I(J)+B @ R(J)=R(J)+A @
      I(J)=I(J)-E
1720 NEXT J
1730 A=E*P2+C*Q @ C=C*P2-E*Q @ E
     =A
1740 NEXT R
1750 NEXT I
1760 IF F=-1 THEN RETURN
1770 A=PI/N2 @ P2=COS(A) @ Q=F*S
     IN(A)
1780 A=R(1) @ R(1)=A+I(1) @ I(1)
     =A-I(1)
1790 IF F=-1 THEN 1810
1800 R(1)=R(1)/2 @ I(1)=I(1)/2
1810 C=F @ E=0
1820 FOR J=2 TO N2/2
1830 A=E*P2+C*Q @ C=C*P2-E*Q @ E
     =A @ K=N2-J+2 @ A=R(J)+R(K)
1840 B=(I(J)+I(K))*C-(R(J)-R(K))
     *E @ U=I(J)-I(K)
1850 V=(I(J)+I(K))*E+(R(J)-R(K))
     *C
1860 R(J)=(A+B)/2 @ I(J)=(U-V)/2
      @ R(K)=(A-B)/2 @ I(K)=-(U+
     V)/2
1870 NEXT J
1880 I(N2/2+1)=-I(N2/2+1)
1890 IF F=-1 THEN 1540
1900 BEEP 150,250 @ BEEP 20,30
1910 DISP "  FINISHED FFT COMPUT
     ATION        "
1920 DISP "  CALCULATING ABSOLUT
     E VALUE"
1930 RETURN
```

G.3 Computation of Nominal Tractive Efficiency

```
10 ! **************************
20 ! *        COMPUTE          *
30 ! *  TRACTIVE EFFICIENCY    *
40 ! *          FOR            *
50 ! *    RANDOM  SURAFACE     *
60 ! * - STANDAPD DEVIATION    *
70 ! *    USE EXP  EQUATIONS   *
80 ! *        no shock         *
90 ! *       *EFFI-RAND"       *
100 ! **************************
110 DISP "DATA FILE NAME"
120 INPUT F$
130 CREATE F$&" D701",200.16
140 ASSIGN# 1 TO F$&" D701"
150 PRINT "    TRACTIVE EFFICIEN
    CY"
160 PRINT
170 G=4/1000000 @ ! ROUGH COEFF
180 FOR J9=1 TO 3
190 IF J9=1 THEN 220
200 IF J9=2 THEN 230
210 IF J9=3 THEN 240
220 P=310300 @ LINETYPE 1 @ GOTO
     250
230 P=137900 @ LINETYPE 4 @ GOTO
     250
240 P=34500 @ LINETYPE 3, 8
250 N=2
260 PRINT "        ROUGH COEEF =
    ".G
270 PRINT "        N= ".N
280 PRINT "        INFLATION PRES
    SURE (Pa)=",P
290 PRINT " ------------------
    --------------------------
    --"
300 PRINT "    V(m/s)  SLIP  TOR
    QUE(Nm)  E[dZ/dt^2]   E[DP]
      DPsigma  EFFICIENCY(%)"
310 PRINT " ------------------
    --------------------------
    --"
320 !
330 ! input data ------------
340 V=5
350 R= 374 @ ! RADIUS
360 R1= 5* 15 @ ! STOPPER
370 T2=330
380 M=200 @ ! MASS
390 M1=M*9 81
400 H5= 17 @ ! SECTION HEIGHT
410 FOR S=2 TO 65
420 S1=S/100
430 K1=-30 @ ! EXP
440 !
450 ! ----------------------
460 K=30000+ 773*P
470 Q=(-4 61*LGT(P)+26 82)/1000
480 E=- 1363*LGT(P)+ 7884
490 L5= 5*Q*SQR(M1)
500 D=R-M1/K
510 U=1-EXP(-7*M1/K/H5)
520 W=V D/(1-S1)
530 F1=SQR(K/M)/2/PI
540 C=E*4*M*F1*PI
550 T1=T2*(1-EXP(K1*S1))+20
560 !
570 !
580 ! print statements -------
590 PRINT "   TYRE---MICHELIN 7 0
    0 (BUFFED)"
600 PRINT "ROUGH COEFF ",G
610 PRINT "V (m/s)=",V
620 PRINT "INFLATION PRESS  (KPa
    ) =".P
630 PRINT "SLIP (%) =",S
640 !
650 ! ----------------------
660 !
670 R8=(T1/8/R^3-U*C*W^2/12/V)*Q
    ^2
680 E8=T1/R+R8*M1
690 E2=R8*C
700 E3=R8*K
710 GOSUB 840 @ ! E[dZ/dt^2] &
    DP-sigma
720 E1=E8-U*E9*C/V
730 !
740 X=(E1-M4)*V/T1/W
750 ! print statements --------
760 IMAGE 3X.2D 3D,3X,2D D,2X,5D
     D ,5X.D 3De.6D 2D,6D 2D,5X,
    3D D
770 PRINT USING 760 , V.S.T1,E9,
    E1,M4.X
780 PRINT# 1 , S,X
790 NEXT S
800 NEXT J9
810 ASSIGN# 1 TO *
820 DISP "****** END ******"
830 END

840 ! ************************
850 ! *  COMPUTE VARIANCE OF *
860 ! *        dZ/dt **2     *
870 ! *        DP-sigma      *
880 ! *    WITH   PSD of Y1  *
890 ! ************************
900 !
910 C9=0 @ Z9=0
920 FOR I=1 TO 200
930 W1=I/10
940 P1=G*V^(N-1)*W1^(-N)
950 B1=W1/F1
960 H1=E3^2+(E2*2*PI*W1)^2
970 H2=(1-B1 2)^2+(2*E*B1)^2
980 B9=2*PI*W1*L5/V
990 H3=SIN(B9)/B9
1000 !
1010 H4=B1^4*H3^2/H2
1020 H6=4*PI^2*H4*W1^2*P1
1030 H7=H4*H1*P1 @ ! (H DP/Y1*P1
     )
1040 !
1050 C9=C9+H6
1060 Z9=Z9+H7
1070 NEXT I
1080 E9=C9* 1
1090 Z3=Z9* 1
1100 M4=SQR(Z3)
1110 RETURN
```